

**Relating the Biogeochemistries of Zinc, Cobalt, and Phosphorus to  
Phytoplankton Activities in the Sea**

by

Rachel J. Wisniewski

B.S. University of Georgia, 2000

Submitted in partial fulfillment of the requirements for the degree of Doctor of Philosophy

at the

MASSACHUSETTS INSTITUTE OF TECHNOLOGY

and the

WOODS HOLE OCEANOGRAPHIC INSTITUTION

June, 2006

© Rachel J. Wisniewski, MMVI. All rights reserved.

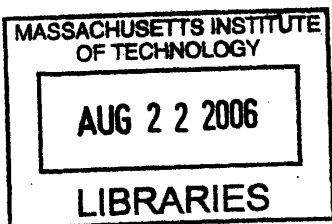
The author hereby grants to MIT and WHOI permission to reproduce paper and electronic copies  
of this thesis in whole or in part and to distribute them publicly.

Signature of Author .....  
Joint Program in Chemical Oceanography  
Massachusetts Institute of Technology  
and Woods Hole Oceanographic Institution  
April 21, 2006

Certified by .....  
Dr. James W. Moffett  
Thesis Supervisor

Certified by .....  
Dr. Sonya T. Dyhrman  
Thesis Supervisor

Accepted by .....  
Dr. Timothy I. Eglinton  
Chair, Joint Committee for Chemical Oceanography  
Senior Scientist  
Woods Hole Oceanographic Institution



**ARCHIVES**



# **Relating the Biogeochemistries of Zinc, Cobalt, and Phosphorus to Phytoplankton Activities in the Sea**

by

Rachel J. Wisniewski

Submitted to the Department of Marine Chemistry and Geochemistry,  
Massachusetts Institute of Technology–Woods Hole Oceanographic Institution,  
Joint Program in Chemical Oceanography  
on April 21, 2006, in partial fulfillment of the  
requirements for the degree of  
Doctor of Philosophy

## **Abstract**

This thesis explores the potential of zinc, cobalt, and phosphorus to influence primary production in the subarctic North Pacific, the Bering Sea, and the North Atlantic Ocean. In the North Pacific and Bering Sea, total zinc concentrations were measured along a near-surface transect and in selected deep profiles. Zinc speciation was also measured with a novel anodic stripping voltammetry method, and the results were consistent with previous studies using different methods. The potential for zinc to impact primary production in the North Pacific was demonstrated in a shipboard incubation and by comparing two phytoplankton pigment markers to total zinc and free zinc ion concentrations. In the North Atlantic, total dissolved zinc and cobalt concentrations were measured and compared to concentrations of dissolved inorganic phosphorus and chlorophyll. In some areas of the North Atlantic the concentrations of zinc and cobalt were decoupled. The relationship between cobalt and inorganic phosphorus suggests that cobalt drawdown may be related to a high alkaline phosphatase related demand at low phosphorus concentrations. This trend compliments a shipboard incubation where alkaline phosphatase activities increased after cobalt addition. The presence of measurable alkaline phosphatase activity indicated that the phytoplankton community in the Sargasso Sea was experiencing phosphorus stress. Shipboard incubations generally confirmed this with inorganic phosphorus additions resulting in chlorophyll increases at 4 out of 5 stations. Further, the addition of dissolved organic phosphorus, as either a phosphate monoester or a phosphonate compound, resulted in a chlorophyll increase in 3 out of 3 incubations. This suggests that dissolved organic phosphorus may be an important phosphorus source for phytoplankton in low phosphorus environments and that the ability to use phosphonates may be more widespread than previously recognized. Overall, this thesis adds to our understanding of how the nutrients phosphorus, zinc, and cobalt may influence primary production.

## **Thesis Supervisors:**

Dr. James W. Moffett

Title: Senior Scientist, Marine Chemistry & Geochemistry Dept., Woods Hole Oceanographic Institution

Dr. Sonya T. Dyhrman

Title: Assistant Scientist, Biology Dept., Woods Hole Oceanographic Institution



## Acknowledgments

I received funding towards my graduate research from the Richard Vanstone Summer Fellowship, the Stanley W. Watson Student Fellowship, the Arch Scurlock Fund for research, the Center for Environmental Bioinorganic Chemistry, the EPA STAR Fellowship, the National Science Foundation (OCE-0136835), and the WHOI Academic Programs Office.

This thesis was heavily influenced by the ideas and support I received from my two advisors: Jim Moffett and Sonya Dyhrman. Jim, I really appreciate the freedom you gave me to pursue questions that I was really interested in. I have also greatly benefited from the numerous opportunities you gave me to go to sea and to attend conferences. Even when I was feeling rather forlorn about my data, you always managed to provide a positive perspective and enthusiasm for what I was doing. I also feel lucky to have had an advisor who encouraged so many of my non-academic pursuits like windsurfing, Millfield parties, and lacrosse coaching. Sonya, thanks for embracing a chemist and helping me expand my skills into the realms of biology. I really value all your efforts in forcing me to come up with deadlines and having detailed comments on drafts done within 24 hours. I am very thankful to you for giving me the opportunity to try my hand at proposal writing. You have been extremely enthusiastic and supportive from the very beginning, which has meant a lot to me. What a nightmare beginning it was...the fateful Weatherbird cruise of losing equipment, breaking back-up equipment, breathing diesel fumes, and somewhat crazy shipmates. Thank goodness we had each other and rum swizzles to make it through!

Thanks to my committee members, Ed Boyle and Mak Saito. I benefited not only from your thoughts and comments in committee meetings, but also from your hands-on help in the lab with various analytical methods and with trace metal clean techniques. Thanks for all your help and insight. Thanks also to Ed Sholkovitz, my thesis defense chair. I really appreciate your taking the time to help out in the home stretch and provide your input on the thesis.

The WHOI Academic Programs Office is a treasure trove of wonderful people who know our names the first day we show up and who are always our advocates. A million thanks to John, Julia, Marsha, and Judy for making WHOI feel like home.

Thanks to the MC&G department's administrative staff who were always helpful and ready with a smile, most especially to Sheila and Lucinda who helped with countless poster printing and room reservations.

Between the Boyle, Moffett, and Dyhrman groups, I've shared lab benches, complaints, and cruise time with a number of people. Thanks to all my past and present lab members for keeping work interesting and teaching me about science and life: Mak, Rick, Bridget, Jay, Sonya, Eric, Gary, Rodrigo, Santiago, Dreux, Sheean, Annette, Tyler, Abigail, Liz, Louie, Alena, Erin, Alicia, Michelle, and Dan.

One of the greatest strengths of the Joint Program is the wonderful students it attracts. I have enjoyed getting to know all of you while pursuing my education on various fronts by doing things

like creating an interpretive dance on Westward cruise, taking classes together, drinking beers at the Kidd, and spending our per diem in far off places during meetings. I have to give a special thanks to those who answered all my L<sup>A</sup>T<sub>E</sub>X, MATLAB, and GMT questions: Linda Kalnejais, Kristy Dahl, Mike Jakuba, Mea Cook, Margaret Boettcher, Chris Roman, and Rachel Stanley. You saved me from complete and utter frustration on a number of occasions! I also need to give a special thanks to Nick Drenzek. Thanks for always being willing to take a walk or get a coffee when I needed to vent and for keeping me up to date on all the latest gossip.

To my Fye girls: Helen, Cara, & Kristy—thank you, thank you, thank you! I don't know how I would have made it through my first year without you girls. I will never forget all the good times and boy crises at OPP #12. You are each an amazing woman and I have learned so many different things from each of you (including important things like how awesome MTV reality TV can be and how miserable making 8 lbs of mac & cheese is!).

Thanks to all the people who made my non-working hours a blast! Thanks to the windsurfing/baby crowd: Chris, Steph, Nick, Amy, Dave, Kate, Claudia, Jason, Lara, Henrick, Mary-Louise, and Jeff. Thanks to the Somerville boys who embraced me (read: began teasing me) immediately and introduced me to many an interesting Boston/Cambridge haunt. Thanks to the Quegs who are the best group of friends I could imagine sharing high school and beyond with. Thanks especially to Lauren, my Royce Road roomie who made the transition to grad school easier. Thanks to my UGA girls, Laurie, Lexi, and Meghan, for always making me laugh, especially Meghan who got to hear about how stressful "the plan" and juice can be.

My family has all been very supportive of me each in their own way. Mark and Luke with their teasing, Mom and Dad with their nagging, and Grandmoms with her bragging. Thanks for being there for me and for all the love and support I have always received from you. And Mark and Luke, that's Dr. Sister to you, now!

Mike, in our first semester, my crush on you was a huge distraction from studying for finals and last month our engagement was a huge distraction from preparing for my thesis defense! I look forward to all the distractions to come. You have had a huge influence on my life over the last five and a half years. There are so many things I may never have done without you: getting serenaded by alpha delts, D-league hockey, windsurfing, beer brewing, canoeing through the rain, riding ATVs on Maui, dancing the tango, curling, learning a little Czech, biking in Bermuda, etc. Thank you for all that you have brought to my life and for always being there for me, especially over the last few stressful months.

## **Dedication**

This thesis is dedicated to the memory of my paternal grandmother, Loretta Wisniewski. She was an extremely sharp woman who loved learning but who was denied the opportunity to pursue an education. Her love of life and laughter taught me lessons that no formal education could.





# Contents

<b>1</b>	<b>Introduction</b>	<b>19</b>
<b>2</b>	<b>A new anodic stripping method for the determination of zinc speciation</b>	<b>31</b>
2.1	Abstract . . . . .	32
2.2	Introduction . . . . .	33
2.3	Methods . . . . .	35
2.3.1	Sample collection . . . . .	35
2.3.2	Total dissolved Zn analysis . . . . .	35
2.3.3	ASV Theory . . . . .	36
2.3.4	ff-ASV Speciation Titrations . . . . .	37
2.3.5	CSV Theory . . . . .	38
2.3.6	CSV Speciation Titrations . . . . .	40
2.4	Results . . . . .	40
2.4.1	ff-ASV Method Analysis . . . . .	40
2.4.2	ff-ASV & CSV Sample Titrations . . . . .	42
2.5	Discussion . . . . .	43
2.6	Conclusions . . . . .	46
2.7	Acknowledgments . . . . .	47
<b>3</b>	<b>Zinc in the subarctic North Pacific and Bering Sea</b>	<b>61</b>
3.1	Abstract . . . . .	62
3.2	Introduction . . . . .	63
3.3	Methods . . . . .	65

3.3.1	Sample Collection and Handling . . . . .	65
3.3.2	Total Dissolved Zn Analysis . . . . .	65
3.3.3	Zn Speciation Determinations . . . . .	67
3.3.4	Shipboard Incubation . . . . .	68
3.3.5	Chlorophyll, Nutrients, and HPLC pigments . . . . .	69
3.4	Results . . . . .	69
3.4.1	Total Dissolved Zn . . . . .	69
3.4.2	Zn Speciation . . . . .	70
3.4.3	Shipboard Incubation . . . . .	71
3.4.4	Chlorophyll, Nutrients, and HPLC pigments . . . . .	71
3.5	Discussion . . . . .	72
3.5.1	Total Dissolved Zn . . . . .	72
3.5.2	Zn Speciation . . . . .	75
3.5.3	Shipboard Incubation . . . . .	76
3.5.4	Zn and HPLC pigments . . . . .	77
3.6	Conclusions . . . . .	78
3.7	Acknowledgments . . . . .	79
<b>4</b>	<b>Trends in phosphorus, zinc, and cobalt concentrations in the western North Atlantic Ocean and their influence on alkaline phosphatase activity</b>	<b>103</b>
4.1	Abstract . . . . .	104
4.2	Introduction . . . . .	105
4.3	Methods . . . . .	107
4.3.1	Sample Collection . . . . .	107
4.3.2	Chlorophyll . . . . .	108
4.3.3	P Analyses . . . . .	108
4.3.4	Near-surface AP Activity . . . . .	109
4.3.5	Dissolved Zn Analysis . . . . .	110
4.3.6	Dissolved Co Analysis . . . . .	111
4.3.7	Shipboard Incubation . . . . .	111
4.3.8	Culture Study . . . . .	112

4.4	Results . . . . .	113
4.4.1	Chlorophyll . . . . .	113
4.4.2	P Analyses . . . . .	114
4.4.3	Near-surface AP Assays . . . . .	114
4.4.4	Dissolved Zn and Co . . . . .	114
4.4.5	Shipboard Incubation . . . . .	115
4.4.6	Culture Study . . . . .	116
4.5	Discussion . . . . .	116
4.5.1	Chlorophyll . . . . .	117
4.5.2	P Analyses . . . . .	117
4.5.3	Near-surface APA Assays . . . . .	117
4.5.4	Dissolved Zn and Co . . . . .	118
4.5.5	Shipboard Incubation . . . . .	122
4.5.6	Culture Study . . . . .	123
4.6	Conclusions . . . . .	124
4.7	Acknowledgments . . . . .	126
<b>5</b>	<b>Phosphonate utilization by marine phytoplankton in the Sargasso Sea</b>	<b>143</b>
5.1	Introduction . . . . .	145
5.2	Methods . . . . .	148
5.3	Results . . . . .	150
5.4	Discussion . . . . .	151
5.5	Conclusions . . . . .	156
5.6	Acknowledgments . . . . .	157
<b>6</b>	<b>Conclusions and Future Directions</b>	<b>169</b>
<b>A</b>	<b>Cleaning Protocols Used</b>	<b>177</b>
A.1	Low Density Polyethylene (LDPE) for acidified totals . . . . .	177
A.2	Teflon for speciation samples . . . . .	178
A.3	Polyethylene Centrifuge tubes for ICP-MS analysis . . . . .	178

<b>B Incubation Experiments</b>	<b>181</b>
B.1 Western North Atlantic, Spring 2004 . . . . .	181
B.1.1 Incubation OCE1 . . . . .	181
B.1.2 Incubation OCE2 . . . . .	184
B.1.3 Incubation OCE3 . . . . .	187
B.1.4 Incubation OCE4 . . . . .	189
B.1.5 Incubation OCE5 . . . . .	190
B.2 North Pacific and Bering Sea, Summer 2003 . . . . .	191
B.2.1 Incubation KM1 . . . . .	191
B.2.2 Incubation KM3 . . . . .	193
B.2.3 Incubation KM4 . . . . .	194
B.2.4 Incubation KM6 . . . . .	195
B.2.5 Incubation KM8 . . . . .	196
B.2.6 Incubation KM10 . . . . .	197
B.2.7 Incubation KM11 . . . . .	198
B.3 Conclusions . . . . .	199

# List of Figures

1-1	Diagram of metal free ion uptake model. . . . .	28
1-2	Zinc versus phosphate data over an entire depth profile from the North Pacific . . . . .	29
1-3	Zinc versus phosphate data in the upper water column (0 - 200 m) from the North Pacific . . . . .	30
2-1	Example of a typical ff-ASV titration (A) and the linear relationship obtained by transforming the titration data (B). . . . .	53
2-2	Example voltammetric scans of a seawater sample with two zinc additions. . . . .	54
2-3	Example of a typical CLE-CSV titration (A) and the linear relationship obtained by transforming the titration data (B). . . . .	55
2-4	ff-ASV titration of UV-irradiated seawater (A) and a dilute (10%) seawater solution (B). . . . .	56
2-5	ff-ASV titration of a solution of 0.1 M potassium chloride and 4 nM EDTA. . . . .	57
2-6	Simulated ASV titrations of a solution with 4 nM ligand of various $K_{cond,Zn^{2+}}$ values. . . . .	58
2-7	An upper water column profile from the North Atlantic of $L_T$ (A) and $K_{cond,Zn^{2+}}$ (B) determined by CLE-CSV and by ff-ASV. . . . .	59
2-8	An upper water column profile from the North Atlantic of total dissolved Zn and $Zn^{2+}$ determined by CLE-CSV and ff-ASV. . . . .	60
3-1	Map of station locations from the North Pacific and Bering Sea visited aboard the R/V Kilo Moana in June-August 2003. . . . .	90
3-2	Total dissolved Zn concentrations from near surface samples in the North Pacific and Bering Sea. . . . .	91
3-3	Depth profiles of total dissolved Zn concentrations from stations 1, 4, and 6 in the North Pacific. . . . .	92

3-4	Comparison of total dissolved Zn concentrations with salinity and temperature profiles in the upper 500 m at St. 4 in the North Pacific. . . . .	93
3-5	Total dissolved Zn concentrations versus PO <sub>4</sub> concentrations from the North Pacific. . . . .	94
3-6	Total dissolved Zn concentrations from stations 1, 4, and 6 in the North Pacific compared to silicate . . . . .	95
3-7	Concentration of Zn binding ligands ( $L_T$ ) in the near surface from the North Pacific and Bering Sea shown in relation to station number and total dissolved Zn concentration . . . . .	96
3-8	Chlorophyll concentrations in a shipboard incubation begun at St. 5 in the North Pacific . . . . .	97
3-9	Total dissolved Zn concentrations several phytoplankton pigments in the North Pacific and Bering Sea. . . . .	98
3-10	Free Zn <sup>2+</sup> concentrations versus several phytoplankton pigments in the North Pacific and Bering Sea. . . . .	99
3-11	Comparison of total dissolved Zn concentrations at St. 1 with previous measurements of Zn in the vicinity of St. 1 in the North Pacific. . . . .	100
3-12	Visualization of the Aerosol Index from NASA's Total Ozone Mapping Spectrometer (TOMS) satellite. . . . .	101
3-13	The concentration of total and free Zn in the near-surface samples from the North Pacific and Bering Sea. . . . .	102
4-1	Map of cruise track from the North Atlantic that was sampled March - April 2004. . . . .	133
4-2	Near surface concentrations of chlorophyll, SRP, and DOP in the North Atlantic. . . . .	134
4-3	Near surface alkaline phosphatase activity in the North Atlantic. . . . .	135
4-4	Near surface concentrations of total dissolved Zn and Co in the North Atlantic. . . . .	136
4-5	Relationship of salinity to Co and Zn for stations 15-25 in the North Atlantic. . . . .	137
4-6	Relationship between chlorophyll <i>a</i> concentration and the concentrations of total dissolved Co, Zn, and SRP in the North Atlantic. . . . .	138
4-7	Relationship between SRP concentration and the concentrations of total dissolved Co and Zn in the North Atlantic. . . . .	139
4-8	Chlorophyll and alkaline phosphatase activity results from the shipboard incubation performed at St. 16 in the North Atlantic. . . . .	140
4-9	Growth rate and alkaline phosphatase results for culture experiment with <i>E. huxleyi</i> . . . . .	141

5-1	Map of time zero locations for incubations performed in the Sargasso Sea. . . . .	163
5-2	Growth curve of <i>E. huxleyi</i> cultures when the sole phosphorus source added was either DIP or a model phosphonate, or when no P was added. . . . .	164
5-3	Chlorophyll concentration at time final in two endpoint incubations (EDR, OCE5) from the Sargasso Sea where P was added as DIP, as a model phosphate monoester, or as a model phosphonate. . . . .	165
5-4	Chlorophyll concentrations in two time-course incubations (OCE1, OCE2) from the Sargasso Sea where P was added as DIP, as a model phosphate monoester, or as a model phosphonate. . . . .	166
5-5	Abundance of picoeukaryotes and <i>Synechococcus</i> in the time course incubation OCE1 from the Sargasso Sea. . . . .	167
5-6	Abundance of picoeukaryotes and <i>Synechococcus</i> at time final of incubation OCE5 from the Sargasso Sea . . . . .	168
B-1	Sargasso Sea time course incubation OCE1 (31°N, 64°W), DIP plus metal additions. Treatments: Control, +DIP, +Co/DIP, +Zn/DIP. . . . .	182
B-2	Sargasso Sea time course incubation OCE1 (31°N, 64°W), metal alone additions. Treatments: Control, +Co, +Zn, +Fe. . . . .	183
B-3	Sargasso Sea time course incubation OCE2 (28°N, 62°W), DIP plus metal additions. Treatments: Control, +DIP, +Co/DIP, +Zn/DIP. . . . .	185
B-4	Sargasso Sea time course incubation OCE2 (28°N, 62°W), metal alone additions. Treatments: Control, +Co, +Zn, +Fe. . . . .	186
B-5	Sargasso Sea endpoint incubation OCE3 (20°N, 46°W), DIP plus metal additions. Treatments: Control, +DIP, +Co/DIP, +Zn/DIP. . . . .	187
B-6	Sargasso Sea endpoint incubation OCE3 (20°N, 46°W), metal alone additions. Treatments: Control, +Co, +Zn. . . . .	188
B-7	Sargasso Sea endpoint incubation OCE4 (32°N, 54°W), DIP plus metal additions. Treatments: Control, +DIP, +Co/DIP. . . . .	189
B-8	Sargasso Sea endpoint incubation OCE5 (34°N, 55°W), DIP plus metal additions. Treatments: Control, +DIP, +Co/DIP, +Zn/DIP. . . . .	190

B-9 North Pacific end point incubation KM1 (41°N, 140°W). Treatments were: control, +Zn, +DIP, +N, +N/Zn. . . . .	192
B-10 North Pacific end point incubation KM3 (44°N, 159°W). Treatments were: control, +Zn, +DIP, +N, +N/Zn. . . . .	193
B-11 North Pacific end point incubation KM4 (47°N, 170°W). Treatments were: control, +Zn, +DIP, +N, +N/Zn. . . . .	194
B-12 North Pacific time course incubation KM6 (46°N, 170°E). Treatments were: control, +Zn, +Fe, +Zn/Fe. . . . .	195
B-13 North Pacific time course incubation KM8 (55°N, 176°E). Treatments were: control, +Zn, +Fe, +Zn/Fe. . . . .	196
B-14 North Pacific end point incubation KM10 (56°N, 167°W). Treatments were: control, +Zn, +Fe, +DIP, +Zn/DIP, +Fe/DIP. . . . .	197
B-15 North Pacific time course incubation KM11 (56°N, 164°W). Treatments were: control, +Zn, +Fe, +Zn/Fe, +DIP, +Zn/DIP, +Fe/DIP. . . . .	198



# List of Tables

2.1	Compilation of the results of voltammetric Zn speciation measurements in oligotrophic regions. . . . .	51
2.2	Voltammetric scan conditions used in this study for the ff-ASV and CLE-CSV methods. . . . .	52
3.1	Total dissolved Zn, Zn speciation, and PO <sub>4</sub> data from the North Pacific and Bering Sea. . . . .	85
3.2	Time final nutrient concentrations and nutrient drawdown ratios from the shipboard incubation performed at St. 5 in the North Pacific. . . . .	86
3.3	Summary table of incubation experiments performed in the North Pacific and Bering Sea during the summer of 2003. . . . .	87
3.4	Estimations of Zn <sup>2+</sup> concentrations in the mixed layer of oligotrophic regions based on voltammetric Zn speciation determinations. . . . .	89
4.1	Free ion concentrations of Co and Zn in the four metal treatments used for <i>E. huxleyi</i> culture experiment. . . . .	131
4.2	Near-surface total dissolved Zn, Co, and P data for the North Atlantic. . . . .	132
5.1	Time zero conditions for DIP and DOP incubations performed in the Sargasso Sea. . . . .	161
5.2	The potential concentration of inorganic nutrients in the P spike solutions. . . . .	162
B.1	Summary table of all the incubation results presented in this thesis. . . . .	201



# **Chapter 1**

## **Introduction**

Phytoplankton are among the smallest organisms in the ocean, yet have a huge impact on the ocean ecosystem and the global environment. At the base of the food chain, phytoplankton fix carbon dioxide (CO<sub>2</sub>) into organic biomass that is consumed by progressively higher trophic levels. Phytoplankton are responsible for the current oxygenated atmosphere of our planet as oxygen is a byproduct of photosynthesis. The consumption of atmospheric CO<sub>2</sub> by phytoplankton results in the ocean serving as a net sink for atmospheric CO<sub>2</sub>. Understanding the ocean's capacity to absorb atmospheric CO<sub>2</sub> is critical to global carbon models that predict future CO<sub>2</sub> concentrations and associated warming.

Primary production depends on numerous factors including light, temperature, nutrient concentrations, ocean circulation, and grazing pressure. Of these factors, nutrient availability seems to be the most important one in the majority of the world's ocean. Traditionally, nitrogen (N) has been considered the limiting nutrient in marine systems based on ammonia and phosphate enrichment experiments (e.g., Ryther and Dunstan 1971). However, in some areas of the ocean, concentrations of N and phosphorus (P) are abundant, yet phytoplankton production is low. One hypothesis to explain the existence of these high-nutrient, low chlorophyll (HNLC) regions is that phytoplankton production is limited by low concentrations of the micronutrient iron (Fe). Fe is critical to the basic metabolic functioning of phytoplankton and was suggested as an important determinant of phytoplankton growth as early as 1931 (Gran, 1931). However, early efforts to understand the importance of Fe to primary production were confounded by Fe contamination. In the mid-1970's, the introduction of "clean" sampling and handling techniques generated new interest in the ability of trace metals to affect primary production with the realization that the concentrations of most trace metals in the ocean were orders of magnitude lower than previously thought (e.g., Cu: Boyle and Edmond 1975, Zn: Bruland et al. 1978, Fe: Gordon et al. 1982). Since then, numerous Fe addition experiments to bottles and mesoscale ocean patches have demonstrated the ability of Fe to limit marine primary production (e.g., Martin and Fitzwater 1988, Coale et al. 1996, Boyd et al. 2000). Thus, Fe and N have been the focus of much of the effort to date on understanding controls on primary production. This thesis centers on two lesser studied nutrients that are also important for marine primary production: zinc and phosphorus.

Zinc (Zn) is the third most abundant trace metal in diatom cells (after iron and manganese, Morel et al. 1991). It is a cofactor in numerous enzyme systems involved in basic metabolic functioning such as carbon and nutrient acquisition and DNA replication (Sunda, 1989). In fact, there are more known Zn-metalloproteins than Fe-metalloproteins (Maret, 2002). Culture studies have demonstrated that low free Zn ion (Zn<sup>2+</sup>) concentrations can limit phytoplankton growth (Anderson et al., 1978) and that Zn concentra-

tions may influence species composition, as oceanic phytoplankton are able to grow at much lower  $Zn^{2+}$  concentrations than coastal species (Brand et al., 1983). The ability of oceanic phytoplankton to survive at lower  $Zn^{2+}$  concentrations is largely a result of a decreased cellular Zn requirement relative to coastal species (Sunda and Huntsman, 1992). A lowering of the growth requirement could be achieved by more efficient utilization of internal Zn pools, replacement of Zn-metalloenzymes with non-metal containing ones, or by substituting a Zn-metalloenzyme with one that contained a more readily available metal (Sunda, 1989). Increasing Zn uptake rates does not seem a viable option for oceanic species since coastal species already approach the limit imposed by diffusion (Morel et al., 1991; Sunda and Huntsman, 1992).

Even though open ocean  $Zn^{2+}$  concentrations can be exceedingly low (e.g., Bruland 1989), there is little evidence for in situ Zn limitation (e.g., Coale 1991; Coale et al. 1996). There are several possible explanations for this discrepancy. First, Zn bioavailability has been described by the free ion model (Fig. 1-1) based on culture studies with the synthetic ligand EDTA (e.g., Anderson et al. 1978; Sunda and Huntsman 1992). The free ion model dictates that cell surface Zn transport molecules will only react with  $Zn^{2+}$  or inorganic complexes that rapidly dissociate to  $Zn^{2+}$ . According to this model, the majority of the oceanic Zn is not available to phytoplankton due to its complexation by strong organic ligands (e.g., Bruland 1989). It is possible that phytoplankton have a siderophore-like Zn uptake system whereby organisms secrete specific Zn binding ligands and the entire Zn-ligand complex is transported into the cell. This situation would be congruent with Zn-EDTA complexes being non-bioavailable but would allow for some fraction of the organically bound Zn in the ocean to be bioavailable.

Another factor that may prevent Zn limitation in the ocean is biochemical substitution. When Zn concentrations are low, some organisms can substitute either cobalt (Co) or cadmium (Cd) for Zn in order to alleviate Zn stress (e.g., Sunda and Huntsman 1995; Lee et al. 1995; Yee and Morel 1996). Sunda and Huntsman (1995) examined the potential influence of biochemical substitution on dissolved Zn and Co concentrations in the North Pacific by plotting Zn and Co against phosphate. At high phosphate, there is a linear relationship between Zn and phosphate and no relationship between Co and phosphate (Fig. 1-2). At low phosphate values, when Zn is near zero, there is a linear relationship between Co and phosphate (Fig. 1-2). The authors interpret this as evidence that Co is biologically drawn down once low Zn concentrations necessitate Co substitution. However, it is important to note that the plots consist of data that is taken from all depths in the water column, not only from the euphotic zone where phytoplankton uptake occurs. Zn concentrations have a nutrient-type distribution with deep concentrations that can be over two

orders of magnitude higher than surface concentrations (Bruland et al., 1978). Though surface depletion of Co due to phytoplankton uptake can occur (e.g., Martin and Fitzwater (1988)), Co does not behave as a classic nutrient-type element. Co is strongly scavenged from oxic water columns, and Co concentrations do not accumulate in the deep waters moving from the North Atlantic to the North Pacific (Martin and Fitzwater, 1988; Saito and Moffett, 2002). Thus, even where surface depletions of Co are observed, the surface concentration is generally the same order of magnitude as the deep concentration (e.g., Saito and Moffett (2002)), as opposed to the 2-3 orders of magnitude concentration difference that can be observed for Zn (e.g., Bruland et al. (1978)).

I have re-plotted the Zn-phosphate and Co-phosphate data with only data from the upper water column (0 - 200 m) where phytoplankton uptake is likely to occur. The relationship still seems to hold, though it is not as clear (Fig. 1-3). Further study is required to determine the relevance of in situ biochemical substitution. The effectiveness of biochemical substitution for alleviating Zn stress should be limited by the fact that Co and Cd concentrations are generally lower than those of Zn (e.g., Martin et al. 1989). Nevertheless, it is important to bear in mind that the Zn nutritional status of a phytoplankter may actually reflect its combined Zn-Co-Cd nutritional status.

The ecological importance of Zn in the ocean may be related to its influence on phytoplankton species composition rather than total primary production. As previously mentioned, the Zn requirements of species and their spatial distributions suggest that Zn may exert a selective influence (Brand et al., 1983). Concentrations of Zn may also influence enzyme activity. Zn is a cofactor in many enzyme systems, including that of alkaline phosphatase (Plocke et al., 1962). Alkaline phosphatase (AP) is an enzyme that is typically expressed under conditions of phosphorus stress. The expression of AP by natural phytoplankton populations in the Sargasso and Mediterranean Seas supports the idea that phosphorus (P) can be limiting in these areas (Zohary and Robarts, 1998; Ammerman et al., 2003; Vidal et al., 2003).

In the Sargasso Sea, surface concentrations of dissolved inorganic phosphorus (DIP) are extremely low (<1 - 10 nM, Wu et al. 2000; Cavender-Bares et al. 2001). The ratio of dissolved nitrogen (N) to P in the water column can reach more than twice the classical Redfield value of 16N:1P in this environment (dissolved inorganic N:P  $\approx$  40-50, Cavender-Bares et al. 2001). Field studies in the Sargasso Sea, using metrics of P physiology such as P uptake, AP activity, and P quotas, provide further evidence of P-limitation in this system (Cotner et al., 1997; Wu et al., 2000; Sanudo-Wilhelmy et al., 2001; Dyhrman et al., 2002; Ammerman et al., 2003). For example, with only a few exceptions, AP activities in the upper 100 m at

BATS were detectable year-round (Ammerman et al., 2003).

Studies of nutrient dynamics and phytoplankton production have primarily focused on inorganic nutrients as they are generally considered the most bioavailable forms. The composition of marine dissolved organic P (DOP) is largely uncharacterized and the ability of organisms to access P from this pool is not well resolved. The concentration of DOP generally accounts for over 80% of the total dissolved phosphorus (TDP) in Sargasso Sea surface waters and the DON:DOP exceeds the Redfield ratio all year. Most phosphorylated compounds cannot be transported across membranes, so the ability of microorganisms to use DOP is largely based on cell surface enzymes. Two enzymes important in the marine environment are AP and 5'-nucleotidase. Both enzymes cleave a phosphate monoester bond separating a bioavailable phosphate molecule from the larger DOP molecule. 5'-nucleotidase has a greater substrate specificity, acting only on nucleotides, whereas AP can hydrolyze a variety of substrates that contain phosphate monoester bonds (Ammerman and Azam, 1985, 1991). The enzyme 5'-nucleotidase seems to be associated primarily with bacteria (Ammerman and Azam, 1985, 1991), although the enzyme is present in some phytoplankton (Dyhrman and Palenik, 2003). Nevertheless, 5'-nucleotidase may provide a significant P-source for phytoplankton because uptake of 5'-nucleotidase cleaved P is only tightly coupled at low DIP concentrations (Ammerman and Azam, 1991).

AP is a metalloenzyme that typically has Zn as a co-factor. Zn concentrations correlate strongly with DIP and are also extremely low in the Sargasso Sea (Bruland and Franks, 1983). This suggests possible constraints on the utilization of phosphate monoesters if low Zn levels restrict the AP biosynthesis. A recent study indicates this may be the case. Low-density batch cultures of *Emiliania huxleyi* grown at low P conditions had lower AP activity when grown at low Zn than when grown at high Zn (Shaked et al., 2006). In an incubation in the Bering Sea, Shaked et al. (2006) observed increased AP activity in bottles amended with Zn over that in control and iron addition bottles. From their data, the authors predict that Zn-P co-limitation is not likely to be a widespread phenomenon, however they suggest it may occur in the Sargasso Sea. The importance of Co or Cd substitution was not considered.

This thesis addresses some of the questions brought up in the preceding paragraphs. In Chapter 2, a new method for measuring Zn speciation was tested and applied to a short profile in the North Atlantic. The literature contains few measurements of Zn speciation in the ocean. These measurements are an important tool for understanding Zn bioavailability. Zn speciation was also measured on a surface transect in the North Pacific and Bering Sea, where DIP concentrations were relatively high (Chapter 3). In this chapter, total Zn

concentrations were compared with previous studies and the major macronutrients P and silicate. This chapter highlights the spatial variability in the concentrations of Zn and Zn binding ligands. The potential for atmospheric inputs of Zn and for Zn to constrain primary production was also considered.

The possibility of Zn-P co-limitation in the low P, low metal environment of the Sargasso Sea was explored (Chapter 4). Zn, Co, DIP, and DOP concentrations and AP activities were measured in a transect from the northern seasonally well-mixed waters into the permanently stratified southern Sargasso Sea. Zn, Co, and DIP concentrations were compared to chlorophyll concentrations. Relationships of Zn and Co draw down were examined with respect to each other and with respect to phosphate concentrations. AP activities were considered both as raw rates of phosphomonoester cleavage and as chlorophyll normalized rates. This has a marked effect on the distributional patterns of activity. The effect of Zn and Co on AP activity was examined via bottle incubations and in batch cultures of a model coccolithophore.

The majority of the total dissolved P pool in the surface waters of the Sargasso Sea occurs as dissolved organic phosphorus (DOP).  $^{31}\text{P}$  nuclear magnetic resonance (NMR) spectroscopy of ultrafiltered DOP suggests that DOP occurs mainly as phosphate esters (75%) and phosphonates (25%). The bioavailability of phosphate monoesters and phosphonates to natural populations was examined in Sargasso Sea (Chapter 5). Bottle incubations were performed with additions of inorganic phosphate, glycerophosphate (monoester), and phosphonoacetic acid (phosphonate). The change in chlorophyll was monitored in both time course and endpoint incubations along with the abundance of the *Synechococcus* and picoeukaryote populations.

Marine primary production is a significant sink for atmospheric carbon dioxide ( $\text{CO}_2$ ). Understanding the controls on that sink is vital as levels of atmospheric  $\text{CO}_2$  continue to rise. This work contributes to the understanding of how the nutrients P, Zn, and Co may influence primary production.



## Bibliography

- AMMERMAN, J. W., and F. AZAM. 1985. Bacterial 5'-nucleotidase in aquatic ecosystems: A novel mechanism of phosphorus regeneration. *Science*. **227**: 1338–1340.
- AMMERMAN, J. W., and F. AZAM. 1991. Bacterial 5'-nucleotidase activity in estuarine and coastal marine waters: Characterization of enzyme activity. *Limnology and Oceanography*. **36**: 1427–1436.
- AMMERMAN, J. W., R. R. HOOD, D. A. CASE, and J. B. COTNER. 2003. Phosphorus deficiency in the Atlantic: An emerging paradigm in oceanography. *EOS*. **84**: 165,170.
- ANDERSON, M. A., F. M. M. MOREL, and R. R. L. GUILLARD. 1978. Growth limitation of a coastal diatom by low zinc ion activity. *Nature*. **276**: 70–71.
- BOYD, P. W., A. J. WATSON, C. S. LAW, E. R. ABRAHAM, T. TRULL, R. MURDOCH, D. C. E. BAKKER, A. R. BOWIE, K. O. BUESSELER, H. CHANG, M. CHARETTE, P. CROOT, K. DOWNING, R. FREW, M. GALL, M. HADFIELD, J. HALL, M. HARVEY, G. JAMESON, J. LAROCHE, M. LIDDI-COAT, R. LING, M. T. MALDONADO, R. M. MCKAY, S. NODDER, S. PICKMERE, R. PRIDMORE, S. RINTOUL, K. SAFI, P. SUTTON, R. STRZEPEK, K. TANNEBERGER, S. TURNER, A. WAITE, and J. ZELDIS. 2000. A mesoscale phytoplankton bloom in the polar Southern Ocean stimulated by iron fertilization. *Nature*. **407**: 695–702.
- BOYLE, E. A., and J. M. EDMOND. 1975. Copper in surface waters south of New Zealand. *Nature*. **253**: 107–109.
- BRAND, L. E., W. G. SUNDA, and R. R. L. GUILLARD. 1983. Limitation of marine phytoplankton reproductive rates by Zn, Mn, and Fe. *Limnology and Oceanography*. **28**: 1182–1198.
- BRULAND, K. W. 1989. Complexation of zinc by natural organic ligands in the central North Pacific. *Limnology and Oceanography*. **34**: 269–285.
- BRULAND, K. W., and R. P. FRANKS. 1983. Mn, Ni, Cu, Zn and Cd in the western North Atlantic. *In* Trace metals in seawater. NATO Conf. Ser. 4 Vol. 9. Plenum. pp. 395–414.
- BRULAND, K. W., G. A. KNAUER, and J. H. MARTIN. 1978. Zinc in north-east Pacific water. *Nature*. **271**: 741–743.
- CAVENDER-BARES, K. K., D. M. KARL, and S. W. CHISHOLM. 2001. Nutrient gradients in the western North Atlantic Ocean: Relationship to microbial community structure and comparison to patterns in the Pacific Ocean. *Deep-Sea Research I*. **48**: 2373–2395.
- COALE, K. H. 1991. Effects of iron, manganese, copper, and zinc enrichments on productivity and biomass in the subarctic Pacific. *Limnology and Oceanography*. **36**: 1851–1864.
- COALE, K. H., K. S. JOHNSON, S. E. FITZWATER, R. M. GORDON, S. TANNER, F. P. CHAVEZ, L. FER-IOLI, C. SAKAMOTO, P. ROGERS, F. MILLERO, P. STEINBERG, P. NIGHTINGALE, D. COOPER, W. P. COCHLAN, M. R. LANDRY, J. CONSTANTINOU, G. ROLLWAGEN, A. TRASVINA, and R. KUDELA. 1996. A massive phytoplankton bloom induced by an ecosystem-scale iron fertilization experiment in the equatorial Pacific Ocean. *Nature*. **383**: 495–501.

- COTNER, J. B., J. W. AMMERMAN, E. R. PEELE, and E. BENTZEN. 1997. Phosphorus-limited bacterio-plankton growth in the Sargasso Sea. *Aquatic Microbial Ecology*. **13**: 141–149.
- DYHRMAN, S. T., and B. PALENIK. 2003. Characterization of ectoenzyme activity and phosphate-regulated proteins in the coccolithophorid *Emiliana huxleyi*. *Journal of Plankton Research*. **25**: 1215–1225.
- DYHRMAN, S. T., E. A. WEBB, D. M. ANDERSON, J. W. MOFFETT, and J. B. WATERBURY. 2002. Cell-specific detection of phosphorus stress in *Trichodesmium* from the Western North Atlantic. *Limnology and Oceanography*. **47**: 1832–1836.
- GORDON, R. M., J. H. MARTIN, and G. A. KNAUER. 1982. Iron in north-east Pacific waters. *Nature*. **299**: 611–612.
- GRAN, H. H. 1931. On the conditions for the production of plankton in the sea. *Rapp. Proc. Verb. Reun. Cons. Int. Explor. Mer.* **75**: 37–46.
- LEE, J. G., S. B. ROBERTS, and F. M. M. MOREL. 1995. Cadmium: a nutrient for the marine diatom *Thalassiosira weissflogii*. *Limnology and Oceanography*. **40**: 1056–1063.
- MARET, W. 2002. Optical methods for measuring zinc binding and release, zinc coordination environments in zinc finger proteins, and redox sensitivity and activity of zinc-bound thiols. *Meth. Enzymol.* **348**: 230–237.
- MARTIN, J. H., and S. E. FITZWATER. 1988. Iron deficiency limits phytoplankton growth in the north-east Pacific subarctic. *Nature*. **331**: 341–343.
- MARTIN, J. H., R. M. GORDON, S. FITZWATER, and W. W. BROENKOW. 1989. VERTEX: phytoplankton/iron studies in the gulf of alaska. *Deep-Sea Research*. **36**: 649–680.
- MOREL, F. M. M., R. J. M. HUDSON, and N. M. PRICE. 1991. Limitation of productivity by trace-metals in the sea. *Limnology and Oceanography*. **36**: 1742–1755.
- PLOCKE, D. J., C. LEVINHAL, and B. L. VALLEE. 1962. Alkaline phosphatase of *Escherichia coli*: a zinc metalloenzyme. *Biochemistry*. **1**: 373.
- RYTHER, J. H., and W. M. DUNSTAN. 1971. Nitrogen, phosphorus, and eutrophication in the coastal marine environment. *Science*. **171**: 1008–1013.
- SAITO, M. A., and J. W. MOFFETT. 2002. Temporal and spatial variability of cobalt in the Atlantic Ocean. *Geochimica et Cosmochimica Acta*. **66**: 1943–1953.
- SANUDO-WILHELMY, S. A., A. B. KUSTKA, C. J. GOBLER, D. A. HUTCHINS, M. YANG, K. LWIZA, J. BURNS, D. G. CAPONE, J. A. RAVEN, and E. J. CARPENTER. 2001. Phosphorus limitation of nitrogen fixation by *Trichodesmium* in the central Atlantic Ocean. *Nature*. **411**: 66–69.
- SHAKED, Y., Y. XU, K. LEBLANC, and F. M. M. MOREL. 2006. Zinc availability and alkaline phosphatase activity in *Emiliana huxleyi*: implications for Zn-P co-limitation in the ocean. *Limnology and Oceanography*. **51**: 299–309.
- SUNDA, W. G. 1989. Trace metal interactions with marine phytoplankton. *Biological Oceanography*. **6**: 411–442.

- SUNDA, W. G., and S. A. HUNTSMAN. 1992. Feedback interactions between zinc and phytoplankton in seawater. *Limnology and Oceanography*. **37**: 25–40.
- SUNDA, W. G., and S. A. HUNTSMAN. 1995. Cobalt and zinc interreplacement in marine phytoplankton: Biological and geochemical implications. *Limnology and Oceanography*. **40**: 1404–1417.
- VIDAL, M., C. M. DUARTE, S. AGUSTI, J. M. GASOL, and D. VAQUE. 2003. Alkaline phosphatase activities in the central Atlantic Ocean indicate large areas with phosphorus deficiency. *Marine Ecology Progress Series*. **262**: 43–53.
- WU, J., W. SUNDA, E. A. BOYLE, and D. M. KARL. 2000. Phosphate depletion in the western North Atlantic Ocean. *Science*. **289**: 759–762.
- YEE, D., and F. M. M. MOREL. 1996. In vivo substitution of zinc by cobalt in carbonic anhydrase of a marine diatom. *Limnology and Oceanography*. **41**: 573–577.
- ZOHARY, T., and R. D. ROBERTS. 1998. Experimental study of microbial P limitation in the eastern Mediterranean. *Limnology and Oceanography*. **43**: 387–395.

Figure 1-1: Diagram of free ion uptake model. Complexation with both inorganic and organic complexes determines the free metal ion ( $M^{n+}$ ) concentration of a metal M. M is bound by a cell surface molecule to be transported into the cell. At equilibrium, the uptake rate will be proportional to the concentration of  $M^{n+}$ . However, the rapid dissociation kinetics and relatively high concentrations of some metal inorganic species (e.g., Fe) result in a disequilibrium that permits the direct exchange of M inorganic species with the transport protein. MX symbolizes the pool of internal metal ligands and ME represents the enzyme-bound metal pool. Figure taken from Sunda (1989).

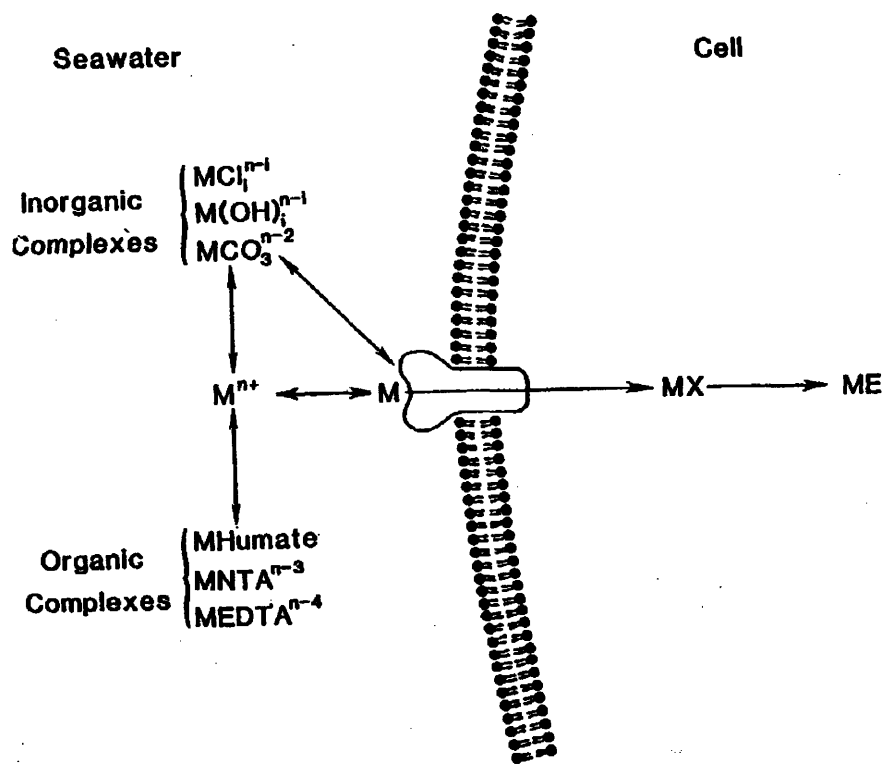


Figure 1-2: The relationship between Zn and phosphate (A) and Co and phosphate (B) in the North Pacific. Data taken from Martin et al. (1989). Plotted after Sunda and Huntsman (1995). Symbols indicate different sampling locations: circles are St. T-5 (39.60°N, 140.77°W); diamonds are St. T-6 (45.00°N, 142.87°W); squares are St. T-8 (55.5°N, 147.5°W).

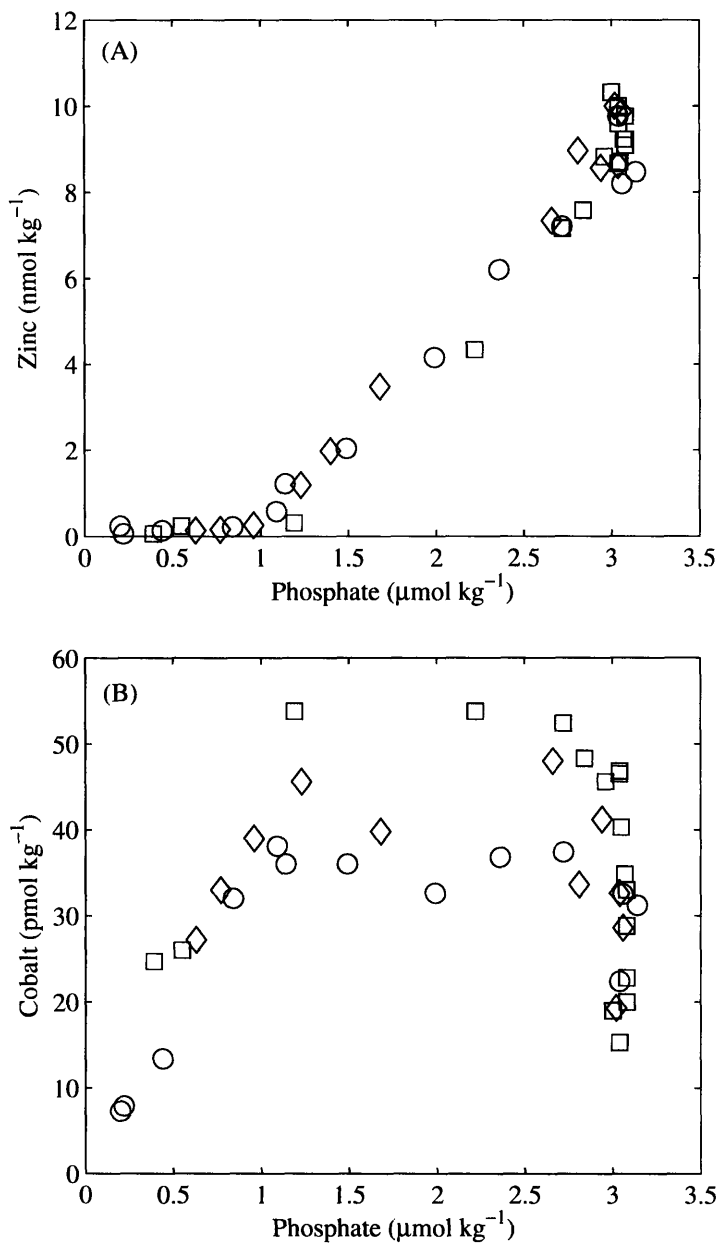
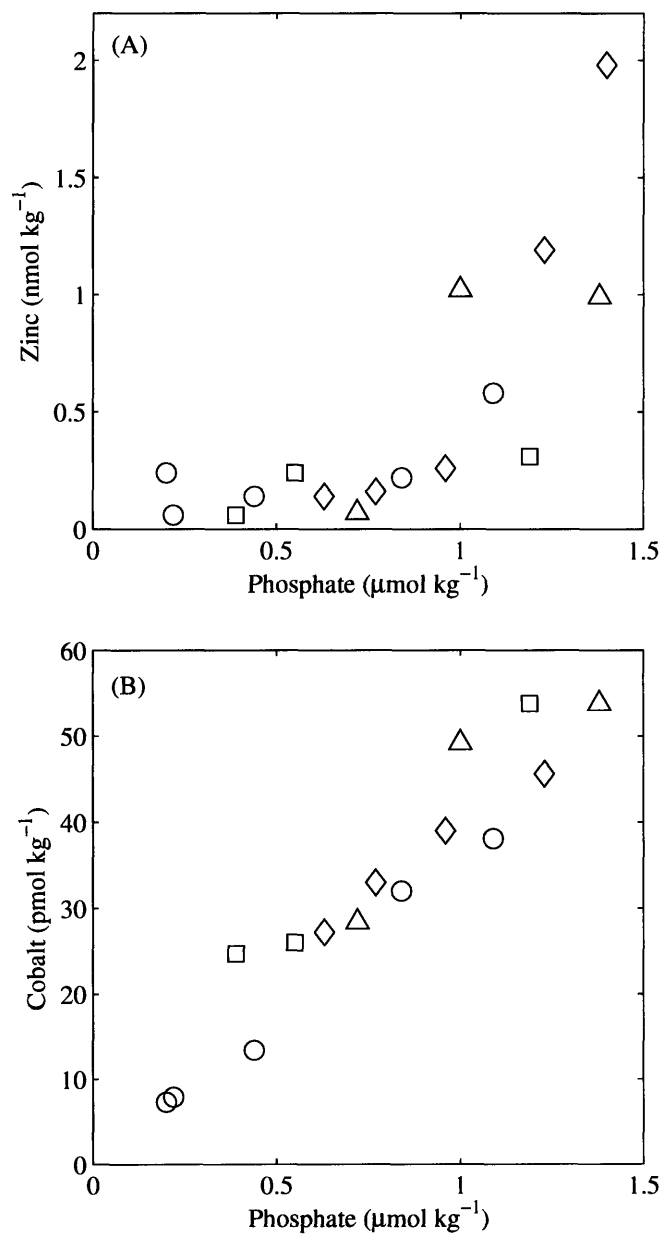


Figure 1-3: The relationship between Zn and phosphate (A) and Co and phosphate (B) in the upper water column of the North Pacific. Plot consists of same data as Fig. 1-2, however data from depths deeper than 200 m or where the Zn concentration was greater than  $4 \text{ nmol kg}^{-1}$  have been deleted. Symbols indicate different sampling locations: circles are St. T-5 ( $39.60^\circ\text{N}$ ,  $140.77^\circ\text{W}$ ); diamonds are St. T-6 ( $45.00^\circ\text{N}$ ,  $142.87^\circ\text{W}$ ); triangles are St. T-7 ( $50.0^\circ\text{N}$ ,  $145.0^\circ\text{W}$ ); squares are St. T-8 ( $55.5^\circ\text{N}$ ,  $147.5^\circ\text{W}$ ).



## **Chapter 2**

# **A new anodic stripping method for the determination of zinc speciation**

## 2.1 Abstract

Zinc concentrations in the open ocean can be extremely low and have the potential to influence the growth and species composition of marine phytoplankton assemblages. The majority of the dissolved zinc pool is complexed to natural organic ligands. This complexation results in an even lower free zinc ion concentration, which is considered the bioavailable form of zinc for phytoplankton. Therefore, measurements of the free zinc ion concentration in the environment are important to understanding the zinc status of natural phytoplankton communities. In this study, an anodic stripping voltammetry method previously developed for the total determination of cadmium and lead was successfully adapted to the measurement of zinc speciation. The method differs from previous zinc speciation anodic stripping voltammetry (ASV) methods in that a fresh mercury film is plated with each sample aliquot. The fresh film ASV (ff-ASV) method was compared to a classic method of zinc speciation analysis using competitive ligand exchange cathodic stripping voltammetry (CSV) in a profile from the North Atlantic Ocean. The ff-ASV method compared favorably with the CSV method though ligand concentrations determined by ff-ASV were generally slightly higher than those determined by CSV. There did not seem to be a systematic difference between methods for the estimates of conditional stability constants. The ligand concentration in the North Atlantic profile was between 0.9 - 1.5 nM as determined by ff-ASV and 0.6 - 1.3 nM as determined by CSV. The conditional stability constants determined by ff-ASV were  $10^{9.8-10.5}$  and by CSV were  $10^{9.8-11.3}$ .



## 2.2 Introduction

Zinc (Zn) is an essential micronutrient used in enzyme systems involved with carbon and phosphorus acquisition. Low Zn bioavailability can limit the growth of phytoplankton cultures (Anderson et al., 1978; Brand et al., 1983; Sunda and Huntsman, 1995). Zn bioavailability or toxicity is controlled by the free Zn ion ( $Zn^{2+}$ ) concentration as opposed to the total concentration of Zn or the concentration of Zn-synthetic ligand complexes (Anderson et al., 1978).

Complexation with natural organic ligands dominates the chemical speciation of Zn in the ocean; greater than 95% of total Zn is organically complexed (Bruland, 1989; Ellwood and van den Berg, 2000; Ellwood, 2004). Thus, the  $Zn^{2+}$  concentration in the open ocean can be extremely low (Bruland, 1989; Donat and Bruland, 1990; Ellwood and van den Berg, 2000; Ellwood, 2004). The source and chemical nature of the Zn binding ligands is unknown. However, there is evidence for biological production of ligands by phytoplankton. Cultures of the diatoms *Skeletonema costatum* and *Thalassiosira weissflogii* and the coccolithophore *Emiliana huxleyi* produced organic exudates with Zn binding capability (Imber and Robinson, 1983; Imber et al., 1985; Vasconcelos et al., 2002). Muller et al. (2003) observed an increase in Zn binding ligands in a mesocosm experiment that was coincident with an increase in dead *E. huxleyi* cells, which suggests ligand release may be passive. At this point, it is also not clear whether the release of Zn binding ligands is a mechanism to prevent toxicity, to aid uptake, or both.

Zn speciation was measured in two recent shipboard incubation experiments (Ellwood, 2004; Lohan et al., 2005). In both cases, high growth occurred in the iron (Fe) addition treatments despite low total Zn concentrations and extremely low  $Zn^{2+}$  concentrations. The  $Zn^{2+}$  concentrations in the +Fe treatments at the end of both experiments was lower than that which limits oceanic phytoplankton in culture, yet Zn limitation was not apparent (Ellwood, 2004; Lohan et al., 2005). This suggests that either the Zn requirements of phytoplankton are much lower than those of the cultured strains, that substitution by cobalt or cadmium successfully supplements the Zn demand in the field, or that the phytoplankton are able to utilize the organically bound Zn. In the open ocean, substitution by cobalt and cadmium should be limited by the fact that the concentrations of these metals are also low (e.g., Ellwood 2004).

The free ion model of Zn bioavailability is based on culture studies where the synthetic ligand ethylenediaminetetraacetic acid (EDTA) was added (e.g., Anderson et al. 1978; Sunda and Huntsman 1995). The

inability of phytoplankton to utilize Zn-EDTA does not necessarily preclude them from using all organically bound Zn. Phytoplankton may produce Zn-binding ligands that require specific uptake sites, akin to the chemical warfare scenario proposed for Fe siderophores. Fe's bioavailability has also been described in culture by the free ion model, however exceptions to the free ion model have been found. For example, Hutchins et al. (1999) observed uptake of organically bound Fe by natural phytoplankton populations in the North Atlantic. This experiment also showed taxonomic differences in that prokaryotes were able to assimilate Fe bound by enterobactin but not by protoporphyrin, and eukaryotes were able to assimilate both compounds (Hutchins et al., 1999). Further study of the uptake of organically bound Zn and Zn speciation are required to resolve our understanding of Zn bioavailability.

The two classic methods of Zn speciation determination are competitive ligand exchange cathodic stripping voltammetry (CLE-CSV, van den Berg 1985) and anodic stripping voltammetry (ASV, Bruland 1989). CLE-CSV is an indirect method where a synthetic Zn-binding ligand is added to compete with the naturally occurring ligands and the concentration of the Zn-synthetic ligand complex is detected. The method of ASV gives a direct measure of the inorganic Zn species in a sample.

Application of the two methods to oligotrophic seawater by different researchers has resulted in relatively uniform results (Table 2.1). The concentration of Zn binding ligands is generally 1 - 2.5 nM and the conditional stability constants of the ligands are  $\sim 10^{10}$  -  $10^{11}$ . A direct intercomparison of the two methods was performed on two seawater samples from the North Pacific (Donat and Bruland, 1990). This experiment found that the concentration of ligands measured by the two methods were in good agreement (1.60 and 2.14 nM for CSV; 1.76 and 2.22 nM for ASV). However, the conditional binding strengths predicted by ASV ( $10^{11.2}$ ) were a log unit higher than those predicted by CSV ( $10^{10.3}$ ). Another study compared the ASV and CSV methods on a single sample from the Southern Ocean (Ellwood, 2004). The average ligand concentrations determined by ASV (1.2 nM) and CSV (1.3 nM) were similar (Ellwood, 2004). A log unit difference in conditional stability constants was not observed (ASV =  $10^{10.2}$ , CSV =  $10^{10.6}$ , Ellwood 2004).

In this study, a new method for Zn speciation was evaluated and used to measure Zn speciation over a profile of the upper water column in the North Atlantic.

## 2.3 Methods

### 2.3.1 Sample collection

Samples were collected aboard the R/V Oceanus in April 2004. Water samples were collected using 10 L teflon-coated Go-Flos (General Oceanics) on a kevlar hydrowire. Samples were pumped using filtered ultra-high purity nitrogen gas directly from the Go-Flo bottles by teflon tubing through acid-cleaned 0.4  $\mu\text{m}$  polycarbonate filter sandwiches into rigorously acid-cleaned low density polyethylene (LDPE) or teflon bottles. Samples for total Zn measurement (LDPE bottles) were acidified to approximately pH 2 by the addition of 2 ml HCl (Seastar) per liter of seawater. Speciation samples (teflon bottles) were stored frozen for 9 months and thawed in a refrigerator several days before analysis.

### 2.3.2 Total dissolved Zn analysis

Total dissolved zinc concentrations were measured using isotope dilution inductively coupled plasma mass spectrometry (ICP-MS) after Wu and Boyle (1998) and Saito and Schneider (2006). Briefly, 15 ml centrifuge tubes (Globe Scientific) were filled to approximately 13.5 mls (exact volume determined gravimetrically). Samples were then spiked with  $^{66}\text{Zn}$  (98.9% as  $^{66}\text{Zn}$ , Cambridge Isotope Laboratories, Inc.), which was allowed to equilibrate overnight. The following day, 125  $\mu\text{l}$  of ammonia (Seastar) was added to each tube. After 90 sec, the tube was inverted and after an additional 90 sec, tubes were centrifuged for 3 min at 3000xg (3861 rpm) using a swinging bucket centrifuge (Eppendorf 5810R). The majority of the supernatant was carefully decanted. The tubes were then respun for 3 min and the remaining supernatant was shaken out. Pellets were dissolved on the day of ICP-MS analysis using 0.5 - 1.5 ml of 5% nitric acid (Seastar). ICP-MS measurements of sample were made using a Finnigan ELEMENT2 in medium resolution, which was sufficient to resolve  $^{64}\text{Zn}$  from the potential interference peak due to Mg-Ar. To measure the procedural blank, one ml of surface seawater was treated the same as samples, and calculations were performed as though it was a 13.5 ml sample.

### 2.3.3 ASV Theory

The theory of using ASV to determine the concentration and conditional stability constants of Zn binding ligands has been described in detail by Bruland (1989) and Donat and Bruland (1990). Briefly, the ASV method is based on the principle that Zn bound in strong organic complexes is inert with respect to ASV because dissociation will not occur within the diffusion layer of the rotating disc electrode (RDE, dissociation rate constants  $<0.1 \text{ sec}^{-1}$ , Bruland 1989). ASV will detect inorganic Zn species:  $\text{Zn}^{2+}$  and those complexes which dissociate rapidly in the electrode diffusion layer producing  $\text{Zn}^{2+}$  such as  $\text{ZnCl}^+$ . Within the electrode diffusion layer  $\text{Zn}^{2+}$  can be reduced to  $\text{Zn}^0$  at which point it will form an amalgam with the mercury (Hg) film. The Zn deposited in the film is measured as an oxidation current peak as the voltage is stripped in the positive direction.

A titration curve is generated by adding increasing concentrations of Zn to a natural sample. Initially, the added Zn is all bound by any Zn binding ligands in the sample, thus no increase in inorganic Zn species ( $\text{Zn}'$ ) is detected at the Hg film. Once the binding capacity is saturated, there will be a linear response between the Zn oxidation peak current and the concentration of  $\text{Zn}'$ . From the Zn titration curve, the concentration of naturally occurring binding ligands ( $L_T$ ) and their conditional stability constant with respect to  $\text{Zn}'$  ( $K'_{\text{cond},\text{Zn}'}$ ) can be calculated. The peak oxidation current ( $i_p$ ) of  $\text{Zn}'$  deposited at the RDE can be described by the equation

$$[\text{Zn}'] = i_p/S \quad (2.1)$$

where S is the sensitivity once the Zn binding ligands have been saturated. Then, the concentration of Zn bound to the natural organic ligands (ZnL) can be calculated as

$$[\text{ZnL}] = [\text{Zn}]_T - [\text{Zn}'] \quad (2.2)$$

where  $[\text{Zn}]_T$  is the total concentration of Zn (i.e., Zn in sample plus added Zn). In the situation where a single ligand binds a single metal, the  $K'_{\text{cond},\text{Zn}'}$  and  $L_T$  are related to  $\text{Zn}'$  and ZnL as follows

$$\frac{[\text{Zn}']}{[\text{ZnL}]} = \frac{[\text{Zn}']}{[L]_T} + \frac{1}{(K'_{\text{cond},\text{Zn}'} * [L]_T)} \quad (2.3)$$

Thus, assuming the data fits the one metal, one ligand model, if plotted as  $[Zn']/[ZnL]$  versus  $[Zn']$ ,  $[L]_T$  can be calculated as  $1/\text{slope}$  and  $K'_{cond,Zn'}$  as  $1/([L]_T * \text{y-intercept})$  (Ruzic, 1982; van den Berg, 1982). An example of a typical ASV titration is presented in Fig. 2-1.

In the classic ASV method applied to Zn speciation (Bruland, 1989), a Hg film is deposited on the RDE at the beginning of the day and used for multiple sample aliquots and then physically removed at the end of the day. Problems can be encountered with this method due to surfactant interference and low sensitivity (Fischer and van den Berg, 1999). To circumvent these problems, Fischer and van den Berg (1999) developed an ASV method where Hg was added to each sample aliquot and a fresh Hg film was plated for each sample aliquot and then electrochemically removed. This has the advantage of producing a thinner mercury film in which Zn is plated simultaneously with Hg, resulting in higher relative Zn concentrations than with a pre-plated film. Thus, the method yields high sensitivity even at relatively short deposition times (3 min). Ammonium thiocyanate is added along with Hg. This ensures good reproducibility of Hg films with each sample aliquot and also allows for complete electrochemical removal of the Hg film (Fischer and van den Berg, 1999). The effect of the thiocyanate is as a result of the formation of Hg(II)-thiocyanate complexes which prevent mercuric oxide formation at the surface of the RDE. The Fischer and van den Berg (1999) method was developed for total determination of lead and cadmium. Here, it has been adapted as a method for Zn speciation analysis.

#### **2.3.4 ff-ASV Speciation Titrations**

Measurements were made using a 663 VA stand (Metrohm) consisting of a glassy carbon RDE, a glassy carbon rod counter electrode, and a double junction Ag, AgCl, saturated KCl reference electrode. The electrode was interfaced to a PC (IBM) using an IME663 and  $\mu$ autolab I (Eco Chemie). A teflon cell cup was used. Before each day of speciation analysis, the glassy carbon RDE was manually polished with aluminum oxide. Then, a cyclic voltammetry step was performed cycling the voltage between -0.8 V and 0.8 V 50 times. Reagents used included 4-(2-Hydroxyethyl)-1-piperazinepropanesulfonic acid (EPPS), ammonium thiocyanate, and mercuric chloride. The pH of the EPPS buffer was adjusted to 8.1 with the addition of clean ammonia (Seastar). EPPS and thiocyanate reagents were run through a pre-cleaned chelex column to remove trace metal contamination (Price and Morel, 1990).

Titration were set up in 15 ml teflon vials (Savillex). In order to prevent wall loss, vials were equilibrated with specific concentrations of Zn before use, and each vial was always used for the same concentration of Zn. Before a titration, the vials were rinsed with 12 ml of sample. Then, 12 ml sample was added into each vial along with 1.7 mM EPPS. For each sample aliquot, the appropriate concentration of Zn was allowed to equilibrate with the sample in the sample vial for 10 min. Then, the sample aliquot was poured into the voltammetric cell and 4.2 mM ammonium thiocyanate and 10.4  $\mu$ M mercuric chloride were added. Each sample aliquot was purged with filtered ultra-high purity nitrogen gas for 5 min to remove oxygen. The voltammetric scan conditions are listed in Table 2.2. The voltammetric cell cup was not rinsed between samples. Zn<sup>0</sup> was evident as a current peak at -1.1 V. Peak height was measured using the GPES software (Eco Chemie). As an example, scans of a seawater sample with additions of 10 and 20 nM are shown (Fig. 2-2).

### 2.3.5 CSV Theory

CLE-CSV was performed after van den Berg (1982) and Donat and Bruland (1990). The CSV method is based on principles similar to that of ASV. In the method of CLE-CSV, a competitive equilibrium is set up between the natural Zn binding ligands in a sample and the added synthetic chelator ammonium pyrrolidinedithiocarbamate (APDC). The ZnPDC complex is electroactive and adsorbs onto the hanging Hg drop (HMD). When the electrode potential is stripped to more negative values, the reduction of Zn<sup>2+</sup> in the adsorbed ZnPDC complexes produces a current peak at -1.1 V. Again, a titration curve is produced by adding increasing concentrations of Zn. The total Zn concentration of sample can now be described as

$$[Zn_T] = [Zn'] + [ZnL] + [ZnPDC]. \quad (2.4)$$

Assuming that the naturally occurring ligands have a greater affinity for Zn than PDC, low concentrations of added Zn will be bound by the natural ligands and no increase in current will be observed. A typical CLE-CSV titration curve is presented with the data from the 21 m sample (Fig. 2-3A). Once the natural ligands are saturated with Zn, all added Zn will be bound by PDC and the increase in peak current will be

proportional to the concentration of Zn added. The reduction peak current is related to  $[Zn^{2+}]$  as follows

$$[Zn^{2+}] = i_p/S * \alpha' \quad (2.5)$$

where

$$\alpha' = \alpha_{Zn} + \alpha_{ZnPDC} \quad (2.6)$$

where  $\alpha_{Zn}$  is the inorganic side reaction coefficient for Zn (a value of 2.2 was used, Turner et al. 1981) and  $\alpha_{ZnPDC}$  is the side reaction coefficient for Zn with PDC.  $\alpha_{ZnPDC}$  can be calculated as

$$\alpha_{ZnPDC} = K'_{ZnPDC} * [PDC-]. \quad (2.7)$$

[PDC-] was approximated as  $[APDC]_T$  since  $[APDC]_T \gg [ZnPDC]$ .  $K'_{ZnPDC}$  has been determined to be  $10^{4.4}$  by van den Berg (1985) and Donat and Bruland (1990).  $[ZnL]$  is now calculated as:

$$[ZnL] = [Zn]_T - (i_p/S). \quad (2.8)$$

Combining equations 2.5 and 2.8,  $[Zn^{2+}]/[ZnL]$  can be directly calculated as

$$\frac{[Zn^{2+}]}{[ZnL]} = \frac{i_p}{\alpha' * ((S * [Zn]_T) - i_p)}. \quad (2.9)$$

In analogy to ASV, the titration data can now be plotted as  $[Zn^{2+}]/[ZnL]$  versus  $[Zn^{2+}]$  (e.g., Fig. 2-3B). When the data fits a one metal, one ligand model, a straight line is produced that can be described by an equation analogous to equation 2.3 (Ruzic, 1982; van den Berg, 1982):

$$\frac{[Zn^{2+}]}{[ZnL]} = \frac{[Zn^{2+}]}{[L]_T} + \frac{1}{(K'_{cond,Zn^{2+}} * [L]_T)}. \quad (2.10)$$

Hence,  $[L]_T$  can be calculated as 1/slope and  $K'_{cond,Zn^{2+}}$  as  $1/([L]_T * \text{y-intercept})$ .  $K'_{cond,Zn^{2+}}$  can be related to  $K'_{cond,Zn'}$  by the equation

$$K'_{cond,Zn^{2+}} = K'_{cond,Zn'} * \alpha_{Zn}. \quad (2.11)$$

### 2.3.6 CSV Speciation Titrations

The voltammetric system used was a 663 VA stand (Metrohm) consisting of a Hg mercury drop working electrode (HMDE), a glassy carbon rod counter electrode, and a double junction Ag, AgCl, saturated KCl reference electrode. A teflon cell cup was used. The electrode was interfaced to a PC (IBM) using an IME663 and  $\mu$ autolab I (Eco Chemie).

Reagents used were EPPS (Aldrich) and APDC (Fluka). The pH of the EPPS buffer was adjusted to 8.1 as above. Zn contamination was removed by passing the EPPS buffer through a pre-cleaned chelex column (Price and Morel, 1990). The APDC solution was prepared in 1% ammonia (Seastar) and washed twice with ~10 ml aliquots of chloroform to remove metal impurities. The APDC solution was made fresh every several days and was stored at 4°C.

Teflon sample vials were equilibrated with specific Zn concentrations as above. Before a titration, the vials were rinsed with 12 ml of sample. Then, 12 ml of sample was measured into each vial and 2.4 mM EPPS and the appropriate concentrations of Zn added. After 1 hour, 24.25  $\mu$ M APDC was added to each vial. The APDC was allowed to equilibrate with the Zn and natural ligands for a minimum of 11 hours.

Starting with the 0 nM Zn addition vial, and working in order of increasing Zn concentration, the sample aliquots were poured into the voltammetric cell and de-aerated for 200 sec with filtered ultra high purity nitrogen gas. Voltammetric scan conditions are listed in Table 2.2. The cell cup was not rinsed between sample aliquots. -0.6 V was used rather than the -0.3 V used by Donat and Bruland (1990). At deposition potentials of -0.3 V or -0.4 V no increase in peak height occurred with Zn addition. Peak height was measured using the GPES software (Eco Chemie).

## 2.4 Results

### 2.4.1 ff-ASV Method Analysis

ff-ASV titrations were performed on UV-irradiated and dilute (10%) seawater. UV-irradiation destroys carbon-carbon bonds, thereby releasing Zn from any organic complexes. In dilute seawater, the ligand concentration is diluted to ~0.1 nM. Thus, in both cases, no significant concentration of Zn binding ligands is expected to be present. The titration of these samples with Zn produced a straight line with no evidence



of curvature (Fig. 2-4). This indicates that when no Zn binding ligands are present, a ff-ASV titration results in a straight line with Zn' increasing immediately when Zn is added. Loss of Zn to the walls of the teflon cell cup can be a significant problem that is important to avoid. For example, the Zn peak current was reduced by a factor of 5 when a sample was left for 2 hr (data not shown). The routine practice of equilibrating sample aliquot vials with a specific Zn concentration was employed to prevent wall loss. The above titrations confirm that wall loss is not significant on the timescales of the titration.

The accuracy of the ff-ASV method was examined by performing a titration on a 0.1 M KCl solution that had 4 nM EDTA added. EDTA reacts with  $\text{Ca}^{2+}$  and  $\text{Mg}^{2+}$ , and the high concentration of these ions in seawater reduces the ability of EDTA to bind Zn. In the 0.1 M KCl solution, the  $K'_{\text{cond,Zn}^{2+}}$  of EDTA is  $10^{13.8}$ , whereas it is only  $10^{7.6}$  in seawater (Bruland, 1989). The ff-ASV titration of the KCl + EDTA solution produced a titration curve where low concentration additions of Zn did not produce significant increases in the Zn peak height (Fig. 2-5). The calculated concentration of Zn binding ligands was 4.3 nM which is in good agreement with the concentration of EDTA added (4.0 nM). The  $K'_{\text{cond,Zn}^{2+}}$  calculated from the titration data was  $10^{11.0}$ . Bruland (1989) performed an analogous ASV titration where 10 nM EDTA was added to a 0.1 M KCl solution. The calculated  $K'_{\text{cond,Zn}^{2+}}$  in that study was also  $10^{11.0}$ . This emphasizes that  $K'_{\text{cond,Zn}^{2+}}$  must be considered a lower limit estimation of the actual  $K'_{\text{cond,Zn}^{2+}}$ .

The values of  $L_T$  and  $K'_{\text{cond,Zn}^{2+}}$  are dependent on each other since  $K'_{\text{cond,Zn}^{2+}}$  is calculated using  $L_T$ . For a set concentration of  $L_T$ , there is a specific range of  $K'_{\text{cond,Zn}^{2+}}$  values which can be measured using the ASV technique. For example, the concentration of Zn' can be calculated for a theoretical solution containing 4 nM ligand with  $K'_{\text{cond,Zn}^{2+}}$  values ranging from  $10^7$  -  $10^{13}$  (Fig. 2-6). This simulated data shows that for a  $L_T$  of 4 nM, the titration curves of a ligand with  $K'_{\text{cond,Zn}^{2+}}$  values of  $10^{11}$ ,  $10^{12}$ , and  $10^{13}$  are virtually indistinguishable. The detection window of the method is thus between  $10^7$  and  $10^{11}$ . For ligands with  $K'_{\text{cond,Zn}^{2+}}$  values greater than  $10^{11}$ , only the ligand concentration and a lower limit of the  $K'_{\text{cond,Zn}^{2+}}$  value can be determined. In the case of EDTA, the true conditional stability constant of  $10^{13.8}$  is outside our detection window and the calculated  $K'_{\text{cond,Zn}^{2+}}$  of  $10^{11}$  represents the lower limit of the actual value.

## 2.4.2 ff-ASV & CSV Sample Titrations

ff-ASV and CSV titrations were performed on samples from a 4 depth profile of the upper water column in the North Atlantic. Using the ff-ASV method, the concentration of  $L_T$  was between 0.9 and 1.5 nM with an average concentration of 1.2 nM (Fig. 2-7A). The concentration of  $L_T$  determined by CSV was between 0.6 and 1.3 nM with an average concentration of 1.0 nM (Fig. 2-7A). In 3 out of 4 samples analyzed, the  $[L_T]$  value determined by ff-ASV was higher than the value determined by CSV. The average difference in the concentration of  $L_T$  calculated by the two methods is 0.3 nM.

The  $K'_{cond,Zn^{2+}}$  of the natural ligands were  $10^{9.8} - 10^{10.5}$  when calculated from the ff-ASV titrations (Fig. 2-7B). The CSV titrations resulted in  $K'_{cond,Zn^{2+}}$  values that were between  $10^{9.8} - 10^{11.3}$  (Fig. 2-7B). In half of the samples, a higher  $K'_{cond,Zn^{2+}}$  was predicted based on the ff-ASV titration than that predicted by the CSV titration. The average difference of the  $\log K'_{cond,Zn^{2+}}$ 's calculated by the two methods was 0.7.

The concentration of  $L_T$  observed in this study (0.6 - 1.5 nM) is in the range of values previously measured in the North Atlantic (0.4 - 2.5 nM, Ellwood and van den Berg 2000). It is also similar to the concentration of Zn binding ligands measured in the North Pacific (1.0 - 2.2 nM, Bruland 1989; Donat and Bruland 1990) and in subantarctic waters (1.6 - 2.2 nM, Ellwood 2004). The  $K'_{cond,Zn^{2+}}$  values calculated in this study ( $10^{9.8} - 10^{11.3}$ ) cover a wider range than those previously measured in the North Atlantic ( $10^{10.2} - 10^{10.6}$ , Ellwood and van den Berg 2000).

There was no apparent vertical structure over the top 150 m with either the  $L_T$  or the  $K'_{cond,Zn^{2+}}$ , regardless of which method was used, similar to previous studies of Zn speciation (Bruland, 1989; Ellwood and van den Berg, 2000; Ellwood, 2004). Concentrations of  $Zn^{2+}$  were calculated from the total Zn concentration ( $Zn_T$ ) and the above speciation parameters (Fig. 2-8).  $Zn^{2+}$  ranged from 4 - 50 pM based on the ff-ASV titrations and 6 - 68 pM based on the CSV titrations. The  $Zn^{2+}$  concentrations predicted by both methods were similar at every depth except 60 m, which is the depth where the concentration of  $L_T$  was most different. The speciation of  $Zn_T$  was dominated by complexation to organic ligands. The  $[Zn^{2+}]$  calculated by ff-ASV was on average 5.6% of the  $[Zn_T]$ . The average  $[Zn^{2+}]$  predicted by CSV was higher at 9.1% of the  $[Zn_T]$ . However, this was largely due to the 60 m titration where the  $[Zn^{2+}]$  accounted for 18.7% of the  $[Zn_T]$ . If this depth is neglected,  $[Zn^{2+}]$  is only 5.9% of the  $[Zn_T]$ , similar to that calculated by ff-ASV.

## 2.5 Discussion

The free ion model predicts that Zn bioavailability is related to the  $Zn^{2+}$  concentration rather than the total Zn concentration. Zn speciation measurements provide a measure of the  $Zn^{2+}$  concentration, allowing a better evaluation of Zn bioavailability. Intercomparisons of ASV and CSV Zn speciation techniques have generally showed good agreement between the two techniques (Donat and Bruland, 1990; Ellwood, 2004). That is also the case for the intercomparison presented here of the ff-ASV method and the CSV method. Fundamental to the intercomparison of two methods is an accurate estimate of the error on  $[L_T]$  and  $K'_{cond,Zn^{2+}}$ . Because ASV and CSV titrations take significant time (~5 hr, plus ~12 hr equilibration for CLE-CSV), performing replicate titrations of the same sample is not common practice (Bruland, 1989; Ellwood and van den Berg, 2000; Ellwood, 2004) and was not performed on the vertical profile.

Over the course of one month, 4 separate ff-ASV titrations were performed as above on a water sample from the N. Pacific (data not shown). The sample was stored at 4°C between analyses. The concentration of  $L_T$  in this sample was determined to be  $2.8 \pm 0.5$  nM and had a  $\log K'_{cond,Zn^{2+}}$  of  $11.0 \pm 0.6$  (average  $\pm$  standard deviation). The final titration of these four was performed 3 weeks after sampling and indicated a  $[L_T]$  considerably lower than the other 3 titrations and may reflect the break down of natural ligands during storage. If this titration is neglected, the standard deviation of  $[L_T]$  is reduced to 0.2 nM. This is similar to results of Ellwood (2004) who found a standard deviation of 0.1 nM on triplicate ASV titrations of a sample from the Antarctic. Ellwood (2004) observed a slightly higher standard deviation of 0.2 nM for duplicate CSV titrations of the same sample. On duplicate samples, Donat and Bruland (1990) had lower average standard deviations on  $[L_T]$  of  $<0.1$  nM for ASV titrations and 0.1 nM for CSV titrations. The standard deviations for the  $\log K'_{cond,Zn^{2+}}$  values from the above three studies range from 0.2 - 0.6 for ASV and 0.1 - 0.3 for CSV.

Based on the replicate titrations discussed above, the error on the  $[L_T]$  for the ff-ASV method is 0.2 - 0.5 nM. The 0.3 nM overestimation of the  $[L_T]$  in the KCl + EDTA titration also suggest an error on this order. The studies of Donat and Bruland (1990) and Ellwood (2004) suggest that the error in  $[L_T]$  calculated by CSV is 0.1 - 0.2 nM. The average difference between the  $[L_T]$ 's calculated by ff-ASV versus CSV was 0.3 nM. Considering the above errors on the estimation of  $[L_T]$ , the 0.3 nM difference between the ff-ASV and CSV methods may be due to the error on  $[L_T]$ . However, there does seem to be a pattern emerging

of slightly lower  $[L_T]$  measured by CSV than by ASV (Table 2.1). Though the difference is on the order of the estimated error, the fact that it was observed in all 3 intercomparisons suggests that it may be a real systematic difference.

The average difference in  $\log K'_{cond,Zn^{2+}}$  values for ff-ASV and CSV was 0.7. Again, with errors on the  $\log K'_{cond,Zn^{2+}}$  values of  $\sim 0.6$  for the ff-ASV method and around 0.1 - 0.3 for the CSV method, the differences between the  $\log K'_{cond,Zn^{2+}}$  values is not likely significant. Donat and Bruland (1990) found that the  $\log K'_{cond,Zn^{2+}}$  values predicted by ASV were one log unit higher than those predicted by CSV. This systematic difference was not observed by Ellwood (2004) or in this study. Ellwood (2004) notes that in studies of Bruland (Bruland, 1989; Donat and Bruland, 1990), successive Zn additions are made to the voltammetric cell cup (i.e., whole titration is performed on one sample aliquot). In this study and in Ellwood (2004), Zn additions were made to separate sample aliquots in Zn-conditioned vials. Ellwood (2004) suggests this difference in protocols may influence the  $K'_{cond,Zn^{2+}}$  values and could potentially explain the log unit higher  $K'_{cond,Zn^{2+}}$  values observed by Bruland. The Zn-conditioned sample vials are employed to prevent wall loss. If wall loss was occurring in the Bruland ASV titrations, one would expect a decrease in sensitivity, which would tend to increase the  $K'_{cond,Zn^{2+}}$  value. However, this effect seems to be small. Artificially doubling the sensitivity in the 60 m ff-ASV titration, resulted in a  $K'_{cond,Zn^{2+}}$  that was only 0.04 log units higher than that at the lower sensitivity.

For future studies, it would be ideal to reduce, or at least better quantify, the error on the estimations of  $[L_T]$  and  $K'_{cond,Zn^{2+}}$ . This would be improved by performing replicated titrations on the same sample in a short time period (i.e., few days) for each speciation study. However, the estimations of  $[L_T]$  and  $K'_{cond,Zn^{2+}}$  are also affected by the method used to fit the titration data. Zn titration curves are typically fit using the Ruzic/van den Berg linear method for one-metal, one-ligand (Bruland, 1989; Donat and Bruland, 1990; Ellwood and van den Berg, 2000; Ellwood, 2004). The titration data can also be modeled using a non-linear fit as has been done for copper speciation (e.g., Moffett and Brand 1996). When a non-linear fit was applied to the Zn titration data from this study, there was generally good agreement between the  $[L_T]$  calculated by the linear method (differences of  $\leq 0.1$  nM); however, in one case (79 m sample), the difference between the two fits (0.6 nM) was greater than the estimated error (0.2 - 0.5 nM). The average difference between the  $\log K'_{cond,Zn^{2+}}$  values calculated by the non-linear method and that of the linear method was

the same as the estimated error (0.6).

Bruland et al. (2000) compared different voltammetric techniques for copper (Cu) speciation and found the estimations of  $[L_T]$  and  $K'_{cond,Zn^{2+}}$  of the CSV methods were influenced by the "analytical competition strength". The analytical competition strength was defined as  $\alpha_{Cu(AL)_2} = \beta_{Cu(AL)_2,Cu^{2+}} * [AL]^2$ . Thus, competition strength of the synthetic added ligand (AL) was improved when its concentration was increased. There was a systematic decrease of the estimated  $[L_T]$  and increase in  $K'_{cond,Cu^{2+}}$  with increasing analytical competition strength (Bruland et al., 2000). The Cu intercomparison also indicated that there was generally better agreement between the calculated  $Cu^{2+}$  than that of either  $[L_T]$  or  $K'_{cond,Cu^{2+}}$ . That was also the case here where estimates of  $Zn^{2+}$  were very similar, excluding the 60 m CSV titration.

Only one concentration of APDC was used in this study. A decreased concentration of APDC would be expected to decrease the analytical competition strength thereby increasing the estimates of  $[L_T]$  and decreasing the estimates of  $K'_{cond,Zn^{2+}}$ . This would generally bring the estimates of CSV into better agreement with those of the ASV method. The analytical competition strength of APDC in this study was calculated as 0.61. The average "analytical window" in this study, calculated as  $L_T * K'_{cond,Zn^{2+}}$  (Buckley and van den Berg, 1986), is 25 for ASV and 74 for CSV. Thus, the analytical windows of the two voltammetric methods used here are the same order of magnitude. Another factor to consider in terms of the analytical window is the potential for APDC to form colloids. A high concentration of APDC is added, some of which may react to form colloids. In the oligotrophic samples analyzed here, there is a large excess of APDC relative to Zn and a low concentration of particulate matter. These two factors likely result in the effect of APDC-colloid formation being small in this study. However, in coastal systems or at high Zn concentrations this effect may be significant.

Another factor that will affect the estimation of  $[L_T]$  and  $K'_{cond,Zn^{2+}}$  is the ability to consistently fit a Zn current peak on the voltammetric scan. The ff-ASV method presented here was developed only because problems with the established methods for Zn speciation made their use intractable. In trying the classic ASV method of Bruland (1989), we found that with the voltammetric system available (different manufacturer than Bruland (1989)), the baseline had too high a level of noise. Even at deposition times of 15 minutes, we could not get a signal to noise ratio sufficient for detection of low levels of Zn. In addition, the CLE-CSV method of van den Berg (1985) was tried repeatedly with unsuccessful results. With the voltammetric sys-

tem employed here, the baseline of the voltammetric scan was not flat in the vicinity of -1.1 V where the Zn peak occurs. Additionally, there was an interfering peak such that Zn sometimes occurred as a double peak, but the interference was not consistent. Problems were also encountered where the addition of Zn caused no increase in the height of the Zn peak. This method was only made to work on our system with the help of an expert whose perseverance with tweaking all the scan parameters finally resulted in consistent baseline scans where Zn occurred as half of a double peak that increased with Zn addition. Thus, one key advantage of the ff-ASV method presented here was the low-noise baseline that had no other peaks in the vicinity of -1.1 V (Fig. 2-2). Another advantage of the ff-ASV method presented here is that short deposition times can be used (3 min) and a long equilibration period is not necessary (such as the overnight equilibration required with CLE-CSV).

The observed Zn-binding ligand appears to be Zn specific. The similar  $L_T$  concentrations in the ASV and CSV titrations indicates that the high concentration of  $Hg^{2+}$  added ( $10 \mu M$ ) in the ASV titrations did not affect the Zn binding capacity of  $L_T$ . This is similar to previous studies of Zn speciation, where Zn binding was not influenced by additions of Cu (Bruland, 1989) or cadmium (Ellwood, 2004). Apparently, the natural cadmium binding ligands are less specific than those of Zn, as Zn addition sometimes reduced the concentration of cadmium-binding ligand (Ellwood, 2004).

## 2.6 Conclusions

Herein, an ASV method was successfully adapted to the measurement of Zn speciation. This ff-ASV method was able to predict the concentration and a lower estimate of  $K'_{cond,Zn^{2+}}$  of EDTA. The ff-ASV method predicted similar  $K'_{cond,Zn^{2+}}$  values and  $L_T$  concentrations of 4 samples in the North Atlantic as those predicted by CLE-CSV. The concentrations of  $L_T$  and the values of  $K'_{cond,Zn^{2+}}$  in the North Atlantic are similar to values measured previously and to those in the North Pacific and Southern Ocean. A consistent picture with respect to Zn speciation in the oligotrophic ocean seems to be emerging. The recent application of Zn speciation analysis to Fe and Zn grow-out experiments begs a reconsideration of the established free ion model of Zn bioavailability. The Zn speciation method developed here adds to the arsenal of Zn speciation techniques, which have the potential to provide significant insight into Zn bioavailability.

## **2.7 Acknowledgments**

Thanks to Mak Saito for help with method development and generously sharing his voltammetric equipment. The author is indebted to Maeve Lohan for sharing her expertise of the CSV method. Thanks to Ken Bruland for his generosity in opening his lab to me. The author would like to thank the captain and crew of the R/V Oceanus. This research was supported by NSF grant OCE-0136835 to J.W.M. and S.D. R.J.W. was supported by an EPA STAR Fellowship.

## Bibliography

- ANDERSON, M. A., F. M. M. MOREL, and R. R. L. GUILLARD. 1978. Growth limitation of a coastal diatom by low zinc ion activity. *Nature*. **276**: 70–71.
- BRAND, L. E., W. G. SUNDA, and R. R. L. GUILLARD. 1983. Limitation of marine phytoplankton reproductive rates by Zn, Mn, and Fe. *Limnology and Oceanography*. **28**: 1182–1198.
- BRULAND, K. W. 1989. Complexation of zinc by natural organic ligands in the central North Pacific. *Limnology and Oceanography*. **34**: 269–285.
- BRULAND, K. W., E. L. RUE, J. R. DONAT, S. A. SKRABAL, and J. W. MOFFETT. 2000. Intercomparison of voltammetric techniques to determine the chemical speciation of dissolved copper in a coastal seawater sample. *Analytica Chimica Acta*. **405**: 99–113.
- BUCKLEY, P. J. M., and C. M. G. VAN DEN BERG. 1986. Copper complexation profiles in the Atlantic Ocean: a comparative study using electrochemical and ion exchange techniques. *Marine Chemistry*. **19**: 281–296.
- DONAT, J. R., and K. W. BRULAND. 1990. A comparison of two voltammetric techniques for determining zinc speciation in Northeast Pacific Ocean waters. *Marine Chemistry*. **28**: 301–323.
- ELLWOOD, M. J. 2004. Zinc and cadmium speciation in subantarctic waters east of New Zealand. *Marine Chemistry*. **87**: 37–58.
- ELLWOOD, M. J., and C. M. G. VAN DEN BERG. 2000. Zinc speciation in the Northeastern Atlantic Ocean. *Marine Chemistry*. **68**: 295–306.
- FISCHER, E., and C. M. G. VAN DEN BERG. 1999. Anodic stripping voltammetry of lead and cadmium using a mercury film electrode and thiocyanate. *Analytica Chimica Acta*. **385**: 273–280.
- HUTCHINS, D. A., A. E. WITTER, A. BUTLER, and G. W. LUTHER III. 1999. Competition among marine phytoplankton for different chelated iron species. *Nature*. **400**: 858–861.
- IMBER, B. E., and M. G. ROBINSON. 1983. Complexation of zinc by exudates of *Thalassiosira fluxiatilis* grown in culture. *Marine Chemistry*. **14**: 31–41.
- IMBER, B. E., M. G. ROBINSON, A. M. ORTEGA, and J. D. BURTON. 1985. Complexation of zinc by exudates from *Skeletonema costatum* grown in culture. *Marine Chemistry*. **16**: 131–139.
- LOHAN, M. C., D. W. CRAWFORD, D. A. PURDIE, and P. J. STATHAM. 2005. Iron and zinc enrichments in the northeastern subarctic pacific: Ligand production and zinc availability in response to phytoplankton growth. *Limnology and Oceanography*. **50**: 1427–1437.
- MOFFETT, J. W., and L. E. BRAND. 1996. Production of strong, extracellular Cu chelators by marine cyanobacteria in response to Cu stress. *Limnology and Oceanography*. **41**: 388–395.
- MULLER, F. L. L., S. JACQUET, and W. H. WILSON. 2003. Biological factors regulating the chemical speciation of Cu, Zn, and Mn under different nutrient regimes in a marine mesocosm experiment. *Limnology and Oceanography*. **48**: 2289–2302.



- PRICE, N. M., and F. M. M. MOREL. 1990. Cadmium and cobalt substitution for zinc in a marine diatom. *Nature*. **344**: 658–660.
- RUZIC, I. 1982. Theoretical aspects of the direct titration of natural waters and its information yield for trace metal speciation. *Analytica Chimica Acta*. **140**: 99–113.
- SAITO, M. A., and D. L. SCHNEIDER. 2006. Examination of precipitation chemistry and improvements in precision using the  $Mg(OH)_2$  preconcentration ICP-MS method for high-throughput analysis of open-ocean Fe and Mn in seawater. *Analytica Chimica Acta*. *in press*.
- SUNDA, W. G., and S. A. HUNTSMAN. 1995. Cobalt and zinc interreplacement in marine phytoplankton: Biological and geochemical implications. *Limnology and Oceanography*. **40**: 1404–1417.
- TURNER, D. R., M. WHITFIELD, and A. G. DICKSON. 1981. The equilibrium speciation of dissolved components in freshwater and seawater at 25°C and 1 atm pressure. *Geochimica et Cosmochimica Acta*. **45**: 855–882.
- VAN DEN BERG, C. M. G. 1982. Determination of copper complexation with natural organic ligands in seawater by equilibration with  $MnO_2$  I. theory. *Marine Chemistry*. **11**: 307–342.
- VAN DEN BERG, C. M. G. 1985. Determination of the zinc complexing capacity in seawater by cathodic stripping voltammetry of zinc APDC complex-ions. *Marine Chemistry*. **16**: 121–130.
- VASCONCELOS, M. T. S. D., M. F. C. LEAL, and C. M. G. VAN DEN BERG. 2002. Influence of the nature of the exudates released by different marine algae on the growth, trace metal uptake and exudation of *Emiliania huxleyi* in natural seawater. *Marine Chemistry*. **77**: 187–210.
- WU, J., and E. A. BOYLE. 1998. Determination of iron in seawater by high-resolution isotope dilution inductively couple plasma mass spectrometry after  $Mg(OH)_2$  coprecipitation. *Analytica Chimica Acta*. **367**: 183–191.



Table 2.1: Compilation of the results of voltammetric Zn speciation measurements in oligotrophic regions.

Study Region	Sample	[L <sub>T</sub> ] (nM)	logK* <sub>cond,Zn<sup>2+</sup></sub>	Reference	Speciation Method
North Pacific	profile	1.0 - 1.5	10.7 - 11.3	Bruland 1989	ASV
North Pacific	60 & 150 m	1.7 - 2.3	11.0 - 11.5	Donat and Bruland 1990	ASV
	60 & 150 m	1.6 - 2.3	10.1 - 10.5		CLE-CSV
North Pacific	15 m	0.7	10.5	Lohan et al. 2005	CLE-CSV
North Pacific	near-surface transect	1.1 - 3.6	9.4 - 11.0	Chapter 3	ff-ASV
North Atlantic	surface transect	0.4 - 2.5	10.0 - 10.5	Ellwood and van den Berg 2000	CLE-CSV
North Atlantic	profile	0.9 - 1.5	9.8 - 10.5	this study	ff-ASV
	profile	0.6 - 1.3	9.8 - 11.3		CLE-CSV
Southern Ocean	mixed layer	1.2 - 2.4	10.0 - 10.8	Ellwood 2004	ASV
	comparison sample	1.3	10.6		ASV
	comparison sample	1.2	10.2		CLE-CSV

Table 2.2: Voltammetric scan conditions used in this study for the ff-ASV and CLE-CSV methods.

Parameter	ff-ASV	CLE-CSV
conditioning potential	0.6 V	
conditioning time	60 sec	
deposition potential	-1.5 V	-0.6 V
deposition time	600 sec	180 sec
equilibration time	10 sec	8 sec
frequency	50 Hz	
modulation time		0.017 sec
interval time		0.2 sec
initial potential	-1.3 V	-0.75 V
End potential	0.6 V	-1.3 V
step potential	4.95 mV	4.95 mV
modulation amplitude	50 mV	100 mV
RDE stirrer speed	1500 rpm	
waveform	square wave	differential pulse

Figure 2-1: A typical ff-ASV titration (60 m sample) showing the response of Zn peak height with increasing Zn additions (A) and the linear relationship obtained by transforming the titration data using equations 2.1 - 2.3 (B).

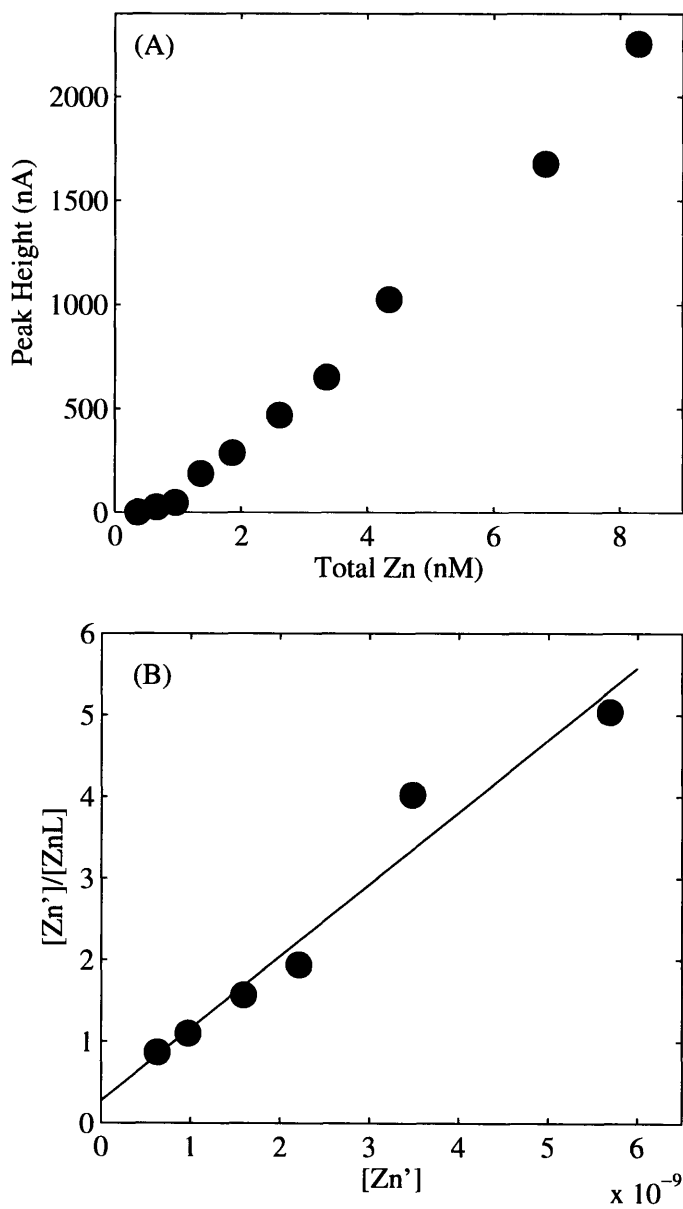


Figure 2-2: Voltammetric scans of a seawater sample and two Zn standard additions obtained using ff-ASV method. (A) Shows the scans at full scale. The large Hg peak is visible at 0 V. (B) Shows the same set of scans on a smaller scale in order for the Zn peaks to be visible.

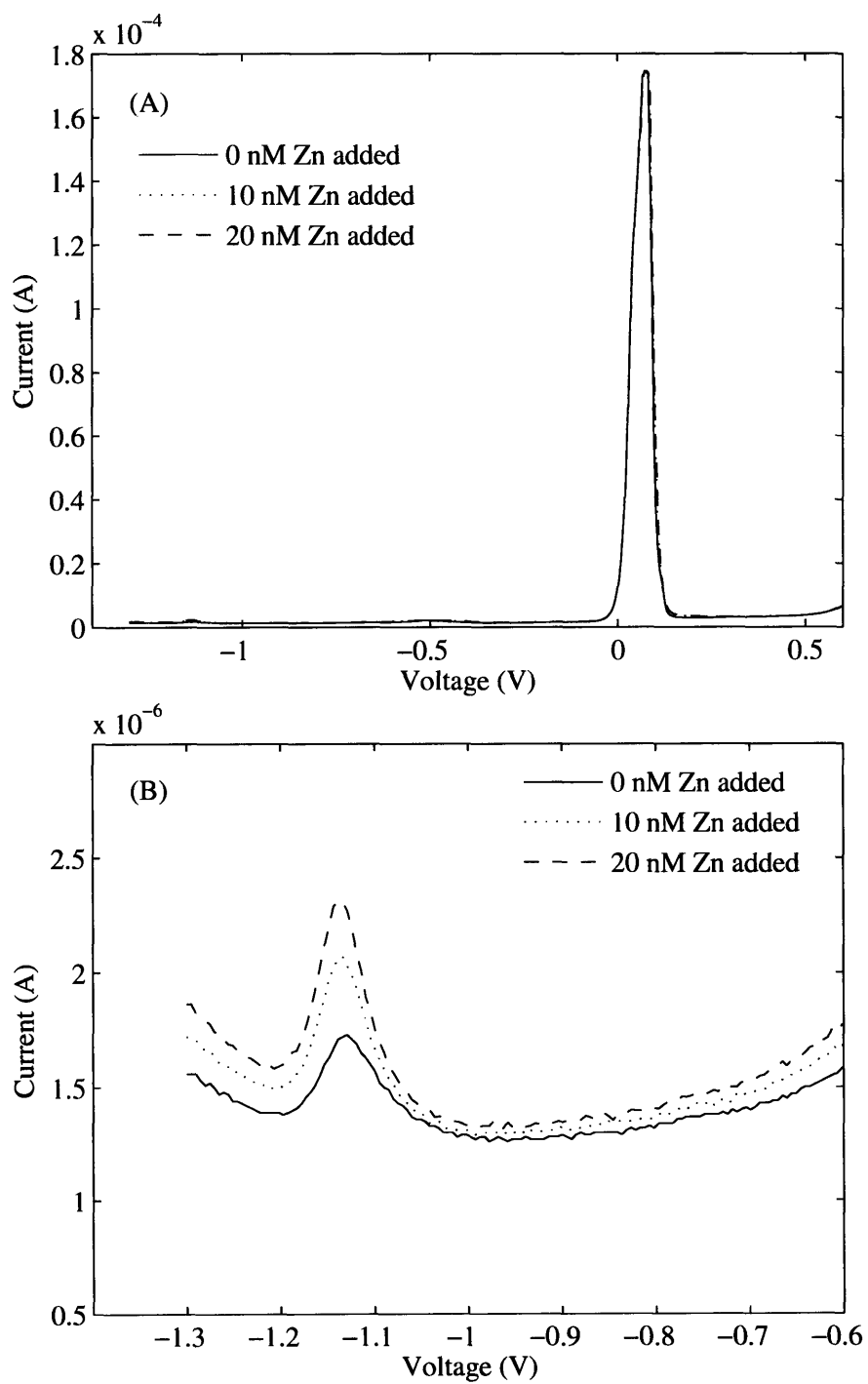


Figure 2-3: A typical CLE-CSV titration (data from the 21 m sample) showing the response of Zn peak height with increasing Zn additions (A) and the linear relationship obtained by transforming the titration data using equations 2.5 - 2.10 (B).

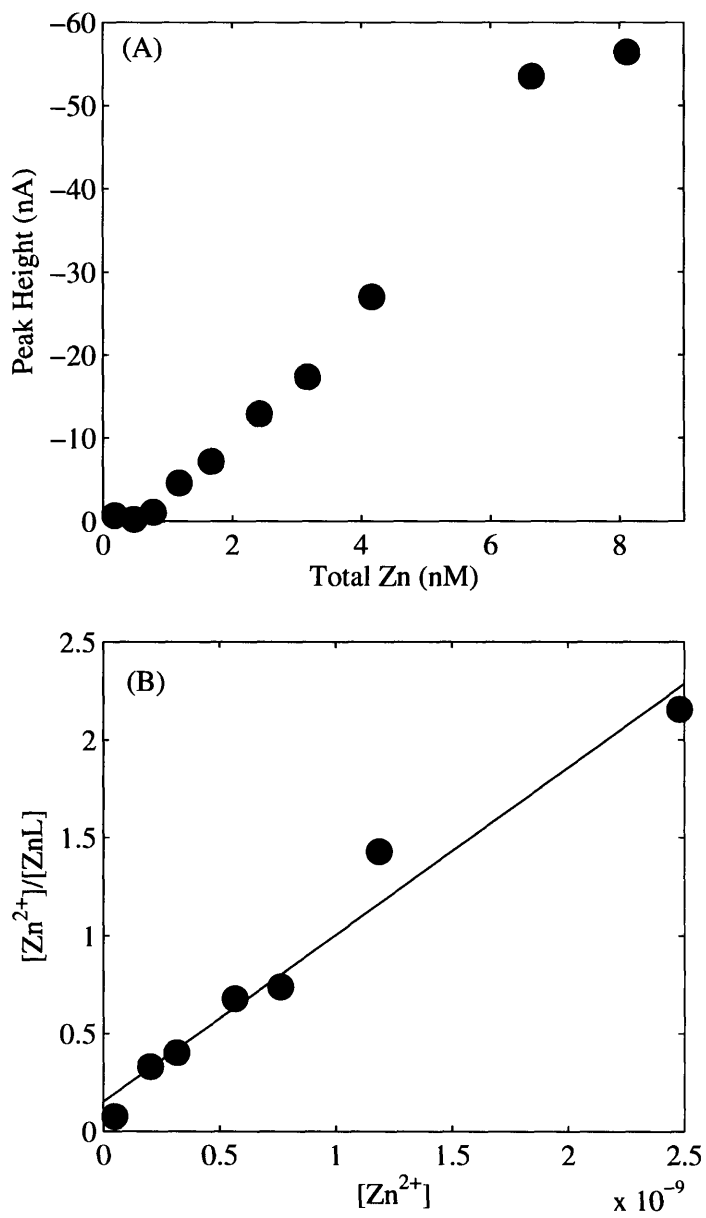


Figure 2-4: ff-ASV titrations of UV-irradiated seawater (A) and a dilute (10%) seawater solution (B). Notice that in both cases, no curvature is observed.

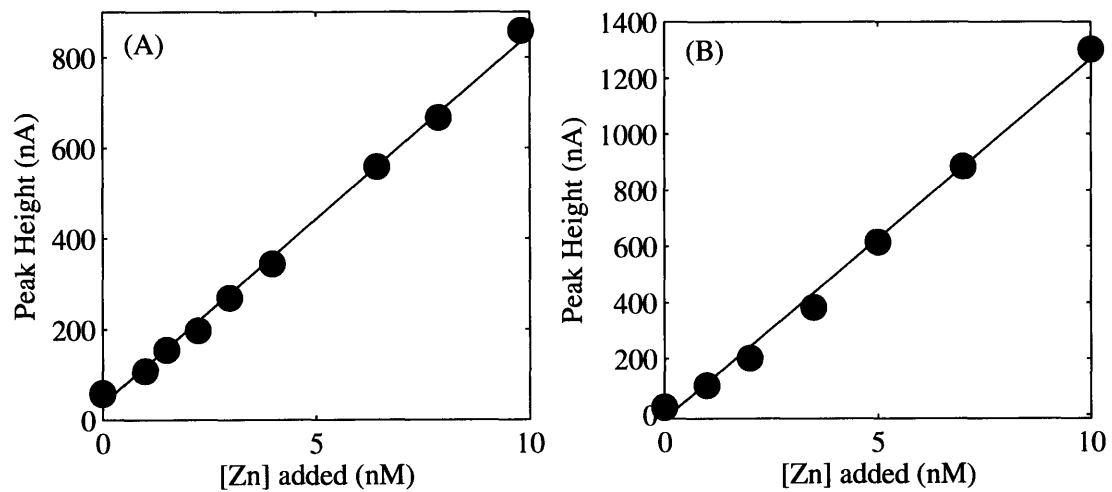




Figure 2-5: ff-ASV titration of 0.1 M KCl solution where 4 nM EDTA was added. (A) Peak height increase with increasing Zn standard additions. (B) the linear relationship obtained by transforming the titration data using equations 2.1 - 2.3.

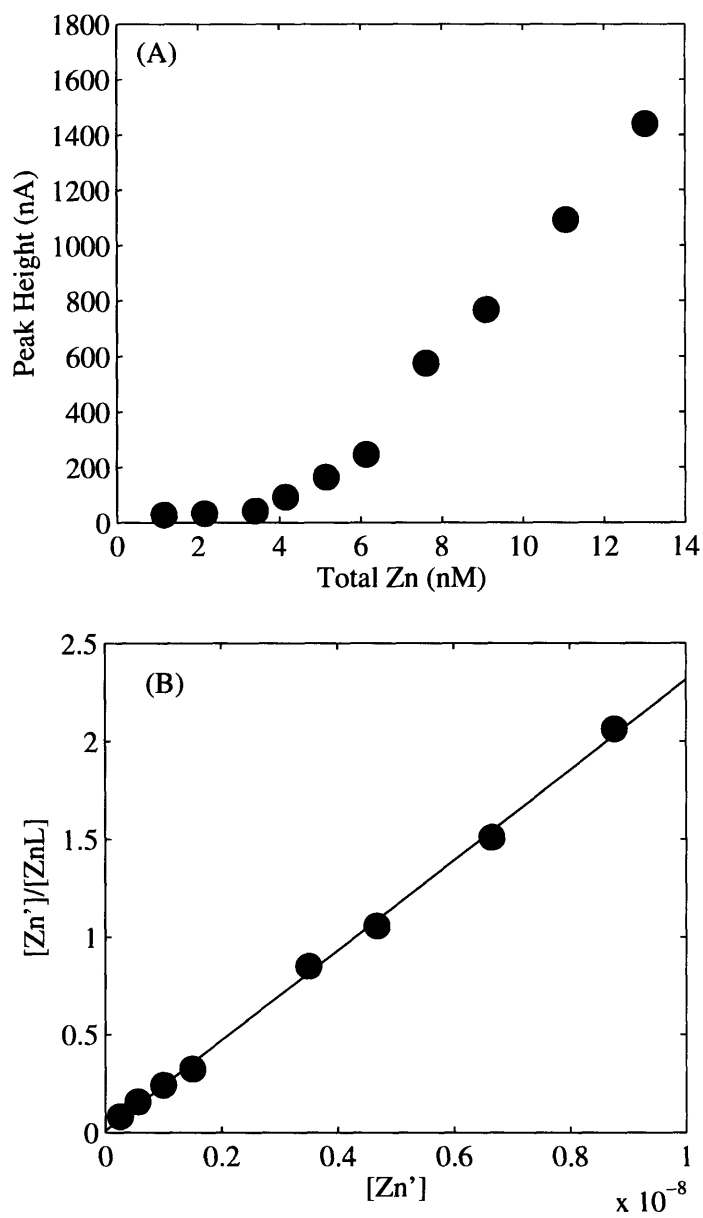


Figure 2-6: Simulated ASV titrations of a solution with 4 nM ligand of various  $K_{cond,Zn^{2+}}$  values.  $K_{cond,Zn^{2+}}$  values used for each titration are listed on plot.

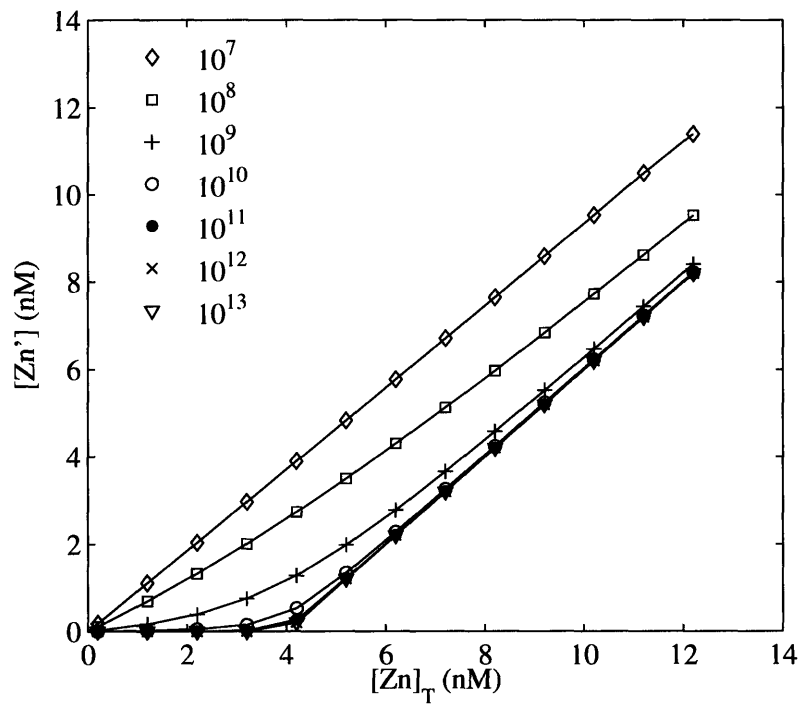


Figure 2-7: Profiles of  $[L]_T$  (A) and  $K_{cond, Zn^{2+}}$  (B) determined by CSV (filled circles) and by ff-ASV (open squares). Samples were collected in April 2004 from the North Atlantic Ocean ( $34^{\circ}38'N$ ,  $55^{\circ}35'W$ ).

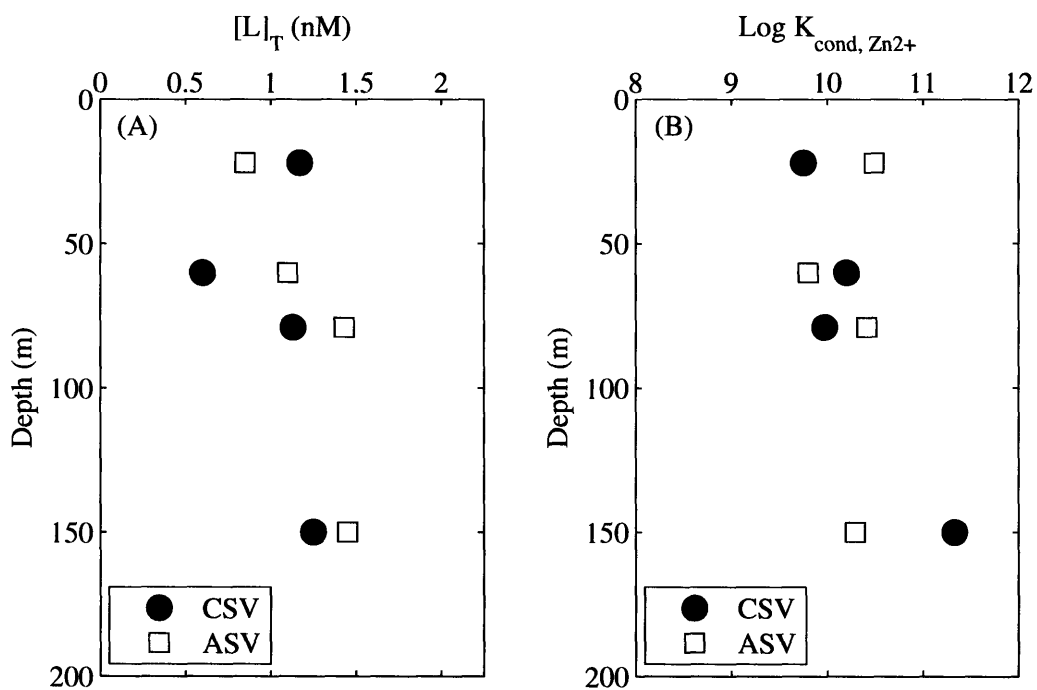
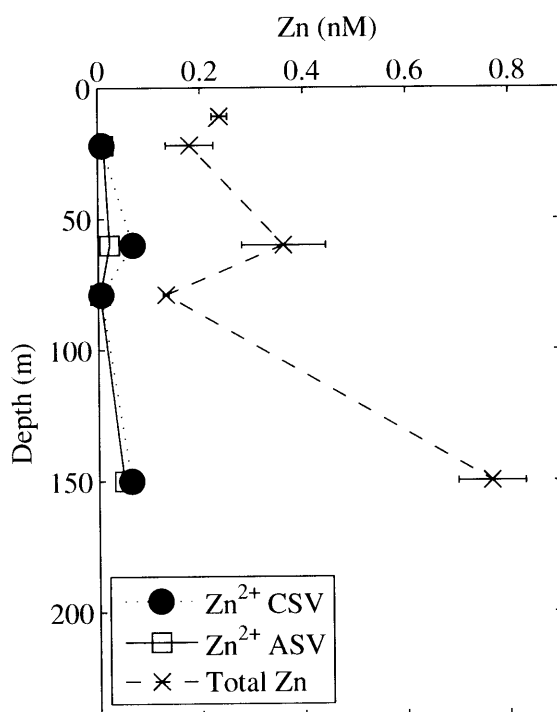


Figure 2-8: Profile of total dissolved Zn (X's) along with  $Zn^{2+}$  determined by CSV (filled circles) and ff-ASV (open squares).



## **Chapter 3**

# **Zinc in the subarctic North Pacific and Bering Sea**

### **3.1 Abstract**

The eastern subarctic North Pacific, an area of high nutrients and low chlorophyll, has been often studied with respect to the potential for iron to control primary production. In comparison, the geochemistry of zinc in the region or in the western portion of the subarctic North Pacific is relatively uncharacterized. In this study, total zinc concentrations and zinc speciation were measured in the near-surface on a transect across the subarctic North Pacific and across the Bering Sea. Total dissolved zinc concentrations in the near-surface ranged from 0.10 nM to 1.15 nM with lowest concentrations in the eastern portions of both the North Pacific and Bering Sea. The speciation of total dissolved zinc was dominated by complexation to strong organic ligands whose concentration ranged from 1.1 to 3.6 nM with conditional stability constants of  $10^{9.1}$  -  $10^{10.7}$ . The importance of zinc to primary producers was evaluated by comparison to phytoplankton pigment concentrations and by performing a shipboard incubation. Zinc concentrations were positively correlated with two pigments that are characteristic of diatoms. At one station in the N. Pacific, the addition of 0.75 nM zinc resulted in a doubling of chlorophyll after four days. This study adds to our understanding of zinc geochemistry and bioavailability in the subarctic North Pacific and Bering Sea.

## 3.2 Introduction

Surface macronutrient concentrations (nitrate, phosphorus, silicate) in the subarctic N. Pacific are not depleted by phytoplankton growth (McAllister et al., 1960), leading to its characterization as a high nutrient, low chlorophyll (HNLC) region. Surface concentrations of iron (Fe), an essential plant nutrient, in this region are very low (e.g., 0.06 nM, Martin et al. 1989). Additions of Fe to both bottle incubations (Martin and Fitzwater, 1988; Coale, 1991; Boyd et al., 1996; Lam et al., 2001; Crawford et al., 2003; Leblanc et al., 2005) and meso-scale ocean patches (Tsuda et al., 2003; Boyd et al., 2004) have demonstrated the ability of Fe to regulate primary production in this region.

Zinc (Zn) concentrations are also very low in the surface waters of the subarctic N. Pacific (Bruland et al., 1978; Martin et al., 1989; Lohan et al., 2002). Though Zn is an important micronutrient for phytoplankton, the role of Zn in determining marine primary production is not as clear as that of Fe. Low Zn concentrations can limit phytoplankton growth in cultures (Anderson et al., 1978; Brand et al., 1983; Morel et al., 1991). Similarly low Zn concentrations are found in the open ocean. However, unlike Fe, Zn additions to bottle experiments have had little or no effect on total chlorophyll biomass (Coale, 1991; Coale et al., 1996; Scharek et al., 1997; Gall et al., 2001; Coale et al., 2003; Crawford et al., 2003; Franck et al., 2003; Ellwood, 2004; Lohan et al., 2005; Leblanc et al., 2005).

Zn has the potential to influence primary production in ways other than by controlling phytoplankton biomass. Zn is a cofactor in a number of important enzyme systems such as carbonic anhydrase and alkaline phosphatase, which are involved in carbon and phosphorus acquisition. In the subarctic N. Pacific, low dissolved concentrations of Zn have been suggested to limit activities of the bacterial ectoenzyme leucine aminopeptidase (Fukuda et al., 2000). Low Zn availability resulted in reduced activity of alkaline phosphatase in Zn and phosphorus co-limited cultures of *E. huxleyi*, and Zn addition increased alkaline phosphatase activity in a shipboard incubation in the Bering Sea (Shaked et al., 2006). Thus Zn availability can affect the functioning of enzyme systems.

Studies with cultured phytoplankton demonstrate that cobalt (Co) and cadmium (Cd) are able to substitute for Zn in the enzyme systems of some phytoplankton (Lee et al., 1995; Yee and Morel, 1996). Co is actually preferentially utilized over Zn by some phytoplankton species (Sunda and Huntsman, 1995; Saito et al., 2002), which suggests that the ratio of Zn to Co may influence species composition in the ocean (Sunda

and Huntsman, 1995). While this hypothesis has not been explicitly tested, the ability of Zn to influence species composition has been shown. In an incubation in the eastern subarctic N. Pacific, the addition of Zn and Fe together (+Zn/+Fe) resulted in a higher proportion of phytoplankton in the smaller size fraction (0.2 - 5  $\mu\text{m}$ ) compared to the addition of Fe alone (Crawford et al., 2003). The community in the +Zn/+Fe addition had a higher abundance of small diatoms and small flagellates and less coccolithophores and ciliates than the Fe alone addition (Crawford et al., 2003). Zn may influence not only which taxa dominate, but which species within a taxa are most successful. In a bottle incubation experiment in the sub-Antarctic zone, the addition of Zn caused a community shift from a large colonial pennate diatom to a smaller, less-silicified, solitary pennate diatoms species (Leblanc et al., 2005).

Zn deficiency can also effect the extent of calcification of *E. huxleyi*, a ubiquitous marine coccolithophore (Schulz et al., 2004). Under Zn limitation, *E. huxleyi* cells become more heavily calcified due to a slowing of growth rates with no corollary decrease in calcium carbonate ( $\text{CaCO}_3$ ) production rate (Schulz et al., 2004). This effect, along with Zn's potential to influence species composition, suggests that Zn may be an important determinant of the organic carbon: $\text{CaCO}_3$  rain ratio. At low Zn:Co, coccolithophores and small cyanobacteria would be expected to dominate over diatoms based on their growth rates at low Zn:Co (Sunda and Huntsman, 1995). This community shift would decrease the organic carbon: $\text{CaCO}_3$  rain ratio, as coccolithophores have  $\text{CaCO}_3$  shells. In addition, the coccolithophores growing under low Zn would be more highly calcified than those experiencing replete levels of Zn, further decreasing the organic carbon: $\text{CaCO}_3$  rain ratio.

Zn bioavailability is related to the Zn free ion ( $\text{Zn}^{2+}$ ) concentration rather than the total Zn concentration, based on culture studies with the synthetic ligand EDTA (e.g., Anderson et al. 1978). Natural organic ligands in the surface ocean strongly bind Zn (Donat and Bruland, 1990; Bruland, 1989; Ellwood and van den Berg, 2000; Ellwood, 2004). These ligands dominate the speciation of the total Zn pool, with  $\text{Zn}^{2+}$  accounting for 5% or less of the total dissolved Zn. Recent evidence demonstrates that the inventory of Zn binding ligands can be extremely dynamic with production and removal of ligands occurring on timescales of 1 day (Lohan et al., 2005). Zn speciation measurements of shipboard incubation experiments suggest that the phytoplankton community can survive at lower  $\text{Zn}^{2+}$  than is known to limit phytoplankton cultures (Ellwood, 2004; Lohan et al., 2005). These results indicate that either the natural community has



much lower Zn requirements than cultured strains, that it is able to meet its Zn requirement by substituting Co or Cd, or alternately, that the community is able to utilize organically complexed Zn.

This study examines total dissolved Zn and Zn speciation across the subarctic N. Pacific and Bering Sea and the effect of Zn addition on phytoplankton in the N. Pacific.

### **3.3 Methods**

#### **3.3.1 Sample Collection and Handling**

Samples were collected in the N. Pacific and Bering Sea aboard the R/V Kilo Moana in the summer of 2003 (Fig. 3-1). Water samples were collected using 10 L teflon-coated Go-Flos (General Oceanics) on a kevlar hydrowire. Seawater was collected from the Go-Flo bottles by connecting teflon tubing to both ports and over-pressuring the top port with filtered ultra-high purity nitrogen gas. Seawater passed directly from teflon tubing through a sandwich filter (acid-cleaned 0.4  $\mu\text{m}$  polycarbonate) and into rigorously acid-washed low density polyethylene (LDPE) or teflon bottles (see Appendix A for full acid-washing procedure). Samples for total dissolved Zn analysis (LDPE bottles) were acidified to approximately pH 2 by the addition of 2 ml HCl (Seastar) per liter of seawater. Samples for Zn speciation analysis (teflon bottles) were stored refrigerated until analysis. All manipulation of the samples occurred in a laminar flow bench inside a clean laboratory.

#### **3.3.2 Total Dissolved Zn Analysis**

Total dissolved zinc ( $Zn_T$ ) concentrations were measured using isotope dilution and magnesium hydroxide pre-concentration followed by analysis using inductively coupled plasma mass spectrometry (ICP-MS) after Wu and Boyle (1998) and Saito and Schneider (2006). 15 ml centrifuge tubes (Globe Scientific) were cleaned by soaking in 2N HCl (J.T. Baker intra-analyzed) at 60°C for 48 hours followed by rinsing 5 times with pH 2 HCl (J.T. Baker intra-analyzed) and once with pH 2 HCl (Seastar). Finally, tubes were filled to a positive meniscus with pH 2 HCl (Seastar) and capped until use. At the time of analysis, tubes were rinsed once with sample and then filled to approximately 13.5 ml (exact volume determined gravimetrically). Samples were then spiked with  $^{66}\text{Zn}$  (98.9% as  $^{66}\text{Zn}$ , Cambridge Isotope Laboratories, Inc.) to an estimated

$^{66}\text{Zn}:$  $^{64}\text{Zn}$  ratio of 9. This ratio minimizes error magnification (Heumann, 1988):

$$R_{optimum} = \sqrt{\left(\frac{^{66}\text{Zn}}{^{64}\text{Zn}}\right)_{sample} * \left(\frac{^{66}\text{Zn}}{^{64}\text{Zn}}\right)_{spike}} \quad (3.1)$$

The added  $^{66}\text{Zn}$  spike was allowed to equilibrate with the samples overnight. The following day, 125  $\mu\text{l}$  of ammonia (Seastar) was added to each tube. After 90 sec, the tube was inverted and after an additional 90 sec, tubes were centrifuged for 3 min at 3000xg (3861 rpm) using a swinging bucket centrifuge (Eppendorf 5810R). The majority of the supernatant was carefully decanted. Tubes were then respun for 3 min to firm pellet and the remaining supernatant was shaken out. Pellets were dissolved on the day of ICP-MS analysis using 0.5 - 1.5 ml of 5% nitric acid (Seastar). ICP-MS measurements were made using a Finnigan ELEMENT2 in medium resolution mode, which was sufficient to resolve  $^{64}\text{Zn}$  from the potential interference peak due to Mg-Ar.  $\text{Zn}_T$  concentrations were calculated as

$$[\text{Zn}_T] = \frac{f_{64 \text{ spike}}}{f_{64 \text{ natural}}} * [\text{Zn}_{spike}] * \frac{\text{spike volume}}{\text{sample volume}} * \left( \frac{R_{measured} - R_{spike}}{R_{natural} - R_{measured}} \right) \quad (3.2)$$

where  $f_{64}$  is the fraction of the abundance of  $^{64}\text{Zn}$  over the abundance of all the Zn isotopes and R is the ratio of  $^{66}\text{Zn}:$  $^{64}\text{Zn}$ . To measure the procedural blank, 1 ml of surface seawater was treated the same as samples, and calculations were performed as though it was a 13.5 ml sample. The average blank value was 0.12 nM with a detection limit of 0.09 nM (calculated as three times the standard deviation of the blank).

The efficiency of the magnesium hydroxide precipitate at scavenging Zn was tested. 1 ml aliquots of acidified seawater (n=3) were equilibrated with the radioisotope  $^{65}\text{Zn}$  (approximately 0.5  $\mu\text{Ci}$ ) for 2 hours. 30  $\mu\text{l}$  of ammonia was added to each sample and after 1.5 minutes, the samples were centrifuged for 3 minutes. The amount of  $^{65}\text{Zn}$  was quantified in the seawater before precipitation, in the precipitate, and in the supernatant using a sodium iodide detector. The percent of  $^{65}\text{Zn}$  that was captured, on average, by the magnesium hydroxide pellet was 96% and the fraction remaining in the supernatant was 2%. The accuracy of the method was evaluated by measuring a NASS-5 seawater standard (National Research Council of Canada). The NASS standard has a certified value of  $1.56 \pm 0.60$  nM Zn. The value obtained by this method ( $1.00 \pm 0.03$  nM) was in good agreement with the certified value.

### 3.3.3 Zn Speciation Determinations

Zn speciation was determined by anodic stripping voltammetry (ASV) using a method adapted from that of Fischer and van den Berg (1999) for the measurement of total lead and cadmium. This method is different than ASV methods that have been used in the past for the determination of zinc speciation (Bruland, 1989; Donat and Bruland, 1990). In previous methods, a mercury film was plated onto a glassy carbon electrode and that film was used repeatedly for multiple sample aliquots. In the fresh film ASV (ff-ASV) method used here, dissolved mercury is added to each sample aliquot and a new mercury film is plated for each aliquot. This has the advantage of producing a thinner mercury film in which Zn is plated simultaneously with mercury, resulting in higher relative Zn concentrations than with a pre-plated film. Thus, the method yields high sensitivity even at relatively short deposition times (3 min).

Measurements were made using a 663 VA stand (Metrohm) consisting of a glassy carbon rotating disc working electrode, a glassy carbon rod counter electrode, and a double junction Ag, AgCl, saturated KCl reference electrode. The electrode was interfaced to a PC (IBM) using an IME663 and  $\mu$ autolab I (Eco Chemie). Before each day of speciation analysis, the glassy carbon rotating disc electrode (RDE) was manually polished with aluminum oxide. Then, a cyclic voltammetry step was performed cycling the voltage between -0.8 V and 0.8 V 50 times. Reagents used included 4-(2-Hydroxyethyl)-1-piperazinepropanesulfonic acid (EPPS), ammonium thiocyanate, and mercuric chloride. The pH of the EPPS buffer was adjusted to 8.1. EPPS and thiocyanate reagents were run through a pre-cleaned chelex column to remove trace metal contamination. The thiocyanate reagent is added to improve the reproducibility of the mercury film and to ensure full de-plating of the film between samples (Fischer and van den Berg, 1999).

Zn speciation titrations were set up in 15 ml teflon vials (Savillex). In order to prevent wall loss, teflon vials were equilibrated with specific concentrations of Zn before use and each vial was always used for the same concentration of Zn. Before a titration, the vials were rinsed with 12 ml of sample. Then, 12 ml of sample was added into each vial, along with 1.7 mM EPPS. For each sample aliquot, the appropriate concentration of Zn was allowed to equilibrate with the sample in the sample vial for 10 minutes. Then, the sample aliquot was poured into the voltammetric cell and 4.2 mM ammonium thiocyanate and 10.4  $\mu$ M mercuric chloride were added. Each sample aliquot was purged with ultra-high purity nitrogen gas for 5 min to remove oxygen. A conditioning potential of 0.6 V was held for 60 sec. The mercury film and Zn' were

then deposited at a potential of -1.5 V for 180 sec. After a 10 sec equilibration time, the voltage was ramped in square wave mode from -1.3 V to 0.6 V. A frequency of 50 Hz was used and the step potential and modulation amplitude were 4.95 mV and 49.95 mV, respectively. A peak in current was evident at -1.1 V representing the concentration of inorganic Zn species ( $Zn'$ ). The total ligand concentration ( $[L_T]$ ) and conditional stability constant ( $K'_{cond,Zn'}$ ) with respect to  $Zn'$  were calculated by performing a linearization of the titration data (Ruzic, 1982; van den Berg, 1982), where  $[Zn']/[ZnL]$  is plotted versus  $[Zn']$ . The equation for the resulting line is

$$\frac{[Zn']}{[ZnL]} = \frac{[Zn']}{[L_T]} + \frac{1}{(K'_{cond,Zn'} * [L_T])}. \quad (3.3)$$

Hence,  $[L_T]$  can be calculated as 1/slope and  $K'_{cond,Zn'}$  as  $1/([L_T] * y\text{-intercept})$ . The  $Zn^{2+}$  concentrations in Table 3.1 were calculated based on the relationships:

$$K'_{cond,Zn'} = \frac{[ZnL]}{[Zn'][L']} \quad (3.4)$$

$$[Zn'] = \alpha_{Zn} * [Zn^{2+}] \quad (3.5)$$

$[Zn']$  was calculated from equation 3.3, assuming that  $[L]_T - [Zn]_T = [L']$  and that  $[ZnL] = [L]_T - [L']$ . A value of 2.2 was used for  $\alpha_{Zn}$  (Turner et al., 1981).

### 3.3.4 Shipboard Incubation

Trace metal clean water was collected with an air-driven Teflon pump that pumped water from approximately 15 m depth directly into an acid-washed HDPE carboy, housed in a trace-metal free bubble constructed of a HEPA filter and plastic sheeting. Acid-washed polycarbonate bottles were filled with unfiltered seawater from the carboy. A time zero sample for chlorophyll was also collected from the carboy. Additions were made to duplicate polycarbonate bottles as follows: control (no addition), +Fe (2.5 nM  $FeCl_3$ ), +Zn (0.75 nM  $ZnCl_2$ ), +Zn/+Fe (0.75 nM  $ZnCl_2$ , 2.5 nM  $FeCl_3$ ). Bottles were tightly capped and placed in an on-deck water bath supplied with flowing seawater for temperature control. Sunlight was attenuated with blue-gel shading (Roscolux 65: Daylight Blue, Stage Lighting Store) to mimic 15 m irradiances. On days 2 and 4,

one bottle was removed from the incubator and sampled for chlorophyll. Samples for analysis of dissolved nutrients from select bottles were also collected, filtered, and frozen.

### **3.3.5 Chlorophyll, Nutrients, and HPLC pigments**

For chlorophyll analysis, seawater was passed through a GF/F filter. Filters were extracted in 90% acetone overnight at -20°C and analyzed following the procedure of Jeffrey and Humphrey (1975). All samples for nutrient analysis were passed through an acid-cleaned 0.4  $\mu\text{m}$  filter into acid-cleaned polypropylene tubes and stored frozen until analysis. Analysis was performed by the Ocean Data Center (ODC) at the Scripps Institution of Oceanography for nitrate, nitrite, ammonium, silicate, and phosphate using an autoanalyzer. In addition, the Popp group ran phosphate analyses onboard at select stations using the molybdate blue method (Murphy and Riley, 1962). Sample collection and analysis of HPLC pigments was performed by the Bidigare group at University of Hawaii after Bidigare (1991) and Bidigare and Trees (2000).

## **3.4 Results**

### **3.4.1 Total Dissolved Zn**

$Zn_T$  was measured in the near-surface at 5 stations in the N. Pacific (mixed layer 15-80 m) and 4 stations in the Bering Sea (mixed layer 15-25 m).  $Zn_T$  concentrations in the near-surface ranged from 0.10 to 1.15 nM (Table 3.1, Fig. 3-2). Concentrations increased from east to west in the North Pacific. In the Bering Sea, concentrations were lowest over the shelf and highest at St. 9, which was close to the shelf/slope break. Profiles of 8-11 depths were collected at three stations in the N. Pacific (Fig. 3-3). The  $Zn_T$  concentrations observed in these profiles are oceanographically consistent with lowest concentrations observed in surface waters, increasing to a maximum concentration around 500 m. At the majority of stations, the near-surface samples collected were close to the base of the mixed layer (e.g., St. 4, Fig. 3-4). Only at St. 1 were multiple samples collected at different depths within the mixed layer. In the N. Pacific, the thermocline extended down to roughly 80-100 m. In the Bering Sea, the thermocline occurred over more compressed depths with the minimum temperature reached between 30-50 m.

When  $Zn_T$  concentrations from the 3 profiles are plotted against phosphate ( $PO_4$ ), the data agree well

with a previous study (Martin et al., 1989) from the N. Pacific in the vicinity of St. 1 (Fig. 3-5A). However, there are some discrepancies. At the high  $\text{PO}_4$ , high  $\text{Zn}$  end of the spectrum, there are three data points that fall above the trend (St. 4 3000 m; St. 6 1000 m; St. 6 3000 m). These data occur at depths in the profile (1000-3000 m) where  $\text{PO}_4$  concentrations are expected to remain constant with depth, yet the  $\text{PO}_4$  in these samples is significantly lower than the two depths surrounding it or the depth above it in the case of the 3000 m points. If the  $\text{PO}_4$  values for these three data points are replaced with the average value for the two surrounding depths or the value above it in the case of 3000 m, the St. 6 1000 m point falls back in line with the expected trend (Fig. 3-5B). The final two data points (St. 4 3000 m; St. 6 3000 m) fall closer to the line but still seem to have higher than expected  $\text{Zn}_T$  concentrations. The 3000 m samples were collected with Go-Flo bottles attached to the CTD rosette frame because sufficient kevlar was not available to reach 3000 m depth. The fact that these samples continue to fall above the trend and were collected on a metal hydrowire suggest that the values are influenced by contamination and that the true  $\text{Zn}_T$  concentrations are lower than those reported here. A final point that seems to fall somewhat off the trend is that at  $1.2 \mu\text{M}$   $\text{PO}_4$  and  $2.7 \text{ nM}$   $\text{Zn}_T$  (St. 6 80 m).  $\text{PO}_4$  concentrations were measured both shipboard and by the ODC for this sample. The shipboard value of  $1.7 \mu\text{M}$   $\text{PO}_4$  is significantly higher than the ODC number of  $1.2 \mu\text{M}$  and is a value that matches the trend. This suggests that  $\text{PO}_4$  was lost during storage before analysis by ODC, a potential problem of sample storage (Maher and Woo 1998, and references therein).

A tight correlation was observed between silicate (Si) and  $\text{Zn}_T$  concentrations (Fig 3-6,  $R^2 = 0.93$ ). Again, however, there are a few outliers. The highest Zn values again fall above the trendline—the likely contamination of these samples has already been noted. The Zn/Si relationship is generally linear, but data from both this study and Martin et al. (1989) trend slightly above the linear relationship in the mid-values. This suggests that at mid-depths (~300-500 m) Zn may be remineralized faster from sinking particulate matter than Si.

### 3.4.2 Zn Speciation

Zn speciation titrations were performed on near-surface samples for stations 1-8. The concentration of Zn binding ligands ( $L_T$ ) ranged from 1.1 to 3.6 nM in the near-surface with an average concentration of 2.2 nM (Table 3.1, Fig. 3-7). The concentration of  $L_T$  followed a general trend of increasing concentrations from

east to west in the N. Pacific. The highest concentration of  $L_T$  was observed at St. 8 in the western Bering Sea. The  $K'_{cond,Zn'}$  of the natural organic ligands ranged from  $10^{9.1}$  to  $10^{10.7}$  with an average value of  $10^{10.1}$  (Table 3.1). The resultant  $Zn^{2+}$  concentrations in these samples ranged from 5-23 pM. Where multiple depths of a profile were analyzed for speciation, the Zn binding ligands had similar concentrations and conditional stability constants at each depth (Table 3.1).

### 3.4.3 Shipboard Incubation

The shipboard incubation began at St. 5. At time zero of the incubation, chlorophyll concentrations were  $0.99 \mu\text{g L}^{-1}$ . The dominant phytoplankton pigments at St. 5 were hexanoyloxyfucoxanthin, fucoxanthin, chlorophyll c, and chlorophyll b. This suggests that the initial community in our incubation bottles consisted mainly of prymnesiophytes, diatoms, and green algae. The near-surface  $Zn_T$  concentration at St. 5 was 0.65 nM. Chlorophyll values remained constant in the control treatment over 4 days (Fig. 3-8). In the +Zn treatment, chlorophyll concentrations increased over the control by 25% on day 2 and reached twice the value in the control on day 4. An even more pronounced effect was seen in the treatments where Fe was added (+Fe, +Zn/+Fe). In these treatments, chlorophyll increased by between 60-80% over the control on day 2 and reached over 3 times the chlorophyll values observed in the control on day 4. The drawdown of nutrients in the incubation bottles matched the chlorophyll trend (Table 3.2). At the end of the experiment, nutrients were most depleted in the treatments where Fe was added. Nutrient concentrations in the +Zn treatment were intermediate between those of the control and the Fe additions.

### 3.4.4 Chlorophyll, Nutrients, and HPLC pigments

Chlorophyll concentrations in the near-surface were lowest in the eastern N. Pacific (Table 3.1). Chlorophyll increased moving west from St. 1 to St. 5. Moderate chlorophyll values were observed for stations 6-10 in the western N. Pacific and Bering Sea, and the highest chlorophyll concentration encountered was at St. 11 on the Bering Shelf.

In the N. Pacific, near-surface  $PO_4$  was lowest in the east and increased significantly between St. 1 and St. 3 and then remained relatively constant moving west (Table 3.1). In the Bering Sea,  $PO_4$  was highest in the west and decreased significantly on the Bering shelf.

There was no relationship between  $Zn_T$  concentration and total chlorophyll *a* (Fig. 3-9A). However, for the pigments fucoxanthin and chlorophyll *c*, a positive relationship was observed between  $Zn_T$  and the relative contribution of each pigment to total chlorophyll *a* (Fig. 3-9B, 3-9C). The relative contribution of a pigment was calculated as

$$\text{Relative contribution (\%)} = \frac{\text{Concentration of a pigment (ng L}^{-1}\text{)}}{\text{Total chlorophyll a concentration (ng L}^{-1}\text{)}} * 100 \quad (3.6)$$

A significant relationship was observed between the free  $Zn^{2+}$  concentration and total chlorophyll *a* (Fig. 3.10A). The free  $Zn^{2+}$  concentration was better correlated than the  $Zn_T$  concentration to both fucoxanthin (Fig. 3.10B) and chlorophyll *c* (Fig. 3-10C).

## 3.5 Discussion

### 3.5.1 Total Dissolved Zn

Near-surface concentrations of  $Zn_T$  increased along an east to west transect in the N. Pacific. This trend agrees well with the trend of integrated Zn in the upper 100 m from a previous study in the region (Fukuda et al., 2000). The low value at St. 1 (0.10 nM) is in the range of values reported for the near-surface in that vicinity (0.06 - 0.25 nM, Martin et al. 1989). During the SEEDS Fe enrichment experiment, which was performed further west of St. 6 (48.5°N, 165°W), near-surface  $Zn_T$  concentrations were even higher than those observed at St. 6 (1.18 - 2.35 nM, Kinugasa et al. 2005). In the Bering Sea, highest  $Zn_T$  concentrations were observed in the western portion of the Bering Sea, which can experience high dust inputs from Asian deserts (Boyd et al., 1998; Nishioka et al., 2003). Lower  $Zn_T$  was observed in the eastern Bering Sea on the Bering Shelf where chlorophyll concentrations were high.

The  $Zn_T$  depth profiles reported here agree well with previous studies, exhibiting nutrient-like behavior (Bruland et al., 1978; Bruland, 1980; Martin et al., 1989; Bruland et al., 1994; Lohan et al., 2002).  $Zn_T$  concentrations from St. 1 are plotted with  $Zn_T$  concentrations from two studies (Martin et al., 1989; Fujishima et al., 2001) where profiles were measured in close proximity to St. 1 (Fig. 3-11). The profiles from all three studies are in close agreement, with values approaching zero in the upper 100 m of the water column, increasing most significantly between 150 and 500 m and reaching a maximum concentration of ~10 nM.



Excluding the likely contaminated 3000 m data, the profiles from this study reach maximum concentrations of 10-10.5 nM. These values agree well with Martin et al. (1989) who found  $Zn_T$  concentrations of 10-10.5 nM at 1500 m for VERTEX stations T-5 thru T-8 and Fujishima et al. (2001) who found deep water  $Zn_T$  concentrations across the subarctic N. Pacific to be 10-11 nM. In the central North Pacific, between 20 - 30°N,  $Zn_T$  concentrations reached maximums of only about 9.5 nM (Bruland et al., 1978; Bruland, 1980; Bruland et al., 1994). Lohan et al. (2002) report  $Zn_T$  profiles down to 400 m in the eastern subarctic N. Pacific. The maximum values at 400 m were generally 8-10 nM, though at St. P4,  $Zn_T$  was 14.4 nM at 400 m. This station was on the shelf and had elevated concentrations throughout the profile which the authors attribute to coastal upwelling (as evidenced by temperature and salinity data). The higher deep Zn values in the subarctic N. Pacific relative to the central N. Pacific are likely due to increasing time for remineralized Zn to reach the deep waters as they move northward.

At St. 4,  $Zn_T$  concentrations from the same profile were also measured using isotope dilution, magnesium hydroxide pre-concentration coupled with an anion exchange resin (S. John, unpubl. data). The results from that method showed excellent agreement with the shape of the entire profile from this study. In addition, the  $Zn_T$  concentrations were usually the same within the error of the measurement. In the upper 1500 m, only three samples out of ten had significantly different concentrations, where the ranges based on the standard deviations did not overlap (100, 150, and 1500 m). In two of three of these samples S. John observed a lower  $Zn_T$  concentration than this study (150 and 1500 m). The discrepancy between the  $Zn_T$  values at these three depths warrants the re-analysis of those depths. However, it is very encouraging that the two studies agree for the majority of the samples, especially considering the high precision of the measurements (standard deviations generally ~0.1 nM). Additionally, the two studies match at the low  $Zn_T$  end of the profile, which should be the more difficult measurements to make.

Near-surface  $Zn_T$  concentrations in the Bering Sea were high (~1 nM) in the deep western portion of the basin and low in the eastern waters over the Bering shelf. Previous studies of Zn in the Bering Sea have shown elevated  $Zn_T$  concentrations at depth (3.5 nM at 30 m and 20 nM at 3000 m) in the western Bering Sea (Fujishima et al., 2001), but low surface  $Zn_T$  concentrations (<0.41 nM, Fujishima et al. 2001; Leblanc et al. 2005). At St. 8, the mixed layer was only 15 m, and the  $PO_4$  concentration at 20 m was 1.56  $\mu$ M compared with only 1.25  $\mu$ M at the surface. Thus, the high  $Zn_T$  at St. 8 is likely a result of sampling below

the mixed layer, at a depth where significant remineralization is occurring. The mixed layer at St. 9 is about 18-20 m and the near-surface sample from this station was taken from 20 m. Unfortunately, nutrient data is not available for St. 9, so it is difficult to conclusively say that the high  $Zn_T$  value is due to the sample being below the mixed layer. An alternate explanation for the elevated  $Zn_T$  concentration observed is that it is a result of recent atmospheric inputs.

Dust from Asian deserts and loess regions is deposited to the N. Pacific and Bering Sea with highest depositions occurring at mid to high latitudes (Duce and Tindale, 1991). A map of aerosol index, a proxy for dust concentration, compiled for July 20, 2003 (shortly before we sampled stations 8 & 9) is shown in Fig. 3-12. The most striking feature of this map is the Saharan dust plume over the tropical Atlantic. However, it also shows a high concentration of dust over the Chukchi peninsula of Russia, just north of the Bering Sea.

Dust has the potential to input significant amounts of trace metals to the surface ocean. Bruland (1980) calculated that atmospheric deposition rates of copper and Zn could be similar to inputs from vertical mixing, and data collected as part of the Sea-Air Exchange (SEAREX) experiments generally support this conclusion (Arimoto et al. 1989, and references therein). Dust deposition to the N. Pacific is typically maximal in March-June, though deposition can be very episodic (Arimoto et al., 1989).

In order to assess of whether or not atmospheric flux could realistically explain the high  $Zn_T$  values in this study, an attempt was made to calculate atmospheric Zn fluxes for St. 9. To increase the Zn concentration by 0.8 nM in the upper 19 m, would require  $15 \mu\text{mol m}^{-2}$  of Zn. Tsunogai et al. (1985) calculate a relationship for mineral dust concentration based on the distance from the Asian coast:

$$C = 0.76 + 53.5^{(-1.43e-3 * X)} \quad (3.7)$$

where C is the dust concentration in  $\mu\text{g m}^{-3}$ , X is distance in km, and where the constants are calculated for stations above 30°N. From this relationship, a dust concentration of  $1.42 \mu\text{g m}^{-3}$  is calculated for St. 9. The concentration of dust was converted to Zn concentration based on dust containing 8% Al (crustal abundance) and on an Al:Zn ratio of 123.5 which has been observed in Asian dust (Duce et al., 1983). The calculated Zn concentration ( $0.9 \text{ ng m}^{-3}$ ) is the same order of magnitude as the Zn concentration measured in dust at the Enewetak Atoll in the equatorial N. Pacific ( $0.2 \text{ ng m}^{-3}$ , Duce et al. 1983). The depositional flux of dust

can be described by the equation

$$F = V * C \quad (3.8)$$

where  $F$  is the flux in  $\mu\text{g sec}^{-1} \text{ m}^{-2}$ ,  $V$  is the depositional velocity in  $\text{cm sec}^{-1}$  and  $C$  is the dust concentration in  $\mu\text{g m}^{-3}$ . A depositional velocity for the central N. Pacific was calculated as  $2 \text{ cm sec}^{-1}$  (Uematsu et al., 1985), however  $1 \text{ cm sec}^{-1}$  is a more commonly used depositional velocity. Using a depositional velocity of  $2 \text{ cm sec}^{-1}$  and the Zn dust concentration calculated above, to get the desired Zn flux of  $15 \mu\text{mol m}^{-2}$  would require 6 days. At the more commonly used depositional velocity of  $1 \text{ cm sec}^{-1}$ , this time is increased to 12 days. This calculation assumes that all the Zn in the dust dissolves. Determining the amount of metals which dissolve in the ocean upon dust deposition is an active area of research (e.g., Sedwick et al. (2006)). A 100% dissolution value is certainly an overestimation, and the true dissolution value is likely closer to 10%, though this value is not well constrained. Air-mass trajectories produced by the NOAA HYSPLIT model ([www.arl.noaa.gov/ready](http://www.arl.noaa.gov/ready)), show that air reaching St. 9 on July 24, 2003 spent time over the Asian land mass and the tropical Pacific where dust concentrations can be high. Thus, it is possible that atmospheric deposition may influence the Zn concentration in the mixed layer at this site.

### 3.5.2 Zn Speciation

At all stations, Zn speciation was dominated by complexation to organic ligands with an average  $[L_T]$  of 2.2 nM and  $K'_{cond,Zn'}$  of  $10^{10.1}$ . These results agree fairly well with previous measurements of Zn speciation in the North Pacific where Bruland (1989); Donat and Bruland (1990) observed ligand concentrations of 1.0-2.2 nM that had  $K'_{cond,Zn'}$ 's of  $10^{10.6} - 10^{11.2}$ . In general, the  $[L_T]$ 's in this study were higher and the  $K'_{cond,Zn'}$ 's lower than those of Bruland (1989). The values observed in this study are more similar to those in subantarctic waters near New Zealand where the  $[L_T]$  ranged from 1.3 - 2.5 nM and  $K'_{cond,Zn'}$  was between  $10^{9.7}$  and  $10^{10.4}$  (Ellwood, 2004). The  $\text{Zn}^{2+}$  concentrations in this study are similar to those predicted by previous studies in the oligotrophic ocean (Table 3.3). The lowest  $\text{Zn}^{2+}$  concentration was observed in the eastern portion of the subarctic N. Pacific where the majority of previous studies have focused.

The concentration of Zn binding ligands generally increased along the transect from east to west, similar to the trend in  $\text{Zn}_T$  (Fig. 3-7B). This resulted in a more stable  $\text{Zn}^{2+}$  concentration (changed by ~4-fold) than

total Zn concentration (changed by almost 9-fold, Fig. 3-13). The  $Zn^{2+}$  accounted for 2-5% of the total Zn concentration, similar to previous studies of Zn speciation in the open ocean (Bruland, 1989; Ellwood and van den Berg, 2000). Culture work has shown that phytoplankton can exude Zn binding ligands (Vasconcelos et al., 2002). In this study, the highest  $[L_T]$  was observed at St. 8, where chlorophyll was also highest and the lowest  $[L_T]$  was observed at St. 1 where the chlorophyll concentration was lowest. However, there did not appear to be a significant relationship between chlorophyll and  $[L_T]$  ( $R^2 = 0.49$ ).

The  $[L_T]$  at St. 8 in the Bering Sea (3.6 nM) is the highest reported value of Zn binding ligands in the open ocean measured by voltammetric methods. Ligand concentrations as high as 6 nM have been reported in bottle incubations after the addition of Zn (Lohan et al., 2005) and much higher concentrations (>20 nM) have been observed in coastal waters and phytoplankton cultures (van den Berg, 1985; Vasconcelos et al., 2002). St. 8 had the highest  $Zn_T$  concentration of any station where Zn speciation measurements were performed (0.89 nM). The concentration of Zn binding ligands measured represent a snapshot of a pool that is dynamic and can change on short timescales in response to the addition of Zn (Lohan et al., 2005). As previously discussed, the  $Zn_T$  concentrations in the Bering Sea may have been influenced by recent atmospheric deposition, in which case, the high  $[L_T]$  may be due to active production of Zn binding ligands by the microbial community in order to enhance the residence time of Zn in the surface mixed layer. A high abundance of copper binding ligands was also observed at St. 8 (J. Moffett, unpubl. data).

### 3.5.3 Shipboard Incubation

Previous shipboard incubations in the N. Pacific have shown little (Coale, 1991; Crawford et al., 2003) or no effect (Lohan et al., 2005; Leblanc et al., 2005) on total chlorophyll concentration due to the addition of Zn. In this study, Zn additions were performed at a number of stations (Table 3.3). A chlorophyll response to Zn addition was only observed at St. 5. Near-surface  $Zn_T$  concentrations at St. 5 were relatively high, as was the concentration of  $Zn^{2+}$  at 22 pM. The pigment distribution at St. 5 was very similar to that at St. 6, where Zn addition had no effect. There is no obvious difference at St. 5 which explains why Zn should be limiting at that station rather than the others. Thus, this study adds to the enigmatic story of Zn limitation of phytoplankton. Though the importance of Zn to phytoplankton growth is exhibited by its nutrient-like profile and numerous culture studies, traditional grow-out experiments do not clearly demonstrate Zn's ability to

control marine primary production.

Fe contamination is a possible explanation for the positive result to Zn addition at this site. No growth was observed in the control bottles or in a treatment of 500 pM added Co (M. Saito et al., unpubl. data). Thus it seems unlikely that contamination would have randomly occurred in the two +Zn bottles and not in any of the four control or +Co bottles.

Previous studies have examined the ability of Fe and Zn limitation to affect nitrate ( $\text{NO}_3$ ) and Si utilization (De La Rocha et al., 2000; Franck et al., 2003). In cultures of the diatom *T. weissflogii*, Fe and Zn deficiency resulted in a higher Si content than in Fe and Zn replete diatoms (De La Rocha et al., 2000). Franck et al. (2003) performed a series of incubation experiments in Fe-limited upwelling regions and often observed an increase in the Si: $\text{NO}_3$  utilization ratio when Zn was added and a decrease in the Si: $\text{NO}_3$  utilization ratio when Fe or Fe and Zn together were added. In this study, a decrease in the Si: $\text{NO}_3$  utilization ratio was observed in all the metal treatments relative to the control (Table 3.2).

### 3.5.4 Zn and HPLC pigments

Fucoxanthin is a classic marker of diatom biomass and chlorophyll c is also a pigment found in diatoms. These two pigments were the only pigments that showed any significant correlation with the total Zn concentration. Diatoms have a high Zn requirement (Sunda and Huntsman, 1995). The relationship observed here is suggestive of Zn being a potential determinant of diatom biomass. An even stronger correlation was observed between the two diatom pigments and the free  $\text{Zn}^{2+}$  concentration. This is consistent with the free ion model of Zn bioavailability. Unfortunately, these relationships are based on limited data. Interpreting pigment data can be difficult because organisms contain multiple pigments and the pigment composition of field organisms does not accurately match those of cultured organisms (B. Bidigare, pers. comm.). It would be ideal to have diatom cell counts or biogenic silica for this data set to evaluate this relationship. However, the presented correlations are interesting, as they are the only data to the author's knowledge comparing Zn and phytoplankton pigment signatures in the open ocean.

### 3.6 Conclusions

This study builds on previous work in the Pacific, providing a transect of near-surface  $Zn_T$  concentrations in the subarctic North Pacific and Bering Sea and deep profiles of  $Zn_T$  in the central and western subarctic North Pacific.  $Zn_T$  concentrations in the North Pacific followed an increasing east to west gradient consistent with previous studies. High concentrations of  $Zn_T$  in the near-surface of the western Bering Sea are likely an artifact of sampling below the shallow mixed layer and may not necessarily reflect a spatial trend. However atmospheric deposition from the nearby Asian continent may influence metal concentrations in the Bering Sea. Zn was tightly bound by natural organic ligands, the concentration of which was correlated well with  $Zn_T$  concentration. Zn addition resulted in an increase in chlorophyll at one station in the North Pacific. This result supports the assertion that Zn is an important micronutrient that may be able to limit phytoplankton growth. However, negative results to Zn additions at similar sites confound the conclusion. A positive correlation was observed between two pigments found in diatoms and the total and free  $Zn^{2+}$  concentrations. This suggests that Zn may be a determinant of diatom growth in the region, though this relationship warrants further study.

### **3.7 Acknowledgments**

The author would like to thank the captain and crew of the R/V Kilo Moana, Bob Bidigare and Chief Scientist Brian Popp who invited the authors on the Kilo Moana cruise. Thanks also to Mak Saito and Yan Xu who partnered the incubation experiment and ran chlorophyll analyses. The author would also like to thank Dave Schneider and Lary Ball of the WHOI Plasma Mass Spectrometry Facility for assistance with ICP-MS measurements. Thanks to Seth John for motivating and partnering the Zn radiotracer work and for sharing his analyses of  $Zn_T$  at St. 4. Brian Popp and Adriana Eskinasy provided the shipboard phosphate data and Bob Bidigare's group provided the HPLC pigment data. Thanks to Ed Boyle for helpful discussions on the total Zn analysis. Thanks to Gary Fones and Chris Dupont for assistance with sampling. This research was supported by NSF grant OCE-0136835 and by an EPA STAR Fellowship.

## Bibliography

- ANDERSON, M. A., F. M. M. MOREL, and R. R. L. GUILLARD. 1978. Growth limitation of a coastal diatom by low zinc ion activity. *Nature*. **276**: 70–71.
- ARIMOTO, R., R. A. DUCE, and B. J. JAY. 1989. Chemical oceanography. J. P. RILEY and R. CHESTER [Eds.]. *Chemical Oceanography*. . volume 10. chapter 56: Concentrations, sources and air-sea exchange of trace elements in the atmosphere over the Pacific Ocean, pp. 107–149. New York, USA. Academic Press.
- BIDIGARE, R. R. 1991. Marine particles: analysis and characterization. D. C. HURD and D. W. SPENCER [Eds.]. *Marine particles: analysis and characterization*. chapter Analysis of algal chlorophylls and carotenoids, pp. 119–123. Washington, D. C. American Geophysical Union.
- BIDIGARE, R. R., and C. C. TREES. 2000. Ocean optics protocols for satellite ocean color sensor validation, revision 2. J. MUELLER and G. FARGION [Eds.]. *Ocean optics protocols for satellite ocean color sensor validation, revision 2*. chapter HPLC phytoplankton pigments: sampling, laboratory methods, and quality assurance procedures, pp. 154–161. NASA Technical Memorandum 2000-209966.
- BOYD, P. W., C. S. LAW, C. S. WONG, Y. NOJIRI, A. TSUDA, M. LEVASSEUR, S. TAKEDA, R. RIVKIN, P. J. HARRISON, R. STRZEPEK, J. GOWER, R. M. MCKAY, E. ABRAHAM, M. ARYCHUK, J. BARWELL-CLARKE, W. CRAWFORD, D. CRAWFORD, M. HALE, K. HARADA, K. JOHNSON, H. KIYOSAWA, I. KUDO, A. MARCHETTI, W. MILLER, J. NEEDOBA, J. NISHIOKA, H. OGAWA, J. PAGE, M. ROBERT, H. SAITO, A. SASTRI, N. SHERRY, T. SOUTAR, N. SUTHERLAND, Y. TAIRA, F. WHITNEY, S. E. WONG, and T. YOSHIMURA. 2004. The decline and fate of an iron-induced subarctic phytoplankton bloom. *Nature*. **428**: 549–553.
- BOYD, P. W., D. L. MUGGLI, D. E. VARELA, R. H. GOLDBLATT, R. CHRETIEN, K. J. ORIAN, and P. J. HARRISON. 1996. In vitro iron enrichment experiments in the NE subarctic Pacific. *Marine Ecology Progress Series*. **136**: 179–193.
- BOYD, P. W., C. S. WONG, J. MERRILL, F. WHITNEY, J. SNOW, P. J. HARRISON, and J. GOWER. 1998. Atmospheric iron supply and enhanced vertical carbon flux in the NE subarctic Pacific: Is there a connection? *Global Biogeochemical Cycles*. **12**: 429–441.
- BRAND, L. E., W. G. SUNDA, and R. R. L. GUILLARD. 1983. Limitation of marine phytoplankton reproductive rates by Zn, Mn, and Fe. *Limnology and Oceanography*. **28**: 1182–1198.
- BRULAND, K. W. 1980. Oceanographic distributions of cadmium, zinc, nickel, and copper in the North Pacific. *Earth and Planetary Science Letters*. **47**: 176–198.
- BRULAND, K. W. 1989. Complexation of zinc by natural organic ligands in the central North Pacific. *Limnology and Oceanography*. **34**: 269–285.
- BRULAND, K. W., G. A. KNAUER, and J. H. MARTIN. 1978. Zinc in north-east Pacific water. *Nature*. **271**: 741–743.
- BRULAND, K. W., K. J. ORIAN, and J. P. COWEN. 1994. Reactive trace metals in the stratified central North Pacific. *Geochimica et Cosmochimica Acta*. **58**: 3171–3182.



- COALE, K. H. 1991. Effects of iron, manganese, copper, and zinc enrichments on productivity and biomass in the subarctic Pacific. *Limnology and Oceanography*. **36**: 1851–1864.
- COALE, K. H., K. S. JOHNSON, S. E. FITZWATER, R. M. GORDON, S. TANNER, F. P. CHAVEZ, L. FERIOLO, C. SAKAMOTO, P. ROGERS, F. MILLERO, P. STEINBERG, P. NIGHTINGALE, D. COOPER, W. P. COCHLAN, M. R. LANDRY, J. CONSTANTINOU, G. ROLLWAGEN, A. TRASVINA, and R. KUDELA. 1996. A massive phytoplankton bloom induced by an ecosystem-scale iron fertilization experiment in the equatorial Pacific Ocean. *Nature*. **383**: 495–501.
- COALE, K. H., X. J. WANG, S. J. TANNER, and K. S. JOHNSON. 2003. Phytoplankton growth and biological response to iron and zinc addition in the Ross Sea and Antarctic Circumpolar Current along 170 degrees W. *Deep-Sea Research II*. **50**: 635–653.
- CRAWFORD, D. W., M. S. LIPSEN, D. A. PURDIE, M. C. LOHAN, P. J. STATHAM, F. A. WHITNEY, J. N. PUTLAND, W. K. JOHNSON, N. SUTHERLAND, T. D. PETERSON, P. J. HARRISON, and C. S. WONG. 2003. Influence of zinc and iron enrichments on phytoplankton growth in the northeastern subarctic Pacific. *Limnology and Oceanography*. **48**: 1583–1600.
- DE LA ROCHA, C. L., D. A. HUTCHINS, M. A. BRZEZINSKI, and Y. ZHANG. 2000. Effects of iron and zinc deficiency on elemental composition and silica production by diatoms. *Marine Ecology Progress Series*. **195**: 71–79.
- DONAT, J. R., and K. W. BRULAND. 1990. A comparison of two voltammetric techniques for determining zinc speciation in Northeast Pacific Ocean waters. *Marine Chemistry*. **28**: 301–323.
- DUCE, R. A., R. ARIMOTO, B. J. RAY, C. K. UNNI, and P. J. HARDER. 1983. Atmospheric trace elements at Enewetak Atoll: I, concentrations, sources, and temporal variability. *Journal of Geophysical Research*. **88**: 5321–5342.
- DUCE, R. A., and N. W. TINDALE. 1991. Atmospheric transport of iron and its deposition in the ocean. *Limnology and Oceanography*. **36**: 1715–1726.
- ELLWOOD, M. J. 2004. Zinc and cadmium speciation in subantarctic waters east of New Zealand. *Marine Chemistry*. **87**: 37–58.
- ELLWOOD, M. J., and C. M. G. VAN DEN BERG. 2000. Zinc speciation in the Northeastern Atlantic Ocean. *Marine Chemistry*. **68**: 295–306.
- FISCHER, E., and C. M. G. VAN DEN BERG. 1999. Anodic stripping voltammetry of lead and cadmium using a mercury film electrode and thiocyanate. *Analytica Chimica Acta*. **385**: 273–280.
- FRANCK, V. M., K. W. BRULAND, D. A. HUTCHINS, and M. A. BRZEZINSKI. 2003. Iron and zinc effects on silicic acid and nitrate uptake kinetics in three high-nutrient, low-chlorophyll (HNLC) regions. *Marine Ecology Progress Series*. **252**: 15–33.
- FUJISHIMA, Y., K. UEDA, M. MARUO, E. NAKAYAMA, C. TOKUTOME, H. HASEGAWA, M. MATSUI, and Y. SOHRIN. 2001. Distribution of trace bioelements in the subarctic North Pacific Ocean and the Bering Sea (the R/V Hakuho Maru cruise KH-97-2). *Journal of Oceanography*. **57**: 261–273.

- FUKUDA, R., Y. SOHRIN, N. SAOTOME, H. FUKUDA, T. NAGATA, and I. KOIKE. 2000. East-west gradient in ectoenzyme activities in the subarctic pacific: Possible regulation by zinc. *Limnology and Oceanography*. **45**: 930–939.
- GALL, M. P., R. STRZEPEK, M. MALDONADO, and P. W. BOYD. 2001. Phytoplankton processes. part 2: Rates of primary production and factors controlling algal growth during the Southern Ocean Iron RElease Experiment (SOIREE). *Deep-Sea Research II*. **48**: 2571–2590.
- HEUMANN, K. G. 1988. Isotope dilution mass spectrometry, chapter 7, pp. 301–375. *In* F. ADAMS, R. GIBBELS and R. VAN GRIEKEN [Eds.], *Inorganic Mass Spectrometry*, volume 95. John Wiley & Sons. New York, USA.
- JEFFREY, S. W., and G. F. HUMPHREY. 1975. New spectrophotometric equations for determining chlorophylls a, b, c1, and c2 in higher-plants, algae and natural phytoplankton. *Biochemie und Physiologie der Pflanzen*. **167**: 191–194.
- KINUGASA, M., T. ISHITA, Y. SOHRIN, K. OKAMURA, S. TAKEDA, J. NISHIOKA, and A. TSUDA. 2005. Dynamics of trace metals during the subarctic Pacific iron experiment for ecosystem dynamics study (SEEDS2001). *Progress in Oceanography*. **64**: 129–147.
- LAM, P. J., P. D. TORTELL, and F. M. M. MOREL. 2001. Differential effects of iron additions on organic and inorganic carbon production by phytoplankton. *Limnology and Oceanography*. **46**: 1199–1202.
- LEBLANC, K., C. E. HARE, P. W. BOYD, K. W. BRULAND, B. SOHST, S. PICKMERE, M. C. LOHAN, K. BUCK, M. ELLWOOD, and D. A. HUTCHINS. 2005. Fe and Zn effects on the Si cycle and diatom community structure in two contrasting high and low-silicate HNLC areas. *Deep-Sea Research I*. **52**: 1842–1864.
- LEE, J. G., S. B. ROBERTS, and F. M. M. MOREL. 1995. Cadmium: a nutrient for the marine diatom *Thalassiosira weissflogii*. *Limnology and Oceanography*. **40**: 1056–1063.
- LOHAN, M. C., D. W. CRAWFORD, D. A. PURDIE, and P. J. STATHAM. 2005. Iron and zinc enrichments in the northeastern subarctic pacific: Ligand production and zinc availability in response to phytoplankton growth. *Limnology and Oceanography*. **50**: 1427–1437.
- LOHAN, M. C., P. J. STATHAM, and D. W. CRAWFORD. 2002. Total dissolved zinc in the upper water column of the subarctic North East Pacific. *Deep-Sea Research II*. **49**: 5793–5808.
- MAHER, W., and L. WOO. 1998. Procedures for the storage and digestion of natural waters for the determination of filterable reactive phosphorus, total filterable phosphorus and total phosphorus. *Analytica Chimica Acta*. **375**: 5–47.
- MARTIN, J. H., and S. E. FITZWATER. 1988. Iron deficiency limits phytoplankton growth in the north-east Pacific subarctic. *Nature*. **331**: 341–343.
- MARTIN, J. H., R. M. GORDON, S. FITZWATER, and W. W. BROENKOW. 1989. VERTEX: phytoplankton/iron studies in the gulf of alaska. *Deep-Sea Research*. **36**: 649–680.
- MCALLISTER, C. D., T. R. PARSONS, and J. D. H. STRICKLAND. 1960. Primary productivity and fertility at station "P" in the north-east Pacific Ocean. *Journal du Conseil*. **25**: 240–259.

- MOREL, F. M. M., R. J. M. HUDSON, and N. M. PRICE. 1991. Limitation of productivity by trace-metals in the sea. *Limnology and Oceanography*. **36**: 1742–1755.
- MURPHY, J., and J. P. RILEY. 1962. A modified single solution method for the determination of phosphate in natural waters. *Analytica Chimica Acta*. **27**: 31–36.
- NISHIOKA, J., S. TAKEDA, I. KUDO, D. TSUMUNE, T. YOSHIMURA, K. KUMA, and A. TSUDA. 2003. Size-fractionated iron distributions and iron-limiting processes in the subarctic NW Pacific. *Geophysical Research Letters*. **30**: 1730.
- RUZIC, I. 1982. Theoretical aspects of the direct titration of natural waters and its information yield for trace metal speciation. *Analytica Chimica Acta*. **140**: 99–113.
- SAITO, M. A., J. W. MOFFETT, S. W. CHISHOLM, and J. B. WATERBURY. 2002. Cobalt limitation and uptake in *Prochlorococcus*. *Limnology and Oceanography*. **47**: 1629–1636.
- SAITO, M. A., and D. L. SCHNEIDER. 2006. Examination of precipitation chemistry and improvements in precision using the Mg(OH)<sub>2</sub> preconcentration ICP-MS method for high-throughput analysis of open-ocean Fe and Mn in seawater. *Analytica Chimica Acta*. *in press*.
- SCHAREK, R., M. A. VAN LEEUWE, and H. J. W. DEBAAR. 1997. Responses of Southern Ocean phytoplankton to the addition of trace metals. *Deep-Sea Research II*. **44**: 209–227.
- SCHULZ, K. G., I. ZONDERVAN, L. J. A. GERRINGA, K. R. TIMMERMANS, M. J. W. VELDHUIS, and U. RIEBESELL. 2004. Effect of trace metal availability on coccolithophorid calcification. *Nature*. **430**: 673–676.
- SEDWICK, P. N., E. R. SHOLKOVITZ, and T. M. CHURCH. 2006. Solubility of aerosol iron in the surface ocean: a new paradigm based on field observations in the Sargasso Sea. *Eos Trans. AGU*. **87** (36). *Ocean Sci. Meet. Suppl.*, Abstract OS11N-03.
- SHAKED, Y., Y. XU, K. LEBLANC, and F. M. M. MOREL. 2006. Zinc availability and alkaline phosphatase activity in *Emiliana huxleyi*: implications for Zn-P co-limitation in the ocean. *Limnology and Oceanography*. **51**: 299–309.
- SUNDA, W. G., and S. A. HUNTSMAN. 1995. Cobalt and zinc interreplacement in marine phytoplankton: Biological and geochemical implications. *Limnology and Oceanography*. **40**: 1404–1417.
- TSUDA, A., S. TAKEDA, H. SAITO, J. NISHIOKA, Y. NOJIRI, I. KUDO, H. KIYOSAWA, A. SHIOMOTO, K. IMAI, T. ONO, A. SHIMAMOTO, D. TSUMUNE, T. YOSHIMURA, T. AONO, A. HIMUMA, M. KINUGASA, K. SUZUKI, Y. SOHRIN, Y. NOIRI, H. TANI, Y. DEGUCHI, N. TSURUSHIMA, H. OGAWA, K. FUKAMI, K. KUMA, and T. SAINO. 2003. A mesoscale iron enrichment in the western subarctic Pacific induces a large centric diatom bloom. *Science*. **300**: 958–961.
- TSUNOGAI, S., T. SUZUKI, T. KURATA, and M. UEMATSU. 1985. Seasonal and areal variation of continental aerosol in the surface air over the western North Pacific region. *Journal of the Oceanographical Society of Japan*. **41**: 427–434.
- TURNER, D. R., M. WHITFIELD, and A. G. DICKSON. 1981. The equilibrium speciation of dissolved components in freshwater and seawater at 25°C and 1 atm pressure. *Geochimica et Cosmochimica Acta*. **45**: 855–882.

- UEMATSU, M., R. A. DUCE, S. NAKAYA, and S. TSUNOGAI. 1985. Short-term temporal variability of eolian particles in surface waters of the northwestern North Pacific. *Journal of Geophysical Research*. **90**: 1167–1172.
- VAN DEN BERG, C. M. G. 1982. Determination of copper complexation with natural organic ligands in seawater by equilibration with  $\text{MnO}_2$  I. theory. *Marine Chemistry*. **11**: 307–342.
- VAN DEN BERG, C. M. G. 1985. Determination of the zinc complexing capacity in seawater by cathodic stripping voltammetry of zinc APDC complex-ions. *Marine Chemistry*. **16**: 121–130.
- VASCONCELOS, M. T. S. D., M. F. C. LEAL, and C. M. G. VAN DEN BERG. 2002. Influence of the nature of the exudates released by different marine algae on the growth, trace metal uptake and exudation of *Emiliania huxleyi* in natural seawater. *Marine Chemistry*. **77**: 187–210.
- WU, J., and E. A. BOYLE. 1998. Determination of iron in seawater by high-resolution isotope dilution inductively couple plasma mass spectrometry after  $\text{Mg}(\text{OH})_2$  coprecipitation. *Analytica Chimica Acta*. **367**: 183–191.
- YEE, D., and F. M. M. MOREL. 1996. In vivo substitution of zinc by cobalt in carbonic anhydrase of a marine diatom. *Limnology and Oceanography*. **41**: 573–577.

Table 3.1: Dissolved Zn and PO<sub>4</sub> data. Values in parentheses represent the standard deviation of duplicate or triplicate analyses for Zn<sub>T</sub>. Values in bold are likely contaminated, see Results section for details. PO<sub>4</sub> was measured by both the Popp group at sea (Ship PO<sub>4</sub>) and by the Ocean Data Center at Scripps Institute of Oceanography (ODC PO<sub>4</sub>).

St.	Dates Occupied	Latitude	Longitude	Depth (m)	Zn <sub>T</sub> (nM)	Ship PO <sub>4</sub> (μM)	ODC PO <sub>4</sub> (μM)	Chl a (μg L <sup>-1</sup> )	L <sub>T</sub> (nM)	logK <sup>*</sup> Zn <sub>T</sub> /Zn <sup>2+</sup>	Zn <sup>2+</sup> (nM)
1	24 Jun - 28 Jun 2003	41°60'N	140°06'W	15	0.10 (0.02)	0.24	0.29	0.14	1.1	9.1	0.005
				50	0.35 (0.01)	0.33		0.99			
				75	0.10 (0.02)	0.48		0.27			
				150	1.99 (0.02)						
				300	2.80 (0.10)						
				500	6.82 (0.03)						
				1000	8.89 (0.03)						
3	4 Jul - 5 Jul 2003	44°02'N	159°59'W	1500	10.30 (0.17)	1.10		0.37	1.9	9.7	0.006
				20	0.20 (0.03)	1.40	1.34	0.72			
				13	0.56 (0.10)	1.48	1.35	1.01	2.0	10.5	0.023
				26	0.71 (0.06)	1.56	1.47	0.41	2.8	10.6	0.020
				40	0.89 (0.08)	1.63	1.20	0.16			
				60	1.24 (0.11)	1.64	1.57	0.03	2.7	9.9	0.059
				100	1.51 (0.01)	2.08		0.01			
4	7 Jul - 8 Jul 2003	47°01'N	170°30'W	150	5.10 (0.07)						
				300	8.57 (0.59)		2.86				
				500	8.84 (0.14)		2.23				
				1000	7.95 (0.13)		2.86				
				1500	10.70 (0.06)		3.17				
				3000	<b>13.51 (0.04)</b>		2.20				
				25	0.65 (0.02)	1.41	1.40	0.81	1.9	10.7	0.022
				20	0.78 (0.11)	1.39	1.40	0.56	2.7	9.3	0.020
				40	1.66 (0.09)		1.45		2.4	9.8	0.104
				50	2.39 (0.29)	1.64		0.65			
				80	2.73 (0.01)	1.74	1.23	0.13			
				150	5.26 (0.02)	2.18	2.33	0.02			
				300	8.52 (0.02)	2.91	3.13				
				500	8.71 (0.10)						
1000	9.76 (0.10)										
1500	9.58 (0.27)										
3000	<b>12.27 (0.19)</b>										
8	21 Jul - 22 Jul 2003	55°18'N	176°31'E	20	0.89 (0.01)	1.56	1.46	0.86	3.6	9.2	0.016
				20	1.15 (0.02)						
9	24 Jul 2003	56°19'N	174°15'W	20	1.15 (0.02)						
10	26 Jul 2003	56°43'N	167°50'W	14	0.42 (0.05)	0.31		0.63			
11	27 Jul 2003	56°45'N	164°60'W	16	0.29 (0.02)	0.24		1.21			

Table 3.2: Time final (day 4) nutrient concentrations and nutrient drawdown ratios from the shipboard incubation performed at St. 5 in the North Pacific.

Treatment	NO <sub>3</sub> ( $\mu$ M)	PO <sub>4</sub> ( $\mu$ M)	Si ( $\mu$ M)	$\Delta$ Si/ $\Delta$ NO <sub>3</sub>	$\Delta$ Si/ $\Delta$ PO <sub>4</sub>
Time Zero	14.3	1.3	14.5		
Control	13.0	1.2	12.4	1.62	21.0
+Fe	7.4	0.8	9.2	0.77	10.6
+Zn/Fe	7.9	0.9	9.5	0.78	12.5
+Zn	10.6	1.0	11.4	0.84	10.3

Table 3.3: Summary table of incubation experiments performed in the North Pacific and Bering Sea during the summer of 2003. An X indicates that a treatment resulted in an increase in chlorophyll above a no-addition control. n.i. indicates no increase. Where spaces are empty, the treatment was not performed at that station. +Fe additions were performed by Saito et al. (unpubl. data) at stations 1, 3 & 4. A chlorophyll increase due to Fe addition was observed at stations 3 & 4, but not at St. 1.

Subarctic North Pacific							
St.	Location	+Zn	+DIP	+N	+Zn/N	+Fe	+Zn/Fe
1	41.60°N, 140.06°W	n.i.	n.i.	X	X		
3	44.02°N, 159.59°W	n.i.	n.i.	n.i.	n.i.		
4	47.01°N, 170.30°W	n.i.	n.i.	n.i.	n.i.		
5	46.59°N, 179.58°W	X				X	X
6	46.60°N, 170.20°E	n.i.				X	X
Bering Sea							
St.	Location	+Zn	+DIP	+Zn/DIP	+Fe/DIP	+Fe	+Zn/Fe
8	55.18°N, 176.31°E	n.i.				X	X
10	56.43°N, 167.50°W	n.i.	n.i.	n.i.	n.i.	n.i.	
11	56.45°N, 164.60°W	n.i.	n.i.	n.i.		n.i.	





Table 3.4: Estimations of  $Zn^{2+}$  concentrations in the mixed layer of oligotrophic regions based on voltammetric Zn speciation determinations.

Study Region	Sample	$Zn^{2+}$ (pM)	Reference	Speciation Method
North Pacific	50 m	<1 - 4	Bruland 1989	ASV
North Pacific	60 m	<1 - 5	Donat and Bruland 1990	ASV, CSV
North Pacific	15 m	2	Lohan et al. 2005	CSV
North Pacific	15 - 26 m transect	5 - 23	this study	ff-ASV
North Atlantic	3 m transect	6 - 23	Ellwood and van den Berg 2000	CSV
Southern Ocean	less than 80 m	<1 - 11	Ellwood 2004	ASV

Figure 3-1: Map of station locations from the North Pacific and Bering Sea visited aboard the R/V Kilo Moana in June-August 2003.

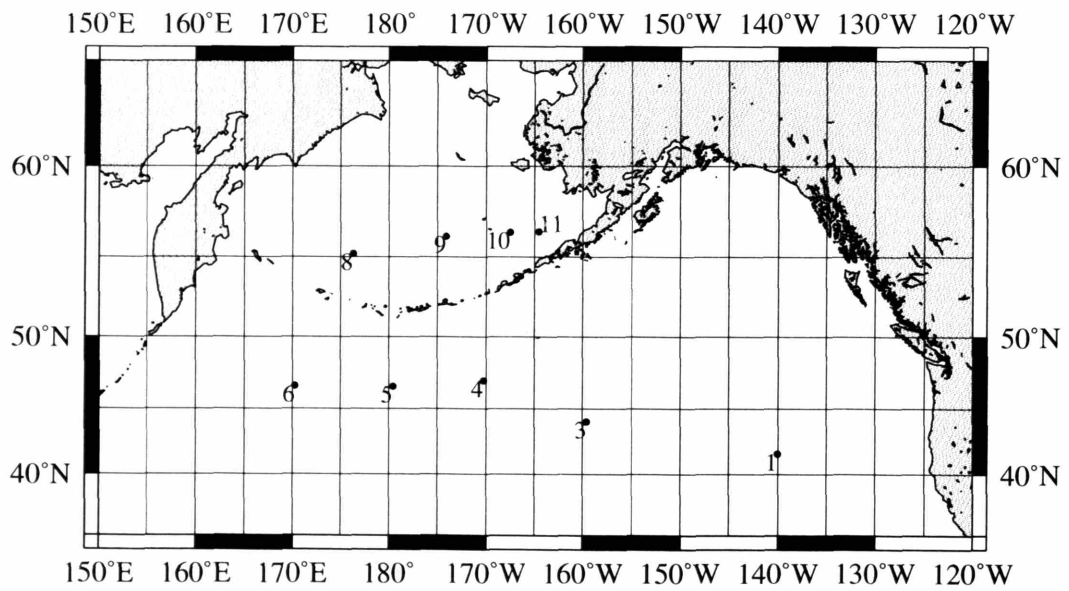


Figure 3-2: Total dissolved Zn concentrations from near surface samples along the transect. Presented on the station map (A) and (B) plotted by station number. Error bars represent the standard deviation of duplicate or triplicate analyses. Dashed line represents the average detection limit.

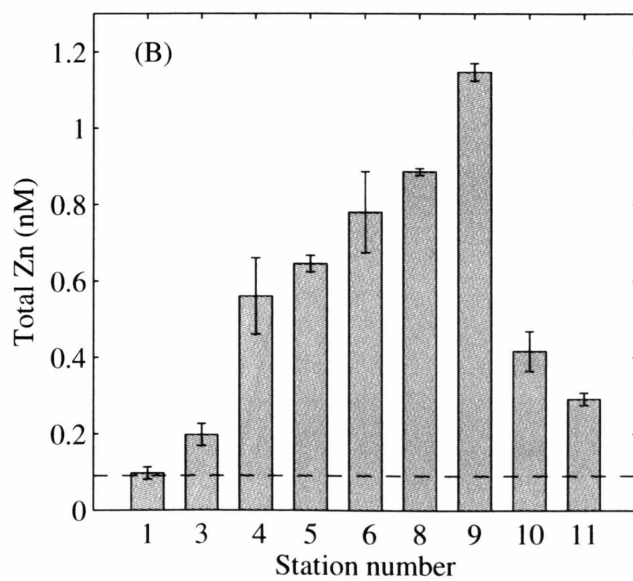
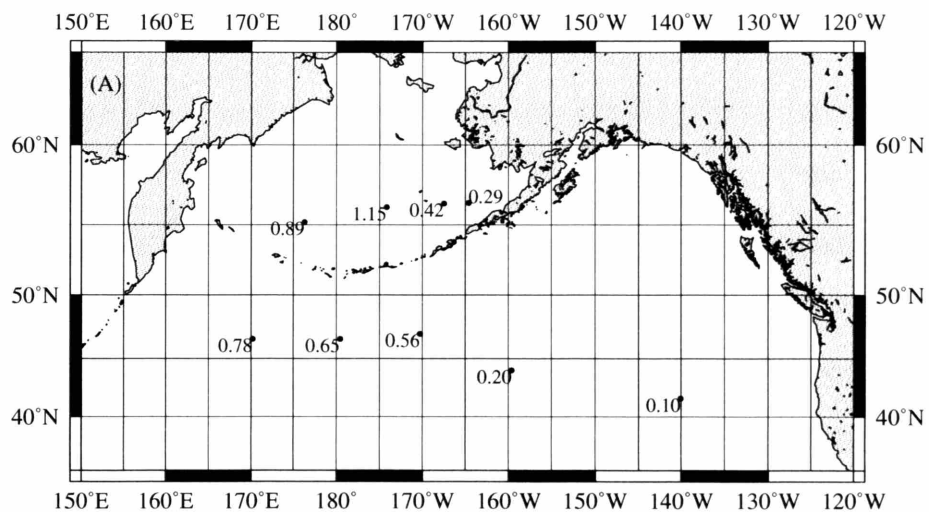


Figure 3-3: Depth profiles of total dissolved Zn concentrations from stations 1 (A), 4 (B), and 6 (C). Error bars represent the standard deviation of duplicate or triplicate analyses. Dashed line represents the detection limit. Note the change in y-scale between A and B & C.

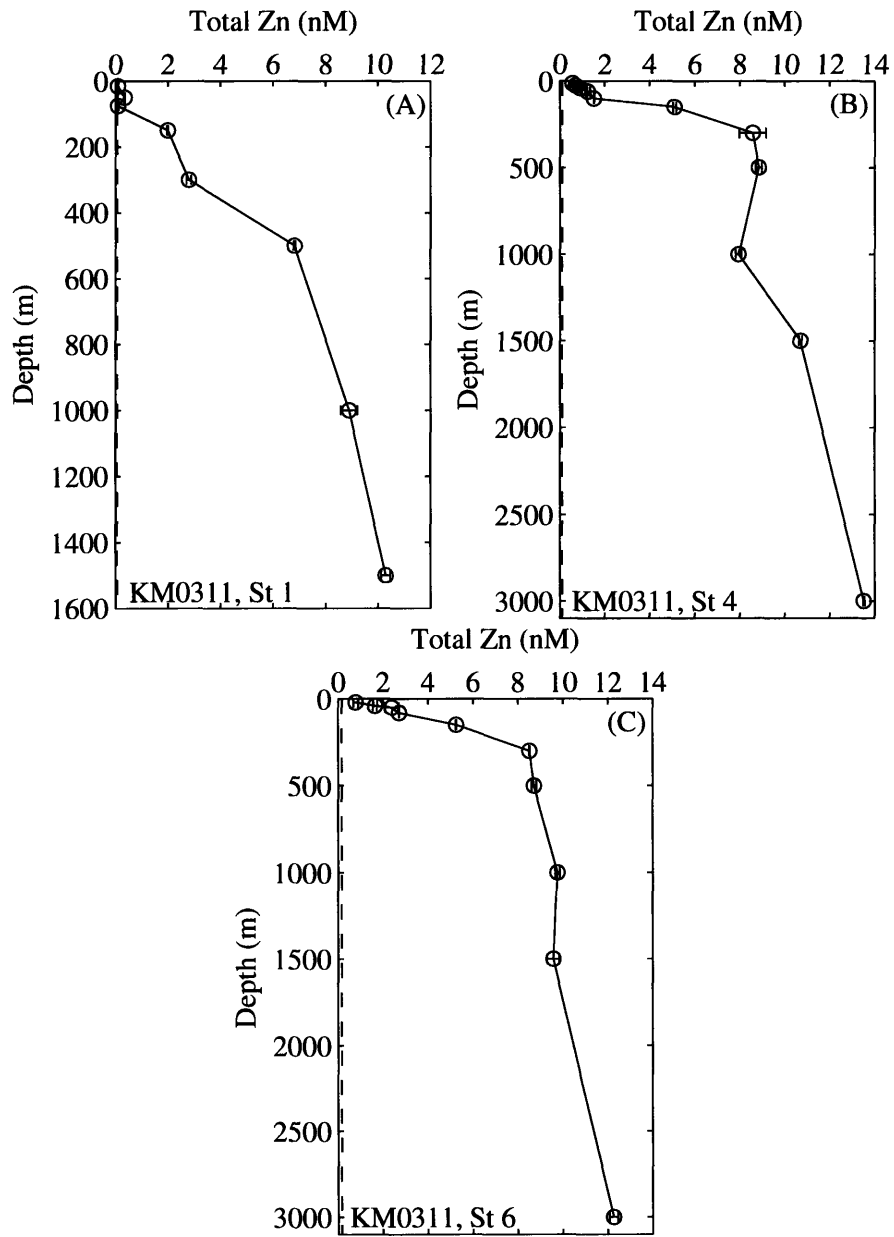


Figure 3-4: Comparison of total dissolved Zn concentrations (A) with salinity (B) and temperature profiles (C) in the upper 500 m at St. 4 . Dotted line and error bars in (A) as Fig. 3-3.

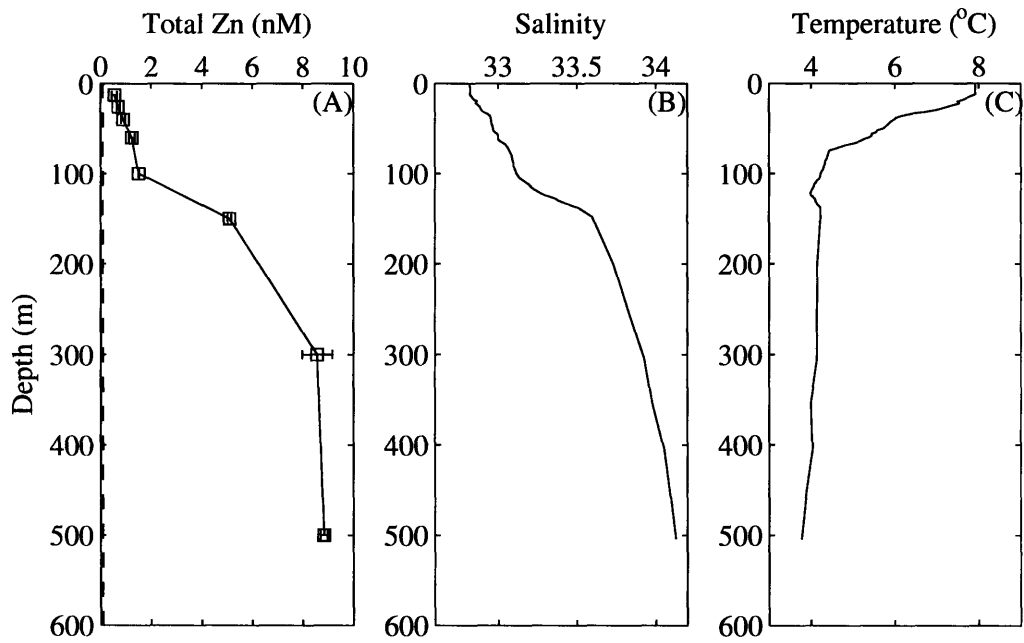


Figure 3-5: Total dissolved Zn concentrations versus PO<sub>4</sub> concentrations phosphate from all stations (A). In (B), suspect PO<sub>4</sub> values have been replaced with average values from surrounding depths (see Results section for more detail). Open circles represent data from this study and closed circles represent data from this study where the PO<sub>4</sub> values are suspected outliers. Open squares represent data from VERTEX stations T-5 and T-6, which are in close proximity to St. 1 (Martin et al., 1989). Zinc error bars as Fig. 3-3.

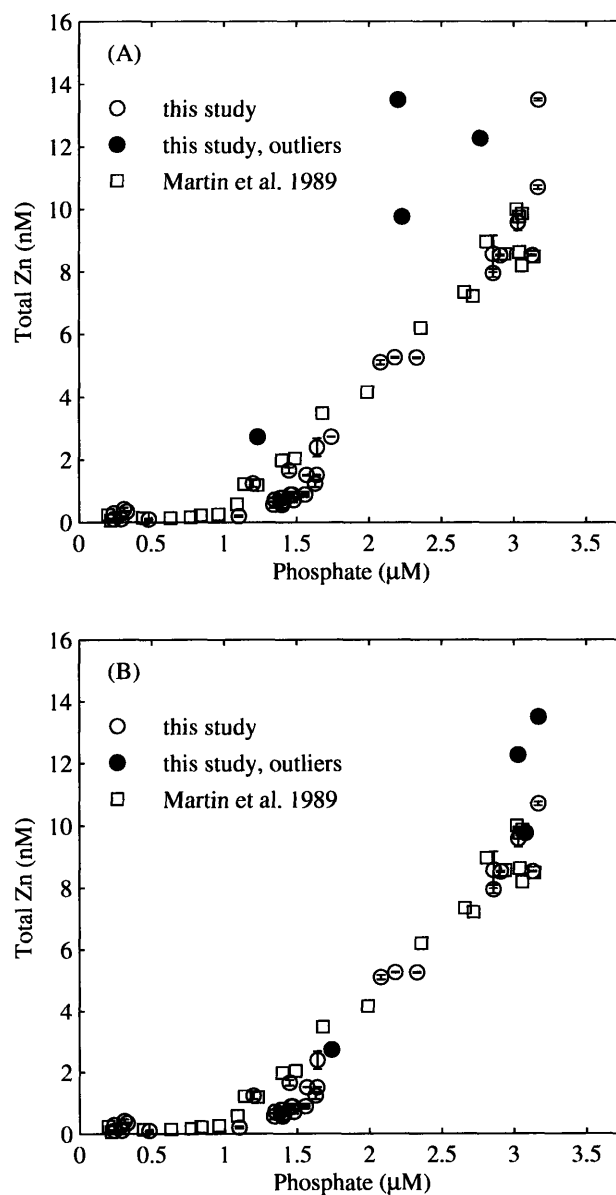


Figure 3-6: Total dissolved Zn concentrations from stations 1, 4, and 6 compared to silicate taken from the WOCE archive from stations close to these stations (Triangles). Squares are data taken from VERTEX stations T-5 and T-6, which are in close proximity to St. 1 (Martin et al., 1989). Line is a least-squares fit line for the  $Zn_T$  concentrations from this study and the WOCE silicate data ( $R^2 = 0.93$ ). Zn error bars as Fig. 3-3.

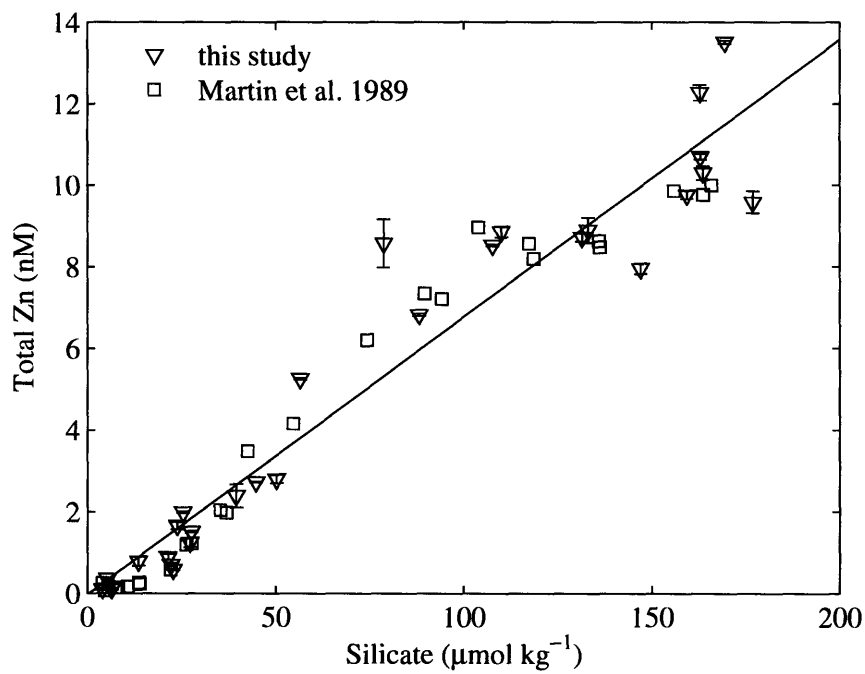


Figure 3-7: Concentration of Zn binding ligands ( $L_T$ ) in the near surface along the first portion of the transect shown in relation to station number (A) and total dissolved Zn concentration (B). Line in (B) is a least-squares fit line ( $R^2 = 0.68$ ).

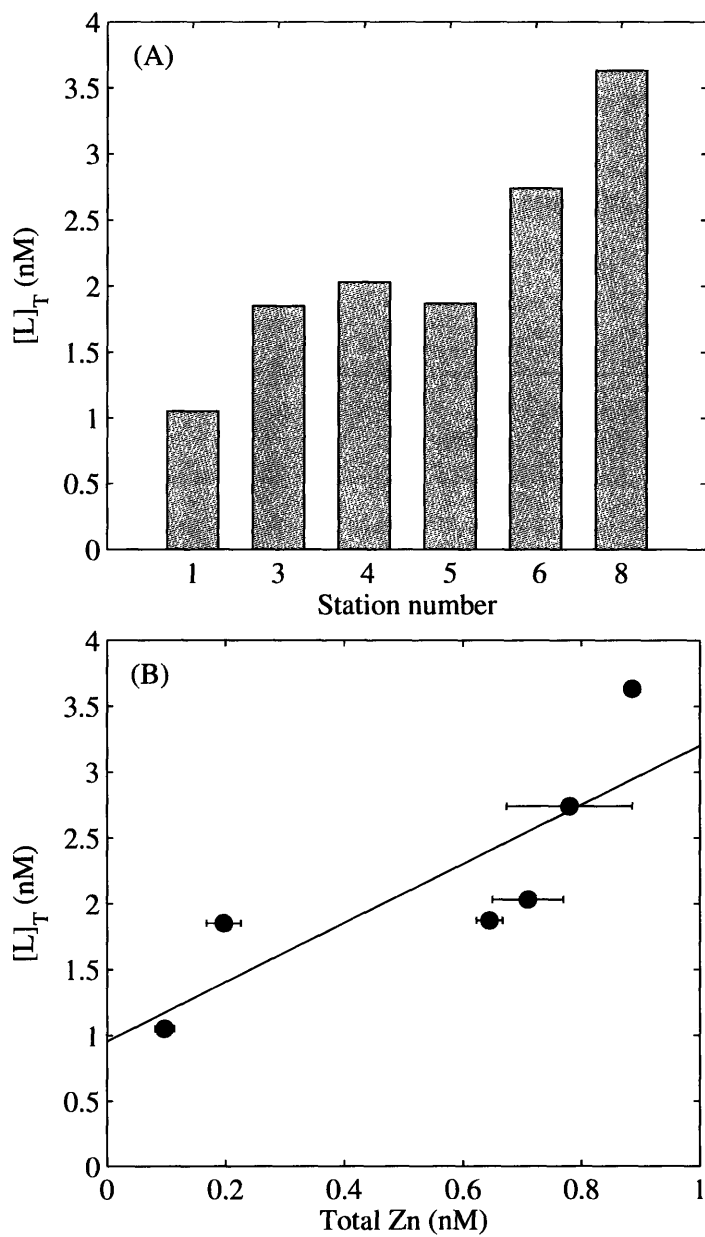




Figure 3-8: Results from a bottle incubation experiment examining the influence of Zn and Fe on phytoplankton biomass. The incubation was performed at St. 5 in the North Pacific. Chlorophyll concentrations are shown over the 4 days of the experiment. One bottle was sacrificed at each time point. Additions were: Control (no addition), +Fe (2.5 nM FeCl<sub>3</sub>), +Zn (0.75 nM ZnCl<sub>2</sub>), +Zn/+Fe (0.75 nM ZnCl<sub>2</sub>, 2.5 nM FeCl<sub>3</sub>).

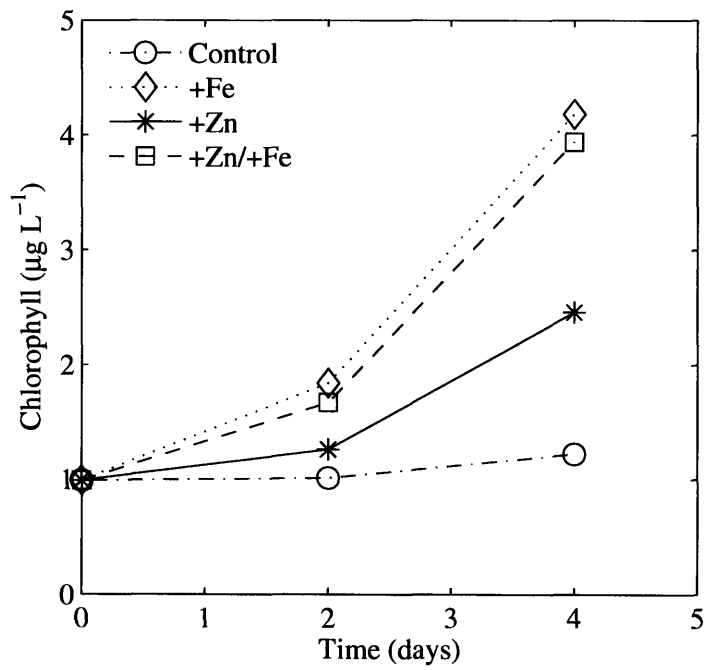


Figure 3-9: Comparison of total Zn concentrations and several phytoplankton pigments (as determined by HPLC). There is no significant relationship between total chlorophyll *a* and Zn (A,  $R^2 = 0.08$ ); however, there is a significant positive correlation between Zn and the relative contribution of two pigments found in diatoms: fucoxanthin (B,  $R^2 = 0.60$ ) and chlorophyll *c* (C,  $R^2 = 0.56$ ). Error bars as Fig. 3-3. Lines are least-squares fit lines.

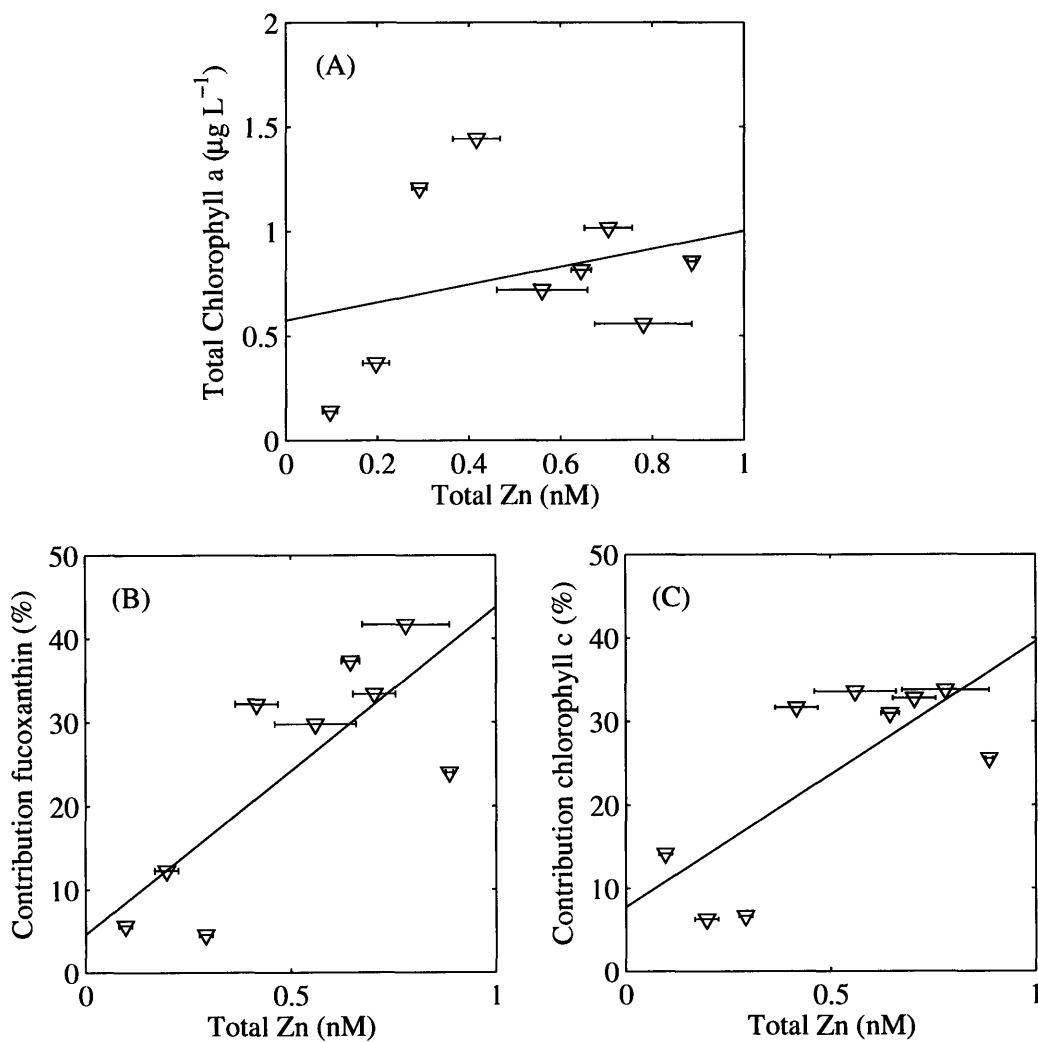


Figure 3-10: Comparison of free  $Zn^{2+}$  concentrations and several phytoplankton pigments (as determined by HPLC). There are significant correlations between the concentration of free  $Zn^{2+}$  and the concentration of total chlorophyll *a* (A,  $R^2 = 0.87$ ), and the relative contribution of two pigments found in diatoms: fucoxanthin (B,  $R^2 = 0.87$ ) and chlorophyll *c* (C,  $R^2 = 0.94$ ). Lines are least-squares fit lines.

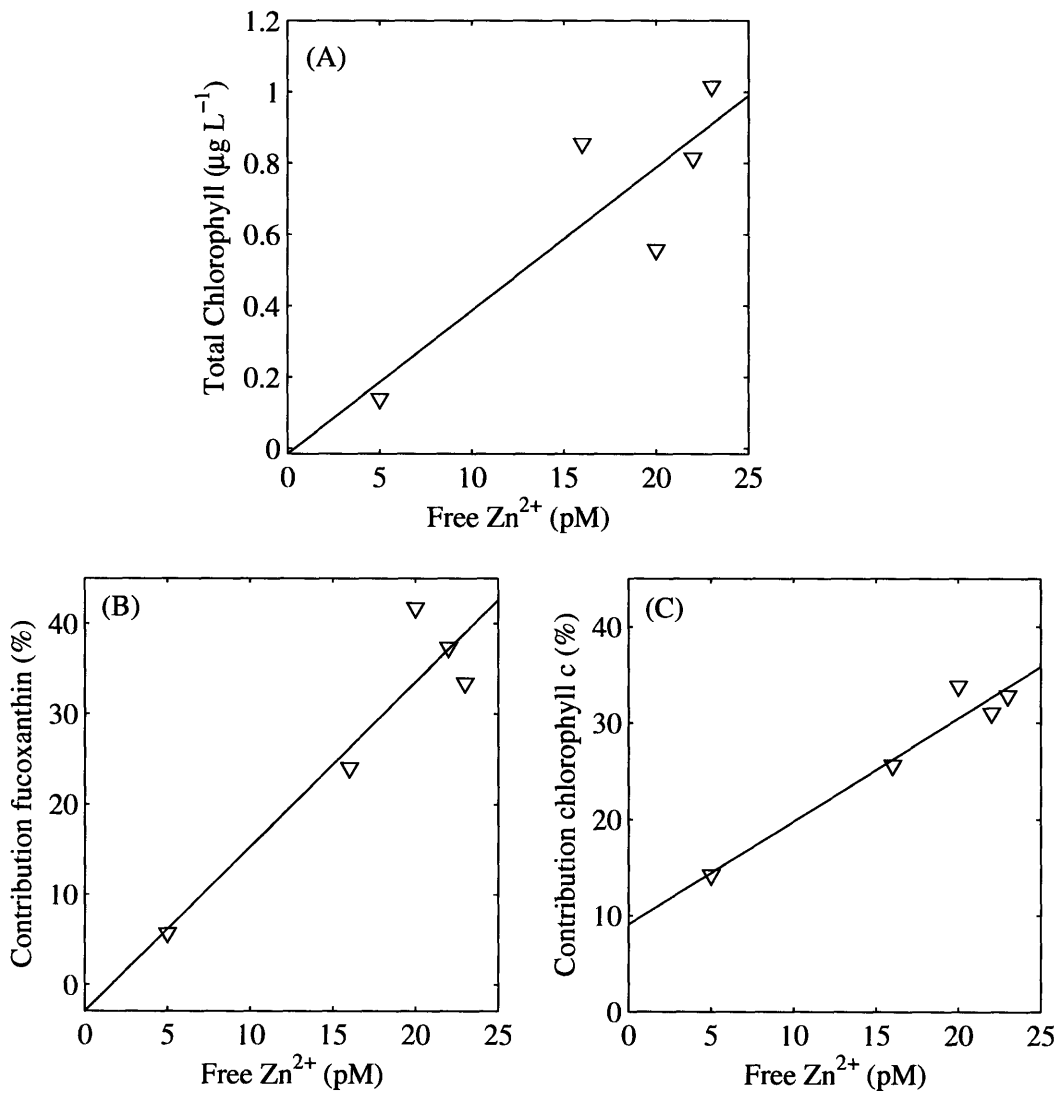


Figure 3-11: Comparison of total dissolved Zn concentrations at St. 1 measured in this study (A) with Zn concentrations reported previously in the vicinity of St. 1: Fujishima et al. 2001 (B); Martin et al. 1989 (C). Scales are the same on all three plots. Dotted lines represent the detection limit where reported.

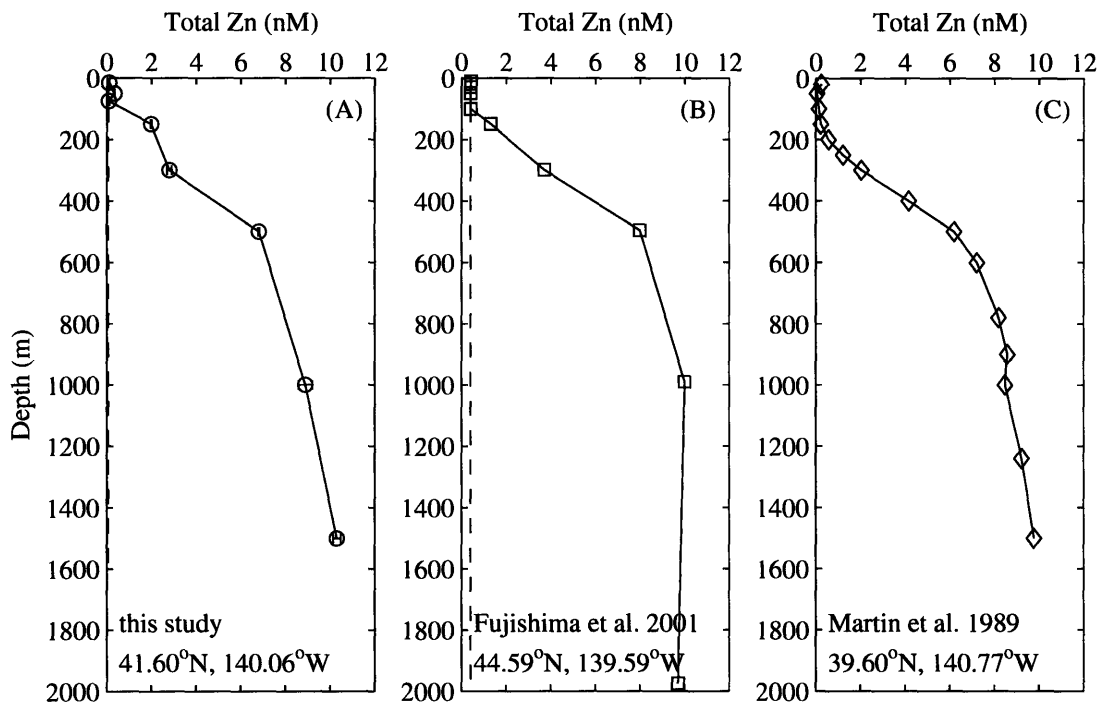


Figure 3-12: Visualization of the Aerosol Index from NASA's Total Ozone Mapping Spectrometer (TOMS) satellite. Produced at [http://toms.gsfc.nasa.gov/aerosols/aerosols\\_v8.html](http://toms.gsfc.nasa.gov/aerosols/aerosols_v8.html).

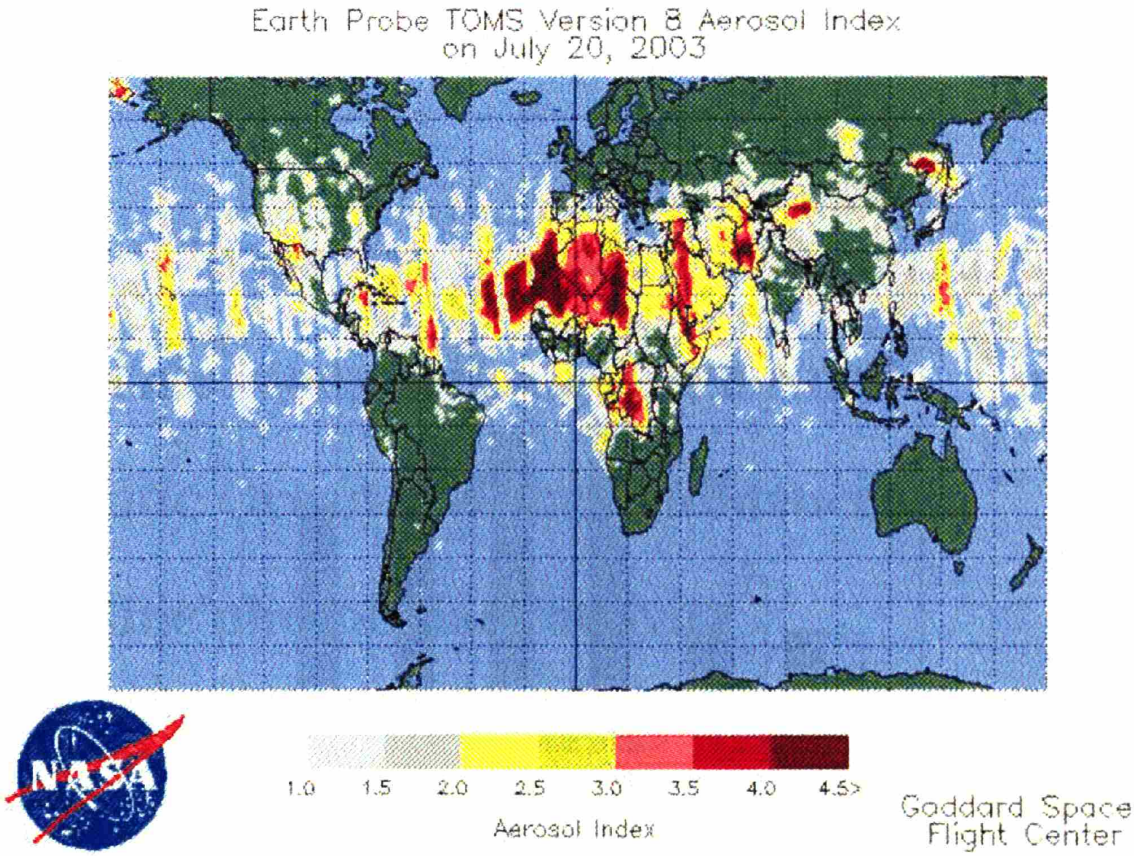
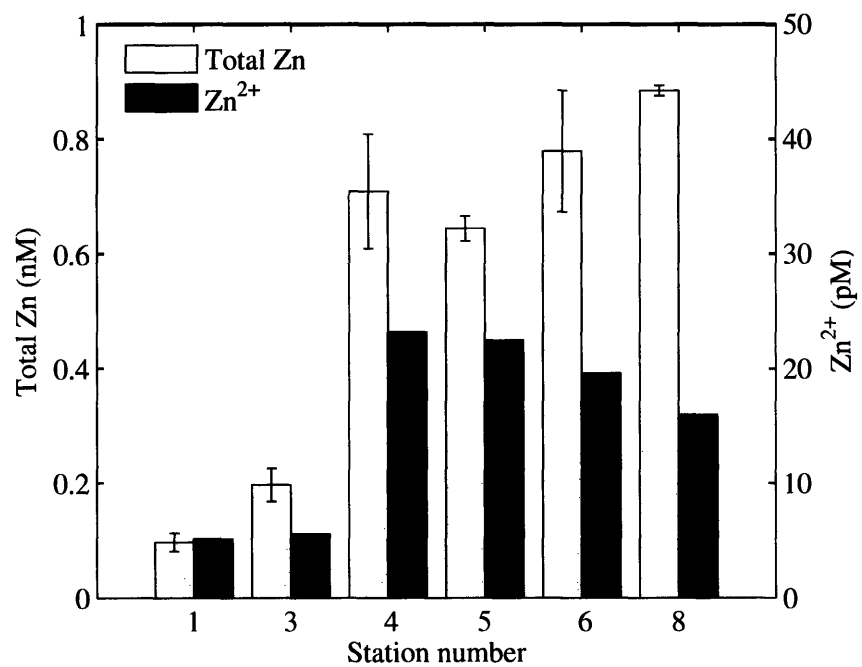


Figure 3-13: The concentration of total (light bars) and free (dark bars) Zn in the near-surface samples where Zn speciation was measured. Notice the different y-axis scales.



## **Chapter 4**

# **Trends in phosphorus, zinc, and cobalt concentrations in the western North Atlantic Ocean and their influence on alkaline phosphatase activity**

## 4.1 Abstract

Zinc and cobalt are both important micronutrients for phytoplankton due to their involvement as cofactors in enzyme systems and vitamins. Some phytoplankton are able to substitute one metal for the other when the first is in short supply, thus the relative abundance of the two metals may influence species composition or metalloenzyme activity (e.g., carbonic anhydrase, alkaline phosphatase). Phosphorus deficient phytoplankton often produce alkaline phosphatase, a metalloenzyme (typically zinc) that cleaves an orthophosphate from phosphomonoesters. In the oligotrophic gyres, the concentrations of zinc, cobalt, and phosphorus can all be low. In such a scenario, alkaline phosphatase activity may link the biogeochemistries of these three elements leading to co-limitation scenarios. In order to better understand how the biogeochemistries of these elements interact and how they influence primary production, total dissolved zinc, cobalt, and phosphorus concentrations were measured on near-surface samples from the North Atlantic Ocean. The samples were collected on a cruise track that extended from the continental shelf off Massachusetts, USA to the permanently stratified southern Sargasso Sea. The concentrations of zinc, cobalt, and inorganic phosphorus were generally lowest at the southern end of the transect and higher approaching the shelf, as expected from historic data. However, the high spatial coverage of this cruise provided additional insights. For example, transecting off the continental shelf, the concentrations of zinc and cobalt were decoupled, with the concentration of zinc being depleted before that of cobalt. Cobalt concentrations were strongly correlated with chlorophyll over the entire transect. This may reflect the dominance of cyanobacteria in the oligotrophic Atlantic, organisms whose primary requirement is for cobalt rather than zinc. Inorganic phosphorus concentrations were extremely low in the southern half of the transect (generally less than 4 nM). Alkaline phosphatase activity, an indicator of phosphorus stress, was detectable at all stations where it was measured. This suggests phosphorus may be an important determinant of primary production in this environment and that the phytoplankton community may rely on the organic phosphorus pool for a portion of their phosphorus requirement. In a shipboard incubation, alkaline phosphatase activity doubled after the addition of cobalt but there was no significant effect after the addition of zinc. This cobalt effect is consistent with culture studies where cobalt limitation caused a decrease in alkaline phosphatase activity in a model coccolithophore. The array of information collected on samples across large spatial, physical, and biogeochemical gradients provides insight into the various processes effecting the zinc, cobalt, and phosphorus cycles.



## 4.2 Introduction

The subtropical gyre of the North Atlantic Ocean, commonly referred to as the Sargasso Sea, is an extremely oligotrophic environment. Inorganic nitrogen (N) concentrations are as low as 2.5 nM (Cavender-Bares et al., 2001) and inorganic phosphorus (DIP) concentrations can be less than 1 nM (Wu et al., 2000; Cavender-Bares et al., 2001). The Sargasso Sea can be divided into two distinct regions. In the northern Sargasso Sea (north of  $\sim 31^\circ$ ), seasonal mixing in the winter results in the injection of nutrients to the euphotic zone leading to eutrophic conditions and spring phytoplankton blooms, followed by increasing stratification and nutrient depletion in the summer (Michaels and Knap, 1996). In the southern Sargasso Sea (south of  $\sim 31^\circ$ ), the water column remains stratified throughout the year, constantly exhibiting signs of oligotrophy (Michaels and Knap, 1996). Though rates of production in oligotrophic gyres can be quite low, because they cover such a large area, they account for over 80% of total marine primary production (Ryther, 1969). This production results in a net oceanic sink of atmospheric carbon dioxide. Understanding controls on the biological pumping of carbon to the deep sea is critical to predicting its behavior as atmospheric carbon dioxide levels continue to rise.

There has been significant debate over what element limits primary production in the Sargasso Sea including N (Graziano et al. 1996; Mills et al. 2004), P (Wu et al. 2000; Sanudo-Wilhelmy et al. 2001), and iron (Berman-Frank et al. 2001). Recently, a growing number of studies have highlighted P as the potential limiting nutrient (e.g., Wu et al. 2000; Ammerman et al. 2003). In the Sargasso Sea, the ratio of dissolved N to P in the water column can reach more than twice the classical Redfield value of 16N:1P (dissolved inorganic N:P  $\approx$  40-50, Cavender-Bares et al. 2001). Field studies in the Sargasso Sea, using metrics of P physiology such as P uptake, alkaline phosphatase activity, and P quotas, provide further evidence of P-limitation in this system (Cotner et al., 1997; Wu et al., 2000; Sanudo-Wilhelmy et al., 2001; Dyrhman et al., 2002; Ammerman et al., 2003).

Under conditions of P stress, some phytoplankton induce alkaline phosphatase activity, a cell surface enzyme that cleaves phosphate monester bonds, thereby releasing a bioavailable phosphate from DOP molecules with monoester bonds. This enzyme allows organisms to access some of the dissolved organic phosphorus (DOP) pool, which accounts for the majority of the total dissolved P pool in the North Atlantic (94-99%, Wu et al. 2000; Cavender-Bares et al. 2001). Because alkaline phosphatase is repressible by in-

organic P, its presence can be used as an indicator of P stress. With a few exceptions, alkaline phosphatase activities in the upper 100 m at BATS are detectable year-round (Ammerman et al., 2003). This implies that DOP may potentially support much of the primary production at BATS and that alkaline phosphatase activity could be critical to sustaining a supply of P for primary production.

Alkaline phosphatase (AP) is a metalloenzyme that has been characterized as a zinc (Zn) enzyme in *Escherichia coli* (Plocke et al., 1962). This suggests possible constraints on AP activity and DOP cycling when Zn concentrations are low. The Sargasso Sea is an example of an environment where both DIP and Zn concentrations are very low, so there may be the potential for Zn/P co-limitation. Some of the lowest reported concentrations in the world's oceans of Zn and cobalt (Co) are from the Sargasso Sea (Bruland and Franks, 1983; Saito and Moffett, 2002). Both Co and Zn are highly complexed by organic ligands in the North Atlantic which further decreases their free ion concentrations (e.g., Ellwood and van den Berg (2000, 2001); Saito and Moffett (2001)). In fact, the free  $Zn^{2+}$  ion concentrations found in seawater are low enough to restrict growth of phytoplankton in culture (Brand et al., 1983).

AP activity can be affected by metal ion concentrations in solution. Inhibition of AP activity has been shown to occur with increasing free cupric ion activity (Rueter, 1983). Low-density batch cultures of *Emiliania huxleyi* grown at low P conditions had lower AP activity when grown at low Zn (0.4 pM Zn') than when grown at high Zn (15 pM Zn', Shaked et al. 2006). In an incubation in the Bering Sea, Shaked et al. (2006) observed increased AP activity in bottles amended with Zn over that in control and iron addition bottles. Extrapolating their results to field concentrations of P and Zn, the authors do not predict Zn-P co-limitation to be a widespread phenomenon, however they suggest it may occur in the Sargasso Sea.

The Zn and Co ions are close in size and charge and some phytoplankton are able to substitute Co for Zn in order to meet their cellular demand (Price and Morel, 1990; Morel et al., 1994; Sunda and Huntsman, 1995; Yee and Morel, 1996). Culture studies have revealed different metal "preferences" between phytoplankton taxa (Sunda and Huntsman, 1995; Saito et al., 2002). Diatoms have Zn requirements that could be partially met with Co, a coccolithophore had a Co requirement that could be partially met with Zn, and picocyanobacteria have absolute Co requirements that could not be met with Zn (Sunda and Huntsman, 1995; Saito et al., 2002). The relative proportion of Zn to Co may therefore favor the growth of certain species over others (Sunda and Huntsman, 1995). This may have important implications for the global carbon cycle

since the carbon:carbonate rain ratio (a parameter that influences the effectiveness of the biological pump in removing carbon dioxide from the atmosphere, Archer and Maier-Reimer 1994) is largely controlled by the dominance of diatoms versus coccolithophores.

In the North Atlantic, the phytoplankton distribution transitions from a eukaryote-dominated regime in the north to a picoeukaryote-dominated regime in the south. Spring blooms in the northern Sargasso Sea generally consist of relatively large phytoplankton (e.g., diatoms, coccolithophores). For example, a bloom in 1985 consisted primarily of large (10  $\mu\text{m}$ ) diatoms; the diatom marker pigment fucoxanthin indicated that diatoms accounted for 80% of the total chlorophyll *a* (Siegel et al., 1990). As nutrients became depleted, the community shifted to smaller species (5  $\mu\text{m}$  and less) of green alga, prasinophytes, prymnesiophytes, and coccolithophores (Siegel et al., 1990). A springtime survey of phytoplankton showed that large phytoplankton (ultra & nano, cryptophytes, and coccolithophores) had highest concentrations north of 29°N, whereas concentrations of the small picocyanobacteria, *Prochlorococcus*, steadily increased going southward from 32-26°N (Cavender-Bares et al., 2001). The picocyanobacteria *Synechococcus* and *Prochlorococcus* accounted for a majority of total phytoplankton biomass (72% of the total phytoplankton  $\text{mg C m}^{-2}$ ) south of 25°N, whereas at the most northern stations (~35°N), eukaryotes became the dominant contributor to phytoplankton biomass (52%, Veldhuis and Kraay 2004).

This study examines the interplay of P, Zn, and Co and their effect on phytoplankton along a near surface transect in the western North Atlantic. The results are expanded upon with a shipboard incubation and a culture study using a model coccolithophore.

## **4.3 Methods**

### **4.3.1 Sample Collection**

All sampling took place aboard the R/V Oceanus between March 20, 2004 and April 9, 2004 (Fig. 4-1). Samples were collected using rigorous protocols to prevent trace metal contamination. Water samples were collected from approximately 10 m using either 10 L teflon-coated Go-Flos (General Oceanics) on a kevlar hydrowire or using an air-driven teflon pump fitted with teflon tubing.

### 4.3.2 Chlorophyll

For chlorophyll analysis, seawater was passed through a GF/F filter. Filters were extracted in 90% acetone overnight at -20°C and analyzed following the procedure of Jeffrey and Humphrey (1975) using a handheld Aquafuor fluorometer (Turner Designs).

### 4.3.3 P Analyses

For P analyses, water samples were filtered (0.4  $\mu\text{m}$  polycarbonate filter) through an acid-cleaned filter tower into acid-cleaned bottles and were immediately frozen and stored at -20°C. DIP was measured based on the MAGIC method developed by Karl and Tien (1992) as modified by Rimmelin and Moutin (2005) for the majority of the samples. Analysis of the few remaining samples is describe elsewhere (Chapter 5, Dyhrman et al. 2006). The P concentrations measured by this method are typically termed soluble reactive phosphorus since hydrolysis of some DOP compounds may occur under the acidic reaction conditions. Sample aliquots of 50 ml were pre-concentrated by adding 350  $\mu\text{l}$  of 1 M sodium hydroxide (Fluka), followed by centrifugation at 3000 rpm (1811xg) for 10 min. The supernatant was carefully decanted using a pipette. The precipitate was dissolved in 1-2 ml of 0.1 M hydrochloric acid (Seastar HCl) and subsequently analyzed using the molybdate blue method (Murphy and Riley, 1962) and corrected for arsenic interference as per Johnson (1971). Standards were prepared by adding 0-200 nM  $\text{NaH}_2\text{PO}_4$  to 50 ml aliquots of Sargasso seawater and were treated identically to samples. Synthetic blanks were prepared as in Rimmelin and Moutin (2005). The average detection limit (calculated as three times the standard deviation of the blank) was 1.03 nM. In cases where the measured SRP value fell below the detection limit (n=2), values are plotted as the detection limit or listed as <daily detection limit. For stations 21-25, where the SRP values were greater than 300 nM, samples were analyzed without the MAGIC pre-concentration. For TDP analysis, 15 ml of sample was placed in a quartz test tube and 40  $\mu\text{l}$  of hydrogen peroxide was added. Samples were then UV digested (Armstrong et al., 1966) for twelve hours followed by analysis with the molybdate blue method (Murphy and Riley, 1962). DOP concentration was defined as the difference between the TDP and the SRP measurements.

#### 4.3.4 Near-surface AP Activity

AP activity was assayed using the 6,8-difluoro-4-methylumbelliferyl phosphate (diFMU-P, Molecular Probes) substrate, after Perry (1972). The 6,8-difluoro-4-methylumbelliferyl (diFMU) product fluoresces in UV light and diFMU-P does not, so AP activity of a sample can be measured as the change in fluorescence over time. For each sample, 500 ml of seawater was passed through a 0.4  $\mu\text{m}$  polycarbonate filter. The filter was placed in a petri dish and stored frozen. At the time of analysis, 2 ml of autoclaved artificial seawater with no P added (Lyman and Fleming, 1940) was added to each petri dish. Petri dishes were agitated on a shaker table for 10 minutes. Then, 10  $\mu\text{M}$  of diFMU-P substrate was added to each petri dish. Fluorescence of the sample was measured by pipetting 200  $\mu\text{l}$  from the filter solution into a well-plate which was inserted into a Cyto-fluor fluorescence reader (Applied Biosystems). A fresh 200  $\mu\text{l}$  sample aliquot was pipetted into the well-plate and fluorescence measured every 5-10 minutes for 5 time points. For the first three stations, AP activity was also assayed on <0.4  $\mu\text{m}$  filtered water samples to determine whether or not there was a significant dissolved component to the total AP activity. For these assays, 1 ml filtered water was pipetted into a petri dish and 10  $\mu\text{M}$  diFMU-P substrate added. Fluorescence of the sample over time was measured as above. All AP assays were performed with saturating levels of substrate (10  $\mu\text{M}$ ). Thus, the AP activities reported are maximum phosphomonoester cleavage rates. This approach has been previously applied in other systems (Ruttenberg and Dyhrman, 2005).

AP activity is often reported normalized to biomass (e.g., Li et al. 1998; Shaked et al. 2006). This is informative as it provides a way to distinguish between a low level of activity expressed by a large number of cells and a high level of activity on a per cell basis. In the field, chlorophyll *a* can be used as a biomass proxy for AP activity normalization. However, it is important to consider what caveats or potential problems this involves. First, chlorophyll *a* is a bulk parameter encompassing the entire phytoplankton community. However, the presence of AP activity within the community can be quite varied over small spatial scales (Dyhrman et al., 2002; Lomas et al., 2004), and some species may have AP activity while others do not. Additionally, AP activity is not exclusive to photosynthetic organisms; therefore, there is likely a heterotrophic component to the measured AP activity. Finally, though AP activity is typically associated with the cell surface, AP activity can be detected in the dissolved fraction (e.g., Vidal et al. 2003). Single-cell assays of enzyme activity are valuable for elucidating some of these complexities (Dyhrman

et al., 2002). However, they do not provide a quantitative measure of activity, and at this point, cannot be uniformly applied to all taxa; there has been difficulty labeling the pico-cyanobacteria which predominate in much of the Sargasso Sea. AP activity in this study was determined by passing seawater through filters and then measuring the AP activity associated with the filter. Thus, the activity reported represents the greater than 0.4  $\mu\text{m}$  activity. Measuring AP activity in this manner attempts to eliminate AP activity due to the dissolved fraction, thus improving the rationale for normalization to chlorophyll *a*.

#### 4.3.5 Dissolved Zn Analysis

All samples were collected using trace metal clean techniques. Samples were piped directly from the Go-Flo bottles by teflon tubing through acid-cleaned 0.4  $\mu\text{m}$  polycarbonate filter sandwiches into rigorously acid-cleaned low density polyethylene bottles (Appendix A for further details). After filtration, samples were acidified to approximately pH 2 by the addition of 2 ml concentrated HCl (Seastar) per liter of seawater. Total dissolved Zn concentration was measured using isotope dilution inductively coupled plasma mass spectrometry (ID ICP-MS) after Wu and Boyle (1998). 15 ml centrifuge tubes (Globe Scientific) were cleaned by soaking in 2N HCl at 60°C for 48 hours, followed by rinsing 5 times with trace-metal grade pH 2 HCl (J.T. Baker intra-analyzed) and once with ultra-pure pH 2 HCl (Seastar). Finally, tubes were filled to a positive meniscus with ultra-pure pH 2 HCl (Seastar) and capped until use. At the time of analysis, tubes were rinsed once with sample and then filled to approximately 13.5 ml (exact volume determined gravimetrically). Samples were then spiked with a  $^{66}\text{Zn}$  spike (98.9% as  $^{66}\text{Zn}$ , Cambridge Isotope Laboratories, Inc.) to an estimated  $^{66}\text{Zn}:$  $^{64}\text{Zn}$  ratio of 9. This ratio minimizes error magnification (Heumann, 1988). The spike was allowed to equilibrate with the samples overnight. The following day, 125  $\mu\text{l}$  of ammonia (Seastar) was added to each tube. After 90 sec, the tube was inverted and after an additional 90 sec, tubes were centrifuged for 3 min at 3000xg (3861 rpm) using a swinging bucket centrifuge (Eppendorf). The majority of the supernatant was carefully decanted and then tubes were respun for 3 min to firm pellet and the remaining supernatant was shaken out. Pellets were dissolved on the day of ICP-MS analysis using 0.5 - 1.5 ml of 5% nitric acid (Seastar). ICP-MS measurements were made using a Finnigan ELEMENT2 in medium resolution mode, which was sufficient to resolve  $^{64}\text{Zn}$  from the potential interference peak due to Mg-Ar. To measure the procedural blank, one ml of surface seawater was treated as the samples but calculations

were performed as though it was a 13.5 ml sample. The average blank value was 0.14 nM and the average detection limit was 0.07 nM.

#### **4.3.6 Dissolved Co Analysis**

The same samples were used for both Zn and Co analyses (see above for collection procedure). The total dissolved Co concentration was measured using Cathodic Stripping Voltammetry (CSV) following the method of Saito and Moffett (2001). Reagents included N-(2-Hydroxyethyl)piperazine-N'-(3-propanesulfonic acid) (EPPS, Sigma) buffer, sodium nitrite (Fluka Puriss), and dimethylglyoxime (DMG, Aldrich). Both the EPPS and nitrite reagents were treated with chelex to remove any contaminating metals. DMG salt was supplied by the Saito lab and purified as per Saito and Moffett (2001).

Acidified samples were poured into quartz tubes that were cleaned by soaking overnight in 10% HCl (J.T. Baker instra-analysed) and rinsed several times with pH 2 HCl (J.T. Baker instra-analyzed). Samples were then UV-irradiated for 1 hour using a 500 Watt high-pressure mercury lamp (Metrohm). Samples were pipetted from the quartz tubes into a teflon cell cup of a 663 VA Stand for a hanging mercury drop mode (Metrohm). The pH of the sample was then adjusted to between 8.0 and 8.5 using ammonia (Seastar). EPPS buffer (pH adjusted to 8.1) was added to a concentration 2.5 mM, DMG was added to a concentration of 0.3 mM, and sodium nitrite was added to a concentration of 0.225 M. Next, the sample was purged with ultra-high purity nitrogen gas for 200 sec. Then a voltage of -0.6 V was applied to the voltammetric cell for 90 sec followed by a 10 sec equilibration period before the potential was ramped from -0.6 to -1.4 V. The scan was performed using the linear sweep wave form at a speed of  $7.01 \text{ V s}^{-1}$  with a step potential of 0.01 V. The zero addition scan was repeated 3 times, followed by one scan each of 3 successive 20 pM additions of cobalt. Seawater blanks were prepared by chelexing UV-irradiated seawater and then UV-irradiating it a second time. The average blank was 4.6 pM and the detection limit was 2.7 pM.

#### **4.3.7 Shipboard Incubation**

A shipboard incubation was performed at St. 16 (34°07 N 55°35 W). Trace metal clean water was collected with an air-driven Teflon pump, which sampled water from approximately 10 m depth directly into an acid-washed HDPE carboy, housed in a trace-metal free bubble constructed of a HEPA filter and plastic sheeting.

Twelve acid-washed polycarbonate bottles were filled with unfiltered seawater from the carboy. Time zero samples for chlorophyll and AP activity were also collected from the carboy. The polycarbonate bottles were spiked in triplicate as follows: Control (no addition), +P (8.4  $\mu\text{M}$   $\text{Na}_2\text{H}_2\text{PO}_4$ ), +Zn (1.7 nM  $\text{ZnCl}_2$ ), +Co (630 pM  $\text{CoCl}_2$ ). For P addition, a solution was made up from monosodium phosphate ( $\text{NaH}_2\text{PO}_4$ , Sigma), chelexed to remove any potential trace metal contamination, and stored in acid-clean teflon bottles at 4°C. Zn addition was made from a serial dilution of a 1000 mg  $\text{L}^{-1}$  Zn stock (Spex CertiPrep). Co addition was made from a serial dilution of a 17.5 mM Co stock (Sigma, ACS reagent) Bottles were tightly capped and placed in on-deck incubators. Surface seawater continuously flowed through the incubators and excess surface irradiance was controlled with blue-gel shading. After 3 days, the bottles were removed from incubators and sampled for AP activity and chlorophyll.

#### 4.3.8 Culture Study

Culture media was prepared using clean and sterile techniques in a class 100 clean room. The base of the medium was Sargasso seawater, collected from a teflon pump at St. 12. Seawater was filtered through a 0.4  $\mu\text{m}$  polycarbonate filter and microwave sterilized. This seawater base was amended with chelexed and filter-sterilized stocks of nitrate and vitamins up to *f*/2 levels (Guillard, 1975; Guillard and Ryther, 1962). Trace metals were added with EDTA to final total concentrations of 100  $\mu\text{M}$  EDTA (SigmaUltra, disodium salt), 40 nM copper, 500 nM Fe, 50 nM manganese, 52 nM molybdenum, and varying levels of Co and Zn. The free ion concentrations for the metals of each treatment were calculated using the computer program visual MINTEQL. There were 4 metal conditions: Replete Zn and Co; 0 Zn added, low Co; 0 Co added, low Zn; 0 Zn added, 0 Co added (for abbreviations and free metal ion concentrations see Table 4.1) and two P conditions (low P, high P) for a total of 8 treatments. For the high P treatments, 36  $\mu\text{M}$   $\text{Na}_2\text{HPO}_4$  was added to the media, and 1  $\mu\text{M}$   $\text{Na}_2\text{HPO}_4$  was added for the low P treatments.

An axenic culture of *Emiliania huxleyi* (CCMP 374) was obtained from the Provasoli-Guillard Center for Culture of Marine Phytoplankton. Before beginning the experiment, *E. huxleyi* was transferred to low metal media to dilute any carryover contamination. All cultures were grown in 30 ml acid-washed polycarbonate tubes, in triplicate. Growth of the cultures was monitored daily by measuring *in vivo* chlorophyll *a* fluorescence on a Turner Designs model 10-AU Fluorometer (Turner Designs) and by performing cell



counts with a haemocytometer on days where AP activity was measured.

For the low P treatments, AP activity was measured daily for 4 days once growth of cultures had entered the log-stationary transition (beginning day 7 for the Replete, day 8 for the -Zn, and day 12 for both the -Co and -Zn/-Co treatments), known from prior work to encompass peak AP activity (Dyhrman and Palenik, 2003). In a previous experiment with *E. huxleyi*, there was no activity detectable at the high P level used here. As such, AP assays were only performed on one day for the high P treatments (3rd day of stationary phase for Replete, -Zn, -Zn/-Co and 1st day of stationary phase for -Co). For the AP assays, 650  $\mu\text{l}$  of culture was removed from each tube, using sterile techniques and acid-washed pipette tips. This aliquot was split: 500  $\mu\text{l}$  was placed in an acid-washed well plate for the enzyme assay and the remaining 150  $\mu\text{l}$  was placed in an epitube for cell counts. 20  $\mu\text{M}$  diFMU-P substrate was added to each well using sterile acid-washed tips. The plate was then inserted into a Fluorstar fluorescence reader (BMG Labtech). Fluorescence was measured every 30-90 seconds for up to 45 minutes. Fluorescence in a no-cells control of autoclaved artificial seawater with no P added (Lyman and Fleming, 1940) plus diFMU-P substrate was subtracted from culture samples. To obtain a rate measurement a line was fitted to at least 6 points with an  $R^2$  of 0.9 or better. If no line could be fit using these conditions, the activity was deemed undetectable. Samples for SRP analysis were collected at the end of the experiment (last day of AP analysis). The culture tubes were centrifuged at 8000 rpm for 10 min to concentrate the cells into a pellet. The supernatant was transferred by pipette into acid-clean tubes and frozen at  $-20^\circ$  until analysis. SRP was measured using the standard molybdate blue method without preconcentration on duplicate supernatants (Murphy and Riley, 1962).

## 4.4 Results

### 4.4.1 Chlorophyll

Chlorophyll *a* concentrations were generally low ( $0.02 - 0.06 \mu\text{g L}^{-1}$ , Fig. 4-2A, Table 4.2) in the southern half of the transect (south of  $31^\circ\text{N}$ ) and rose to much higher levels ( $0.10 - 1.90 \mu\text{g L}^{-1}$ ) in the northern half of the transect (north of  $32^\circ\text{N}$ ). These chlorophyll *a* concentrations are similar in magnitude and spatial distribution to previous studies in the Sargasso Sea (Siegel et al., 1990; Cavender-Bares et al., 2001).

#### 4.4.2 P Analyses

SRP concentrations ranged from sub-nanomolar values (reported as below detection limit) in the southern portion of the transect to 585 nM near the continental shelf (Fig. 4-2B, Table 4.2). In the southern permanently stratified region, SRP was generally less than 4 nM and increased significantly only north of 35°N. DOP ranged from 51 to 308 nM with an average value of 133 nM (Fig. 4-2C, Table 4.2). The DOP distribution was similar to SRP in that the highest values were observed at the northern-most stations. However, there seemed to be more structure to the DOP concentrations south of 35°N, whereby the lowest DOP concentrations were between roughly 28-38°N with intermediate concentrations south of 28°N.

#### 4.4.3 Near-surface AP Assays

AP activities along the transect are presented both normalized to chlorophyll *a* concentrations (Fig. 4-3A) and as raw rates of phosphomonoester cleavage (Fig. 4-3B). When normalized to chlorophyll, AP activity is relatively high, though variable, in the southern half of the transect and steadily decreases northward of 30°N. This trend is inversely related to the SRP concentrations with higher AP activities in the south where the SRP is low. There is not as obvious a latitudinal trend when AP activity is considered without normalization to chlorophyll *a* (Fig 4-3B). However, the average activity for the entire transect is 4.1 nmol P hr<sup>-1</sup> L<sup>-1</sup>. The average activity for the portion of the transect between 28.3 and 36.1°N is nearly double that at 7.2 nmol P hr<sup>-1</sup> L<sup>-1</sup>. The measured AP activity in this study agrees well with previous measurements of AP activity at the BATS time series site which were 1-10 nmol P hr<sup>-1</sup> L<sup>-1</sup> in March-April of 1996-1998 (Ammerman et al., 2003).

#### 4.4.4 Dissolved Zn and Co

Total dissolved Zn concentrations along the transect ranged from being undetectable (average detection limit was 0.07 nM) to 1.3 nM (Table 4.2, Fig. 4-4A). Three samples had Zn concentrations below the detection limit (stations 12, 14, 16). Transecting off the coast, the Zn concentrations dropped sharply from 1.3 nM to 0.14 nM at 37.4°N. Zn concentrations in the middle of the transect oscillated between undetectable values and 0.42 nM without an obvious spatial trend (Fig. 4-4A). Along 20°N latitude, Zn concentrations were very low (~0.1 nM) except for the western most station (0.58 nM). Dissolved Co was detectable at all stations and

ranged from 3.8 to 111.4 pM (Table 4.2, Fig 4-4B). Total Co concentrations also decreased transecting off the coast, though not as rapidly as Zn. However, Co continued to decrease more consistently with latitude with the lowest Co concentrations measured along 20°N (3.8-7.1 pM).

The relationships of Co (Fig. 4-5A) and Zn (Fig. 4-5B) to salinity were examined for stations 15 to 25. Station 15 was chosen as the pelagic end member because it had a salinity of 37.4 which is similar to many of the other pelagic stations. Co and Zn both exhibited negative relationships with salinity, such that the lowest Co and Zn concentrations were associated with the highly saline waters of the oligotrophic gyre.

The correlation between chlorophyll *a* and Co (Fig. 4-6A), Zn (Fig. 4-6B), and SRP (Fig. 4-6C) was also examined. Co concentrations were tightly coupled to chlorophyll *a* concentrations with an  $R^2$  value of 0.90. Unlike Co, there was not a simple linear correlation between Zn and chlorophyll ( $R^2$  of linear fit = 0.37). There is a somewhat better correlation between Zn and chlorophyll ( $R^2 = 0.40$ ) if only stations 15-25 are considered (excluding the high Zn stations in the oligotrophic south). The correlation between SRP and chlorophyll is intermediate between that of Co and Zn with an  $R^2$  value of 0.78.

When the concentrations of SRP are compared with those of Co (Fig. 4-7A) and Zn (Fig. 4-7B), positive relationships are seen. The correlation between Co and SRP is more significant ( $R^2 = 0.78$ ) than that of Zn and SRP ( $R^2 = 0.57$ ).

#### 4.4.5 Shipboard Incubation

The water from St. 16 that was collected for the shipboard incubation had an initial chlorophyll concentration of  $0.27 \mu\text{g L}^{-1}$  and an SRP concentration of  $2.9 \pm 0.2 \text{ nM}$ . Zn was below the daily detection limit of 0.12 nM and Co was 14.3 pM. After 3 days, there was no increase in chlorophyll *a* due to any of the experimental additions and chlorophyll concentrations decreased in the +Zn and +Co treatments (Fig. 4-8A). AP activity is reported both normalized to chlorophyll *a* (Fig. 4-8B) and as raw rates of phosphomonoester cleavage (Fig. 4-8C). In both cases, the trends in AP activity are the same. AP activity remained constant in our no addition control and in our +Zn treatment. AP activity dropped roughly in half in the +P treatment as expected since AP is an enzyme repressible by high inorganic P concentrations (Fig 4-8B, 4-8C). There was a large increase in AP activity in the +Co treatment. Raw rates of phosphomonoester cleavage in the +Co treatment increased by a factor of 50% over the control, and chlorophyll-normalized AP activity increased

by over 100% (Fig. 4-8B, 4-8C). In both cases, the increase in AP activity in the +Co treatment is significant ( $p < 0.02, 0.14$ , respectively)

#### 4.4.6 Culture Study

The growth rate of *E. huxleyi* was highest in the Replete metal treatments and decreased from the -Zn to the -Co to the -Zn/-Co added treatments at both P conditions (Fig. 4-9A, 4-9C). This trend in growth rates follows the pattern of previous culture studies (Sunda and Huntsman, 1995), where coccolithophores have a primary growth requirement for Co that can be partially substituted with Zn. The maximum AP activity in the -Zn, low P and -Co, low P treatments was only 60% of the maximum activity in the Replete, low P treatment (Fig. 4-9C). This trend also holds when the average AP activity of 4 days is considered (data not shown). AP activity in the -Zn/-Co, low P treatment was generally undetectable. For the high P treatments, AP activity was only detectable in two of the Replete, high P treatments, but is not visible on the same scale as the activity in the low P treatments (Fig. 4-9D). The re-addition of P to the Replete, low P, -Zn, low P, and -Co, low P treatments caused AP activity to decrease (data not shown). There was no detectable SRP ( $<20$  nM) at the end of the experiment in the Replete, low P; -Zn, low P; and -Co, low P treatments. In the -Zn/-Co, low P treatment, there was  $592 \pm 30$  nM SRP left in the media at the end of the experiment. The low growth observed and the relatively high levels of SRP remaining in the -Zn/-Co, low P media suggest that SRP was not sufficiently drawn down to induce AP activity. Thus, the absence of activity in the -Zn/-Co treatment is probably due to P-sufficient conditions rather than metal limitation of AP.

The concentration of SRP in all of the high P treatments was above our highest standard ( $1 \mu\text{M}$ ). Extrapolating the standard curve upwards to the observed absorbances yields SRP concentrations of approximately  $25 \mu\text{M}$  for all the high P metal treatments.

## 4.5 Discussion

This study is a valuable addition to the current body of literature on the biogeochemistry of the North Atlantic. It provides a uniquely comprehensive data set of chlorophyll, SRP, DOP, alkaline phosphatase activity, Co, and Zn on the same suite of samples covering a large section of the western North Atlantic Ocean. The large spatial coverage and the simultaneous measurement of multiple parameters allows us to

better understand and interpret the interactions between the cycles of P, Zn, and Co in the North Atlantic Ocean.

#### **4.5.1 Chlorophyll**

The observed chlorophyll distribution follows the pattern described by Siegel et al. (1990) where seasonal mixing in the northern Sargasso injects nutrients into the mixed layer that fuel higher production and chlorophyll concentrations. Whereas the low concentrations of chlorophyll observed in the southern half of the transect are typical of the permanently stratified waters that are extremely nutrient-deprived and do not support high levels of primary production.

#### **4.5.2 P Analyses**

The SRP concentrations observed in this study agree well with past studies in this region (0.5 - 400 nM, Cavender-Bares et al. 2001). At 17 out of 25 total stations, the SRP concentration was below the detection limit (30-50 nM) of the standard molybdate blue method (Murphy and Riley, 1962). Extreme care was taken in analysis of SRP samples and the high grades of reagents used (Seastar HCl, Fluka NaOH, ACS certified plus H<sub>2</sub>SO<sub>4</sub>) were found to be essential for obtaining low blank values which made detection of nanomolar SRP possible. DOP concentrations from this study are also similar to previous research (Wu et al., 2000; Cavender-Bares et al., 2001). South of 35°N, DOP accounted for the majority of the dissolved P pool (96% of total on average). North of 35°N, where SRP concentrations were higher (>65 nM), SRP was the dominant fraction, and DOP accounted for less than half of the total dissolved P pool (45% on average).

#### **4.5.3 Near-surface APA Assays**

AP activity was detected at all stations along the transect where we sampled (no AP data for stations 24, 25). There are two important implications for this observation. First, it suggests that some portion of the community is experiencing P stress. Secondly, it suggests that the phosphomonoester portion of the DOP pool may be an important P source for primary production. The addition of DIP in our shipboard incubation caused a decrease in AP activity, further showing that the community in the Sargasso Sea is experiencing

P-stress and that AP activity is a useful marker of P status.

The trend in AP activity changes dramatically depending on whether or not it is normalized to chlorophyll *a* concentration. There are plausible explanations for the distributional pattern of AP activity in both cases. When AP activity is normalized to chlorophyll *a*, activity is highest in the south and declines north of ~32°N. This pattern fits with the inverse of SRP concentrations. In the south, where SRP is lowest and presumably cells are experiencing a high level of P-stress, AP activity is high. Then, north of ~34°N, the SRP concentrations begin increasing and AP activity declines.

Raw rates of phosphomonoester cleavage had peak values at 34°N and were highest between 28 and 36°N. This latitudinal range covers the transition zone from permanent stratification to seasonally mixed waters and encompasses the portion of the Sargasso where dissolved N:P ratios are highest ([N+N]:[SRP] up to 70, Cavender-Bares et al. 2001). N:P ratios above the classic Redfield ratio (16N:1P) are often used as a metric of P stress. If P-stress is correlated with a high N:P, then we would expect higher AP activity at these intermediate latitudes, as observed with raw phosphomonoester cleavage rates. Further, this portion of the transect with high phosphomonoester cleavage rates coincides with the area of minimum DOP concentration. It is also important to note that the same level of raw phosphomonoester cleavage rates was observed in the southern stations as in the northern stations, even though the photosynthetic biomass level is sometimes 10-fold lower in the south.

#### **4.5.4 Dissolved Zn and Co**

Previous measurements of total dissolved Zn in the surface waters of the North Atlantic range from 0.06-0.34 nM Zn in the open ocean to 0.59-2.4 nM Zn closer to the coast (Bruland and Franks, 1983; Martin et al., 1993; Ellwood and van den Berg, 2000). Our measurements of <0.07-1.32 nM agree well with these previous studies. The concentrations of Co observed (3.8-111.4 pM) also agree well with previous measurements (Martin et al., 1993; Saito and Moffett, 2002), though the concentrations in this study fell mainly in the lower range of previous observations (<20 pM).

The concentrations of Zn and Co appeared to be de-coupled along parts of the transect. Transecting off the coast (36-40°N), Zn concentrations decreased more dramatically at the northern stations than Co concentrations. This may indicate a higher biological demand for Zn than Co in the most northern part

of our transect. This area encompassed colder continental shelf waters into the pelagic northern Sargasso Sea, waters where diatoms can account for the majority of chlorophyll *a* in the spring (Siegel et al., 1990). Diatoms have a high Zn requirement and little or no absolute Co requirement (Sunda and Huntsman, 1995). The presence of a diatom-dominated community between 36-40°N may explain the more dramatic Zn draw-down relative to Co in this region.

There were also several stations in the south where Zn concentrations increased without a corollary increase in Co. South of 30°N, the Zn concentration was generally less than 0.25 nM; however, at five stations (5, 6, 7, 11, and 13), the Zn concentration was greater than 0.25 nM. There was no corollary increase in Co concentration at these stations. There are several possible explanations for this discrepancy. One possibility is that Zn contamination may have occurred during sampling. Zn is a very contamination prone element (more so than Co), and great care was taken to prevent contamination. Teflon coated Go-Flo bottles were suspended on a kevlar line around a derin metering block and tripped with teflon-coated messengers. The Go-Flo bottles were immediately transferred to a portable clean van for sampling. The bottles were pressurized with filtered ultra-high purity nitrogen gas and samples transferred through acid-cleaned teflon tubing and a polycarbonate filter sandwich in a laminar flow hood. The high Zn values were generally at the beginning of the cruise, a time when shipboard contamination issues are not always resolved. However, low Zn values (0.15 - 0.21 nM) were observed at the first three stations sampled (1, 2, & 4).

Alternately, the higher Zn concentrations may be the result of increased Zn inputs from the atmosphere or shelf. Dust deposition from the Saharan dust plume is an important source of Fe to the North Atlantic Ocean (e.g., Duce and Tindale 1991). Zn is a thousand-fold less abundant than Fe in crustal material (Taylor and McLennen, 1985) and the importance of aeolian deposition of Zn to the surface ocean is not as well understood. Atmospheric dust would be expected to deposit a higher concentration of Zn than Co since Zn is over four times as abundant as Co in crustal material (Taylor and McLennen, 1985). Zinc is also considered an enriched element because it is present in dust at concentrations 10-100,000 times above that expected due to crustal abundances (Duce et al., 1983; Arimoto et al., 1989).

Based on the Zn concentration of dust collected at Bermuda (Duce et al., 1976), a 1 cm sec<sup>-1</sup> depositional velocity, and a 10% Zn solubility, it would take about two weeks of dust deposition to increase the Zn concentration by 0.3 nM in a 20 m mixed layer. Dust deposition does not appear to be a significant source of

Co to the North Atlantic (Saito and Moffett, 2002). Saito and Moffett (2002) calculate that it would take 3 months to increase the dissolved Co concentration in a 20 m mixed layer by 3 pM. In the southern Sargasso Sea, the residence time of Zn in the surface layer may be enhanced relative to the northern Sargasso Sea due to a decreased biological demand for Zn in the southern Sargasso where the biomass is typically dominated by picocyanobacteria. Both *Synechococcus* and *Prochlorococcus* have absolute growth requirements for Co, that cannot be substituted for with Zn (Sunda and Huntsman, 1995; Saito et al., 2002). The meridional trend of decreasing Co with latitude supports the idea that Co demand is high in the southern Sargasso Sea.

Previous studies have examined the relationships of Co and Zn with salinity. Saito and Moffett (2002) observed a tight correlation between Co and salinity indicative of conservative mixing. The slope of their relationship is plotted along with the data from this study (Fig. 4-5A). The slope of our relationship is similar to that of Saito and Moffett (2002), however one data point pulls down the slope of our trend. This data point (33.5, 59.9) represents St. 25, which is the station closest to the coast. Data from this station are somewhat difficult to interpret. Chlorophyll and Co concentrations dropped in half from the previous station yet Zn and SRP increased. A similar precipitous drop in chlorophyll around 40°N with no drop in SRP was observed by Cavender-Bares et al. (2001). In both Saito and Moffett (2002) and this study, the Co-salinity relationship breaks down somewhat at the high salinity end with Co concentrations decreasing more rapidly than salinity increases.

Bruland and Franks (1983) observed a relationship between Zn and salinity in the North Atlantic that suggested the possibility of Zn removal during mixing of coastal and pelagic waters. Data from this study also supports the possibility of Zn removal during mixing. Zn concentrations rapidly decrease as salinity increases from 33.5 to 34.5, with Zn values falling below the least squares regression line. This is also the portion of the transect where biological demand for Zn is expected to be high.

A tight correlation was observed between Co and chlorophyll *a* over the entire transect. This may indicate that Co is an important driver of phytoplankton biomass or reflect the dominance of prokaryotes in the western Atlantic. The fact that the relationship holds even at the high chlorophyll, high Co end of the spectrum (and breaks down at very low Co/low chlorophyll) suggest that Co may be important to the array of phytoplankton communities sampled across the transect. It also indicates that the community's Co demand is not based solely on AP, since even at high P, Co and chlorophyll are tightly coupled. *Synechococcus*



and *Prochlorococcus* both have absolute Co requirements at high P concentrations (Sunda and Huntsman, 1995; Saito et al., 2002), which may be due to Co's use in vitamin B<sub>12</sub>, carbonic anhydrase, or DNA transcription. Incubations where both Co and DIP were added together were performed at 5 stations (Appendix B). In two of these incubations (begun at St. 1 and St. 2), the addition of Co and DIP together caused increases in chlorophyll higher than those due either to DIP addition alone or to the addition of DIP and Zn together. The start points of these two incubations fall in cluster of low Co, low chlorophyll points in the Co/chlorophyll relationship. That Co and DIP together had a greater effect than P alone supports the idea that the community's Co demand goes beyond use in AP because the Co was still important after P-stress was relieved.

The relationship between Zn and chlorophyll is more complex. At the very low chlorophyll end, there are a range of Zn concentrations. These data points represent the southern oligotrophic stations. It appears that in this region, Zn inputs do not result in any increase in chlorophyll. At higher chlorophyll values, there is a positive relationship between Zn and chlorophyll; however, it is skewed by one high Zn, moderate chlorophyll point. This data point is from St. 25, which was also anomalous in the Co/salinity relationship. The fact that Co and chlorophyll trended together over these changes emphasizes the tight correlation between these two parameters and suggests that either one parameter is influencing the other or that both chlorophyll and Co concentrations are being regulated by some other factor (perhaps nitrogen).

There is a good correlation between chlorophyll and SRP on the transect ( $R^2 = 0.78$ ), though not as significant as the correlation between Co and chlorophyll ( $R^2 = 0.90$ ). The majority of the stations cluster near the origin of the plot of chlorophyll versus SRP. There are three points at the very low P end which fall above the least squares fit line. These three values represent stations 16, 17, and 19 which are right at the transition to a surface temperature of 19°C and are where the chlorophyll increased above the very oligotrophic values of less than  $0.1 \mu\text{g L}^{-1}$ . The fact that chlorophyll values increased before that of SRP, may be due to the phytoplankton community's ability to supplement their P demand with DOP.

The relationship between Co and SRP seems to have a non-zero y-intercept, such that it is only when SRP concentrations are very low (less than ~10-15 nM), that Co is drawn down below 20 pM. One explanation for this relationship may be that at low SRP values, elevated production of AP creates an increased demand for Co. There is a fair amount of scatter over the entire range of values in the Zn-SRP plot, which

suggests these two elements are not tightly coupled in this region. There is no evidence from this relationship for an AP-related Zn demand.

#### **4.5.5 Shipboard Incubation**

As previously stated, AP activity is a repressible enzyme that is typically expressed when cells experience P-stress. AP activity was present at significant levels at time zero and decreased by 50% in the +P treatment further establishing a link between community P-stress level and AP activity. Yet, no chlorophyll increase was observed in the +P treatment. This non-intuitive result suggests that additional factors were significantly influencing biomass levels. These may include grazing or a complex co-limitation situation between metals and P.

The chlorophyll decrease in the +Zn and +Co treatments was not expected. The concentrations of metals added were over an order of magnitude greater than the ambient concentrations, but the presence of natural organic ligands should have buffered the increase in free metal ion concentrations, such that a toxic effect is unlikely. Grazing coupled with co-limitation of growth by P may explain the chlorophyll decrease in these treatments. As with the +P treatment, the AP activity results for the two metal additions were more straightforward than the chlorophyll results. AP activity doubled in the +Co treatment, whereas the addition of Zn had no effect on AP activity. At time zero of the incubation, Zn was very low ( $<0.12$  nM) whereas Co was only moderately low (14 pM). Yet, the addition of Zn had no effect on AP activity. This may be explained a couple of ways. First, the concentration of Zn binding ligands in surface waters is generally in excess of the total Zn concentration by  $\sim 1$  nM (e.g., Bruland 1989). By contrast, the concentration of Co binding ligands is generally very similar to the total Co concentration (e.g., Saito and Moffett 2001). Thus, the lack of response in the +Zn addition may be due to most of the added Zn being immediately bound by natural ligands, which are not typically considered bioavailable. The majority of the added Co would be expected to remain in the inorganic fraction. Another possible explanation for the lack of response in the +Zn addition is that the Zn requirement for AP was extremely low or non-existent. This in turn suggests that some organisms may have AP enzymes that have Co rather than Zn as cofactors. An AP enzyme that appears to have Co rather than Zn as its primary cofactor was isolated from a hot spring bacteria (Gong et al., 2005). This incubation experiment indicates that in the natural environment, the concentration of the

metal micro-nutrient Co may limit the level of AP activity and hence DOP hydrolysis.

These results are counter to those for the Bering Sea where Zn addition resulted in an increase in AP activity (Shaked et al., 2006). This may not be surprising for several reasons. The two incubations took place in very different regimes where the photosynthetic community structure would be expected to differ significantly. Sea surface temperature in the Bering Sea was 10.7°C compared to 19.0°C in this study. Initial concentrations of DIP and chlorophyll in the Bering Sea were an order of magnitude higher than the initial concentrations observed in this study. Zn in the Bering Sea was moderately low at 0.25 nM. In this study, the Zn concentration was lower than the detection limit (<0.12 nM). Based on the conclusions of Shaked et al. (2006), one would expect a stimulation of AP activity by Zn addition at the low initial Zn values observed here. However Co, rather than Zn, stimulated an increase in AP activity. The phytoplankton community in the Sargasso may be adapted for chronically low levels of Zn. This may mean that the species present have very low Zn requirements or have enzymes with Co or cadmium cofactors rather than Zn.

AP incubations were attempted at a few other stations in the Sargasso Sea. Some of these incubations were set-up as time course experiments with single bottles sacrificed at each time point. These data were thrown out because the high variability between bottles of the same treatment at the different time points made it impossible to determine coherent trends between different treatments. A 2-day endpoint incubation with triplicate bottles was performed at St. 11. In this incubation, no increase of AP activity was observed in either the +Zn or +Co treatments.

In summary, the incubation result of this study and that of (Shaked et al., 2006) demonstrate that Zn and Co have the potential to influence AP activity in diverse natural environments. However, considering the negative Zn result in this study and the negative Zn and Co result at St. 11, it is clear that the situation is a complex one. More field studies are required to establish how common it is for AP activity to be reduced due to low metal concentrations and to explore which metals result in increased AP activity.

#### **4.5.6 Culture Study**

This study and work by Shaked et al. (2006) confirm the importance of trace metals to levels of AP activity using cultures of the model coccolithophore *E. huxleyi*. Though the conclusions from both studies are similar, the approaches taken to reach them are very different. Shaked et al. (2006) had two Zn treatments

(high =  $10^{-10.8}$  Zn'; low =  $10^{-12.4}$  Zn') and made no additions of Co or cadmium. In this study, a matrix of Zn and Co concentrations were considered (Table 4.1) similar to the seminal work of Sunda and Huntsman (1995); no cadmium was added. Because no Co was added to the media in Shaked et al. (2006), their low Zn treatment is actually a low Zn, low Co treatment and is most appropriately compared to the -Co treatment of this study based on free metal ion concentrations.

The low Zn, low P treatment of Shaked et al. (2006) had 86% the growth rate and 56% the AP activity of the high Zn, low P treatment. In this study, the -Co treatment grew at 60% the rate and had 64% the AP activity of the Replete metal, low P treatment. Thus, in this study there was a larger reduction in growth rate, yet not as large a decrease in AP activity as that seen by Shaked et al. (2006). Part of this difference may be due to differences in the sampling schemes of the two studies.

Previous research has shown that in batch cultures of *E. huxleyi*, AP activity increases over time and has maximum values during stationary phase (Dyhrman and Palenik, 2003). With that in mind, in this study, treatments were sampled for 4 days once they reached stationary phase, even if that meant sampling days of each treatment did not overlap. Shaked et al. (2006) sampled all treatments at the same 4 time points which resulted in sampling different portions of the growth curve. The high Zn, low P culture was sampled for 1 day in exponential phase and 3 days of stationary phase and the low Zn, low P culture was sampled for 2 days in exponential phase and 2 days in stationary phase. In both treatments, AP activity was increasing daily. The AP activity from the 2<sup>nd</sup> day of stationary phase growth is indistinguishable between the two treatments (low Zn =  $42.3 \pm 1.9$ , high Zn =  $40.0 \pm 16$  fmol diFMU cell<sup>-1</sup> min<sup>-1</sup>).

The fact that similar decreases in AP activity were observed when either Zn or Co was removed from the media, may reflect some plasticity in the metal requirements of *E. huxleyi*'s AP, but underscore the potential for Zn and Co to constrain AP activity. This result compliments our shipboard incubation and again highlights that at low P, the Zn and Co cycles are intertwined with that of P, implying that Zn and Co have the potential to influence P-limitation and DOP cycling.

## 4.6 Conclusions

The low concentrations of SRP observed and the presence of measurable AP activity along the transect suggest that many phytoplankton in the Sargasso Sea experience P-stress and that DOP may support a

significant fraction of the phytoplankton community's P requirement. In cultures of *E. huxleyi* that were either Zn or Co stressed, AP activity was 60% the activity in Replete metal cultures. In addition, adding Co to a bottle incubation resulted in a significant increase in AP activity. This suggests that Zn and Co concentrations can be important factors in the level of AP activity and that DOP hydrolysis in the ocean may be linked to the availability of Zn and Co. Co is less often touted as a critical micronutrient than Zn; however, this study highlights the potential importance of Co more so than that of Zn in the Sargasso Sea. The concentration of Co was tightly coupled to chlorophyll *a* concentrations, and the addition of Co, not Zn, resulted in an increase of AP activity in a bottle incubation. These observations suggest that Co may be an important determinant of phytoplankton biomass and DOP cycling in the Sargasso Sea. The distributions of Zn and Co were sometimes decoupled and suggest that a main driver of Zn and Co concentrations may be phytoplankton predominance, though continental input processes may also be important. In summary, this study supports the hypothesis that low P concentrations in the Sargasso Sea may limit primary production and suggests that Zn and particularly Co may be linked to P acquisition in SRP-deficient environments such as the Sargasso Sea.

## **4.7 Acknowledgments**

The authors would like to thank the captain and crew of the R/V Oceanus. Thanks to Tyler Goepfert and Dreux Chappell for assistance at sea. The authors would also like to thank Dave Schneider and Lary Ball of the WHOI Plasma Mass Spectrometry Facility for assistance with ICP-MS measurements. Thanks to Mak Saito and Abigail Noble for providing the DMG reagent. This research was supported by NSF grant OCE-0136835 to J.W.M. and S.D. R.J.W. was supported by an EPA STAR Fellowship.

## Bibliography

- AMMERMAN, J. W., R. R. HOOD, D. A. CASE, and J. B. COTNER. 2003. Phosphorus deficiency in the Atlantic: An emerging paradigm in oceanography. *EOS*. **84**: 165,170.
- ARCHER, D., and E. MAIER-REIMER. 1994. Effect of deep-sea sedimentary calcite preservation on atmospheric CO<sub>2</sub> concentration. *Nature*. **367**: 260–263.
- ARIMOTO, R., R. A. DUCE, and B. J. JAY. 1989. Chemical oceanography. J. P. RILEY and R. CHESTER [Eds.]. *Chemical Oceanography*. . volume 10. chapter 56: Concentrations, sources and air-sea exchange of trace elements in the atmosphere over the Pacific Ocean, pp. 107–149. New York, USA. Academic Press.
- ARMSTRONG, F. A. J., P. M. WILLIAMS, and J. D. H. STRICKLAND. 1966. Photo-oxidation of organic matter in sea water by ultra-violet radiation, analytical and other applications. *Nature*. **211**: 481–483.
- BERMAN-FRANK, I., J. T. CULLEN, Y. SHAKED, R. M. SHERRELL, and P. G. FALKOWSKI. 2001. Iron availability, cellular iron quotas, and nitrogen fixation in *Trichodesmium*. *Limnology and Oceanography*. **46**: 1249–1260.
- BRAND, L. E., W. G. SUNDA, and R. R. L. GUILLARD. 1983. Limitation of marine phytoplankton reproductive rates by Zn, Mn, and Fe. *Limnology and Oceanography*. **28**: 1182–1198.
- BRULAND, K. W. 1989. Complexation of zinc by natural organic ligands in the central North Pacific. *Limnology and Oceanography*. **34**: 269–285.
- BRULAND, K. W., and R. P. FRANKS. 1983. Mn, Ni, Cu, Zn and Cd in the western North Atlantic. *In* Trace metals in seawater. NATO Conf. Ser. 4 Vol. 9. Plenum. pp. 395–414.
- CAVENDER-BARES, K. K., D. M. KARL, and S. W. CHISHOLM. 2001. Nutrient gradients in the western North Atlantic Ocean: Relationship to microbial community structure and comparison to patterns in the Pacific Ocean. *Deep-Sea Research I*. **48**: 2373–2395.
- COTNER, J. B., J. W. AMMERMAN, E. R. PEELE, and E. BENTZEN. 1997. Phosphorus-limited bacterioplankton growth in the Sargasso Sea. *Aquatic Microbial Ecology*. **13**: 141–149.
- DUCE, R. A., R. ARIMOTO, B. J. RAY, C. K. UNNI, and P. J. HARDER. 1983. Atmospheric trace elements at Enewetak Atoll: 1, concentrations, sources, and temporal variability. *Journal of Geophysical Research*. **88**: 5321–5342.
- DUCE, R. A., G. L. HOFFMAN, B. J. RAY, I. S. FLETCHER, P. R. WALSH, S. R. FASCHING, S. R. PIOTROWICZ, E. J. HOFFMAN, J. M. MILLER, and J. L. HEFFTER. 1976. chapter Trace metals in the marine atmosphere: sources and fluxes, pp. 77–120. *In* H. WINDOM and R. A. DUCE [Eds.], *Marine Pollutant Transfer*. D. C. Heath. Lexington, Mass.
- DUCE, R. A., and N. W. TINDALE. 1991. Atmospheric transport of iron and its deposition in the ocean. *Limnology and Oceanography*. **36**: 1715–1726.
- DYHRMAN, S. T., P. D. CHAPPELL, S. T. HALEY, J. W. MOFFETT, E. D. ORCHARD, J. B. WATERBURY, and E. A. WEBB. 2006. Phosphonate utilization by the globally significant marine diazotroph *Trichodesmium*. *Nature*. **439**: 68–71.

- DYHRMAN, S. T., and B. PALENIK. 2003. Characterization of ectoenzyme activity and phosphate-regulated proteins in the coccolithophorid *Emiliania huxleyi*. *Journal of Plankton Research*. **25**: 1215–1225.
- DYHRMAN, S. T., E. A. WEBB, D. M. ANDERSON, J. W. MOFFETT, and J. B. WATERBURY. 2002. Cell-specific detection of phosphorus stress in *Trichodesmium* from the Western North Atlantic. *Limnology and Oceanography*. **47**: 1832–1836.
- ELLWOOD, M. J., and C. M. G. VAN DEN BERG. 2000. Zinc speciation in the Northeastern Atlantic Ocean. *Marine Chemistry*. **68**: 295–306.
- ELLWOOD, M. J., and C. M. G. VAN DEN BERG. 2001. Determination of organic complexation of cobalt in seawater by cathodic stripping voltammetry. *Marine Chemistry*. **75**: 33–47.
- GONG, N., C. CHEN, L. XIE, H. CHEN, X. LIN, and R. ZHANG. 2005. Characterization of a thermostable alkaline phosphatase from a novel species *Thermus yunnanensis* sp. nov. and investigation of its cobalt activation at high temperature. *Biochimica et Biophysica Acta*. **1750**: 103–111.
- GRAZIANO, L. M., R. J. GEIDER, W. K. W. LI, and M. OLAIZOLA. 1996. Nitrogen limitation of north atlantic phytoplankton: Analysis of physiological condition in nutrient enrichment experiments. *Aquatic Microbial Ecology*. **11**: 53–64.
- GUILLARD, R. R. L. 1975. Culture of marine invertebrate animals. W. L. SMITH and M. H. CHANLEY [Eds.]. *Culture of Marine Invertebrate Animals*. chapter Culture of phytoplankton for feeding marine invertebrates, pp. 26–60. New York, USA. Plenum Press.
- GUILLARD, R. R. L., and J. H. RYTHER. 1962. Studies of marine planktonic diatoms. i. *cyclotella nana* hustedt and *detonula conferevacea* cleve. *Canadian Journal of Microbiology*. **8**: 229–239.
- HEUMANN, K. G. 1988. Isotope dilution mass spectrometry, chapter 7, pp. 301–375. *In* F. ADAMS, R. GIBBELS and R. VAN GRIEKEN [Eds.], *Inorganic Mass Spectrometry*. volume 95. John Wiley & Sons. New York, USA.
- JOHNSON, D. L. 1971. Simultaneous determination of arsenate and phosphate in natural waters. *Environmental Science & Technology*. **5**: 411–414.
- KARL, D. M., and G. TIEN. 1992. MAGIC: A sensitive and precise method for measuring dissolved phosphorus in aquatic environments. *Limnology and Oceanography*. **37**: 105–116.
- LI, H., M. J. W. VELDHUIS, and A. F. POST. 1998. Alkaline phosphatase activities among planktonic communities in the northern Red Sea. *Marine Ecology Progress Series*. **173**: 107–115.
- LOMAS, M. W., A. SWAIN, R. SHELTON, and J. W. AMMERMAN. 2004. Taxonomic variability of phosphorus stress in sargasso sea phytoplankton. *Limnology and Oceanography*. **49**: 2303–2310.
- LYMAN, J., and R. H. FLEMING. 1940. Composition of seawater. *Journal of Marine Research*. **3**: 134–146.
- MARTIN, J. H., S. E. FITZWATER, R. M. GORDON, C. N. HUNTER, and S. J. TANNER. 1993. Iron, primary production and carbon-nitrogen flux studies during the JGOFS North Atlantic Bloom Experiment. *Deep-Sea Research II*. **40**: 115–134.



- MICHAELS, A. F., and A. H. KNAP. 1996. Overview of the U.S. JGOFS Bermuda Atlantic Time-series Study and the Hydrostation S program. *Deep-Sea Research II*. **43**: 157–198.
- MILLS, M. M., C. RIDAME, M. DAVEY, J. L. ROCHE, and R. J. GEIDER. 2004. Iron and phosphorus co-limit nitrogen fixation in the eastern tropical North Atlantic. *Nature*. **429**: 292–294.
- MOREL, F. M. M., J. R. REINFELDER, S. B. ROBERTS, C. P. CHAMBERLAIN, J. G. LEE, and D. YEE. 1994. Zinc and carbon co-limitation of marine phytoplankton. *Nature*. **369**: 740–742.
- MURPHY, J., and J. P. RILEY. 1962. A modified single solution method for the determination of phosphate in natural waters. *Analytica Chimica Acta*. **27**: 31–36.
- PERRY, M. A. 1972. Alkaline phosphatase activity in subtropical central north pacific waters using a sensitive fluorometric method. *Marine Biology*. **15**: 113–119.
- PLOCKE, D. J., C. LEVINHAL, and B. L. VALLEE. 1962. Alkaline phosphatase of *Escherichia coli*: a zinc metalloenzyme. *Biochemistry*. **1**: 373.
- PRICE, N. M., and F. M. M. MOREL. 1990. Cadmium and cobalt substitution for zinc in a marine diatom. *Nature*. **344**: 658–660.
- RIMMELIN, P., and T. MOUTIN. 2005. Re-examination of the MAGIC method to determine low orthophosphate concentration in seawater. *Analytica Chimica Acta*. **548**: 174–182.
- RUETER, J. G., J. 1983. Alkaline phosphatase inhibition by copper: Implications to phosphorus nutrition and use as a biochemical marker of toxicity. *Limnology and Oceanography*. **28**: 743–748.
- RUTTENBERG, K. C., and S. T. DYHRMAN. 2005. Temporal and spatial variability of dissolved organic and inorganic phosphorus, and metrics of phosphorus bioavailability in an upwelling-dominated coastal system. *Journal of Geophysical Research*. **110**: C10S13.
- RYTHER, J. H. 1969. Photosynthesis and fish production in the sea. *Science*. **166**: 72–76.
- SAITO, M. A., and J. W. MOFFETT. 2001. Complexation of cobalt by natural organic ligands in the sargasso sea as determined by a new high-sensitivity electrochemical cobalt speciation method suitable for open ocean work. *Marine Chemistry*. **75**: 49–68.
- SAITO, M. A., and J. W. MOFFETT. 2002. Temporal and spatial variability of cobalt in the Atlantic Ocean. *Geochimica et Cosmochimica Acta*. **66**: 1943–1953.
- SAITO, M. A., J. W. MOFFETT, S. W. CHISHOLM, and J. B. WATERBURY. 2002. Cobalt limitation and uptake in *Prochlorococcus*. *Limnology and Oceanography*. **47**: 1629–1636.
- SANUDO-WILHELMY, S. A., A. B. KUSTKA, C. J. GOBLER, D. A. HUTCHINS, M. YANG, K. LWIZA, J. BURNS, D. G. CAPONE, J. A. RAVEN, and E. J. CARPENTER. 2001. Phosphorus limitation of nitrogen fixation by *Trichodesmium* in the central Atlantic Ocean. *Nature*. **411**: 66–69.
- SHAKED, Y., Y. XU, K. LEBLANC, and F. M. M. MOREL. 2006. Zinc availability and alkaline phosphatase activity in *Emiliana huxleyi*: implications for Zn-P co-limitation in the ocean. *Limnology and Oceanography*. **51**: 299–309.

- SIEGEL, D. A., R. ITURRIAGA, R. R. BIDIGARE, R. C. SMITH, H. PAK, T. D. DICKEY, J. MARRA, and K. S. BAKER. 1990. Meridional variations of the springtime phytoplankton community in the Sargasso Sea. *Journal of Marine Research*. **48**: 379–412.
- SUNDA, W. G., and S. A. HUNTSMAN. 1995. Cobalt and zinc interreplacement in marine phytoplankton: Biological and geochemical implications. *Limnology and Oceanography*. **40**: 1404–1417.
- TAYLOR, S. R., and S. M. MCLENNEN. 1985. *The Continental Crust: Its Composition and Evolution*. Blackwell Scientific Publications.
- VELDHUIS, M. J. W., and G. W. KRAAY. 2004. Phytoplankton in the subtropical Atlantic Ocean: towards a better assessment of biomass and composition. *Deep-Sea Research I*. **51**: 507–530.
- VIDAL, M., C. M. DUARTE, S. AGUSTI, J. M. GASOL, and D. VAQUE. 2003. Alkaline phosphatase activities in the central Atlantic Ocean indicate large areas with phosphorus deficiency. *Marine Ecology Progress Series*. **262**: 43–53.
- WU, J., and E. A. BOYLE. 1998. Determination of iron in seawater by high-resolution isotope dilution inductively couple plasma mass spectrometry after  $Mg(OH)_2$  coprecipitation. *Analytica Chimica Acta*. **367**: 183–191.
- WU, J., W. SUNDA, E. A. BOYLE, and D. M. KARL. 2000. Phosphate depletion in the western North Atlantic Ocean. *Science*. **289**: 759–762.
- YEE, D., and F. M. M. MOREL. 1996. In vivo substitution of zinc by cobalt in carbonic anhydrase of a marine diatom. *Limnology and Oceanography*. **41**: 573–577.

Table 4.1: Free ion concentrations of Co and Zn in the culture media for each metal treatment are presented as log of the molar concentration. Values were calculated using the program visual MINTEQL based on both the background levels of Co and Zn in the seawater base and on the metals added to the media.

Treatment	Abbreviation	log[Zn <sup>2+</sup> ]	log[Co <sup>2+</sup> ]
Replete Zn and Co	Replete	-10.6	-10.1
0 Zn added, low Co	-Zn	-13.0	-12.3
low Zn, 0 Co added	-Co	-12.3	-14.8
0 Zn added, 0 Co added	-Zn/-Co	-13.0	-14.8

Table 4.2: Near-surface (~10 m) dissolved metal and phosphorus data. Values in parentheses represent the standard deviation of duplicate filters for chlorophyll (Chl), triplicate analyses for SRP and DOP, and either duplicate or triplicate analyses for Co and Zn. For chlorophyll, where there are no values in parentheses, only one filter was collected. Zn and SRP values that fell below the detection limit are marked < daily detection limit. No sample for total metal analysis was collected at St. 3. Other abbreviations: Sal = salinity, SST = sea surface temperature.

St.	Date	Location	Sal	SST (°C)	Chl ( $\mu\text{g L}^{-1}$ )	Co <sub>T</sub> (pM)	Zn <sub>T</sub> (nM)	SRP (nM)	DOP (nM)
1	20 Mar	31°41'N, 64°11'W	37.3	20.7	0.06 (0.02)	20.0 (1.2)	0.21 (0.01)	3.6 (1.1)	60.2 (5.0)
2	21 Mar	28°46'N, 62°57'W	37.4	20.8	0.02	10.9 (0.9)	0.19 (0.06)	1.0 (0.4)	92.2 (3.1)
3	21 Mar	28°03'N, 62°37'W	37.4	22.3	0.02			4.5 (0.6)	88.4 (13.0)
4	22 Mar	25°24'N, 61°09'W	37.4	24.7	0.03	10.4 (0.4)	0.15 (0.01)	3.7 (4.9)*	72.8 (15.0)*
5	23 Mar	25°23'N, 61°08'W	37.4	24.7	0.02	16.2 (5.3)	0.42 (0.03)	<1.4	105.0 (11.8)
6	24 Mar	22°48'N, 58°56'W	37.6	25.2	0.03	8.4 (1.4)	0.26 (0.04)	<1.4	123.8 (18.2)
7	25 Mar	20°00'N, 57°00'W	37.9	25.0	0.04	6.8 (0.7)	0.58 (0.03)	13.6 (4.9)*	81.1 (26.5)*
8	26 Mar	20°00'N, 52°58'W	37.8	25.4	0.05	7.1 (2.2)	0.09 (0.01)	1.7 (0.1)	196.4 (21.9)
9	27 Mar	20°00'N, 49°44'W	37.8	25.0	0.02	5.4 (0.3)	0.12 (0.02)	2.0 (0.4)	96.7 (12.9)
10	28 Mar	20°00'N, 45°54'W	37.8	24.6	0.06	3.8 (0.0)	0.15 (0.02)	5.8 (4.9)*	136.8 (8.6)*
11	29 Mar	20°58'N, 46°54'W	37.8	24.8	0.06 (0.00)	4.7 (0.9)	0.34 (0.04)	1.6 (0.4)	135.0 (34.4)
12	30 Mar	23°36'N, 49°41'W	37.7	25.4	0.05 (0.02)	8.7 (4.7)	<0.12	3.3 (0.4)	118.3 (21.3)
13	01 Apr	28°31'N, 53°11'W	37.4	21.9	0.05 (0.00)	10.1 (2.6)	0.37 (0.04)	1.7 (0.7)	74.30 (14.8)
14	01 Apr	29°38'N, 53°37'W	37.2	20.6	0.06	13.7 (0.1)	<0.07	3.2 (0.8)	104.5 (16.1)
15	02 Apr	32°14'N, 54°37'W	37.4	20.4	0.12 (0.00)	18.0 (0.5)	0.24 (0.02)	3.2 (0.2)	108.4 (0.0)
16	04 Apr	34°38'N, 55°35'W	37.2	19.0	0.27 (0.07)	14.3 (1.6)	<0.12	2.9 (0.2)	89.9 (0.0)
17	05 Apr	34°24'N, 58°12'W	37.0	19.0	0.37 (0.17)	13.9 (0.9)	0.11 (0.01)	6.3 (1.5)	73.5 (16.1)
18	06 Apr	36°11'N, 61°54'W	37.1	18.1	0.51 (0.08)	43.0 (3.5)	0.08 (0.02)	66.5 (2.4)	84.8 (7.4)
19	07 Apr	37°43'N, 64°51'W	36.8	19.2	0.49 (0.06)	39.9 (5.2)	0.14 (0.06)	22.5 (1.1)	168.9 (17.0)
20	08 Apr	38°42'N, 67°07'W	37.0	19.5	0.61 (0.14)	51.5 (1.9)	0.35 (0.05)	103.3 (2.8)	50.8 (0.0)
21	08 Apr	38°56'N, 67°33'W	36.3	14.1	0.55 (0.08)	51.8 (0.1)	0.24 (0.02)	400.4 (9.1)	223.3 (34.4)
22	08 Apr	38°59'N, 67°38'W	35.5	8.0	1.40 (0.20)	56.3 (1.7)	0.44 (0.03)	342.6 (37.9)	216.0 (18.7)
23	08 Apr	39°23'N, 68°35'W	34.1	8.4	1.80 (0.59)	90.9 (24.9)	0.96 (0.02)	584.8 (42.1)	233.9 (22.2)
24	09 Apr	40°00'N, 70°01'W	34.1	6.7	1.87 (0.15)	111.4 (18.1)	0.69 (0.10)	416.1 (9.4)	282.4 (24.1)
25	09 Apr	40°27'N, 70°19'W	33.5	5.1	0.84 (0.02)	59.9 (5.7)	1.32 (0.08)	452.6 (38.2)	307.5 (32.1)

\* From Dyrman et al. (2006).

Figure 4-1: Map of cruise track from the North Atlantic that was sampled aboard the R/V Oceanus during March - April 2004.. Shipboard incubation was performed at St. 16.

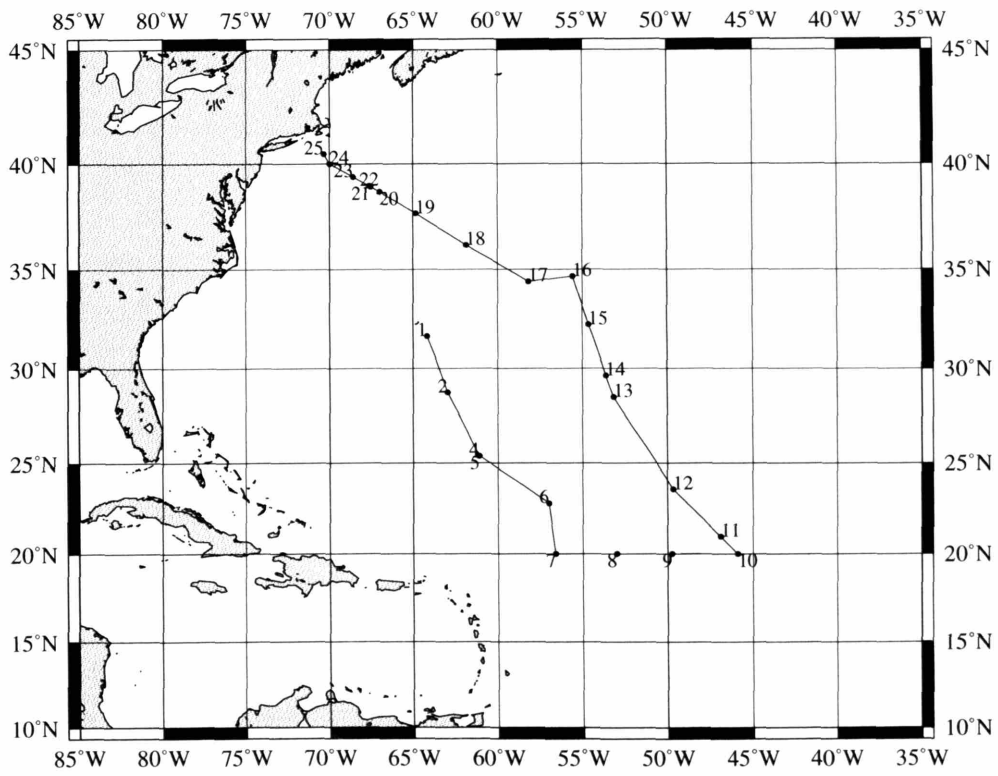


Figure 4-2: Concentrations of chlorophyll, soluble reactive phosphorus (SRP), and dissolved organic phosphorus (DOP) at approximately 10 m along the transect. Error bars represent the standard deviation between duplicate filters for chlorophyll, triplicate analyses for SRP and DOP. SRP and DOP values for stations 4, 7, and 10 have been previously reported elsewhere (Dyhrman et al., 2006) and are not plotted here, though they are included in Table 3.1.

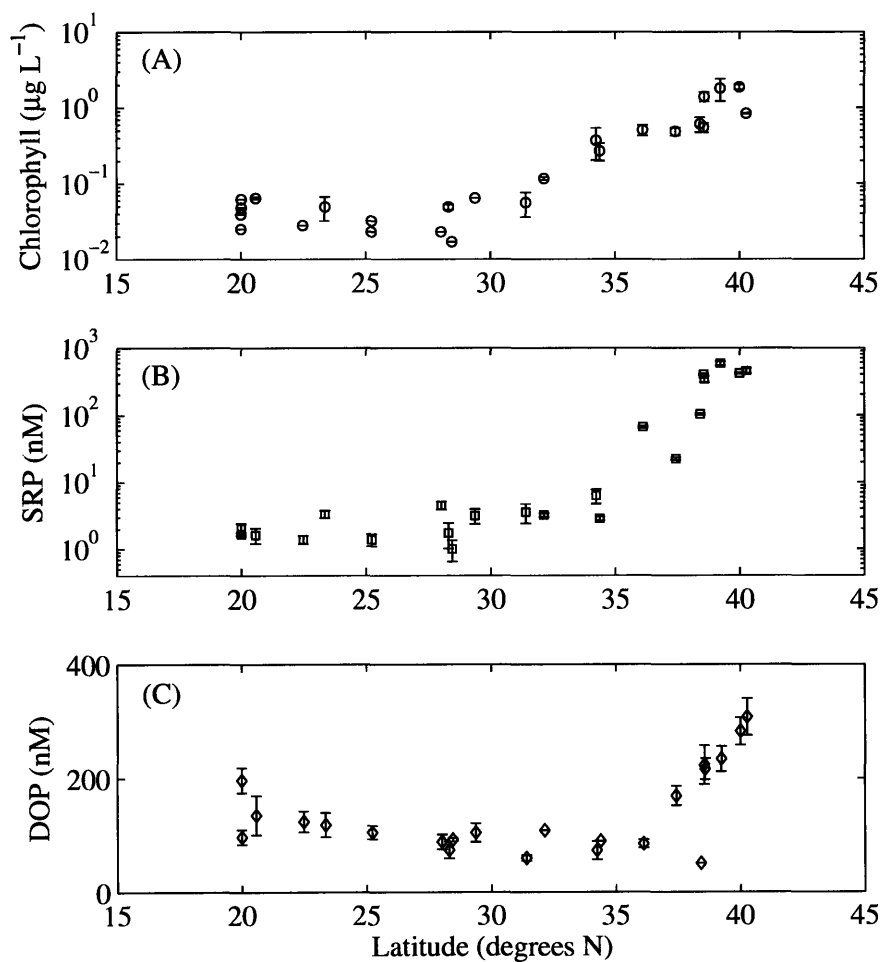


Figure 4-3: Alkaline phosphatase activity (APA) at approximately 10 m along the transect. In (A) activities are normalized to the chlorophyll concentration, whereas in (B), activities are presented as raw rates of phosphomonester cleavage rates.

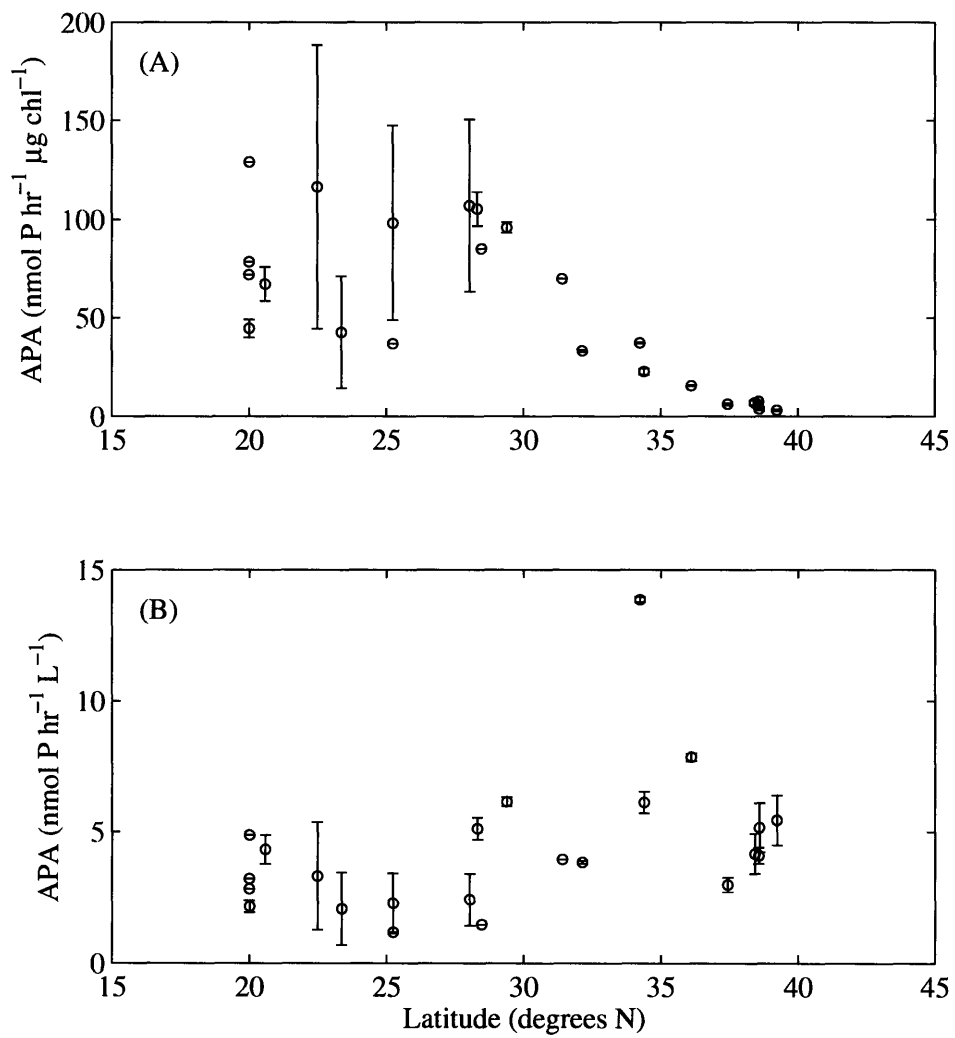


Figure 4-4: Concentrations of total dissolved Zn (A) and Co (B) at roughly 10 m depth along the transect. Error bars represent the standard deviation of duplicate or triplicate analyses. Detection limit of the analyses is denoted by the dashed line. Any values which fell below the detection limit are plotted with the detection limit as their concentration.

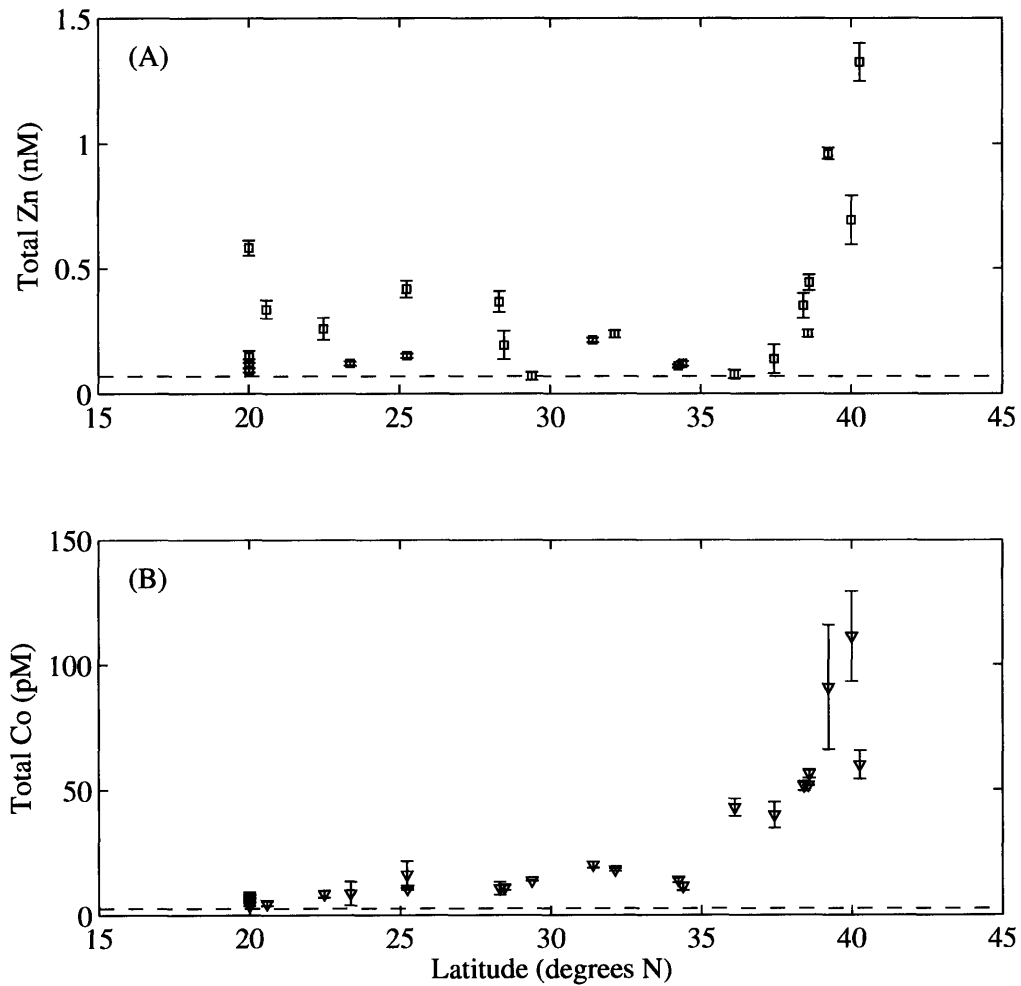




Figure 4-5: Relationship of salinity to Co (triangles in A) and Zn (B) for stations 15-25.  $R^2$  values are as follows: Zn/salinity 0.78; Co/salinity 0.65. Zn and Co error bars represent the standard deviation of duplicate or triplicate analyses. Solid lines are least-squares fit lines. In (A), circles and dashed line are data points and the least squares relationship from Saito and Moffett (2002).

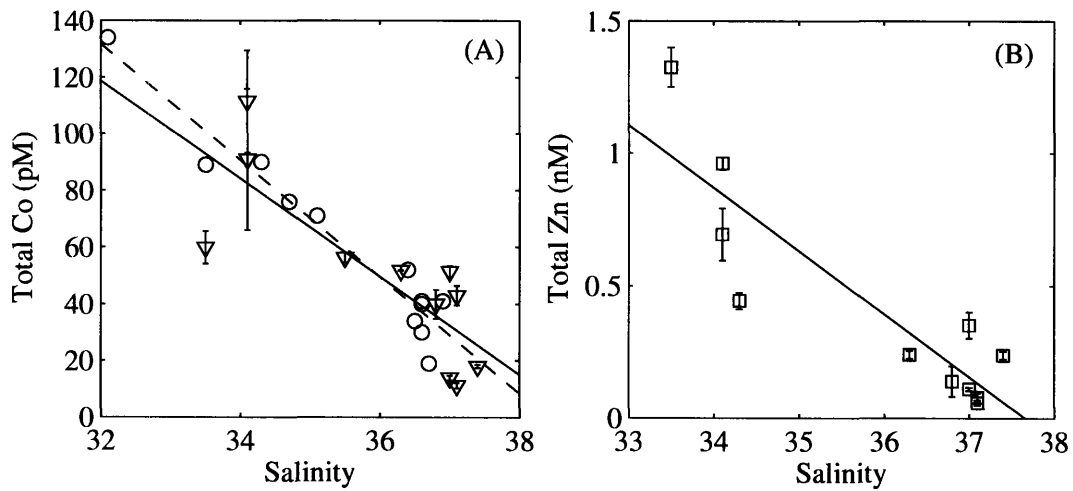


Figure 4-6: Relationship between chlorophyll *a* concentration and the concentrations of total dissolved Co (A) and Zn (B) and SRP (C). Co and Zn error bars represent the standard deviation of duplicate or triplicate analyses. SRP error bars represent the standard deviation of triplicate analyses. Chlorophyll error bars represent the standard deviation of duplicate filters. Lines are least-squares fit lines ( $R^2$  values are 0.90 for Co/chlorophyll, 0.37 for Zn/chlorophyll, and 0.78 for SRP/chlorophyll).

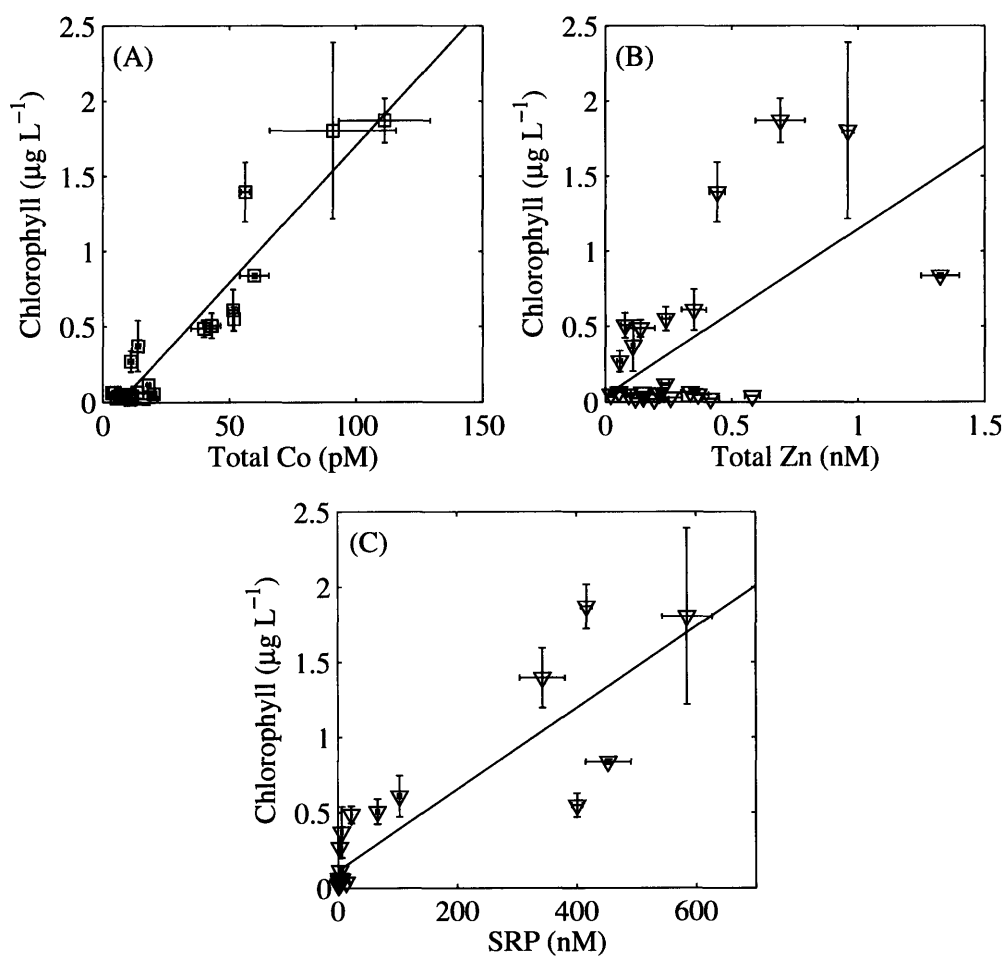


Figure 4-7: Relationship between SRP concentration and the concentrations of total dissolved Co (A) and Zn (B). Error bars as previous figures. Lines are least-squares fit lines ( $R^2$  values are 0.78 for Co/SRP and 0.57 for Zn/SRP).

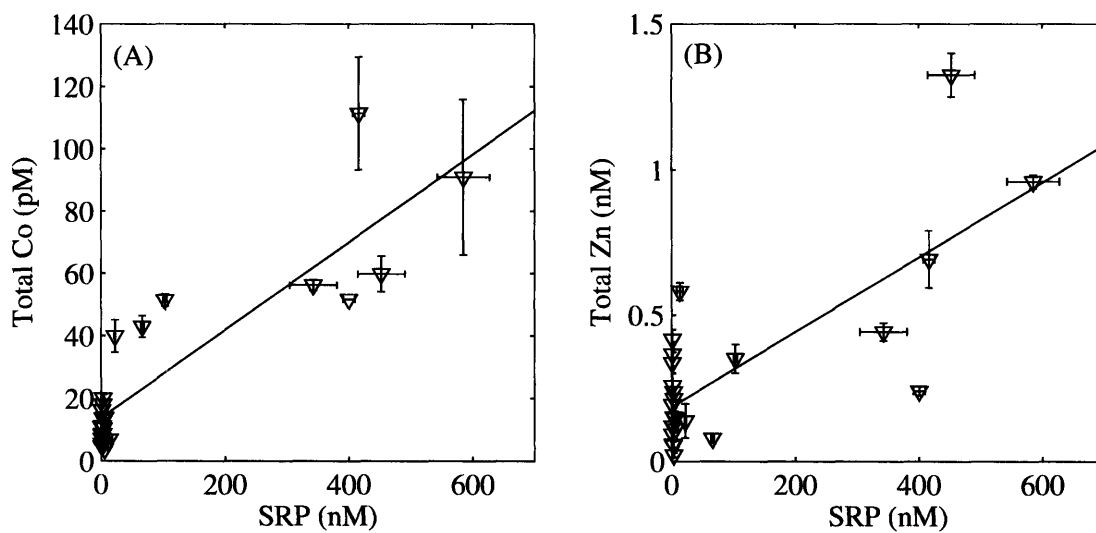


Figure 4-8: Results from the shipboard incubation performed at St. 16: (A) chlorophyll *a*, (B) AP activity normalized to chlorophyll, (C) AP activity as raw phosphomonoester cleavage rates. For all plots, bars represent the average value of triplicate bottles and error bars represent the standard deviation. In both (B) and (C) +Co activity is significantly higher than control with p-values of 0.14 and 0.01, respectively.

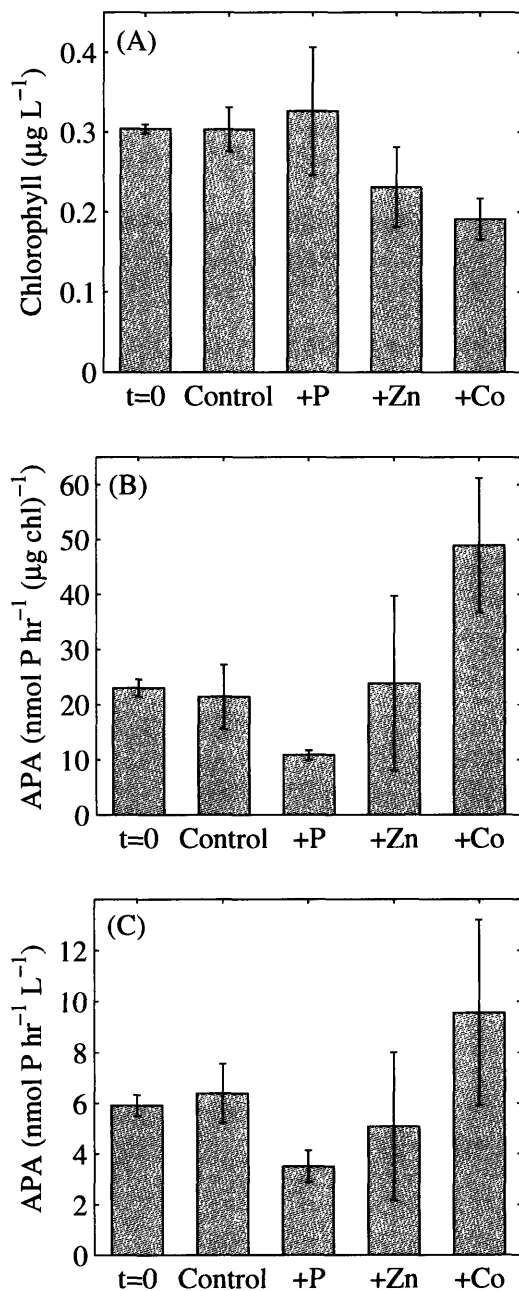
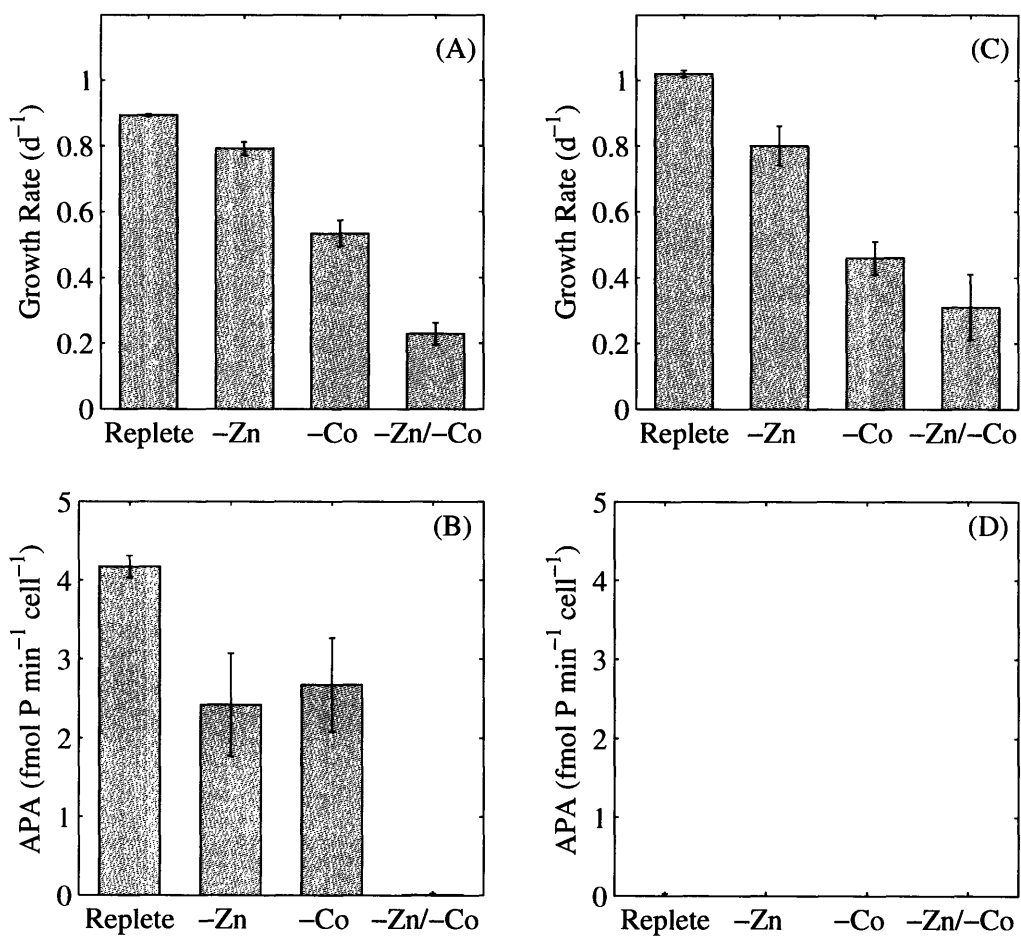


Figure 4-9: Growth rate (A,C) and maximum alkaline phosphatase activity (B,D) of *E. huxleyi*. Data represent culture conditions over varying levels of Zn and Co and two different P levels (low P: A,B; high P: C,D). Average values of triplicate cultures are plotted for each treatment with the standard deviation plotted as error bars.





## **Chapter 5**

# **Phosphonate utilization by marine phytoplankton in the Sargasso Sea**

## **Abstract**

Concentrations of inorganic phosphorus in the Sargasso Sea are extremely low and have the potential to limit the growth of marine phytoplankton. The bioavailability of the comparatively large pool of dissolved organic phosphorus is not well understood. This study uses shipboard incubations from two cruises in the Sargasso Sea to examine the ability of marine phytoplankton to utilize two dominant classes of organic phosphorus: phosphate monoesters and phosphonates. Bottle incubations were performed with additions of inorganic phosphate, glycerophosphate (monoester), and phosphonoacetic acid (phosphonate). In all incubations where glycerophosphate or phosphonoacetic acid were added, an increase in chlorophyll relative to a no-addition control was observed. The chlorophyll increase due to inorganic phosphate addition was generally similar to that due to organic phosphorus addition; however in one incubation, it was significantly less than that caused by the addition of either glycerophosphate or phosphonoacetic acid. Flow cytometry analysis revealed that phosphonate addition stimulated increases in both the *Synechococcus* and picoeukaryote populations. These data suggest that in the Sargasso Sea, where inorganic phosphorus is low, marine phytoplankton are able to obtain phosphorus from dissolved organic phosphorus sources. Furthermore, it suggests that phosphonates, a compound class that has been considered refractory, may be available to the natural phytoplankton community.



## 5.1 Introduction

Phosphorus is an element essential to all living organisms. It is a major component of numerous biomolecules that are used in cells for membrane structure, protein encoding, and energy transfer. Phosphorus (P) in the marine environment occurs as dissolved inorganic phosphorus (DIP, mainly as the  $\text{HPO}_4^{2-}$  ion), dissolved organic phosphorus (DOP), and particulate phosphorus (PP). DIP is the form of P which is most bioavailable to phytoplankton (Bjorkman and Karl, 1994). In the surface ocean, concentrations of DIP are often drawn down to very low levels. For example, concentrations of soluble reactive phosphorus (hereafter equated with and referred to as DIP) in the mixed layer of the North Pacific Ocean are generally 40 - 120 nM (Karl and Tien, 1997). Surface DIP concentrations in the North Atlantic are typically an order of magnitude lower (<1 - 10 nM, Wu et al. 2000; Cavender-Bares et al. 2001).

Low DIP in surface waters may limit production in some ocean regions. Time-series measurements at Station ALOHA in the North Pacific revealed a steady decrease in the DIP concentration over a ten-year period beginning in 1988 (Karl et al., 2001b). Concomitantly, nitrogen (N) fixation increased, which has led to the hypothesis that the North Pacific subtropical gyre is in the process of switching from a predominantly N-limited ecosystem to a predominantly P-limited ecosystem (Karl et al., 2001a). In the Sargasso Sea, the ratio of dissolved N to P in the water column can reach more than twice the classical Redfield value of 16N:1P (dissolved inorganic N:P  $\approx$  40-50, Cavender-Bares et al. 2001). Field studies in the Sargasso Sea, using metrics of P physiology such as P uptake, alkaline phosphatase activity, and P quotas, provide further evidence of P-limitation in this system (Cotner et al., 1997; Wu et al., 2000; Sanudo-Wilhelmy et al., 2001; Dyhrman et al., 2002; Ammerman et al., 2003). In low DIP environments like the Sargasso Sea, the bioavailability of DOP may dramatically influence production.

The concentration of DOP exceeds that of DIP in surface waters, accounting for the majority of the total dissolved P pool: 94–99% in the North Atlantic (Wu et al., 2000; Cavender-Bares et al., 2001) and 70–80% in the North Pacific (Karl and Bjorkman, 2002). Although the organic fraction dominates the total dissolved phosphorus (TDP) pool, relatively little is known about its composition or bioavailability. DOP is produced by organisms through cell growth and death, exudation, viral lysis and grazing, and therefore, phosphorus molecules typically found in the cell are expected to make up the DOP pool in open ocean systems. Several DOP compound classes have been detected in seawater including nucleotides, nucleic acids, phospholipids,

sugar phosphates, and vitamins (Karl and Bjorkman 2002 and references therein).

DOP molecules are often categorized based on the type of bond connecting the  $\text{PO}_4^{3-}$  molecule to the organic structure. In phosphate esters, the P atom is bound through an oxygen atom to a C atom, whereas in phosphonate molecules, the P is directly bonded to a C atom.  $^{31}\text{P}$  nuclear magnetic resonance (NMR) spectroscopy of ultrafiltered DOP (1-100 nm size fraction) suggests that oceanic DOP occurs mainly as phosphate esters (75%) but that a significant proportion (25%) also occurs as phosphonates (Kolowitz et al., 2001). The high proportion of phosphonates is unusual since phosphonates account for only a small percentage of total P in sinking particles (<6%, Paytan et al. 2003). One explanation for this is that phosphonates accumulate in the DOP pool because they are more chemically resistant and therefore less likely to be utilized by microorganisms than phosphate esters (Kolowitz et al., 2001). However, the relative proportion of phosphate esters to phosphonates remains constant with depth, though the total DOP concentration decreases significantly (Kolowitz et al., 2001). This seems to suggest that remineralization of both compounds classes is occurring with depth. It is also important to stress that the NMR data considers only the high molecular weight portion of DOP, which accounts for 25-50% of the total DOP (Kolowitz et al., 2001). There is no comparable knowledge of the composition of the low molecular weight fraction that dominates the total DOP.

Identifying the fraction and type of DOP that is bioavailable to phytoplankton remains elusive. DOP bioavailability is a function of several factors including its concentration, its composition, the taxa present, and their physiological state. Previous research has shown that DIP is the strongly preferred P substrate for plankton growth (Cotner, Jr. and Wetzel, 1992; Bjorkman and Karl, 1994), however the low concentrations of DIP relative to DOP and DIN in many areas of the ocean may select for the ability to use organic forms of P. A number of cultured phytoplankton are able to grow successfully when organic substrates are the sole P source including representatives of the following groups: coccolithophores (Dyhrman and Palenik, 2003), diatoms (Donald et al., 1997), and cyanobacteria (Donald et al., 1997; Scanlan et al., 1997; Stihl et al., 2001; Palenik et al., 2003). This research highlights the complexity of DOP bioavailability. Some organisms were able to grow on some DOP substrates but not on all DOP substrates examined. For example, *Synechococcus* WH7803 was able to grow on a nucleotide and on three different phosphate monoesters, but not on a model phosphate diester (Scanlan et al., 1997). Heterogeneity in bioavailability can also occur between different

strains of the same species. *Emiliana huxleyi* CCMP374 was able to grow on adenosine monophosphate (AMP) or glycerophosphate, but *Emiliana huxleyi* CCMP373 could grow only on glycerophosphate not on AMP (Dyhrman and Palenik, 2003). These studies document the potential for DOP bioavailability with model organisms in culture, however field studies are essential to verify extrapolations from cultured organisms to natural populations.

Several studies have examined the availability of DOP to natural phytoplankton assemblages using both direct and indirect measures. In an incubation experiment off the coast of Hawaii, seven different DOP compounds were added to whole water samples and subsequent P uptake was measured (Bjorkman and Karl, 1994). The microorganisms were able to access P from both nucleotides and phosphate monoesters, however even those DOP compounds that were most bioavailable (nucleotides) were only 20% as bioavailable as DIP (Bjorkman and Karl, 1994). Alkaline phosphatase is a cell surface enzyme that cleaves phosphate monester bonds, thereby releasing a bioavailable  $\text{PO}_4$  from DOP molecules with monoester bonds. Alkaline phosphatase activity provides an indirect measure of DOP bioavailability, as its presence is an indication of potential DOP hydrolysis. Alkaline phosphatase activity has been measured in a number of marine environments, including the Mediterranean (Zohary and Robarts, 1998), the Red Sea (Li et al., 1998; Stihl et al., 2001), and the North Atlantic (Ammerman et al., 2003; Vidal et al., 2003), providing an indirect measure of DOP bioavailability.

The work to date demonstrates that DOP is likely an important P source for phytoplankton; however, our understanding is limited by several factors. One of these is our lack of knowledge about the composition of marine DOP. NMR has provided information about the high molecular weight fraction of DOP, but little is known about the low molecular weight fraction. Additionally, studies of DOP availability have predominantly focused on phosphate monoesters. Phosphonates have not been considered likely P sources for phytoplankton because their more chemically stable C-P bond is difficult to break and because they appear to accumulate in the water column. However, recent evidence from the Cariaco Basin shows a preferential removal of phosphonates from sinking particles relative to phosphate esters, suggesting that under anoxic conditions, phosphonates may be bioavailable (Benitez-Nelson et al., 2004). Genetic evidence indicates that even under the normal aerobic conditions of the upper water column, phosphonates may be bioavailable to *Synechococcus* cultures (Palenik et al., 2003). Furthermore, a recent study documented the

expression of genes predicted to encode a C–P lyase pathway in colonies of *Trichodesmium erythraeum* collected from the Sargasso Sea (Dyhrman et al., 2006). As such, there is a growing literature on the bioavailability of phosphonates to phytoplankton; however, this has not been comprehensively examined in oligotrophic systems.

This study examines the response of natural marine phytoplankton to DOP additions in an oceanic regime where DIP concentrations are extremely low, the Sargasso Sea. Phytoplankton response to DOP was examined by performing incubation experiments with phosphate monoester and phosphonate additions.

## 5.2 Methods

Several phosphorus bottle incubation experiments were performed in the North Atlantic on two separate cruises. In late August 2002, an incubation was performed in the Sargasso Sea aboard the R/V Endeavor (EDR, Fig. 5-1). Additions were made of both inorganic P and a model phosphate monoester (PME). For P additions, solutions were made up from monosodium phosphate ( $\text{NaH}_2\text{PO}_4$ , Sigma) and a glycerophosphate disodium salt (Sigma, no more than 0.1% inorganic P). Each solution was chelexed to remove any potential trace metal contamination and stored in acid-clean teflon bottles at 4°C. Unfiltered water was collected from 60 m depth using Teflon-coated Go-Flo bottles (General Oceanics) and distributed into acid-washed 2.5 L polycarbonate bottles. Triplicate bottles were amended with  $10 \mu\text{mol L}^{-1} \text{NaH}_2\text{PO}_4$  (+DIP), and  $10 \mu\text{mol L}^{-1}$  glycerophosphate (+PME). To serve as the control, no addition was made to one set of triplicates. Bottles were placed in a Percival incubator which was on a 14:10 light/dark cycle where the light flux adjusted to mimic the irradiance at 60 m depth ( $41.5 \mu\text{mol quanta s}^{-1} \text{m}^{-2}$ ). Time zero samples were collected for chlorophyll and dissolved P analyses. After four days, bottles were removed from the incubator and sampled for chlorophyll.

Three shipboard incubations (OCE1, OCE2, OCE5) were performed aboard the R/V Oceanus in March–April 2004 in the Sargasso Sea (Fig. 5-1). Nutrient stocks were prepared as above. For this cruise, a phosphonate treatment was added using phosphonacetic acid (Sigma, no more than 0.02% inorganic P) prepared as above. The phosphonacetic acid (Pnte) stock was cross-checked and confirmed to be free of inorganic P contamination, via a bioassay with *Emiliania huxleyi* CCMP 374. Briefly, cell-free Sargasso Sea water was spiked with cells and changes in biomass were recorded in treatments where P was added as

DIP ( $36 \mu\text{mol L}^{-1} \text{NaH}_2\text{PO}_4$ ) or as Pnte ( $36 \mu\text{mol L}^{-1}$  phosphonoacetic acid) and where no P was added. No growth was observed on Pnte relative to the no P control (Fig. 5-2).

For the OCE incubation experiments, trace metal clean water was collected with an air-driven Teflon pump from approximately 15 m depth directly into an acid-washed HDPE carboy. Twelve acid-washed polycarbonate bottles (1 and 2.5 L) were filled from the carboy and time zero samples were collected for chlorophyll, flow cytometry, and dissolved P analyses. Additions were made to duplicate or triplicate polycarbonate bottles as follows: no addition (control),  $8.4 \mu\text{mol L}^{-1} \text{NaH}_2\text{PO}_4$  (+DIP),  $8.4 \mu\text{mol L}^{-1}$  glycerophosphate (+PME), and  $8.4 \mu\text{mol L}^{-1}$ , phosphonoacetic acid (+Pnte). Bottles were tightly capped and placed in an on-deck water bath supplied with flowing seawater for temperature control. Sunlight was attenuated with blue-gel shading (Roscolux 65: Daylight Blue, Stage Lighting Store) to mimic 15 m irradiances. Incubations were sampled in two different manners: at an end point or along a time course. For the endpoint style incubations, all three bottles were removed from incubators after three days and sampled for chlorophyll. In addition, one bottle of each treatment was sampled for cell counts by flow cytometry. In the time-course style incubations, a single bottle of each treatment was sacrificed at each timepoint. In the endpoint incubations, where triplicate data points were available, t-tests were used to determine the statistical significance of the results with a 95% confidence level and where there were 4 degrees of freedom.

For chlorophyll analysis, seawater was passed through a GF/F filter. Filters were extracted in 90% acetone overnight at  $-20^\circ\text{C}$  and analyzed following the procedure of Jeffrey and Humphrey (1975) using a handheld Aquafluor fluorometer (Turner Designs). For flow cytometry, 1 ml of unfiltered seawater was preserved with 1% paraformaldehyde and stored in liquid nitrogen (Campbell and Vaultot, 1993). These samples were processed by the J. J. MacIsaac Aquatic Cytometry Facility at the Bigelow Laboratory for Ocean Sciences for the abundance of *Synechococcus* and pico-eukaryotes.

For P analyses, samples were filtered (acid-cleaned  $0.4 \mu\text{m}$ -pore, polycarbonate filters) through an acid-cleaned filter tower into acid-cleaned LDPE bottles and were immediately frozen and stored at  $-20^\circ\text{C}$ . DIP was measured using the MAGIC method developed by Karl and Tien (1992). Briefly, sample aliquots of 50 ml were pre-concentrated by adding  $200 \mu\text{l}$  of  $1 \text{mol L}^{-1} \text{NaOH}$ , followed by centrifugation at 3000 rpm ( $1811 \times g$ ) for 1 hour. After decanting the supernatant, the precipitate was dissolved in 1-2 ml of  $0.1 \text{mol L}^{-1}$  hydrochloric acid. This solution was subsequently analyzed using the molybdate blue method (Murphy

and Riley, 1962) and corrected for arsenic interference as per Johnson (1971). Standards and blanks were prepared in DIP-free seawater and treated identically to samples. DIP-free seawater was prepared by performing a MAGIC co-precipitation reaction as above on surface Sargasso seawater; the supernatant was collected and deemed DIP-free since the DIP was co-precipitated in the pellet. For TDP analysis, 10 ml samples were placed in quartz tubes and 40  $\mu\text{l}$   $\text{H}_2\text{O}_2$  was added. The samples were then exposed to strong UV-radiation to photo-oxidize organic matter (Armstrong et al., 1966). UV-digestion was carried out for twelve hours followed by analysis with the molybdate blue method (Murphy and Riley, 1962). DOP concentration was defined as the difference between the TDP and the DIP measurements.

### 5.3 Results

For the four shipboard incubation experiments, the initial surface chlorophyll and P values at each experimental station are given in Table 5.1. The chlorophyll concentration was low at the start of the EDR, OCE1, and OCE2 incubations but was an order of magnitude higher at the start of OCE5. The concentration of DIP was uniformly low (1.0 - 4.8  $\text{nmol L}^{-1}$ ) at all locations. In all cases, the concentration of DOP (60 - 92  $\text{nmol L}^{-1}$ ) was an order of magnitude higher than DIP. Some studies have found that UV-photo-oxidation does not result in complete recovery of DOP from seawater samples (Maher and Woo 1998 and references therein). Therefore, these DOP numbers can be treated as lower limits of the actual DOP concentration.

Changes in chlorophyll concentration were monitored at either single endpoints (EDR, OCE5, Fig. 5-3) or along a time-course (OCE1, OCE2, Fig. 5-4). In the EDR incubation, after four days, chlorophyll increased significantly in both the +DIP and +PME additions, Fig. 5-3A) relative to the control ( $p < 0.01$ ,  $< 0.03$ ). In OCE5, chlorophyll at the three-day endpoint was similar in the control (0.30  $\mu\text{g L}^{-1}$ ) and +DIP (0.32  $\mu\text{g L}^{-1}$ ) treatments (Fig. 5-3B). A doubling of chlorophyll relative to the control was observed after the addition of phosphonoacetic acid (0.69  $\mu\text{g L}^{-1}$ ) and increased even more in the +PME treatment (0.77  $\mu\text{g L}^{-1}$ , Fig. 5-3B). These chlorophyll increases in the DOP treatments were significantly elevated relative to the control with  $p$ -values less than 0.02 and 0.01, respectively.

In time-course incubations OCE1 and OCE2, there was a strong response to the addition of phosphorus (Fig. 5-4). In OCE1, chlorophyll concentrations nearly tripled in the +DIP addition on day 2 (from 0.06 to 0.16  $\mu\text{g L}^{-1}$ ). The addition of DIP in OCE2 resulted in a chlorophyll increase by a factor of 8 on day 2 (from

0.02 to 0.14  $\mu\text{g L}^{-1}$ ). This chlorophyll increase due to DIP addition was not sustained on day 4 in either incubation. In OCE1, the chlorophyll increase on day 2 in the +PME and the +Pnte treatments was slightly higher than that observed in the +DIP treatment. As in the +DIP treatment, after the increase in chlorophyll over the first two days of the experiment, the chlorophyll decreased in both DOP treatments from days 2 to 4. During OCE2, the +PME treatment caused a greater increase in chlorophyll than the +Pnte treatment, and both forms of DOP had a more sustained response than DIP over time, surpassing the DIP addition on day 4 (Fig. 5-4).

Samples were analyzed by flow cytometry for species composition over the time-course incubation OCE1 (Fig. 5-5). Because samples were collected from and incubated to simulate light at near surface depths (15 m), *Prochlorococcus* could not be reliably detected, however *Synechococcus* and picoeukaryote populations were observable. The trends of both *Synechococcus* and picoeukaryote abundance were very similar to that of chlorophyll. In the control, abundance of both picoeukaryote and *Synechococcus* either remained constant or decreased. In each of the added P treatments (+DIP, +PME, +Pnte), abundances increased to peak values on day 2. Picoeukaryote abundance more than tripled on day 2 in each P treatment and the highest response was seen in the +Pnte treatment (Fig. 5-5A). By contrast, the *Synechococcus* response was highest in the +PME treatment where the cell concentration more than doubled (Fig. 5-5B). Increases in *Synechococcus* abundance were slightly more modest in the +DIP and +Pnte treatments on day 2; however, the *Synechococcus* abundance continued increasing on day 4 in the +DIP treatment whereas it declined in both the +Pnte and +PME treatments (Fig. 5-5B).

For OCE5, the flow cytometry data did not track the chlorophyll response as closely. The picoeukaryote and *Synechococcus* abundances were similar in the control and +Pnte treatments (Fig. 5-6). In the +PME treatment, there was a large increase in both picoeukaryote (3-fold) and *Synechococcus* (2-fold) populations. Both picoeukaryote and *Synechococcus* abundance also increased in the +DIP treatment, though less dramatically (Fig. 5-6).

## 5.4 Discussion

In late summer 2002 and early spring 2004, the addition of phosphorus (as either DIP or DOP) caused an increase in chlorophyll in four separate bottle incubations in the Sargasso Sea. Our results support evidence

from other studies (e.g., Wu et al. 2000; Ammerman et al. 2003) that the low concentrations of DIP in the Sargasso Sea may control primary production. In three out of four incubations, DIP addition resulted in a significant increase in chlorophyll. Although DIP has been shown to be the preferred P substrate for phytoplankton near Hawaii (Bjorkman and Karl, 1994), in this study in the Sargasso Sea, the addition of DOP as both a phosphate monoester and a phosphonate caused an increase in chlorophyll similar to, or higher than, that caused by DIP. This suggests that in the Sargasso Sea, phytoplankton are able to utilize DOP as a P source in lieu of DIP. As previously mentioned, DOP dominates the TDP pool in the surface of the Sargasso Sea, yet growth of the phytoplankton community was stimulated by DOP addition. It seems the phytoplankton community has the capacity to use DOP, but this capacity is not saturated despite the relatively high concentration of DOP in situ. This may imply that the majority of the DOP pool in the Sargasso Sea is refractory compared to the low molecular weight model compounds added in this study.

Both the model phosphate monoester and model phosphonate compound added appear to be bioavailable. Phosphate monoesters have been repeatedly shown to be bioavailable to phytoplankton (van Boekel, 1991; Cotner, Jr. and Wetzel, 1992; Bjorkman and Karl, 1994; Scanlan and West, 2002; Dyrhman and Palenik, 2003). However, because phosphonates have a stronger C–P bond that is difficult to break, they have not been considered likely to be bioavailable until recently (Palenik et al., 2003; Benitez-Nelson et al., 2004; Dyrhman et al., 2006). This study is the first demonstration that phosphonate addition can result in the growth of a natural phytoplankton community.

Two different incubation approaches were used, each of which has an associated set of advantages and disadvantages. The time-course incubation allows observation of the evolution of the response and provides a large window to observe chlorophyll increases. The endpoint incubation is valuable because triplicate bottles are sampled at one time allowing for the application of statistics. The combination of both approaches was useful to better understand the results.

Time-course incubations OCE1 and OCE2 provided insight into the speed of community response. The phytoplankton community responded rapidly with chlorophyll values generally peaking at the first time-point (at 48 h) and declining thereafter. The chlorophyll response due to DOP addition seemed to have somewhat different timing and perhaps a slower response than that due to DIP addition. When microorganisms are grown on phosphonate as the sole P source, there can be an extended lag phase prior to growth



(Kononova and Nesmeyanova, 2002). This may explain the more sustained chlorophyll response in the +PME and +Pnte treatments after 4 days in OCE2.

The concentration of P added ( $8.4 \mu\text{mol L}^{-1}$ ) in our incubations was 1000 times greater than the ambient DIP concentration. Without measuring the final DIP concentration in the bottles, it is somewhat difficult to know how much of the added P was consumed. The kinetics of DIP uptake by phytoplankton can generally be described by Michaelis-Menten kinetics. Luxury uptake of P can occur after the removal of P-limitation and may likely have occurred in our bottles (Cembella et al., 1984). A compilation of kinetic parameters for DIP uptake obtained from phytoplankton cultures and natural phytoplankton populations (Cembella et al., 1984) suggest that a P-deficient population with the cell density observed in our bottles, could consume  $9.7 \mu\text{mol L}^{-1}$  P in 48 h. However, using the change in chlorophyll observed, along with a typical phytoplankton C:chlorophyll from the North Atlantic ( $160 \mu\text{g C } \mu\text{g chl}^{-1}$ , Veldhuis and Kraay 2004), and the Redfield C:P molar ratio of 106, the amount of P consumed would only have been  $25 \text{ nmol L}^{-1}$ . Both these calculations require assumptions (e.g., Redfield 106C:1P) that are imperfect (C:P can vary widely, especially under situations of P limitation) but necessary considering our limited information. It is apparent from the ~1000 fold difference between the calculations, that the assumptions strongly influence the calculated value and therefore it is difficult to be confident in a calculated concentration of P drawdown. However, as the Sargasso Sea is an oligotrophic environment, it is unlikely that the phytoplankton in our bottles would have been able to consume  $8.4 \mu\text{mol L}^{-1}$  P before another nutrient such as N or perhaps Fe, Co, or Zn became limiting. Thus, a plausible explanation for the observed trend in chlorophyll over time is that the phytoplankton consumed the necessary P to recover from P limitation in the first 48 h, after which limitation by another nutrient and grazing processes dominated and resulted in the chlorophyll decrease generally seen on day 4.

The time-course incubations described above, provide useful information for understanding the results of the endpoint style incubations EDR and OCE5. The chlorophyll results after four days in EDR are similar to the results from day 4 of OCE1. In both cases, the chlorophyll in the +DIP and +PME treatments were similar and about twice the chlorophyll concentration of the control. For OCE5, the lack of chlorophyll increase in the +DIP bottle coupled with the large chlorophyll increases in the +PME and +Pnte bottles was initially surprising. However, the OCE5 chlorophyll results resemble those from day 4 of OCE2. There may

have been a response to DIP in OCE5 that was missed by not sampling the bottles prior to day 3. Despite the potential for bottle effects and grazing these endpoint incubations clearly demonstrate increased growth on PME and Pnte relative to the control.

The ability of *Synechococcus* WH8102 to utilize phosphonates was predicted from its genome sequence and validated in culture (Palenik et al., 2003; Su et al., 2003). Here, flow cytometry results from OCE1 are the first evidence from the field that natural populations of *Synechococcus* can respond to phosphonate addition. There was previously no available evidence of phosphonate utilization by picoeukaryotes. However, the OCE1 incubation showed that picoeukaryotes also responded to phosphonate addition. These results suggest that the use of phosphonates may not be exclusive to marine prokaryotes and could be present in different phytoplankton taxa.

In OCE5, there was an increase in the abundance of *Synechococcus* and picoeukaryotes in the +DIP treatment and the +PME treatment relative to the control. There was no increase in either *Synechococcus* or picoeukaryote abundance in the +Pnte treatment where a large chlorophyll increase was observed. This may indicate that other phytoplankton, not examined with flow cytometry, may also be capable of responding to phosphonate addition. OCE5 was the most northern incubation performed, where the ambient temperature was lower and the ambient chlorophyll higher than any other station. It is likely that the initial community collected in our bottles for OCE5 differed from the other incubations. Alternately, our results could be due to an increase in the concentration of chlorophyll per cell in the +Pnte treatment, not an actual increase in biomass.

Potential contamination with inorganic N or P of the DIP and DOP stocks was considered. The Sargasso Sea is an extremely oligotrophic environment where concentrations of N are also very low (Cavender-Bares et al. 2001 and references therein) and some studies have suggested that N can limit primary production in the Sargasso Sea (Mills et al., 2004). To ensure that there was no unintended addition of inorganic N or P in our incubations, fresh solutions of the DIP and DOP stocks were prepared and given to the WHOI Nutrient Analytical Facility for analysis of inorganic nutrients. Aliquots of each stock were analyzed before and after treatment with chelex resin, a step which removes trace metal impurities (Table 5.2). For the most part, negligible amounts of inorganic N and small amounts of P were added to the incubations. The exception is the +GP treatment which appears to have gained significant ammonia upon chelexing

(Table 5.2). However, the striking similarity between the results for the +GP and +Pnte treatments in each experiment suggests that this high ammonia number may be due to ammonia contamination of the aliquot measured and not the actual GP stock. If the stock did contain significant ammonia one would expect a higher response than when P alone is added since the P addition would likely drive the community to N limitation.

Designing the ideal experiment is always a difficult task, especially when the experiment is to be done in the field with added time and resource constraints. The results of this experiment illuminate some of its design flaws. In reference to the previous paragraph, adding a +N treatment would constrain the importance of possible contamination with inorganic nitrogen. Though week-long, multi-timepoint incubation experiments have been extremely effective for demonstration of iron limitation (e.g., Martin and Fitzwater 1988), they are not well-suited to the Sargasso Sea. Future experiments should be conducted with replicates focused in the 0 to 48 or perhaps 72 h timeframe. In addition, the amount of P that we added was extremely high relative to the ambient concentration. The results would be more applicable if an environmentally relevant P concentration was used, such as the concentration of DIP at 500 m ( $\sim 100 - 700 \text{ nmol L}^{-1}$ , Cavender-Bares et al. 2001) which could be injected through upwelling. The final issue with these incubation experiments is more difficult to fix. The incubation bottles were filled with whole seawater that contains natural populations of non-photosynthetic microbes. These organisms may have played a potential role in cycling DOP to DIP, which would have then been available to the phytoplankton. Thus, we cannot rule out the possibility that the phytoplankton chlorophyll and abundance increases were due to the indirect availability of DOP. However, a growing body of evidence (e.g., Palenik et al. 2003, Dyhrman et al. 2006), suggests that phosphonates can be bioavailable to marine phytoplankton without microbial transformation. Measuring bacterial cell counts in future incubation experiments might shed light on this distinction.

It is clear that DOP availability can dramatically influence phytoplankton abundance in a low DIP environment. It may also influence what taxa or even what strains, dominate these environments. Further analysis of phosphate monoester and phosphonate bioavailability to both model organisms and field populations is certainly warranted.

## 5.5 Conclusions

This study expands our knowledge of DOP bioavailability. In the Sargasso Sea, where DIP concentrations are low enough to restrict primary production, phytoplankton responded to P additions of both a model phosphate ester and a model phosphonate. This work represents the first demonstration that natural marine phytoplankton assemblages are able to respond to additions of phosphonate. Increased cell numbers after the addition of phosphonate were observed for both picoeukaryotes and *Synechococcus*. Our results suggest that the ability to use phosphonates may be more widespread across phytoplankton taxa than previously recognized. The accumulation of high molecular weight phosphonates in the ocean has been attributed to a lack of bioavailability. This may hold true, however low molecular weight phosphonates may be an important source of P for phytoplankton in regions of the ocean where DIP is depleted.

## **5.6 Acknowledgments**

The authors would like to thank the captain and crew of the R/V Endeavor and the R/V Oceanus, as well as Brian Binder, Chief Scientist on the R/V Endeavor cruise. Thanks to Tyler Goepfert and Dreux Chappell for assistance at sea. The authors would also like to acknowledge Nicole Poulton at the J. J. MacIsaac Aquatic Cytometry Facility for analyzing the flow cytometry samples. This research was supported by NSF grant OCE-0136835 to J.W.M. and S.D and by an EPA STAR Fellowship to R.J.W.

## Bibliography

- AMMERMAN, J. W., R. R. HOOD, D. A. CASE, and J. B. COTNER. 2003. Phosphorus deficiency in the Atlantic: An emerging paradigm in oceanography. *EOS*. **84**: 165,170.
- ARMSTRONG, F. A. J., P. M. WILLIAMS, and J. D. H. STRICKLAND. 1966. Photo-oxidation of organic matter in sea water by ultra-violet radiation, analytical and other applications. *Nature*. **211**: 481–483.
- BENITEZ-NELSON, C. R., L. O'NEILL, L. C. KOLOWITH, P. PELLECHIA, and R. THUNELL. 2004. Phosphonates and particulate organic phosphorus cycling in an anoxic marine basin. *Limnology and Oceanography*. **49**: 1593–1604.
- BJORKMAN, K., and D. M. KARL. 1994. Bioavailability of inorganic and organic phosphorus compounds to natural assemblages of microorganisms in Hawaiian coastal waters. *Marine Ecology Progress Series*. **111**: 265–273.
- CAMPBELL, L., and D. VAULOT. 1993. Photosynthetic picoplankton community structure in the subtropical North Pacific Ocean near Hawaii (station ALOHA). *Deep-Sea Research I*. **40**: 2043–2060.
- CAVENDER-BARES, K. K., D. M. KARL, and S. W. CHISHOLM. 2001. Nutrient gradients in the western North Atlantic Ocean: Relationship to microbial community structure and comparison to patterns in the Pacific Ocean. *Deep-Sea Research I*. **48**: 2373–2395.
- CEMBELLA, A. D., N. J. ANTIA, and P. J. HARRISON. 1984. The utilization of inorganic and organic phosphorus compounds as nutrients by eukaryotic microalgae: A multidisciplinary perspective: Part 1. *CRC Critical Reviews Microbiology*. **10**: 317–391.
- COTNER, J. B., J. W. AMMERMAN, E. R. PEELE, and E. BENTZEN. 1997. Phosphorus-limited bacterioplankton growth in the Sargasso Sea. *Aquatic Microbial Ecology*. **13**: 141–149.
- COTNER, JR., J. B., and R. G. WETZEL. 1992. Uptake of dissolved inorganic and organic phosphorus compounds by phytoplankton and bacterioplankton. *Limnology and Oceanography*. **37**: 232–243.
- DONALD, K., D. SCANLAN, N. CARR, N. MANN, and I. JOINT. 1997. Comparative phosphorus nutrition of the marine cyanobacterium *Synechococcus* WH7803 and the marine diatom *Thalassiosira weissflogii*. *Journal of Plankton Research*. **19**: 1793–1813.
- DYHRMAN, S. T., P. D. CHAPPELL, S. T. HALEY, J. W. MOFFETT, E. D. ORCHARD, J. B. WATERBURY, and E. A. WEBB. 2006. Phosphonate utilization by the globally significant marine diazotroph *Trichodesmium*. *Nature*. **439**: 68–71.
- DYHRMAN, S. T., and B. PALENIK. 2003. Characterization of ectoenzyme activity and phosphate-regulated proteins in the coccolithophorid *Emiliania huxleyi*. *Journal of Plankton Research*. **25**: 1215–1225.
- DYHRMAN, S. T., E. A. WEBB, D. M. ANDERSON, J. W. MOFFETT, and J. B. WATERBURY. 2002. Cell-specific detection of phosphorus stress in *Trichodesmium* from the Western North Atlantic. *Limnology and Oceanography*. **47**: 1832–1836.
- JOHNSON, D. L. 1971. Simultaneous determination of arsenate and phosphate in natural waters. *Environmental Science & Technology*. **5**: 411–414.

- KARL, D. M., R. R. BIDIGARE, and R. M. LETELIER. 2001a. Long-term changes in plankton community structure and productivity in the North Pacific Subtropical Gyre: The domain shift hypothesis. *Deep-Sea Research II*. **48**: 1449–1470.
- KARL, D. M., and K. M. BJORKMAN. 2002. Dynamics of DOP. *In* D.A. HANSELL and C.A. CARLSON [Eds.], *Biogeochemistry of Marine Dissolved Organic Matter*. Elsevier Science. pp. 249–366.
- KARL, D. M., K. M. BJORKMAN, J. E. DORE, L. FUJIEKI, D. V. HEBEL, T. HOULIHAN, R. M. LETELIER, and L. M. TUPAS. 2001b. Ecological nitrogen-to-phosphorus stoichiometry at station ALOHA. *Deep-Sea Research II*. **48**: 1529–1566.
- KARL, D. M., and G. TIEN. 1992. MAGIC: A sensitive and precise method for measuring dissolved phosphorus in aquatic environments. *Limnology and Oceanography*. **37**: 105–116.
- KARL, D. M., and G. TIEN. 1997. Temporal variability in dissolved phosphorus concentrations in the subtropical North Pacific Ocean. *Marine Chemistry*. **56**: 77–96.
- KOLOWITH, L. C., E. D. INGALL, and R. BENNER. 2001. Composition and cycling of marine organic phosphorus. *Limnology and Oceanography*. **46**: 309–320.
- KONONOVA, S. V., and M. A. NESMEYANOVA. 2002. Phosphonates and their degradation by microorganisms. *Biochemistry (Moscow)*. **67**: 220–233.
- LI, H., M. J. W. VELDHUIS, and A. F. POST. 1998. Alkaline phosphatase activities among planktonic communities in the northern Red Sea. *Marine Ecology Progress Series*. **173**: 107–115.
- MAHER, W., and L. WOO. 1998. Procedures for the storage and digestion of natural waters for the determination of filterable reactive phosphorus, total filterable phosphorus and total phosphorus. *Analytica Chimica Acta*. **375**: 5–47.
- MARTIN, J. H., and S. E. FITZWATER. 1988. Iron deficiency limits phytoplankton growth in the north-east Pacific subarctic. *Nature*. **331**: 341–343.
- MILLS, M. M., C. RIDAME, M. DAVEY, J. L. ROCHE, and R. J. GEIDER. 2004. Iron and phosphorus co-limit nitrogen fixation in the eastern tropical North Atlantic. *Nature*. **429**: 292–294.
- MURPHY, J., and J. P. RILEY. 1962. A modified single solution method for the determination of phosphate in natural waters. *Analytica Chimica Acta*. **27**: 31–36.
- PALENIK, B., B. BRAHAMSHA, F. W. LARIMER, M. LAND, L. HAUSER, P. CHAIN, J. LAMERDIN, W. REGALA, E. E. ALLEN, J. MCCARREN, I. PAULSEN, A. DUFRESNE, F. PARTENSKY, E. A. WEBB, and J. WATERBURY. 2003. The genome of a motile marine *Synechococcus*. *Nature*. **424**: 1037–1042.
- PAYTAN, A., B. J. CADE-MENUN, K. MCCLAUGHLIN, and K. L. FAUL. 2003. Selective phosphorus regeneration of sinking marine particles: evidence from <sup>31</sup>P-NMR. *Marine Chemistry*. **82**: 55–70.
- SANUDO-WILHELMY, S. A., A. B. KUSTKA, C. J. GOBLER, D. A. HUTCHINS, M. YANG, K. LWIZA, J. BURNS, D. G. CAPONE, J. A. RAVEN, and E. J. CARPENTER. 2001. Phosphorus limitation of nitrogen fixation by *Trichodesmium* in the central Atlantic Ocean. *Nature*. **411**: 66–69.

- SCANLAN, D. J., N. J. SILMAN, K. M. DONALD, W. H. WILSON, N. G. CARR, I. JOINT, and N. H. MANN. 1997. An immunological approach to detect phosphate stress in populations and single cells of photosynthetic picoplankton. *Applied and Environmental Microbiology*. **63**: 2411–2420.
- SCANLAN, D. J., and N. J. WEST. 2002. Molecular ecology of the marine cyanobacterial genera *Prochlorococcus* and *Synechococcus*. *FEMS Microbiology Ecology*. **40**: 1–12.
- STIHL, A., U. SOMMER, and A. F. POST. 2001. Alkaline phosphatase activities among populations of the colony-forming diazotrophic cyanobacterium *Trichodesmium* spp. (cyanobacteria) in the Red Sea. *Journal of Phycology*. **37**: 310–317.
- SU, Z., P. DAM, X. CHEN, V. OLMAN, T. JIANG, B. PALENIK, and Y. XU. 2003. Computational inference of regulatory pathways in microbes: an application to phosphorus assimilation pathways in *Synechococcus* sp. wh8102. *Genome Informatics*. **14**: 3–13.
- VAN BOEKEL, W. H. M. 1991. Ability of *Phaeocystis* sp. to grow on organic phosphates: direct measurement and prediction with the use of an inhibition constant. *Journal of Plankton Research*. **13**: 959–970.
- VELDHUIS, M. J. W., and G. W. KRAAY. 2004. Phytoplankton in the subtropical Atlantic Ocean: towards a better assessment of biomass and composition. *Deep-Sea Research I*. **51**: 507–530.
- VIDAL, M., C. M. DUARTE, S. AGUSTI, J. M. GASOL, and D. VAQUE. 2003. Alkaline phosphatase activities in the central Atlantic Ocean indicate large areas with phosphorus deficiency. *Marine Ecology Progress Series*. **262**: 43–53.
- WU, J., W. SUNDA, E. A. BOYLE, and D. M. KARL. 2000. Phosphate depletion in the western North Atlantic Ocean. *Science*. **289**: 759–762.
- ZOHARY, T., and R. D. ROBARTS. 1998. Experimental study of microbial P limitation in the eastern Mediterranean. *Limnology and Oceanography*. **43**: 387–395.



Table 5.1: Conditions at time zero for each incubation. Values in parentheses represent the standard deviation of duplicate filters for chlorophyll, triplicate analyses for DIP, and duplicate analyses for DOP.

Incubation	Date	Location	Surface T (°C)	Chlorophyll ( $\mu\text{g L}^{-1}$ )	DIP ( $\text{nmol L}^{-1}$ )	DOP ( $\text{nmol L}^{-1}$ )
EDR	29 Aug 2002	33°13'N, 64°31'W	28.4	0.05 (0.03)	4.8 (1.4)	79.8 (0.9)
OCE1	20 Mar 2004	31°40'N, 64°10'W	20.7	0.06 (0.02)	3.6 (1.1)	60.2 (5.0)
OCE2	21 Mar 2004	28°46'N, 62°57'W	20.8	0.02	1.0 (0.4)	92.2 (3.1)
OCE5	04 Apr 2004	34°38'N, 55°35'W	19.0	0.30 (0.01)	2.9 (0.2)	89.9 (0.0)

Table 5.2: The concentration of inorganic nutrients in P solutions made up in the same manner as those for spiking the incubation experiments is reported. Also reported are the concentrations this would have added to the incubation bottles. Concentrations of PO<sub>4</sub> in the DIP stock are not reported because they were off-scale. Abbreviations: ammonia (NH<sub>4</sub>), phosphate (PO<sub>4</sub>), nitrite plus nitrate (NO<sub>2</sub>+NO<sub>3</sub>).

	NH <sub>4</sub> (μmol L <sup>-1</sup> )	PO <sub>4</sub> (μmol L <sup>-1</sup> )	NO <sub>2</sub> +NO <sub>3</sub> (μmol L <sup>-1</sup> )
Un-chelexed solutions:			
DIP	0	–	0.47
Pnte	0	30.6	1.2
PME	4.6	18.3	2.4
Chelexed solutions:			
DIP	1.5	–	6.9
Pnte	7.5	31.2	0.47
PME	1130	18.6	4.1
	NH <sub>4</sub> (nmol L <sup>-1</sup> )	PO <sub>4</sub> (nmol L <sup>-1</sup> )	NO <sub>2</sub> +NO <sub>3</sub> (nmol L <sup>-1</sup> )
Added to bottles:			
DIP	0	–	2
Pnte	2	9	0
PME	316	5	1

Figure 5-1: Map of incubation locations. Endeavor Incubation (EDR): 29 Aug 2002; Oceanus Incubation 1 (OCE1): 20 Mar 2004; Oceanus Incubation 2 (OCE2): 21 Mar 2004; Oceanus Incubation 5 (OCE5): 04 Apr 2004.

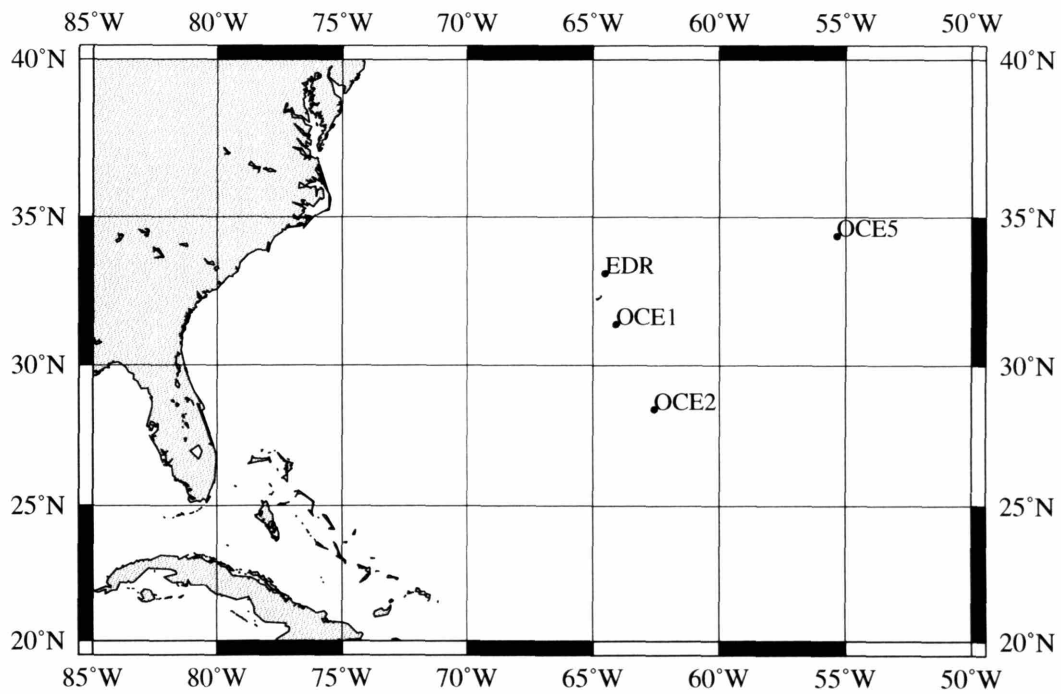


Figure 5-2: Relative fluorescence units, a measure of in vivo chlorophyll a fluorescence, in *E. huxleyi* cultures over time. The Sargasso seawater media base was supplemented with  $36 \mu\text{mol L}^{-1}$  of  $\text{NaH}_2\text{PO}_4$  (+DIP),  $36 \mu\text{mol L}^{-1}$  phosphonacetic acid (+Pnte), or no P added (0 P).

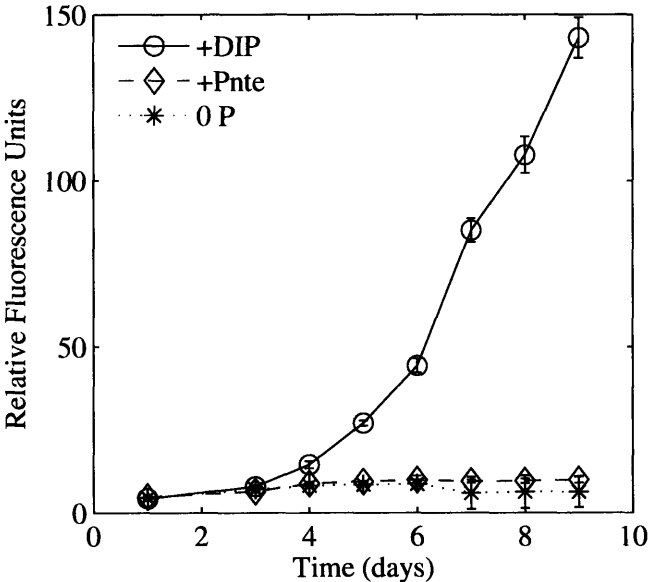


Figure 5-3: Average chlorophyll concentrations of 3 replicate bottles sampled after 4 days (A: EDR incubation) or 3 days (B: OCE5 incubation). Additions for EDR incubation: no addition (control),  $10 \mu\text{mol L}^{-1}$  of  $\text{NaH}_2\text{PO}_4$  (+DIP), and  $10 \mu\text{mol L}^{-1}$  of a phosphate monoester (+PME). Additions for OCE5 incubation: no addition (control),  $8.4 \mu\text{mol L}^{-1}$  of  $\text{NaH}_2\text{PO}_4$  (+DIP),  $8.4 \mu\text{mol L}^{-1}$  of a phosphate monoester (+PME) and  $8.4 \mu\text{mol L}^{-1}$  of a phosphonate (+Pnte). Note change in scale of y axis.

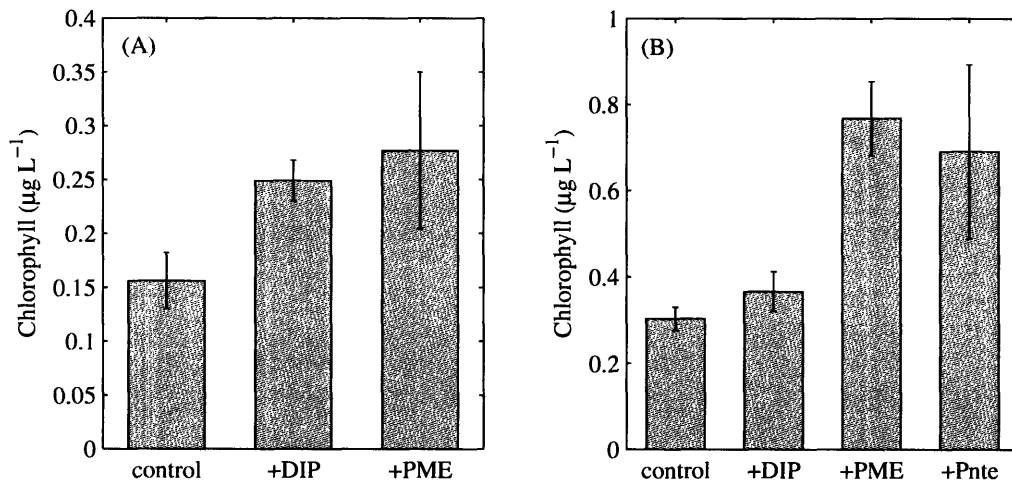


Figure 5-4: Chlorophyll concentrations from time-course incubation experiments OCE1 (A) and OCE2 (B). One bottle was sacrificed at each timepoint. Additions for both incubations are: no addition (control),  $8.4 \mu\text{mol L}^{-1}$  of  $\text{NaH}_2\text{PO}_4$  (+DIP),  $8.4 \mu\text{mol L}^{-1}$  of a phosphate monoester (+PME) and  $8.4 \mu\text{mol L}^{-1}$  of a phosphonate (+Pnte).

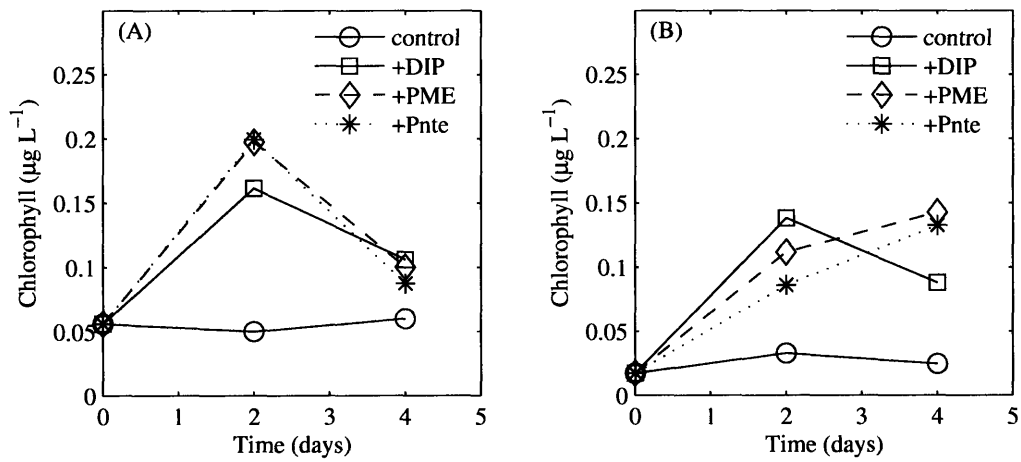


Figure 5-5: Abundance of (A) picoeukaryotes and (B) *Synechococcus* over the time course incubation OCE1. Additions as in Fig. 5-4 label.

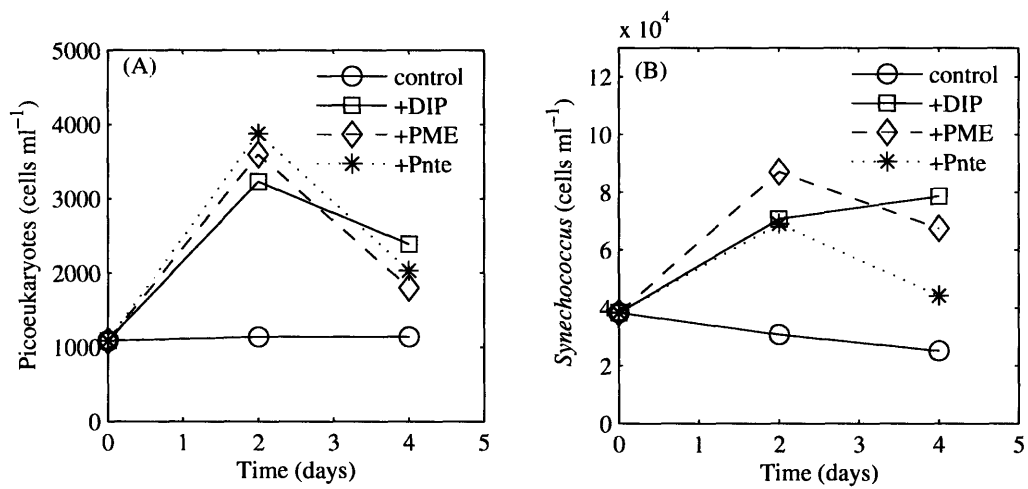
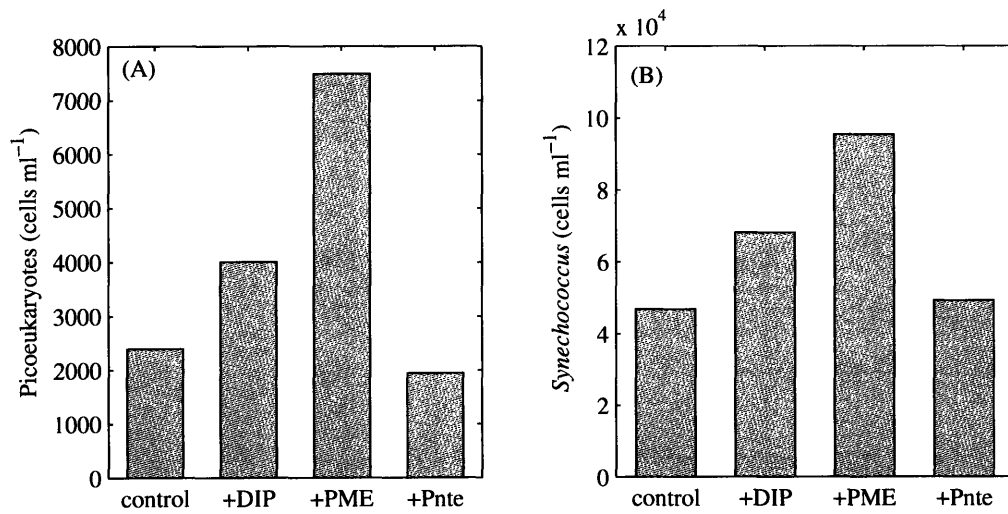


Figure 5-6: Abundance of (A) picoeukaryotes and (B) *Synechococcus* at day 3 of OCE5. Samples were analyzed from one of triplicate bottles for each treatment. Additions as in Fig. 5-3 label.





## **Chapter 6**

# **Conclusions and Future Directions**

Detailed research into a topic often results in the asking of just as many new questions (if not more) than those which were answered. This thesis is no exception.

Zinc (Zn) speciation was successfully measured by adaptation of an anodic stripping voltammetry (ASV) method for total lead and cadmium (Cd) analysis. This fresh film ASV (ff-ASV) method proved better in my hands than the classic competitive ligand exchange cathodic stripping voltammetry (CLE-CSV) method, in terms of consistency and signal to noise ratio. In relating the results of the ff-ASV method to the classic CLE-CSV method, it became clear that the error of Zn speciation methods is ill-defined. The time consuming nature of Zn speciation titrations mean that replicate titrations of a sample are rarely performed and error estimates on the Zn binding ligand ( $L_T$ ) concentration and conditional stability constant ( $K_{cond,Zn'}$ ) values are not generally reported. In the future, the error should be recognized and attempts made to minimize or at least better quantify it.

On the whole, Zn speciation measurements seem to be converging with similar  $L_T$  concentrations (1-3 nM) and  $K_{cond,Zn'}$  values ( $10^{9.5}$  -  $10^{11.5}$ ) measured in the the North Pacific, North Atlantic, and Southern oceans (e.g., Bruland 1989, Ellwood 2004, Chapter 2). The resultant free Zn ion ( $Zn^{2+}$ ) concentrations in the surface ocean range from <1 - 25 pM. The lowest concentrations of  $Zn^{2+}$  in this range cause reduced grow rates of cultured phytoplankton species, including oceanic species (Sunda and Huntsman, 1995). Does the  $Zn^{2+}$  concentration truly represent the bioavailable Zn fraction? The answer is unclear. Zn speciation measurements indicate that oceanic phytoplankton are able to grow at exceedingly low  $Zn^{2+}$  (Ellwood, 2004; Lohan et al., 2005). This suggests that either the phytoplankton Zn requirements are lower than previously thought, that Cd or cobalt (Co) effectively substitutes for Zn, or that some fraction of the organically complexed Zn fraction is bioavailable. If the third scenario is true, the utility of voltammetric Zn speciation analysis is limited. The values of  $L_T$  and  $K_{cond,Zn'}$  are valuable in that they allow calculation of  $Zn^{2+}$ , which is important as long as it is a biologically relevant quantity. The isolation and characterization of metal binding ligands from seawater proves a difficult analytical problem. However, it has the potential to provide more detailed information about the Zn binding ligands and could provide clues to the relevance of the free ion model of bioavailability. For instance, are there multiple classes of ligands that could be traced to specific species? If so, this may suggest a siderophore-like scenario, where specific receptors and transport proteins make the Zn-ligand complex bioavailable.

Measurements of Zn in the western subarctic North Pacific are scarce and the profiles in Chapter 3 are only the second set of the deep profiles measured to date. The trends in total dissolved Zn ( $Zn_T$ ) concentrations matched those previously measured, with lowest concentrations in the eastern portions of both the North Pacific and Bering Sea. High resolution concentration profiles are extremely valuable for comparison with macronutrient concentrations and hydrographic properties. In a cruise track such as ours, which covered a variety of mixed layer depths, a true surface transect would be more valuable than a near-surface transect. The disadvantage of the near-surface transect is that the water sampled not only reflects spatial variability but also whether or not the bottle is in the mixed layer, chlorophyll maximum, etc.

Zn was tightly bound by organic ligands at all stations in the N. Pacific and Bering Sea. The highest concentration of  $L_T$  measured to date in the open ocean was observed in the Bering Sea. There was also a high concentration of  $Zn_T$  at this station that may reflect recent atmospheric deposition. This may suggest that  $L_T$  synthesis by the microbial community has occurred in response to a Zn addition.  $L_T$  synthesis could be a detoxification mechanism or a way to enhance bioavailability either by uptake of the Zn-L complex or by keeping the Zn in solution.

Zn bioavailability in the open ocean remains a complicated and poorly constrained issue. Chlorophyll concentrations increased after Zn addition at one station in the North Pacific, which demonstrates the potential for low Zn bioavailability to limit primary production. However, Zn additions were performed at a number of other stations and no stimulation of chlorophyll due to Zn addition was observed. St. 5, where the response due to Zn addition was observed, does not seem to be anomalous from the other stations in any obvious way ( $Zn_T$ ,  $Zn^{2+}$ , phytoplankton species composition). Thus, the bioavailability of Zn and its importance to primary production is a complicated matter.

Another intriguing result of Chapter 3 was the correlation between Zn and two diatom pigments. The relative contributions of fucoxanthin and chlorophyll c to total chlorophyll were fairly well correlated with  $Zn_T$  ( $R^2 \sim 0.6$ ). An even stronger correlation was observed when the pigments were compared to  $Zn^{2+}$  ( $R^2 \sim 0.9$ ). Diatoms are known to have a relatively high Zn requirement (e.g., Sunda and Huntsman 1995), and these correlations may suggest that Zn is an important driver of diatom biomass. These results are preliminary and interpretation of HPLC pigment data is not always straightforward, since phytoplankton taxa contain multiple pigments. However, these results are encouraging for the potential to use pigment data

to examine the hypothesis that Zn concentrations may affect species composition.

In the North Atlantic Ocean, high sensitivity measurements were made of dissolved organic phosphorus, dissolved organic phosphorus, Co, Zn, and AP activity over a transect of 25 stations encompassing latitudes between 20 and 40°N. Concentrations of dissolved inorganic phosphorus (DIP) were extremely low in the majority of the transect (<7 nM at 16 of 25 stations). Measurement of such low DIP levels required the MAGIC method of sample pre-concentration (Karl and Tien, 1992). The low volume of sample collected (250 ml) and the low concentration of DIP meant that I was pushing the detection limit of the spectrophotometer. Extreme care and patience (similar to that for trace metal work) was required to prevent contamination. The synthetic blank protocol developed by Rimmelin and Moutin (2005) is an important practical advance. It allows rapid blank determination which aids in hunting for a contamination source. One thing that is not reported by authors about this method and that needs to be addressed is whether or not the sample volume is measured after precipitate dissolution. The volume of the precipitate plus acid is higher than the volume of acid added. Therefore, which volume is used for the dilution calculation will affect the concentration of P calculated. Calculations in this study were made without considering the volume increase due to the precipitate.

The low DIP concentration and measurable alkaline phosphatase (AP) activities add to the growing body of evidence that phosphorus (P) may limit primary production in the Sargasso Sea. AP is a phosphohydrolytic enzyme that is typically expressed only under conditions of P-stress and allows organisms to access a portion of the DOP pool. The presence of AP activity also suggests that DOP may be a significant fraction of the P consumed by phytoplankton. However, the measured AP activity is an optimum rate since a hydrolyzable substrate is added in excess. Whether or not all the phosphate monoesters present in seawater (75% of high molecular weight DOP) can be cleaved by AP is an open question.

The importance of Zn and Co for maximum AP activity was demonstrated. In *E. huxleyi* cultures, reducing either the Zn or the Co media concentration resulted in reduced AP activity. In a shipboard incubation, however, Co addition stimulated an increase in AP activity and Zn addition did not. This may suggest that the added Zn was tightly bound by organic ligands and therefore not bioavailable or that the community was expressing a Co-AP rather than a Zn-AP. This thesis focused on Co and Zn. However, Cd also has the potential to replace Zn in AP, and studies in the future should address this possibility. Practically, examining

the synergistic effects of all 3 metals is difficult as the number of experimental treatments quickly multiplies. Further, there are logistical constraints to working in an ultra-oligotrophic environment (i.e., low nutrient and low metals). The complexities of low P, low metal incubations have not been adequately addressed in the literature. Nevertheless, tackling this problem is necessary if we are to gain a complete and accurate picture of metal-AP dynamics.

For example, as no Cd was added to our culture media or to the shipboard incubations, we cannot rule out the possibility that Cd limitation of AP may have been occurring. Similarly, since neither Co or Cd was added to the media in Shaked et al. (2006), making their low Zn treatment most analogous to our -Co treatment, results from that study may be due to Co or Cd limitation of AP. Isolation of the AP enzyme and determination of its metal center under different metal conditions would help clarify these issues. Because AP activity is prevalent in the Sargasso Sea and may therefore be a significant P source for phytoplankton, future work into the metal limitation of AP is warranted as Zn, Co, and Cd concentrations may influence DOP utilization in this and other low P, low metal systems.

Co was mainly considered in this thesis because of its ability to substitute for Zn. The relationship of Zn and Co with phosphate from the North Pacific (Fig. 1-2) suggested that Co was an important nutrient mainly after Zn was depleted (Sunda and Huntsman, 1995). In the Sargasso Sea, Zn was often depleted; however, Co was always depleted, suggesting that Co is an important nutrient in its own right, not simply for Zn substitution. This point was driven home by the striking correlation between Co and chlorophyll ( $R^2 = 0.9$ ). This correlation was more robust than either the relationship between Zn and chlorophyll or DIP. The concentration of Co appears to be an important driver of phytoplankton biomass in the Sargasso Sea. It is possible that another nutrient that was not measured, such as nitrogen (N), is the true driver of phytoplankton biomass and that Co draw down is tightly coupled to the biomass abundance. However, the abundant AP activity over the transect suggests that N is sufficient for growth. Regardless, the tight correlation between Co and chlorophyll highlights the importance of Co as a micronutrient in its own right and perhaps even more so than Zn in the Sargasso Sea.

The concentrations of Co and Zn were decoupled along parts of the transect. This reflects either differences in the input or removal processes of the two elements. Biological drawdown by eukaryotic populations in the northern Sargasso Sea likely explains the more dramatic removal of Zn in these waters. In the south-

ern Sargasso Sea, the situation is more complex. It is possible that some of the high Zn values may reflect Zn contamination during sampling. Alternately, the higher Zn concentrations may be due to atmospheric dust deposition or advective input from the Caribbean shelf. Dust and advective inputs would also supply Co, though at lower concentrations. Co is more particle reactive than Zn. Co inputs maybe more readily removed from the mixed layer than Zn by both biological uptake and particle scavenging.

The relationship between Co and DIP concentrations seemed to have a non-zero y-intercept, such that it was only when DIP concentrations were very low (less than ~10-15 nM), that Co was drawn down below 20 pM. One explanation for this relationship may be that at low DIP values, elevated production of AP creates an increased demand for Co. There was a fair amount of scatter over the entire range of values in the Zn-DIP plot, which suggests these two elements were not tightly coupled in this region. There is no evidence from this relationship for an AP-related Zn demand.

The hypothesis that low DIP concentrations may limit phytoplankton production in the Sargasso Sea was explored by performing shipboard incubation experiments where DIP and DOP compounds were added. In three out of four incubations in the Sargasso Sea, DIP addition resulted in an increase in chlorophyll relative to a no-addition control. This again emphasizes the importance of P to primary production in the Sargasso Sea. The phytoplankton community seems to be adapted to the low DIP levels. Chlorophyll production was stimulated by the addition of dissolved organic phosphorus (DOP) as either a phosphate monoester or as a phosphonate model compound. This supports recent evidence that natural phytoplankton populations can utilize the phosphonate class of DOP compounds, which have largely been considered non-bioavailable (Dyhrman et al., 2006). Populations of both *Synechococcus* and picoeukaryotes were both stimulated by phosphonate addition. Some of this response may be the result of microbial DOP breakdown, however genetic and molecular evidence indicate that some cyanobacteria have the capability for phosphonate utilization (Palenik et al., 2003; Dyhrman et al., 2006). Our results are contrary to a recent study where chlorophyll increases were observed after N addition in the Sargasso Sea (Mills et al., 2004). We have the opportunity to repeat the experiment this spring. The importance of N will be addressed directly by performing N additions.

This thesis examined the importance of three nutrients in two ocean basins. Results were obtained through a variety of methods including high-sensitivity analyses of Zn, Co, and P, shipboard incubations,

and phytoplankton culture experiments. This work highlights the difficulties but also the value in performing high sensitivity analyses of both macronutrients and trace metals. Overall, this thesis adds to our understanding of the Zn, Co, and P cycles and demonstrates that the three may be linked under low P conditions.

## Bibliography

- BRULAND, K. W. 1989. Complexation of zinc by natural organic ligands in the central North Pacific. *Limnology and Oceanography*. **34**: 269–285.
- DYHRMAN, S. T., P. D. CHAPPELL, S. T. HALEY, J. W. MOFFETT, E. D. ORCHARD, J. B. WATERBURY, and E. A. WEBB. 2006. Phosphonate utilization by the globally significant marine diazotroph *Trichodesmium*. *Nature*. **439**: 68–71.
- ELLWOOD, M. J. 2004. Zinc and cadmium speciation in subantarctic waters east of New Zealand. *Marine Chemistry*. **87**: 37–58.
- KARL, D. M., and G. TIEN. 1992. MAGIC: A sensitive and precise method for measuring dissolved phosphorus in aquatic environments. *Limnology and Oceanography*. **37**: 105–116.
- LOHAN, M. C., D. W. CRAWFORD, D. A. PURDIE, and P. J. STATHAM. 2005. Iron and zinc enrichments in the northeastern subarctic pacific: Ligand production and zinc availability in response to phytoplankton growth. *Limnology and Oceanography*. **50**: 1427–1437.
- MILLS, M. M., C. RIDAME, M. DAVEY, J. L. ROCHE, and R. J. GEIDER. 2004. Iron and phosphorus co-limit nitrogen fixation in the eastern tropical North Atlantic. *Nature*. **429**: 292–294.
- PALENIK, B., B. BRAHAMSHA, F. W. LARIMER, M. LAND, L. HAUSER, P. CHAIN, J. LAMERDIN, W. REGALA, E. E. ALLEN, J. MCCARREN, I. PAULSEN, A. DUFRESNE, F. PARTENSKY, E. A. WEBB, and J. WATERBURY. 2003. The genome of a motile marine *Synechococcus*. *Nature*. **424**: 1037–1042.
- RIMMELIN, P., and T. MOUTIN. 2005. Re-examination of the MAGIC method to determine low orthophosphate concentration in seawater. *Analytica Chimica Acta*. **548**: 174–182.
- SHAKED, Y., Y. XU, K. LEBLANC, and F. M. M. MOREL. 2006. Zinc availability and alkaline phosphatase activity in *Emiliania huxleyi*: implications for Zn-P co-limitation in the ocean. *Limnology and Oceanography*. **51**: 299–309.
- SUNDA, W. G., and S. A. HUNTSMAN. 1995. Cobalt and zinc interreplacement in marine phytoplankton: Biological and geochemical implications. *Limnology and Oceanography*. **40**: 1404–1417.



## **Appendix A**

# **Cleaning Protocols Used**

### **A.1 Low Density Polyethylene (LDPE) for acidified totals**

1. Rinse new bottle (Nalgene) with methanol (this step was used for N. Pacific and Bering Sea samples, but was omitted for N. Atlantic and Sargasso Sea samples.)
2. Soak bottle in 1-5% Citranox detergent for 24-48 hours at 60°C. Flip once mid-way through.
3. Rinse bottle 5-6 times with Milli-Q.
4. In fume hood, fill bottles with 6N HCl (J.T. Baker Instra-analysed), exclude air when tightening caps, place filled bottles in 2N HCl (J.T. Baker Instra-analysed) bath for 2-4 weeks.
5. Rinse outside of bottles with Milli-Q.
6. In fume hood, empty bottles of 6N HCl.
7. Rinse bottles once with Milli-Q.
8. Fill bottles with 5% HNO<sub>3</sub> (J.T. Baker Instra-analysed), exclude air when tightening caps, double bag and let sit for two weeks.
9. In laminar flow hood, empty bottles of 5% HNO<sub>3</sub>.
10. In laminar flow hood, rinse once with pH 2 HCl (Seastar).
11. Rinse clean bottle with 100-200 mls sample, before filling with sample.

## **A.2 Teflon for speciation samples**

1. Rinse new bottle (Nalgene) with Milli-Q.
2. Fill bottle with concentrated  $\text{HNO}_3$  (J.T. Baker Instra-analysed).
3. Place bottles in warm water bath ( $50^\circ\text{C}$ ) for 8 hours.
4. Let acid cool, then empty bottles in fume hood.
5. Fill bottles with 2N HCl (J.T. Baker Instra-analysed) and let sit 1 week.
6. Fill bottles with pH 2 HCl (Seastar).

## **A.3 Polyethylene Centrifuge tubes for ICP-MS analysis**

For tubes:

1. Rinse centrifuge tubes (Globe Scientific) with Milli-Q 5 times.
2. Fill High Density Polyethylene (HDPE) jar three-quarters of the way full with 2 N HCl (J.T. Baker Instra-analysed).
3. Put centrifuge tubes in HDPE jar making sure tubes fill with acid.
4. Top up jar with 2N HCl.
5. Put jar in  $60^\circ\text{C}$  oven for 48 hours. Flip once mid-way through.
6. Pour 2N HCl out of jar, leaving tubes behind.
7. In laminar flow hood, shake 10 tubes at a time into a clean gloved hand.
8. Rinse tubes 5 times with pH 2 HCl (J.T. Baker Instra-analysed).
9. Rinse tubes 1 time with pH 2 HCl (Seastar).
10. Fill tubes to a positive meniscus with pH 2 HCl (Seastar).
11. Shake clean cap into a clean gloved hand and cap tubes.
12. Rinse tubes once with sample before filling.

For caps:

1. Rinse caps (Globe Scientific) with Milli-Q 5 times.

2. Place caps in HDPE bottle.
3. Fill bottle with 2 N HCl (J.T. Baker Instra-analysed).
4. Put jar in 60°C oven for 48 hours. Flip once mid-way through.
5. Pour 2N HCl out of bottle, leaving caps behind.
6. Fill bottle 5 times with pH 2 HCl (J.T. Baker Instra-analysed), shake, then pour pH 2 out of bottle, leaving caps behind.
7. Fill bottle 2 times with pH 2 HCl (Seastar), shake, then pour pH 2 out of bottle, leaving caps behind.



## **Appendix B**

# **Incubation Experiments**

This Appendix contains results for incubation experiments that were not presented as part of the first 6 chapters in order for simplicity or clarity of those chapters and largely represent incubations that had negative or inconclusive results.

### **B.1 Western North Atlantic, Spring 2004**

The following incubation experiments were performed as a part of the R/V Oceanus cruise OC399-4 in March-April of 2004 in the western North Atlantic Ocean. The methods used for these incubations are described in Ch. 4. Station numbers are the same as those in Ch. 4, Fig. 4-1.

#### **B.1.1 Incubation OCE1**

Incubation OCE1 was begun at St. 1 (31°N, 64°W) on March 20, 2004. The treatments below were performed in addition to those in chapters 4 and 5. When either Co or Zn was added along with DIP, the chlorophyll response was generally greater than that of DIP addition alone (Fig. B-1). This effect was most pronounced in the +Co/DIP treatment which had chlorophyll values 2.5-4 times higher than the DIP alone treatment and 5-11 times higher than the control. No increase in chlorophyll was observed due to the addition of a single metal alone (including Fe) or the combination of Zn and Co added together (Fig. B-2). These results suggest that P is the limiting nutrient at this site, but that once P-limitation is relieved, the community quickly becomes stressed for Co and/or Zn.

Figure B-1: Incubation OCE1: Metal and DIP additions. Treatments were: Control-no addition; +DIP-8.4  $\mu\text{M}$   $\text{Na}_2\text{H}_2\text{PO}_4$ ; +Co/DIP-630 pM  $\text{CoCl}_2$ , 8.4  $\mu\text{M}$   $\text{Na}_2\text{H}_2\text{PO}_4$ ; and +Zn/DIP-1.7 nM  $\text{ZnCl}_2$ , 8.4  $\mu\text{M}$   $\text{Na}_2\text{H}_2\text{PO}_4$ .

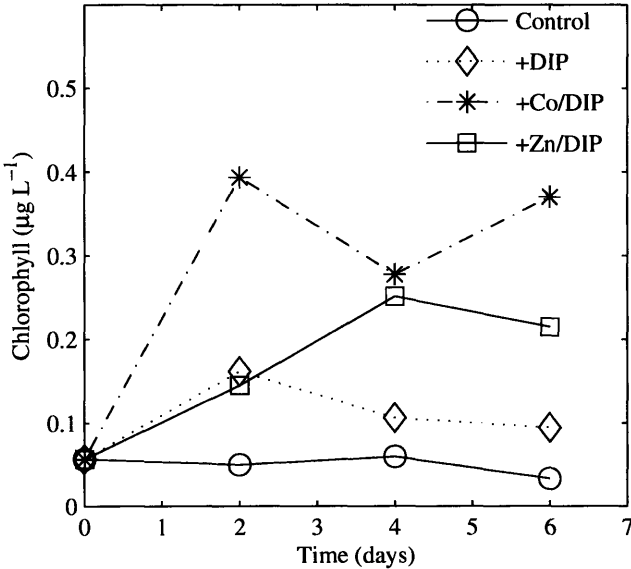
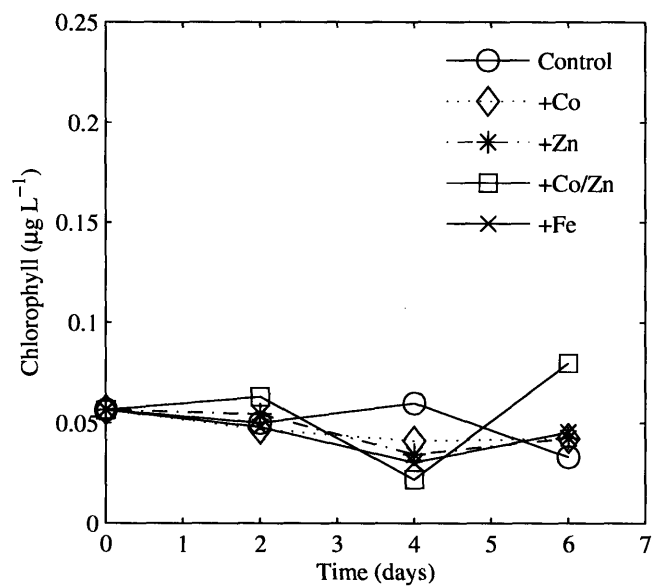


Figure B-2: Incubation OCE1: Metal alone additions. Additions were: Control-no addition; +Co-630 pM  $\text{CoCl}_2$ ; +Zn-1.7 nM  $\text{ZnCl}_2$ ; +Co/Zn-630 pM  $\text{CoCl}_2$ , 1.7 nM  $\text{ZnCl}_2$ ; and +Fe-1.7 nM  $\text{FeCl}_3$ . Notice y-axis scale is half that in Fig. B-1.



### **B.1.2 Incubation OCE2**

Incubation OCE2 began at St. 2 (28°N, 62°W) on March 21, 2004. The treatments presented here were performed in addition to those presented in chapters 4 and 5. At this site, the addition of Co along with DIP resulted in a higher chlorophyll response on days 4 and 6, however the response was not nearly as pronounced as that in OCE1 (Fig. B-3). The addition of Zn along with DIP had a higher chlorophyll response than DIP on day 6 only. The chlorophyll values in +DIP treatments on day 2 were lower at St. 2 than St. 1, however the relative increase was actually higher at St. 2 (4-fold) than St. 1 (3-fold) because the initial chlorophyll values were much lower at St. 2. There was a slight increase in the +Co addition above the control treatment on days 2 and 4, but this diminished on day 6 and had only 30-40% the effect of the addition of DIP (Fig. B-4). Again in OCE2, the limiting nutrient for phytoplankton growth appears to be P. Co and Zn did not have as large an additional effect on chlorophyll as in OCE1, perhaps because the absolute chlorophyll values did not reach as high a level as OCE1 or because another nutrient such as N restricted further growth.



Figure B-3: Incubation OCE2: Metal and DIP additions. Additions were: Control-no addition; +DIP-8.4  $\mu\text{M}$   $\text{Na}_2\text{H}_2\text{PO}_4$ ; +Co/DIP-630 pM  $\text{CoCl}_2$ , 8.4  $\mu\text{M}$   $\text{Na}_2\text{H}_2\text{PO}_4$ ; and +Zn/DIP-1.7 nM  $\text{ZnCl}_2$ , 8.4  $\mu\text{M}$   $\text{Na}_2\text{H}_2\text{PO}_4$ . Notice y-axis scale is one-third that in Fig. B-1.

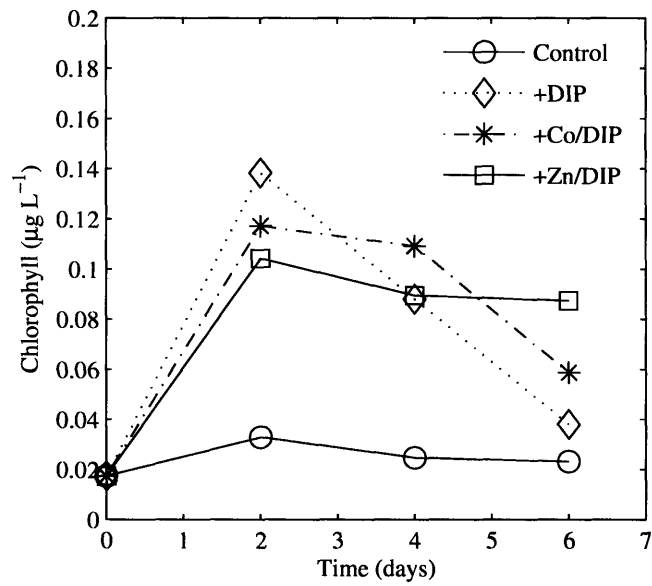


Figure B-4: Incubation OCE2: Metal alone additions. Additions were: Control-no addition; +Co-630 pM  $\text{CoCl}_2$ ; +Zn-1.7 nM  $\text{ZnCl}_2$ ; +Co/Zn-630 pM  $\text{CoCl}_2$ , 1.7 nM  $\text{ZnCl}_2$ ; and +Fe-1.7 nM  $\text{FeCl}_3$ . There was only one +Fe bottle, which was sampled on day 6.

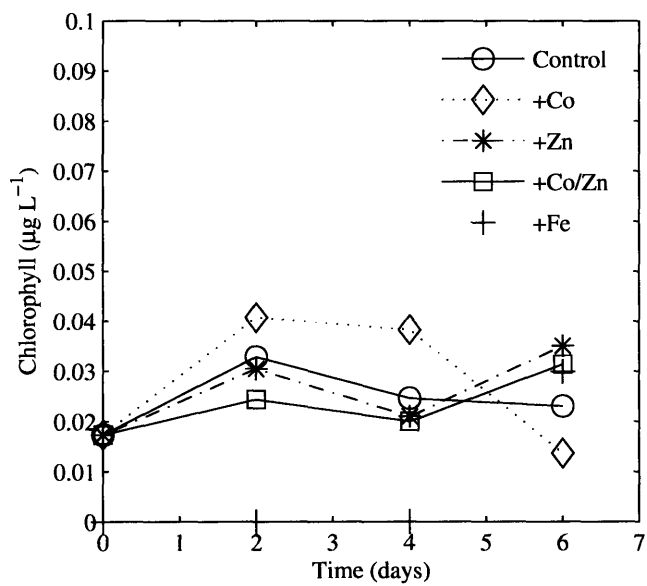
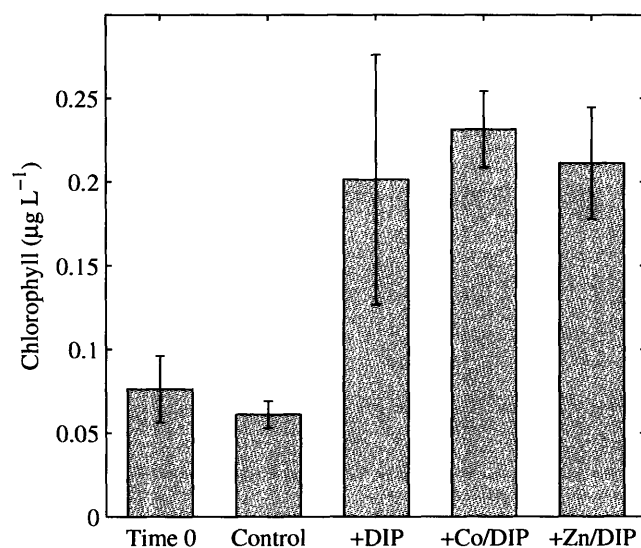


Figure B-5: Incubation OCE3: Metal and DIP additions. Additions were: Control-no addition; +DIP-8.4  $\mu\text{M}$   $\text{Na}_2\text{H}_2\text{PO}_4$ ; +Co/DIP-630 pM  $\text{CoCl}_2$ , 8.4  $\mu\text{M}$   $\text{Na}_2\text{H}_2\text{PO}_4$ ; and +Zn/DIP-1.7 nM  $\text{ZnCl}_2$ , 8.4  $\mu\text{M}$   $\text{Na}_2\text{H}_2\text{PO}_4$ . The bars represent the average chlorophyll value of triplicate bottles which were all sampled after 2 days. Error bars represent the standard deviation of the triplicate values.



### B.1.3 Incubation OCE3

Incubation OCE3 began at St. 11 (20°N, 46°W) on March 29, 2004. This incubation was an end-point incubation where all bottles were sampled after 2 days. The addition of DIP caused an increase in chlorophyll that was roughly 4-times the chlorophyll in the control (Fig. B-5). The addition of Co or Zn in addition of DIP did not have a significant effect over that of the DIP addition. There was a slight decrease in all the metal addition treatments relative to time zero, but there is not a significant difference between the metal additions (Fig. B-6). As in OCE1 and OCE2, P seems to be the limiting nutrient at this site. There was not an enhance effect when Co or was added along with DIP, suggesting that there is sufficient Co and Zn to meet the community's demand at these chlorophyll levels.

Figure B-6: Incubation OCE3: Metal alone additions. Additions were: Control-no addition; +Co-630 pM  $\text{CoCl}_2$ ; and +Zn-1.7 nM  $\text{ZnCl}_2$ . Bars as Fig. B-5.

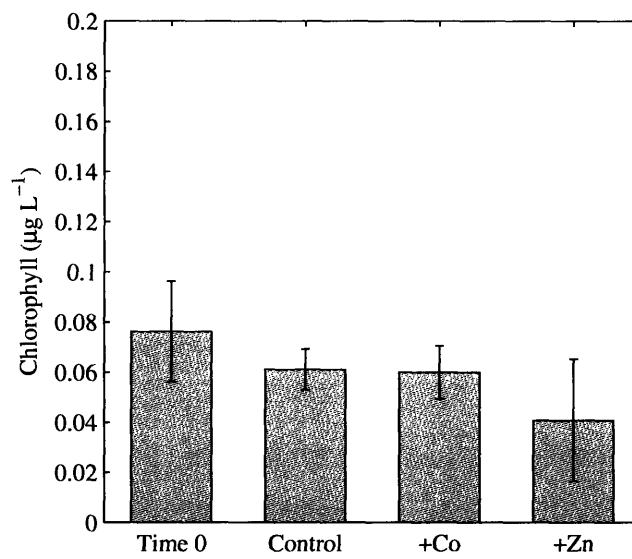
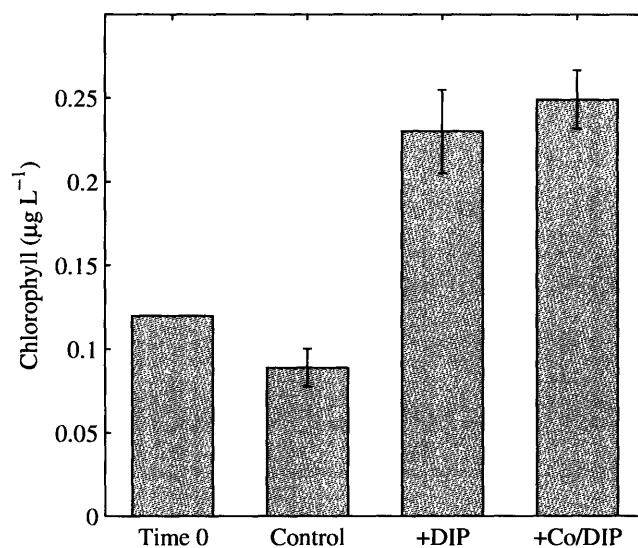


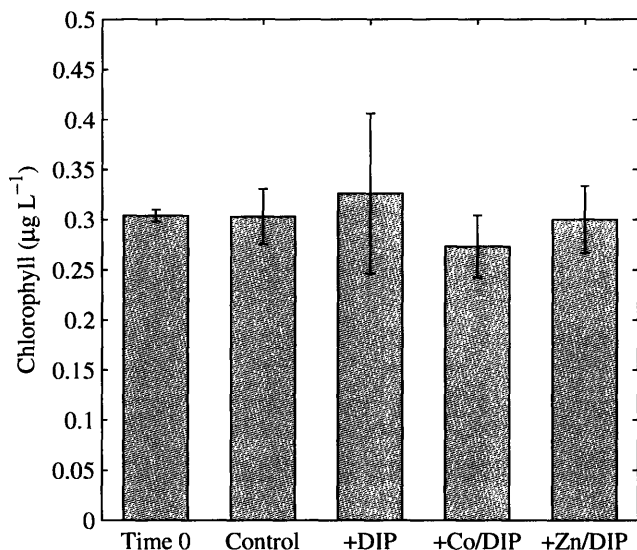
Figure B-7: Incubation OCE4: Metal and DIP additions. Additions were: Control-no addition; +DIP-8.4  $\mu\text{M}$   $\text{Na}_2\text{H}_2\text{PO}_4$ ; and +Co/DIP-630 pM  $\text{CoCl}_2$ , 8.4  $\mu\text{M}$   $\text{Na}_2\text{H}_2\text{PO}_4$ . The bars represent the average chlorophyll value of triplicate bottles which were all sampled after 2 days. Error bars represent the standard deviation of the triplicate values.



#### B.1.4 Incubation OCE4

Incubation OCE4 was started at St. 15 (32°N, 54°W) on April 2, 2004. This incubation was an end-point incubation where all bottles were sampled after 2 days. The addition of DIP caused an increase in chlorophyll that was 3-times the chlorophyll in the control (Fig. B-7). The addition of Co along with DIP did not have a significant effect over that of the DIP addition. Similar to the previous incubation experiments presented, at St. 15, P appeared to be the nutrient limiting phytoplankton growth.

Figure B-8: Incubation OCE5: Metal and DIP additions. Additions were: Control-no addition; +DIP-8.4  $\mu\text{M}$   $\text{Na}_2\text{H}_2\text{PO}_4$ ; +Co/DIP-630 pM  $\text{CoCl}_2$ , 8.4  $\mu\text{M}$   $\text{Na}_2\text{H}_2\text{PO}_4$ ; and +Zn/DIP-1.7 nM  $\text{ZnCl}_2$ , 8.4  $\mu\text{M}$   $\text{Na}_2\text{H}_2\text{PO}_4$ . The bars represent the average chlorophyll value of triplicate bottles which were all sampled after 3 days. Error bars represent the standard deviation of the triplicate values.



### B.1.5 Incubation OCE5

Incubation OCE5 began at St. 16 (34°N, 55°W) on April 4, 2004. This incubation was an end-point incubation where all bottles were sampled after 3 days. This was the only incubation where the addition of DIP had no effect (Fig. B-8). The addition of Co or Zn along with DIP did not have a significant effect over the control either. Chlorophyll was stimulated at this station by the addition of two DOP compounds (Ch. 5). At this site, P does not appear to be limiting based on the lack of chlorophyll response in the +DIP addition. However, the increase in chlorophyll after DOP addition counterdicts this assertion and suggests that perhaps there was a chlorophyll response in the +DIP addition that was missed by not sampling before day 3. This is speculative, but the author does not have a better alternate explanation.

## **B.2 North Pacific and Bering Sea, Summer 2003**

The following incubation experiments were performed as a part of the R/V Kilo Moana cruise KM0311 in June-August of 2003 in the subarctic North Pacific and Bering Sea. The methods used for these incubations are described in Ch. 3. Station numbers are the same as those in Ch. 3, Fig. 3-1. Incubations were performed in collaboration with Mak Saito and Yan Xu.

### **B.2.1 Incubation KM1**

Incubation KM1 began at St. 1 (41°N, 140°W) on June 27, 2003. This incubation was an end-point incubation where all bottles were sampled after 4 days. This incubation took place in the eastern subarctic North Pacific which is classically considered an Fe-limited region. However, when we visited this site, nutrients had been drawn down to low levels (0.07  $\mu\text{M}$   $\text{NO}_3$ , 0.29  $\mu\text{M}$   $\text{PO}_4$ , 0.46  $\mu\text{M}$   $\text{SiO}_3$ ). The addition of  $\text{NO}_3$  caused a quadrupling of chlorophyll relative to the control (Fig. B-9). The addition of Zn along with N had no effect above that of N addition alone. This is interesting considering the total Zn at St. 1 was the lowest Zn measured on this cruise (0.1 nM). It is also interesting to note that the addition of 25 nM Zn did not appear to have a toxic effect on the phytoplankton community. The addition of such a high level of Zn was inadvertent (calculations were performed using the wrong standard). This experiment suggests that N can limit phytoplankton growth at this site (near Ocean Station Papa) and that the ambient Zn appears to be sufficient to meet the community's cellular demand.

Figure B-9: Incubation KM1: Metal and nutrient additions. Additions were: Control-no addition; +Zn-25 nM  $ZnCl_2$ ; +DIP-10  $\mu M Na_2H_2PO_4$ ; +N-75  $\mu M NaNO_3$ ; and +N/Zn-75  $\mu M NaNO_3$ , 25 nM  $ZnCl_2$ . The bars represent the average chlorophyll value of duplicate bottles which were all sampled after 4 days. Error bars represent the standard deviation of duplicate values.

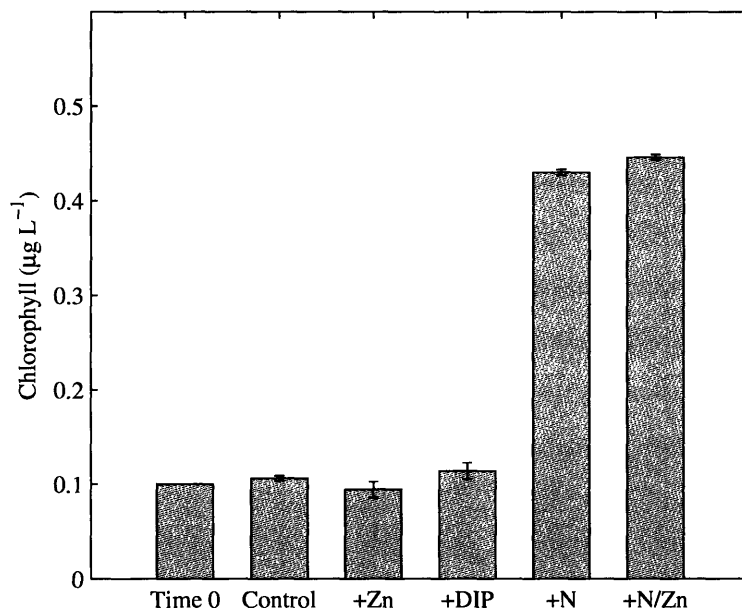
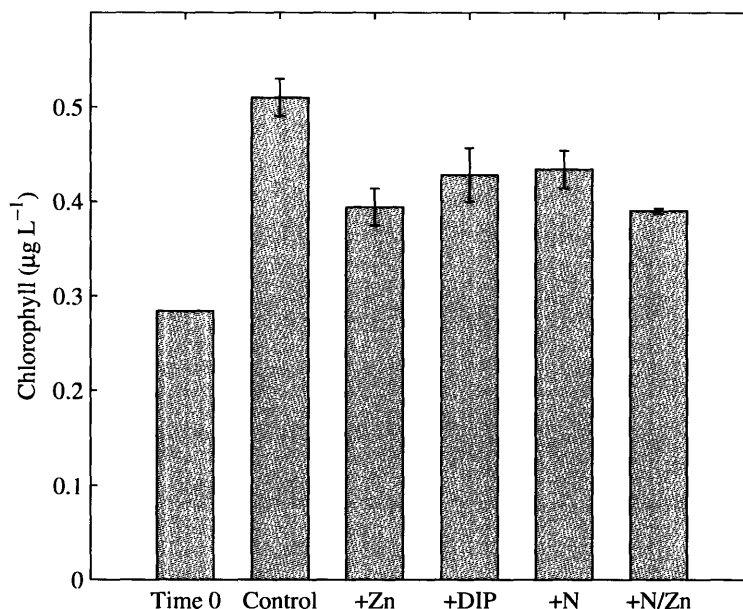




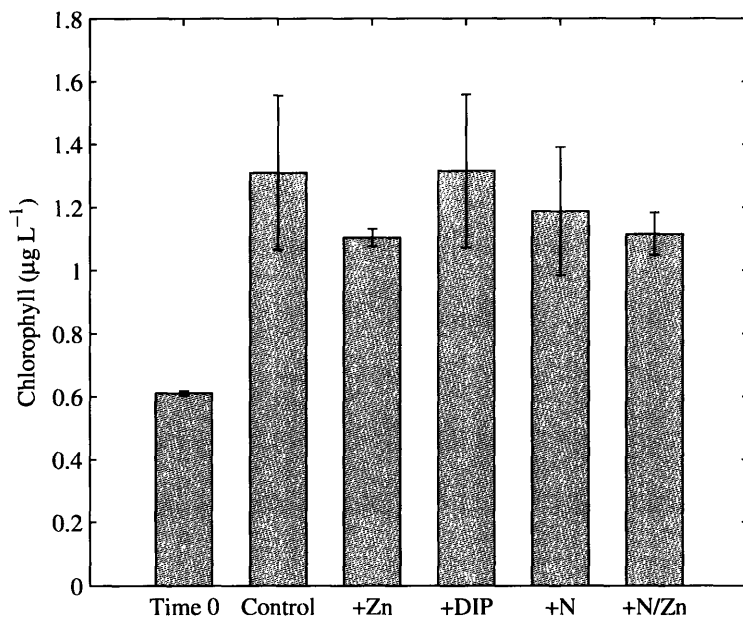
Figure B-10: Incubation KM3: Metal and nutrient additions. Additions were: Control-no addition; +Zn-25 nM ZnCl<sub>2</sub>; +DIP-10 μM Na<sub>2</sub>H<sub>2</sub>PO<sub>4</sub>; +N-75 μM NaNO<sub>3</sub>; and +N/Zn-75 μM NaNO<sub>3</sub>, 25 nM ZnCl<sub>2</sub>. The bars represent the average chlorophyll value of duplicate bottles which were all sampled after 4 days. Error bars represent the standard deviation of duplicate values.



### B.2.2 Incubation KM3

Incubation KM3 was began at St. 3 (44°N, 159°W) on July 5, 2003. This incubation was an end-point incubation where all bottles were sampled after 4 days. The nutrient concentrations at the beginning of this incubation (1.09 μM PO<sub>4</sub>) were higher than those observed at St. 1. There was no increase in chlorophyll due to the addition of Zn, P, N, or Zn and N together (Fig. B-10). In fact, the highest chlorophyll after 4 days was in the no addition control. Incubations performed by Saito and Xu (unpubl. data) at this site suggest that Fe was the limiting nutrient at St. 3.

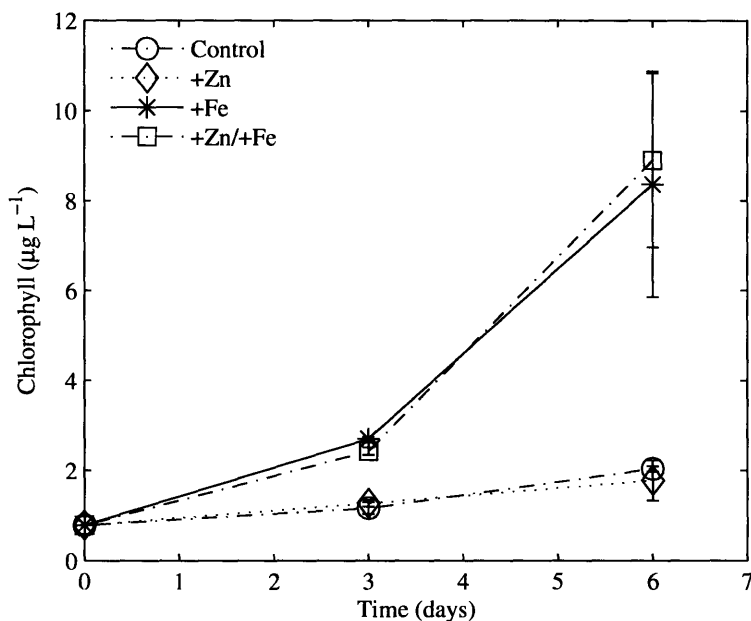
Figure B-11: Incubation KM4: Metal and nutrient additions. Additions were: Control-no addition; +Zn-6 nM ZnCl<sub>2</sub>; +DIP-10 μM Na<sub>2</sub>H<sub>2</sub>PO<sub>4</sub>; +N-75 μM NaNO<sub>3</sub>; and +N/Zn-75 μM NaNO<sub>3</sub>, 6 nM ZnCl<sub>2</sub>. The bars represent the average chlorophyll value of duplicate bottles which were all sampled after 6 days. Error bars represent the standard deviation of duplicate values.



### B.2.3 Incubation KM4

Incubation KM4 was started at St. 4 (47°N, 170°W) on July 10, 2003. This incubation was an end-point incubation where all bottles were sampled after 6 days. Initial nutrient concentrations at St. 4 were 14.5 μM NO<sub>3</sub>, 1.3 μM PO<sub>4</sub>, 13.8 μM SiO<sub>3</sub>. As at St. 3, the addition of Zn, P, N, or Zn and N together had no effect on chlorophyll (Fig. B-11). Again, incubations performed by Saito and Xhu (unpubl. data) indicate that Fe was limiting primary production at St. 4.

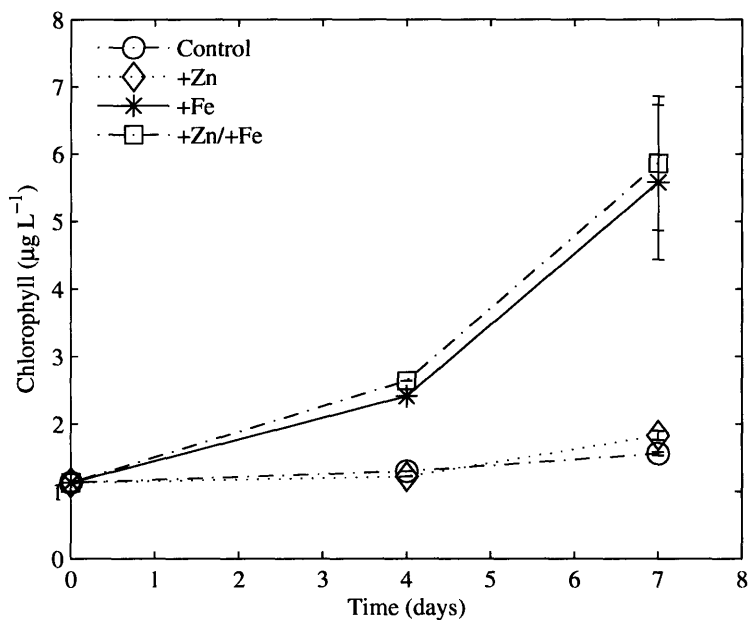
Figure B-12: Incubation KM6: Metal additions. Additions were: Control-no addition; +Zn-1 nM ZnCl<sub>2</sub>; +Fe-2.5 nM FeCl<sub>3</sub>; and +Zn/Fe-1 nM ZnCl<sub>2</sub>, 2.5 nM FeCl<sub>3</sub>. Error bars represent the standard deviation of duplicate values.



#### B.2.4 Incubation KM6

Incubation KM6 was started at St. 6 (46°N, 170°E) on July 17, 2003. This incubation was a time-course incubation where bottles were sampled on days 3 and 6. Initial nutrient concentrations were very similar to those at St. 4 (14.9 µM NO<sub>3</sub>, 1.4 µM PO<sub>4</sub>, 13.5 µM SiO<sub>3</sub>). There were triplicate bottles for each treatment. One bottle from each treatment was sacrificed on day 3, and a second bottle was opened and sampled for chlorophyll and then returned to the incubator. This second bottle and the final unopened triplicate bottle were sampled on day 6. The addition of Zn alone had no effect on chlorophyll concentration, whereas the addition of Fe or Fe and Zn together resulted in a 10-fold increase in chlorophyll after 6 days (Fig. B-12). This indicates that Fe is the ultimate limiting nutrient at this site and that once Fe-limitation is relieved, the ambient concentrations of the other nutrients are sufficient to support ten times the ambient phytoplankton biomass.

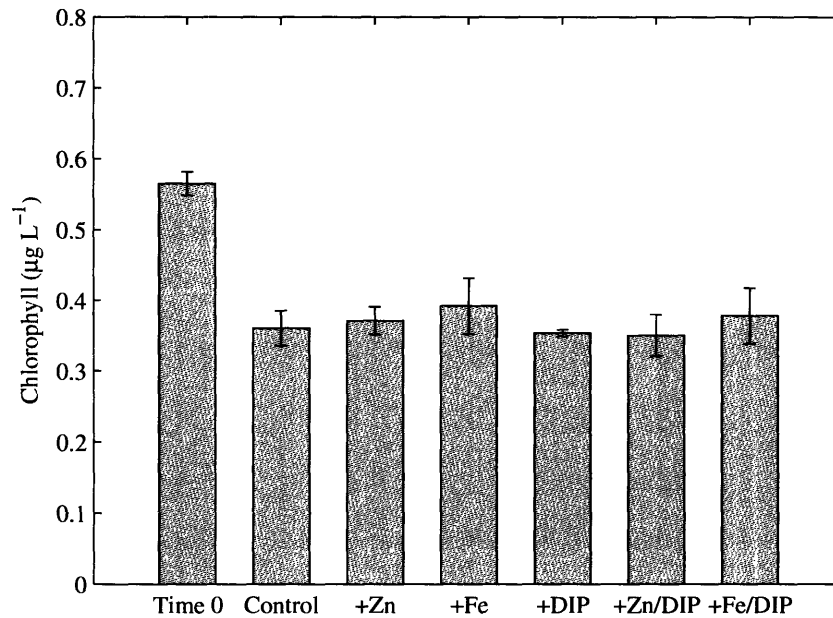
Figure B-13: Incubation KM8: Metal additions. Additions were: Control-no addition; +Zn-1 nM ZnCl<sub>2</sub>; +Fe-2 nM FeCl<sub>3</sub>; and +Zn/Fe-1 nM ZnCl<sub>2</sub>, 2 nM FeCl<sub>3</sub>. Error bars represent the standard deviation of duplicate values.



### B.2.5 Incubation KM8

Incubation KM8 began on July 21, 2003 at St. 8 (55°N, 176°E) in the deep western portion of the Bering Sea. Initial nutrient concentrations were similar to stations 4 and 6 (14.8 µM NO<sub>3</sub>, 1.5 µM PO<sub>4</sub>, 11.6 µM SiO<sub>3</sub>). This incubation was a time-course incubation where bottles were sampled on days 4 and 7. There were duplicate bottles for each treatment. One bottle from each treatment was opened and sampled for chlorophyll on day 4 and then returned to the incubator. This bottle and the unopened duplicate bottle were sampled on day 7. The results from this incubation mimic those of the previous incubation at St. 6 with chlorophyll increases in the +Fe and +Zn/+Fe treatments (Fig. B-13). Notice however that the chlorophyll increase (6-fold) after 7 days at this site was not as high as the chlorophyll increase at the previous site after 6 days (10-fold). This incubation suggests that Fe was limiting phytoplankton growth at St. 8 in the western Bering Sea.

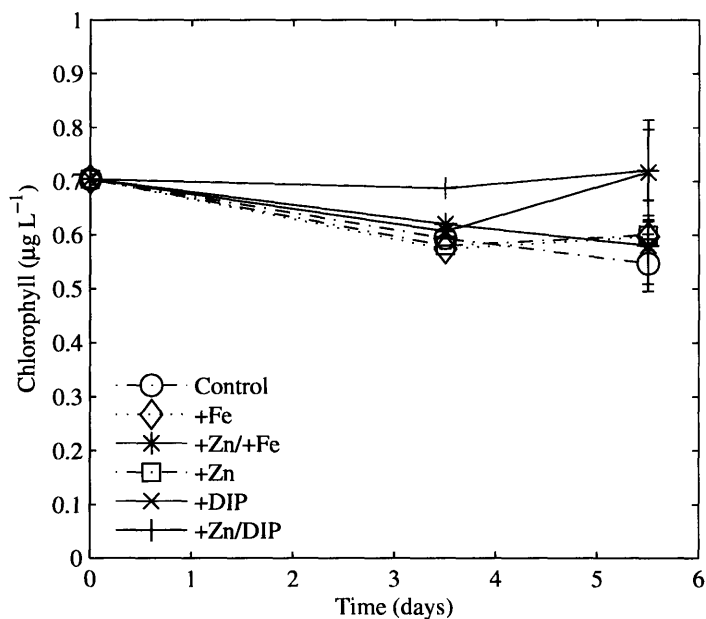
Figure B-14: Incubation KM10: Metal and nutrient additions. Additions were: Control-no addition; +Zn-1 nM ZnCl<sub>2</sub>; +Fe-2 nM FeCl<sub>3</sub>; +DIP-10 μM Na<sub>2</sub>H<sub>2</sub>PO<sub>4</sub>; +Zn/DIP-1 nM ZnCl<sub>2</sub>, 10 μM Na<sub>2</sub>H<sub>2</sub>PO<sub>4</sub>; and +Fe/P-2 nM FeCl<sub>3</sub>, 10 μM Na<sub>2</sub>H<sub>2</sub>PO<sub>4</sub>. Error bars represent the standard deviation of duplicate values.



### B.2.6 Incubation KM10

Incubation KM10 began on July 30, 2003 at St. 10b2 (56°N, 167°W), which is on the Bering Shelf. Initial PO<sub>3</sub> concentration at St. 10b2 (0.31 μM) was lower than all the N. Pacific stations except St. 1. This incubation was an end-point incubation where all bottles were sampled on day 4. There were duplicate bottles for each treatment. There was a decrease in chlorophyll in all treatments relative to time zero (B-14). The addition of Zn, Fe, P, or a combination of metals and P had no effect on chlorophyll concentration relative to the no addition control. This suggests that another nutrient (perhaps N) was limiting primary production at this site.

Figure B-15: Incubation KM11: Metal and nutrient additions. Additions were: Control-no addition; +Zn-1 nM ZnCl<sub>2</sub>; +Fe-2 nM FeCl<sub>3</sub>; +DIP-10 μM Na<sub>2</sub>H<sub>2</sub>PO<sub>4</sub>; +Zn/DIP-1 nM ZnCl<sub>2</sub>, 10 μM Na<sub>2</sub>H<sub>2</sub>PO<sub>4</sub>; and +Fe/P-2 nM FeCl<sub>3</sub>, 10 μM Na<sub>2</sub>H<sub>2</sub>PO<sub>4</sub>. Error bars represent the standard deviation of duplicate values.



### B.2.7 Incubation KM11

Incubation KM11 was begun on July 26, 2003 at St. 11 (56°N, 164°W) which is also on the Bering Shelf. The initial phosphate concentration at St. 11 was similar to that at stations 1 and 10. This incubation was a time-course incubation where bottles were sampled on days 3.5 and 5.5. There were duplicate bottles for each treatment. One bottle from each treatment was opened and sampled for chlorophyll on day 3.5 and then returned to the incubator. Chlorophyll concentrations declined over time in the majority of the treatments, including the control (Fig. B-15). The concentration of chlorophyll remained steady in the +Zn addition such that it had higher chlorophyll values than the control on both sampling days, though the variation between duplicate bottles meant that this effect was not significant on day 5.5. As with the other incubation performed on the Bering Shelf, the limiting nutrient appears to be something other than those which we added.

### **B.3 Conclusions**

In the Sargasso Sea in spring 2004, P was found to be the limiting nutrient based on DIP additions at 4 out of 5 incubation sites. There was strong evidence at one station that Co and Zn could enhance the effect of DIP addition alone. The additions of metals (Fe, Zn, Co) without macronutrients generally had no effect on chlorophyll concentration. These results are in complete contrast to those of the N. Pacific and Bering Sea. In the summer of 2003, N was found to be limiting at the eastern-most station of the N. Pacific. All other stations in the N. Pacific and the western-most Bering Sea station appeared to be Fe limited. Two incubation experiments on the Bering Shelf indicated that the phytoplankton growth was limited by something other than Fe, Zn, and P (perhaps N).





Table B.1: Summary table of all the incubation results presented in this thesis. An X indicates that a treatment resulted in an increase in chlorophyll above a no-addition control. n.i. indicates no increase. Where spaces are empty, the treatment was not performed at that station.

Subarctic North Pacific (summer 2003)										
St.	Location	+Zn	+DIP	+N	+Zn/N	+Fe	+Zn/Fe			
1	41.60°N, 140.06°W	n.i.	n.i.	X	X					
3	44.02°N, 159.59°W	n.i.	n.i.	n.i.	n.i.					
4	47.01°N, 170.30°W	n.i.	n.i.	n.i.	n.i.					
5	46.59°N, 179.58°W	X				X	X			
6	46.60°N, 170.20°E	n.i.				X	X			
Bering Sea (summer 2003)										
St.	Location	+Zn	+DIP	+Fe	+Zn/Fe	+Zn/DIP	+Fe/DIP			
8	55.18°N, 176.31°E	n.i.		X	X					
10	56.43°N, 167.50°W	n.i.	n.i.	n.i.		n.i.	n.i.			
11	56.45°N, 164.60°W	n.i.	n.i.	n.i.		n.i.				
Western North Atlantic (spring 2004)										
St.	Location	+DIP	+Co/DIP	+Zn/DIP	+Co	+Zn	+Co/Zn	+Fe	+PME	+Pnte
1	31.41°N, 64.11°W	X	X	X	n.i.	n.i.	n.i.	n.i.	X	X
2	28.46°N, 62.57°W	X	X	X	?	n.i.	n.i.	n.i.	X	X
11	20.58°N, 46.54°W	X	X	X	n.i.	n.i.				
15	32.14°N, 54.37°W	X	X							
16	34.38°N, 55.35°W	n.i.	n.i.	n.i.	n.i.	n.i.		X	X	X